

The Design and Synthesis of Novel Anti-Viral Agents

PhD Pharmacy

School of Chemistry Food and Pharmacy

Ibrahim Celiker

November 2016

Declaration

I confirm that this is my own work and the use of all material from other sources has been properly and fully acknowledged

Acknowledgements

I would like to thank my supervisors Prof Helen Osborn and Dr Barny Greenland for their invaluable advice and support over the last four years. I would also like to thank Dr Helen Gale, Dr Alex Weymouth-Wilson and Dr Zofia Komsta, and all the members of staff at Dextra Laboratories LTD for their continued support of this research. Thank you to Dr Mark Dallas and the staff in the Hopkins building for their time, assistance and effort in training me in microbiological techniques that enabled me to perform the cell based assays. I would also like to mention the MRC and Dextra Laboratories Ltd for funding this research over the last four years.

This piece of work would not have been possible without the support staff at Reading. A special mention goes to the glassblower Mark McClemont for creating specialist pieces of glassware, to stores for pushing through orders and to the workshop staff for maintaining and repairing electrical equipment.

A special thanks to all of the people in Lab 228, Dr Jay Parshotam and Dr Laura Brierley for their continued friendship and support through the last four years.

A most special thanks to my wife, Mrs Laura Celiker, for her endless love and support, without whom, I could not have done this work. Thank you for believing that I could do the impossible.

Abstract

Viral infections account for 25.4% of all human illnesses. Current anti-viral nucleosides are able to prevent viral replication; however, viruses evolve resistance to available treatments. Ribose nucleosides are ubiquitous; however due to the discriminatory nature of kinases, low intracellular concentrations of the active triphosphate is a significant factor in inactivity. In contrast, oxetane nucleosides have been shown to be phosphorylated by these kinases with high levels of the required active nucleotide triphosphate (NTP) resulting. Oxetane nucleosides, however, have been found to be inactivated by pyrimidine nucleoside phosphorylases (PNPs).

Previous studies have illustrated that sulfur containing nucleosides are not hydrolysed by PNPs. Therefore in this programme a library of 9 novel 3,3-bis(hydroxymethyl)-thietan-2-yl nucleosides was synthesised using Vorbrüggen conditions starting from a fluorothietane precursor, over 8 steps. Cell viability studies using an XTT assay on the thymine ($103\% \pm 4.9\%$), uracil ($95\% \pm 2.3\%$), 5-fluorouracil ($98\% \pm 7.5\%$) and 5,6-dimethyl uracil ($82\% \pm 4.1\%$) derivatives showed no significant loss in cell viability at up to 100 μM concentration, suggesting they were suitable for further study in anti-viral screens. Steps towards the synthesis of a complementary library of 4,4-bis(hydroxymethyl)-thietan-2-yl nucleosides have been optimised with successful synthesis of a novel key intermediate, thietane-2-one, in a yield of 37% over 6 steps. 4'-Thiohamamelose nucleosides show promise as potential anti-viral compounds as previous studies have shown that 4'-thioribose nucleosides are stable to PNPs and have longer half-lives than ribose nucleosides. Increasing the stability of the 4'-thiohamamelose nucleosides could improve the potential for development of the anti-viral profiles of this class of compounds. Therefore the chemistry of 4'-thiohamamelose nucleosides has been explored, with an intermediate hamamelolactone being prepared in a yield of 44% over 5 steps.

Small molecule nucleosides offer the greatest benefits as anti-viral compounds versus other small molecule anti-viral agents as nucleosides are able to directly halt viral replication. The sulfur containing nucleosides are potentially more stable than their ribose counterparts, leading to better pharmacological and pharmacodynamics outcomes.

Contents

Chapter	Title	Page
	Declaration	i
	Acknowledgements	ii
	Abstract	iii
	Contents	iv
	Abbreviations	viii
	List of Figures	xiii
	List of Schemes	xvii
	List of Tables	xxi
1	Introduction	1
	1.1 Lifecycle of Viruses	2
	1.2 Types of Antiviral Agents	4
	1.2.1 Interferons	4
	1.2.2 Inhibitors	5
	1.2.2.1 Integrase Strand Inhibitors	5
	1.2.2.2 Fusion Inhibitors/Co-receptor antagonists	7
	1.2.2.3 Protease Inhibitors	8
	1.2.2.4 Non-nucleoside Inhibitors	11
	1.2.2.4.1 Non-nucleoside Reverse Transcriptase Inhibitors	11
	1.2.2.4.2 Non-nucleoside Replicase Inhibitors	12
	1.2.2.5 Nucleoside Inhibitors	12
	1.2.2.5.1 Nucleoside Reverse Transcriptase Inhibitors	14
	1.2.2.5.2 Nucleoside Polymerase Inhibitors	15
	1.2.2.5.3 Development of Phosphoramidates	19
	1.2.2.5.4 Conformationally Restricted Nucleosides	24
	1.3 Summary and Conclusions	26
	1.4 Aims and Objectives	27
	1.5 References	29
2	The Design and Synthesis of 3,3-bis(hydroxymethyl)-thietan-2-yl Nucleosides	32
	2.1 Background	33

2.1.1 Oxetane and Thietane Nucleosides	34
2.2 Aims and Objectives	40
2.2.1 Formation of Thietane Nucleosides	40
2.3 Synthetic Strategy toward 3,3-bis(hydroxymethyl) thietane nucleosides	46
2.3.1 Synthesis of Thietane Nucleosides via the Pummerer Reaction	56
2.3.2 Synthesis of Thietane Nucleosides under Vorbrüggen Conditions	58
2.3.2.1 Deprotection of the benzoate groups	64
2.4 ¹ H NMR Features of Thietane Nucleosides	68
2.5 Assessment of Cellular Viability	72
2.5.1 The XTT Assay	73
2.5.2 Results and Discussion: General Background	74
2.5.2.1 Results and Discussion	74
2.6 Conclusions	76
2.7 References	78
3 The Design and Synthesis of 4,4-bis(hydroxymethyl)-thietan-2-yl nucleosides	81
3.1 Background	82
3.1.1 Aims and Objectives	83
3.2 Synthetic Strategies towards 4,4-bis(hydroxymethyl) thietane nucleosides	83
3.3 Initial Synthetic Steps Toward 4,4-bis(hydroxymethyl) thietane nucleosides	86
3.3.1 Results and Discussion: Initial Synthesis and Optimisation of Synthetic Route Toward 4,4-bis(hydroxymethyl) thietane Nucleosides	89
3.3.1.1 Oxidation Reactions toward 2-phenyl-1,3-dioxan-5-one	93
144	
3.3.1.2 Swern Oxidation Reactions toward Ketone 144	95
3.3.1.3 Parikh-Doering Oxidation Reactions toward Ketone 144	97
3.3.2 Results and Discussion: Modification of the Protecting	99

	Group	
	3.3.2.1 Results and Discussion: Synthesis of the Ally Aldehyde	100
	3.3.2.2 Divergence of the Synthetic Scheme	104
	3.3.3 Ester Hydrolysis Reactions	107
	3.3.3.1 Use of Potassium Trimethylsilanolate	110
	3.3.3.2 Trimethyltin Hydroxide Hydrolysis of Esters	111
	3.3.3.3 Steps Toward the Target Thietane Molecule	114
	3.3.4 Ester Hydrolysis reactions of Thioether	178
	3.4 References	123
4	The Design and Synthesis of 4'-Thiohamamelose Nucleosides	124
	4.1 The 4'-Thioribose Nucleosides and their Derivatives	125
	4.2 Hamamelose Nucleosides	129
	4.3 Aims	131
	4.3.1 SAR of the 4'-thiohamamelose nucleosides	131
	4.3.2 Synthetic strategy towards the 4'-thiohamamelose nucleosides	133
	4.4 Results and Discussion: Steps Toward the Synthesis of 4'-thiohamamelose Nucleosides	134
	4.4.1 Formylation Model Reactions	139
	4.4.2 Optimisation of the Oxidation Reactions	142
	4.4.3 Hydrolysis Reactions Toward Methyl Ester	203
	4.5 References	152
5	Conclusions and Future Work	156
	5.1 General Conclusions	157
	5.2 Future Work	158
	5.2.1 Synthesis of 3,3-bis(hydroxymethyl) thietane nucleosides	158
	5.2.2 Synthesis of 4,4-bis(hydroxymethyl) thietan-2-yl Nucleosides	160
	5.2.3 Synthesis of 4'-thiohamamelose Nucleosides	161
	5.2.4 HPLC Stability Studies	164
	5.2.5 Synthesis of Phosphoramidates	166
	5.3 Closing Statement	170
	5.4 References	172

6	Experimental	174
	6.1 References	209
	Appendix	210

Abbreviations

1,2-DCE	1,2-dichloroethane
1,2-DMP	1,2-dimethoxypropane
5,6-DMU	5,6-dimethyluracil
5FU	5-fluorouracil
Ac ₂ O	Acetic anhydride
AcO	Acetone
AcSH	Thioacetic acid
AgOTf	Silver triflate
BDMA	Benzylidene dimethylacetal
Bn	Benzyl
BnBr	Benzyl bromide
BnSH	Benzyl mercaptan
Bu ₄ NF	<i>n</i> -Butylammonium fluoride
BVDU	(<i>E</i>)-5-(2-bromovinyl)2'-deoxyuridine
Bz	Benzoyl
BzCl	Benzoyl chloride
Calc	Calculated
CC ₅₀	Cytotoxic Concentration
cLog P	Calculated Partition Coefficient
CMV	Cytomegalovirus
DAA	Directly Acting Anti-viral Agent
DAST	Diethylaminosulfur trifluoride

DCM	Dichloromethane
Deoxofluor	Bis(2-methoxyethyl)aminosulfur trifluoride
DHA	Dihydroxy acetone
DIBAL-H	Diisobutylaluminium Hydride
DKA	Diketo Aryl like Inhibitors
DMAP	4-Dimethylaminopyridine
DMF	Dimethylformamide
DMP	Dess Martin Periodinane
DMSO	Dimethylsulfoxide
DNA	Deoxyribose Nucleic Acid
EBV	Epstein-Barr Virus
EC ₅₀	Effective Concentration
EI	Electron Spray Ionisation
Equiv	Equivalent(s)
Et ₃ N	Triethylamine
EtOH	Ethanol
FGI	Functional Group Interconversion
GI	Gastrointestinal tract
HBV	Hepatitis B Virus
HCl	Hydrochloric Acid
HCV	Hepatitis C Virus
HIV	Human Immunodeficiency Virus
HMDS	Hexamethyldisilazane

HPLC	High Performance Liquid Chromatography
HRMS	High Resolution Mass Spectrometry
Hrs	Hours
HSV	Herpes Simplex Virus
HWE	Horner-Wadsworth-Emmons
IC ₅₀	Inhibitory Concentration
IIs	Integrase Strand Inhibitors
IFN	Interferon
IPA	Isopropyl Alcohol (2-propanol)
IR	Infra red
IV	Intravenous
LG	Leaving Group
Log P	Partition Coefficient
M/Z	Mass Charge Ratio
MeCN	Acetonitrile
MeOH	Methanol
Mins	Minutes
<i>N,O</i> -BSA	<i>N,O</i> -Bis(trimethylsilyl)acetamide
NaOMe	Sodium Methoxide
NMP	Nucleotide monophosphate
NMR	Nuclear Magnetic Resonance
NNRI	Non-Nucleoside Replicase Inhibitor
NNRTI	Non-Nucleoside Reverse Transcriptase Inhibitor

N°	Number
NS	Non-Structural Protein
NTP	Nucleotide triphosphate
Obs	Observed
PBS	Phosphate Buffer Solution
PEG IFN	Pegylated Interferon
PI	Protease Inhibitor
PMB	Peripheral Blood Mononuclear
PMS	Phenazine Methosulfate
PNP	Pyrimidine Nucleoside Phosphorylase
PPh ₃	Triphenylphosphine
<i>p</i> TSA	<i>Para</i> -toluene sulfonic acid
RBV	Ribavirin
RdRp	RNA Dependant RNA Polymerase
RNA	Ribose Nucleic Acid
RT	Room Temperature
SAR	Structure Activity Relationship
SH-SY5Y	Neuroblastoma Cells
SO ₃ .Py	Sulfurtrioxide Pyridine Complex
TBA-OH	<i>tert</i> -butylammonium Hydroxide
TBDPS	<i>tert</i> -butyldiphenylsilyl
TBDPS-Cl	<i>tert</i> -butyldiphenylsilyl chloride
TBME	<i>tert</i> -butylmethyl ether

<i>t</i> -BOC	Di- <i>tert</i> -butyl dicarbonate
TBS	<i>Tert</i> -butyldimethylsilyl
TBS-Cl	<i>Tert</i> -butyldimethylsilyl Chloride
THF	Tetrahydrofuran
TLC	Thin Layer Chromatography
TMSOTf	Trimethylsilyl trimethanesulfonate
TMV	Tobacco mosaic virus
Tr	Trityl
TrCl	Trityl chloride
VZV	Varicella zoster virus
XTT	2,3-bis-(2-methoxy-4-nitro-5-sulfophenyl)-2 <i>H</i> -tetrazolium-5-carboxanilide
μwave	Microwave

List of Figures

	Page
Figure 1.1: Viral genome (DNA or RNA) 1 , capsid 2 , viral envelope 3 , viral glycoproteins 4 , host cell receptors 5 , host cell membrane 6 , virus binds 7 , endocytosis 8 , virus released from endosome in pH dependent manner 9 , virus uncoats 10 , genome replicated 11 , viral protein synthesis at ribosomes 12 , viral assembly 13 , exocytosis of mature virions 14 .	3
Figure 1.2: First generation IIs DKAs tetrazole 1 and acid 2	5
Figure 1.3: Raltagevir 3	6
Figure 1.4: Fusion inhibitors and co-receptor antagonists Arbidol, Neu5Ac2en and Zanamivir	7
Figure 1.5: Telaprevir 7 and Boceprevir 8	8
Figure 1.6: In the HCV protease active site, histadine and serine make up the catalytic core of the enzyme and cleaves the C-N bond.	9
Figure 1.7: Mechanism of action of boceprevir ketoamide in NS3 HCV protease	9
Figure 1.8: Binding interactions of boceprevir	10
Figure 1.9: Saquinavir, an aspartly protease inhibitor for HIV-1	10
Figure 1.10: NNRTIs used to treat HIV infections: Etravirine 10	11
Figure 1.11: HCV-796 11 non-nucleoside replicase inhibitor	12
Figure 1.12: Obligate and non-obligate chain terminators prevent DNA or RNA chain growth by preventing direct bonding between nucleotides, or steric and electronic effects prevent elongation of the DNA or RNA strands.	13
Figure 1.13: Example of an obligate and non-obligate chain terminating DAA. Elvucitabine an anti-HIV obligate chain terminator and 2'-C-methylcytidine an anti-HCV non-obligate chain terminator.	14
Figure 1.14: Current reverse transcriptase inhibitors in clinical use. All lack the 3'-OH group necessary for genome replication. Without this group, chain extension is not possible. 14: Zidovudine (AZT) 15: Didanosine 16: Zalcitabine 17: Stavudine 18: Lamivudine 19: Abacavir 20: Tenofovir diisoproxil fumarate	15
Figure 1.14: 2'-modified ribonucleosides including base modifications	16
Figure 1.15: The phosphorylation steps of the three kinases to the active triphosphate using Zidovudine 14 as an example. Kinase 1 creates the nucleotide monophosphate (NMP) 30 , kinase 2 creates the nucleoside diphosphate (NDP) 32 and kinase 3 creates NTP 33 . As shown, the NMP can be enzymatically cleaved to an inactive form.	20
Figure 1.16: Phosphoramidate prodrugs of NM107 21	22
Figure 1.17: PSI7851 and PSI7977 (Sofosbuvir)	22
Figure 1.18: Guanosine based phosphoramidates	23

Figure 1.19: Chemical hydrolysis of Meier pronucleotides	24
Figure 1.20: North and south puckered nucleotides	25
Figure 1.21: Typical C-2 Spironucleoside active against HCV infection	26
Figure 2.1: North and south puckered nucleotides 44 and 45	33
Figure 2.2: Conformations of oxetane	34
Figure 2.3: Target compounds	45
Figure 2.4: ^1H NMR spectrum of isopropylidene dibromide 93	47
Figure 2.5: ^1H NMR spectrum of isopropylidene thietane 94	48
Figure 2.6: ^1H NMR spectrum of sulfoxide 65	50
Figure 2.7: Sulfoxide 65 coupling patterns. Ha/Hb are conformationally non-equivalent to Hx/Hy	51
Figure 2.8: ^1H NMR spectrum of fluorothietane 76	55
Figure 2.9: Coupling of C-4 protons to the SCHF bond. As can be seen, the protons on C-4 occupy different environments. One proton couples to its neighbour giving rise to the doublet and the other proton couples to the proton and the fluorine on C-1 as a through bond effect	55
Figure 2.10: ^{19}F NMR of fluorothietane 76	56
Figure 2.11: Structure showing the SCH bond that was indicative of product formation	64
Figure 2.12: ^1H NMR spectrum of uracil 80	67
Figure 2.13 Mass spectrum and ^1H NMR spectroscopic data revealed two compounds present: uracil 80 and iodouracil 87	68
Figure 2.14: Candidate compounds chosen for cell viability assays	72
Figure 2.15: Cell viability data for thymine 79	74
Figure 2.16: Cell viability data for uracil 80	75
Figure 2.17: Cell viability data for DMU 89	75
Figure 2.18: Cell viability data for 5FU 84	75
Figure 3.1: Target thietane nucleosides for the 4,4-bis(hydroxymethyl) thietane core compounds	82
Figure 3.2: ^1H NMR spectrum of acetal 147 which shows both cis and trans isomers are present	92
Figure 3.3: ^1H NMR spectrum of ketone 148	99
Figure 3.4: ^1H NMR spectrum of TBS Ketone 166	102
Figure 3.5: ^1H NMR spectrum of methyl ester 167	104
Figure 3.6: ^1H NMR spectrum of acid 177 . No methyl ester protons are present at 3.6 ppm.	113
Figure 3.7: ^1H NMR spectrum of thioether 182	115

Figure 3.8: ¹ H NMR spectrum of acid 178	117
Figure 3.9: ¹ H NMR spectrum of thiol 179	118
Figure 3.10: ¹ H NMR spectrum of thietanone 180	119
Figure 3.11: Top: The IR spectrum for thiol 179 and bottom: The IR spectrum for thietanone 180	120
Figure 4.1: Thymidine and 4'-thiothymidine differ by the sulfur atom at the 4'-position	126
Figure 4.2: Action of pyrimidine nucleoside phosphorylase. No degradation was observed for the 4'-thioribose moiety.	127
Figure 4.3: Hamamelose	129
Figure 4.4: Key anti-HCV compounds	130
Figure 4.5: Hamamelose nucleosides active against HCV	130
Figure 4.6: 4'-thiohamamelose showing potential areas of chemical modification	131
Figure 4.7: Pummerer Reaction for the formation of nucleosides	133
Figure 4.8: ¹ H NMR spectrum of acetamide 200	136
Figure 4.9: ¹ H NMR spectrum of trityl moiety 201	138
Figure 4.10: ¹ H NMR spectrum of TBDPS moiety 204	147
Figure 4.11: ¹ H NMR spectrum of ribolactone 215	150
Figure 5.1: The two thietane scaffolds and the 4'-thiohamamelose scaffolds are shown. The scaffolds for the 3,3-bis(hydroxymethyl) (library 1) and 4,4-bis(hydroxymethyl)-thietane (library 2) nucleosides vary by the position of the hydroxymethyl groups. In library 1, nucleosides are varied. The biological activity of each nucleoside will give an indication of the SAR for this library. In library 2, the hydroxymethyl group position is altered. By using the same nucleobases as those in library 1, the effect of the hydroxymethyl group on the SAR can be determined. Library 3, the 4'-thiohamamelose nucleosides will also use the same nucleobases as the first two libraries, however, the SAR will determine whether 4'-thiohamamelose nucleosides have better anti-viral properties versus hamamelose nucleosides in the literature. From each library, the biological data will be used to determine the SAR with the intent of designing and synthesising more potent compounds for each scaffold	158
Figure 5.2: Thymidine and 4'-thiothymidine	164
Figure 5.3: The control compounds (left) and the target compounds (right)	165
Figure A1.1: Thymine 79 replicate 1	212
Figure A.1.2: Thymine 79 replicate 2	212
Figure A.1.3: Thymine 79 replicate 3	213
Figure A.1.4: Uracil 80 replicate 1	213
Figure A.1.5: Uracil 80 replicate 2	213

Figure A.1.6: Uracil 80 replicate 3	213
Figure A.1.7: 5FU 84 replicate 1	214
Figure A.1.8: 5FU 84 replicate 2	214
Figure A.1.9: 5FU 84 replicate 3	214
Figure A.1.10: 5,6-DMU 89 replicate 1	214
Figure A.1.11: 5,6-DMU 89 replicate 2	215
Figure A.1.12: 5,6-DMU 89 replicate 3	215

List of Schemes

	Page
Scheme 2.1: General mechanism of the Pummerer reaction	41
Scheme 2.2: Thietane core structure affects product yield	41
Scheme 2.3: Top: Pummerer rearrangement proceeds via neighbouring group participation of the –OBz group shown by 69 and 67 . The incoming nucleoside can only attack from the top face resulting in a diastereomerically pure product 68 . Bottom: Major competing reaction resulting in an unreactive intermediate that does not undergo Pummerer rearrangement	42
Scheme 2.4: Fluoro-Pummerer reaction from a sulfoxide 65	43
Scheme 2.5: Fluoro-Pummerer reaction from a sulfide 74 . Note[SbCl ₃ F] [–] liberates fluoride ions as the reaction proceeds.	43
Scheme 2.6: Mechanism of thietane nucleoside formation under Vorbrüggen conditions	44
Scheme 2.7: Conditions: i) <i>p</i> TSA, 1,2-DMP, Acetone, RT, 24 hrs, 91% ii) Na ₂ S.9H ₂ O, DMF, 110° C, 24 hrs, 94% iii) <i>p</i> TSA, MeOH, RT, 86% iv) BzCl, DMAP, DCM, RT, 24 hrs, 78% v) Deoxofluor, SbCl ₃ , DCM, RT, 86% vi) NaIO ₄ , MeOH, RT, 24 hrs, 64%	46
Scheme 2.8: Reaction mechanism of thietane formation	48
Scheme 2.9: Top: Pummerer reaction. Bottom: Vorbrüggen conditions.	49
Scheme 2.10: Pummerer reaction to thymine nucleoside	57
Scheme 2.11: General reaction scheme toward thietane nucleosides	58
Scheme 2.12: General conditions for the Vorbrüggen synthesis	59
Scheme 2.13: Synthesis of cytosine nucleoside 102	60
Scheme 2.14: Nishizono synthesis of 6-chloropurine substituted thietane 108	62
Scheme 2.15: Attempts to synthesise carbamoyl protected guanine 110	63
Scheme 2.16: Nishizono synthesis of adenine 111 using gaseous ammonia	63
Scheme 2.17: Synthesis of diBoc adenine 114	63
Scheme 2.18: General scheme for the removal of benzoate groups	65
Scheme 3.1: Retrosynthetic steps toward 4,4-bis(hydroxymethyl) thietane nucleosides	84
Scheme 3.2: Potential chemistry toward the thietane target using already established chemistry	85
Scheme 3.3: Potential side reactions that could occur by using Na ₂ S.9H ₂ O to furnish thietane 142 from compound 143	85
Scheme 3.4: Initial synthetic strategy toward 4,4-bis(hydroxymethyl) thietane nucleosides i) glycerol, <i>p</i> TSA, Toluene, 40° C, 6 hrs, 62% ii) DMP, DCM, 0° C, 4 hrs, 82% iii) NaH, methyl diethylphosphonoacetate, THF, RT, overnight, 61%	86

Scheme 3.5: Givaudan synthesis of 4-methyl-thietan-2-ol using crotonaldehyde and H ₂ S	87
Scheme 3.6: Application of the Givaudan synthesis to methyl ester 149 to give target thietane 153 i) DIBAL-H, THF, -78° C, 3 hrs ii) H ₂ S, Et ₃ N, -10° C, 6 hrs	88
Scheme 3.7: Pattenden synthesis of thietanone compounds i) BnSH, piperidine, reflux, 24 hrs ii) Na, NH ₃ , -78° C, 2 hrs iii) Isobutyl chloroformate, Et ₃ N, DCM, -10° C, 20 mins	88
Scheme 3.8: Proposed conditions to methyl ester 149 i) NaOH or LiOH, IPA, water ii) Na, NH ₃ , -78° C, 2 hrs iii) Isobutyl chloroformate, Et ₃ N, DCM, -10° C, 20 mins iv) DIBAL-H, THF, -78° C, 3 hrs.	89
Scheme 3.9: Proposed condition: (this chemistry was established in chapter 2 i) deoxofluor, SbCl ₃ , DCM, RT, 24 hrs ii) silylated nucleobase, AgClO ₄ , SnCl ₂	89
Scheme 3.10: General synthesis of acetal 147 using either benzaldehyde or BDMA to furnish acetal 147	90
Scheme 3.11: Optimised reaction conditions for the oxidation of acetal 147 to ketone 148 using DMP	93
Scheme 3.12: Oxidation reaction using DMP	95
Scheme 3.13: Optimised reaction conditions for the Swern oxidation reaction toward ketone 148	96
Scheme 3.14: Parikh-Doering oxidation	97
Scheme 3.15: Proposed synthetic strategy toward 4,4-bis(hydroxymethyl)-thietane nucleosides i) TBS-Cl, imidazole, DCM, RT ii) NaH, Methyl diethylphosphonoacetate, THF, RT iii) DIBAL-H, THF, -78° C iv) H ₂ S, Et ₃ N, -10° C v) BnBr, DMF, RT vi) nBu ₄ NF, THF vii) BzCl, Et ₃ N, DMAP, DCM, RT viii) H ₂ Pd/C, MeOH ix) Deoxofluor, SbCl ₃ , DCM, RT x) silylated nucleobase AgClO ₄ , SnCl ₂ various solvents and conditions (see chapter 2) xi) NaOMe, MeOH, RT	100
Scheme 3.16: Proposed synthetic steps to the allyl aldehyde: i) TBS-Cl, imidazole, DCM, RT, 18 hrs, quantitative yield ii) NaH, Methyl diethylphosphonoacetate, THF, 1 hr then ketone 167 , RT, overnight, 61% iii) DIBAL-H, THF -78° C product not observed, however, compound 181 was (see text) isolated	101
Scheme 3.17: Modification of the Pattenden synthetic steps toward thietanes: i) LiOH or NaOH ii) BnSH, piperidine, 116° C iii) Na/NH ₃ , THF, -78° C iv) Isobutyl chloroformate, Et ₃ N, DCM, -10° C	101
Scheme 3.18: Synthetic scheme and reaction mechanism toward methyl ester 167	103
Scheme 3.19: DIBAL-H reduction of methyl ester 167 did not give aldehyde 168 , but instead gave allyl alcohol 181 i) DIBAL-H, THF, -78° C, 80% for 181 .	105
Scheme 3.20: i) Benzyl mercaptan, piperidine, reflux, 24 hrs, quant ii) Na, NH ₃ , THF, -78° C, quant iii) Isobutyl chloroformate, Et ₃ N, DCM, -10° C, 20 minutes	106
Scheme 3.21: Modification of the synthetic route toward the target thietane i) LiOH or NaOH, various solvents, ii) BnSH, piperidine, 116° C, overnight iii) Na/NH ₃ , THF, -78° C 2-	108

3 hrs iv) isobutyl chloroformate, Et ₃ N, DCM, -10° C, 1-2 hrs	
Scheme 3.22: General hydrolysis reaction of methyl ester 167 with mineral bases	108
Scheme 3.23: Suspected hydrolysis reaction at the TBS group.	110
Scheme 3.24: Optimised reaction conditions toward acid 177 i) 8 equivalents of Me ₃ SnOH, 1,2-DCE, 80° C, 96 hrs, 93% yield	112
Scheme 3.25: Attempts to synthesis thioether 178 from acid 177 i) 1.1 equiv BnSH, piperidine (base and solvent), 116° C, 48 hrs no reaction	113
Scheme 3.26: Synthesis of thioether 182 i) 1.1 equiv BnSH in piperidine, heating to reflux over 24 hours.	114
Scheme 3.27: General hydrolysis reaction toward acid 178	116
Scheme 3.28: Ester hydrolysis using trimethyltin hydroxide	117
Scheme 3.29: The synthesis of thiol 179 using sodium in liquid ammonia	118
Scheme 3.30: Synthesis of thietanone 180 i) isobutylchloroformate, triethylamine, DCM, -10° C, 4 hours, 37%	119
Scheme 3.31: Top: Aldehyde method which requires additional protecting group chemistry and bottom: Optimised route toward thietanone 180 which was achieved after significant optimisation of the each step i) TBS-Cl, imidazole, DCM, RT, 24 hrs, quant ii) Methyl diethylphosphonoacetate, THF, NaH, RT, 24 hrs, 61% iii) BnSH, piperidine, 116° C, 24 hrs, 82% iv) 8 equiv Me ₃ SnOH, 1,2-DCE, 80° C, 96 hrs, 88% v) Na, NH ₃ , THF, -78° C, 2 – 3 hrs, 93% vi) Isobutylchloroformate, Et ₃ N, DCM, -10° C, 37% vii) nBu ₄ NF, THF viii) BzCl, DMAP, Et ₃ N, DCM, RT ix) NaBH ₄ , THF x) Deoxofluor, SbCl ₃ , DCM, RT xi) silylated nucleobase, AgClO ₄ , SnCl ₂ various solvents and temperatures (see chapter 2) xii) NaOMe, MeOH, RT	122
Scheme 4.1: Proposed synthetic steps to 4'-thiohamamelose nucleosides i) Acetone, H ₂ SO ₄ RT 3 hrs ii) TrCl, Pyridine, RT, 20 hrs iii) Formaldehyde, Methanol, K ₂ CO ₃ , 70° C, 20 hrs iv) Br ₂ , K ₂ CO ₃ , DCM, RT, 3 hrs v) TBDPS-Cl, Imidazole, DCM, RT, 12 hrs vi) NaOH, Me ₂ SO ₄ , DMSO, RT, 3 hrs vii) PPh ₃ , Imidazole, I ₂ , DCM, 120°C, 6 hrs viii) AcSH, TBA-OH, toluene, RT, 18 hrs ix) DIBAL-H, toluene, 2 hrs x) CBr ₄ , PPh ₃ , DCM, -25° C, 1 hr xi) AgOTf, 135°C, μ wave, DCE/MeCN, 30 mins	133
Scheme 4.2: Large scale synthesis of acetonide 200 using acetone and sulfuric acid	136
Scheme 4.3: Synthesis of trityl moiety 201 i) trityl chloride, pyridine, RT, 48 hrs, 82%	137
Scheme 4.4: Synthesis of hamamelose 202 i) formaldehyde, methanol, K ₂ CO ₃ , 66° C, 97% (crude yield)	139
Scheme 4.5: Synthesis of hamamelose by Ho <i>et al</i>	139
Scheme 4.6: Synthesis of hamamelolactone 203	143
Scheme 4.7: Synthesis of ribolactone 215 . 1 equivalent bromine 1.1 equivalent K ₂ CO ₃ in water, 98%	143

Scheme 4.8: Optimisation of the bromine oxidation reaction toward ribolactone 216 from trityl ribose 201 . 1 equivalent of bromine, 1.5 equivalents of K ₂ CO ₃ in DCM	144
Scheme 4.9: Synthesis of hamamelolactone 204 i) TBDPS-Cl, imidazole, DCM, RT, 24 hrs, 44% crude product	146
Scheme 4.10: Proposed synthetic steps toward 4'-thiohamamelose 208 i) NaOH, Me ₂ SO ₄ , DMSO, RT, 3 hrs ii) PPh ₃ , Imidazole, I ₂ , DCM, 120°C, 6 hrs iii) AcSH, TBA-OH, toluene, RT, 18 hrs iv) DIBAL-H, toluene, 2 hrs	148
Scheme 4.11: Model hydrolysis reaction toward acid 217 using NaOH	148
Scheme 5.1: General synthetic scheme to target nucleosides from fluorothietane 76 i) silylated nucleobase, AgClO ₄ , SnCl ₂ , DCM, RT, 18 hrs, 57% ii) MeNH ₂ , EtOH, RT, 2 hrs, 98%	159
Scheme 5.2: Proposed synthesis of 4,4-bis(hydroxymethyl)-thietan-2-yl nucleosides i) nBu ₄ NF, THF ii) BzCl, DMAP, Et ₃ N, DCM, RT iii) NaBH ₄ , THF iv) Deoxofluor, SbCl ₃ , DCM, RT v) silylated nucleobase, AgClO ₄ , SnCl ₂ various solvents and temperatures (see chapter 2) vi) NaOMe, MeOH, RT	161
Scheme 5.3 Proposed synthetic method toward 4'-thiohamamelose nucleosides i) NaOH, Me ₂ SO ₄ ii) PPh ₃ , Imidazole, I ₂ , DCM, 120°C, 6 hrs iii) AcSH, TBA-OH, toluene, RT, 18 hrs iv) DIBAL-H, toluene, 2 hrs v) CBr ₄ , PPh ₃ , DCM, -25° C, 1 hr vi) AgOTf, 135°C, μ wave, DCE/MeCN, 30 mins	162
Scheme 5.4: Synthetic strategy for the conversion of the 2'-C-methylhydroxy group to the fluoromethyl group: i) nBu ₄ NF, THF, ii) Deoxofluor, SbCl ₃ , DCM	163
Scheme 5.5: Conversion of the 2'-OH group to the 2'-Fluoro group first requires removal of the acetonide and formation of the benzylidene acetal. The 2'-OH group is converted to a leaving group (LG= Mesylate or tosylate or equivalent) and then deoxofluor is used to add the fluoride in an S _N 1 fashion: i) H ⁺ eg pTSA ii) Benzaldehyde dimethyl acetal then a Mesylate or tosylate added iii) Deoxofluor, SbCl ₃ , DCM	163
Scheme 5.6: Conversion of the 3'-OH group to the fluoride requires removal of the acetonide and re-protection of the trityl group. Since the 3'-OH is a secondary hydroxide, the reaction mechanism of deoxofluor allows displacement by the S _N 2 mechanism. The tertiary hydroxyl group will not react readily: i) pTSA ii) TrCl, pyridine iii) deoxofluor SbCl ₃	163

List of Tables

	Page
Table 1.1: Biological data for 2'- α -fluoro compounds	16
Table 2.1: Anti-viral activity of oxetane nucleosides	35
Table 2.2: Thietane nucleosides active against HIV	37
Table 2.3: Optimisation reactions to glycosyl fluoride 76 . Effect of catalyst	53
Table 2.4: Effect of increased reaction time on yield of fluoride 76	54
Table 2.5: Pummerer reaction conditions	57
Table 2.6: Thietane nucleosides synthesised using Vorbrüggen conditions	61
Table 2.7: Free hydroxyl thietane nucleosides with key data. Reaction conditions: a = NaOMe in MeOH, RT, 24 hrs b = MeNH ₂ in EtOH, RT, 2 hrs	66
Table 2.8: Key ¹ H NMR spectra for the thietane ring in thietane nucleosides. The ppm values are given first, followed by the signal type (s – singlet, d – doublet, t – triplet etc). The number of protons per signal is 1 proton as all the protons on the ring are non-equivalent.	69
Table 3.1: Reaction conditions attempted for the synthesis of acetal 147	90
Table 3.2: Key ¹ H NMR spectroscopic data for both acetal 147 and the 5 membered ring acetal. The bold protons are the protons of interest and uses acetal 147 as the reference compound. (d) doublet, (s) singlet, (m) multiplet (t) triplet (q) quartet	92
Table 3.3: Optimised reaction conditions using DMP toward the synthesis of ketone 148	94
Table 3.4: Parikh-Doering Reaction toward the synthesis of ketone 148	97
Table 3.5: Comparisons between the ¹ H NMR spectra of hydroxyl acetal 147 and keto acetal 148	98
Table 3.6: Optimisation of reaction conditions toward methyl ester 167	103
Table 3.7: Optimisation of the DIBAL-H reduction reaction of methyl ester 167 to allyl alcohol 181 . All reactions performed at -78° C in anhydrous THF	105
Table 3.8: Mineral base hydrolysis of methyl ester 167 to acid 177	108
Table 3.9: Hydrolysis reactions with KOSiMe ₃	110
Table 4.1: Known 4'-thioribose nucleosides (only active nucleosides have been shown with compounds 186 and 187 shown as the ribose counterparts with their associated activity)	127
Table 4.2: Variations to sugar ring groups for assessment of SAR in 4'-thiohamamelose nucleosides	132
Table 4.3: Comparison of yields between the pTSA method and the sulfuric acid method	135
Table 4.4: Optimisation reactions for the protection of the 5'-OH group using trityl chloride	137

Table 4.5: Formylation reaction conditions	139
Table 4.6: Optimisation of the formylation reaction towards 5'-O-trityl-hamamelose	141
Table 4.7: Optimisation of the bromine oxidation reaction in DCM shown in scheme 4.8	144
Table 4.8: Optimisation of the bromine oxidation toward 5'-O-tritylhamamelolactone 203 shown in scheme 4.8	145
Table 4.9: Attempted optimisation for the model hydrolysis reactions	149
Table 5.1: cLog P data for thietane nucleosides compared to known nucleosides	167
Table 5.2: Calculated log P values for 3,3-, 4,4-bis(hydroxymethyl)-thietan-2-yl, 4'-thiohamamelose nucleosides, and the phosphoramidate derivatives	168
Table A.1.1: Raw data for thymine 76	210
Table A.1.2: Raw data for uracil 77	210
Table A.1.3: Raw data for 5FU 81	211
Table A.1.4: Raw data for 5,6-DMU 86	211

Chapter 1:

Introduction

Chapter 1: Introduction

The emergence of severe viral infections coupled with the limited availability of anti-viral agents is a common cause of human illness and death.¹ Of these viral infections, the most severe infections are due to the human immunodeficiency virus (HIV) which infects 28.1-31.7 million people worldwide with 1.3-1.5 million deaths and 1.7-2.1 million new infections per year; and the hepatitis C virus (HCV) which infects 180 million people with 3 – 4 million new cases a year of which 80% of the patients develop a chronic infection that leads to death.²⁻⁵ Although these are the most severe viral infections, there are many other viruses that can cause illness in humans such the influenza virus, the common cold virus, herpes simplex virus (HSV), HIV, varicella zoster virus (VZV), hepatitis B (HBV), HCV and cytomegalovirus (CMV) and the Epstein-Barr virus (EBV) to name a few. New anti-viral agents are needed because viruses are able to replicate quickly and evolve resistance to any anti-viral agents that are used as treatments. The problems of long term toxicity and poor bioavailability of these drugs is also a major concern that requires further investigation into new anti-viral agents.^{1,6}

1.1 Lifecycle of Viruses

The first identified virus was the tobacco mosaic virus (TMV), discovered in 1898 by Martinus Beijerinck. Since then over 5000 types of viruses have been found in almost every ecosystem on Earth and are the smallest known infectious agents.^{1,7-10} There are two broad classifications of viruses: those that contain deoxyribonucleic acid (DNA) in their core and those that contain ribonucleic acid (RNA) in their core. These are termed DNA-viruses and RNA-viruses respectively. These entities are unable to reproduce on their own, and hence require a host cell process to propagate.^{1,7-10} A typical viral lifecycle is shown in figure 1.1.

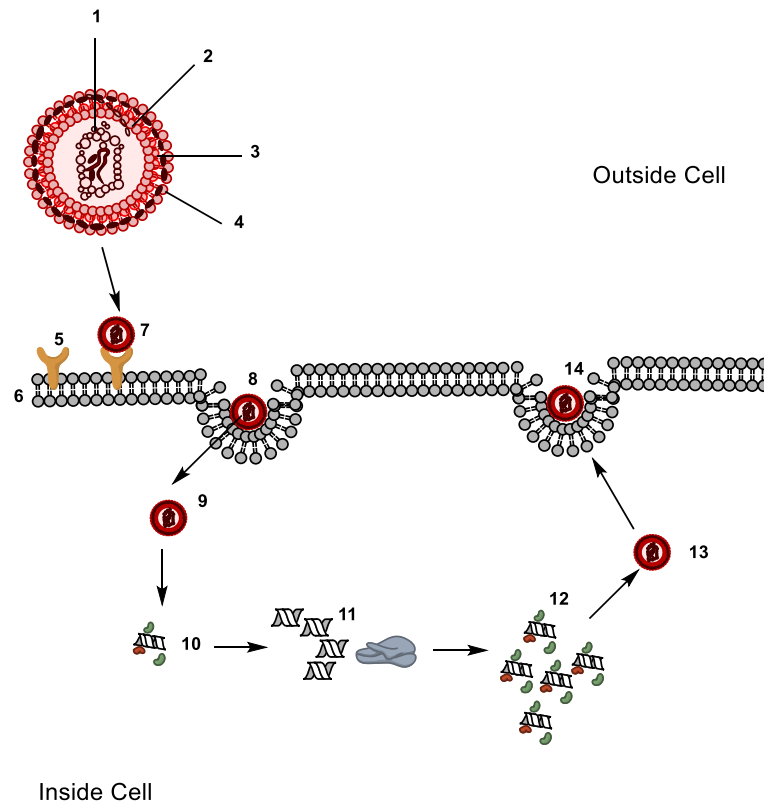


Figure 1.1: Viral genome (DNA or RNA) 1, capsid 2, viral envelope 3, viral glycoproteins 4, host cell receptors 5, host cell membrane 6, virus binds 7, endocytosis 8, virus released from endosome in pH dependent manner 9, virus uncoats 10, genome replicated 11, viral protein synthesis at ribosomes 12, viral assembly 13, exocytosis of mature virions 14.

Viral infections typically eventually kill the host cell. This is due to alterations to host cell metabolism, alterations to the host cell membrane (that usually contain a viral proteins that upon exocytosis, become the new viral envelope) and cell lysis.^{1,11}

By understanding the viral lifecycle there are several potential drug targets that can be exploited to stop infection. Historically, drug targets of interest have been fusion inhibitors, co-receptor antagonists, integrase inhibitors, protease inhibitors, and transcriptase and replicase inhibitors. Each class has shown activity to varying degrees of success.^{11,12} The most important classes of anti-viral drugs are protease inhibitors which prevent the formation of mature viral proteins from the polyprotein precursors; and directly acting anti-viral agents (DAA) nucleosides which act as anti-metabolites to prevent elongation of the viral genome during replication.⁶ These nucleosides are mutagenic, causing error catastrophe at such a rate that they are able to obliterate an entire viral population by preventing genome replication, and hence are the most important class of anti-viral agent available.¹³ However, due to

the speed at which viruses are able to evolve, even when combination therapies of protease inhibitors and DAAs are used, there is an urgent and on-going need for new DAAs.

1.2 Types of Antiviral Agents

There are several classes of antiviral agents available to treat viral infections. Each class acts on a specific part of the viral lifecycle, from preventing binding and fusion (see 7 in figure 1.1), to preventing viral replication (see section 11 in figure 1.1). Each class of antiviral agent will be critically evaluated in the proceeding sections with key developments discussed. Research over the past 30 years has shown that the best methods to treat viral infections use combination therapy of a replicase/transcriptase inhibitor and a protease inhibitor. These drugs act early in the viral lifecycle to prevent an increase in viral load, and in the case of HCV infection, a complete cure. Combination therapy has also been shown to significantly reduce the chance of viral resistance from evolving. This is because the chance of evolving more than one resistance trait to multiple targets is unlikely.

1.2.1 Interferons

Interferons (IFNs) are a class of proteins known as cytokines that are excreted from cells that protects against viral infections.¹⁴ IFNs activate the host immune system via signal transduction by binding to immune receptors, though the mechanism of action is not fully understood.^{11,14} IFNs have broad activity against many cancers and viral infections, including HIV, HCV and HBV.^{11,14,15}

IFN is used in combination with other anti-viral drugs, and is administered via injection. Monotherapy of interferon is associated with a high rate of relapse that necessitates retreatment, which is invariably unsuccessful for patients with HCV infection.¹⁵ Recent advances in anti-viral therapies have occurred because IFN has serious side effects, especially when used in combination with other drugs. Interferon free therapies offer the best patient outcomes as the side effects of these new regimens are not as serious. IFN has been associated with side effects such as influenza like symptoms, depression, fatigue and fever.^{14,15}

IFN activates the immune system but does not prevent the viral infection from spreading. Targeting the virus directly, whether it be by preventing viral replication, preventing binding, or preventing the maturation of the viral polyproteins, are far better methods to combat infection.^{14,17}

1.2.2 Inhibitors

Inhibitors are chemical compounds that block receptors, proteins or enzyme function, and therefore prevent a biological function from occurring. Inhibitors as anti-viral agents are the broadest class of drug as there are several important targets. Inhibitors can target every stage in the life-cycle of the virus, from preventing the virus from binding to a receptor prior to viral attachment, to preventing viral replication (see figure 1.1). In the proceeding sections, the main classes of inhibitors and the key challenges and discoveries are discussed.

1.2.2.1 Integrase Strand Inhibitors

Integrase inhibitors (IIs) are a class of anti-viral agent targeting HIV-1 infection. They prevent the integration of viral DNA into the host cell chromosomes which is achieved by integrase enzymes, thereby preventing viral replication.¹⁶⁻¹⁸ Integrase are essential for viral replication and the absence of a host cell equivalent means that there are potentially less off target side effects.¹⁶ The most common class of IIs are diketo aryl and diketo aryl like inhibitors (DKAs).^{16,18} Shown in figure 1.2 are two of the first generation IIs discovered.^{16,19}

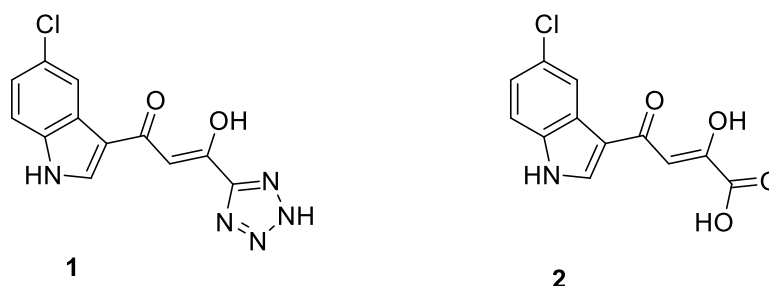


Figure 1.2: First generation IIs DKAs tetrazole 1 and acid 2

Divalent metal cofactors such as Mg^{2+} and Mn^{2+} are important for DKA activity. The tetrazole moiety in figure 1.2 was found to have poor binding affinity to Mg^{2+} ions and hence exhibited lower than expected activity.^{16,18,19} Extensive analysis of structure-

activity relationships (SAR) led to the discovery that replacement of the tetrazole moiety with a carboxylate derivative increased binding affinity to Mg^{2+} and hence, increased activity of the DKAs.^{16,17,19,20}

SAR found that although the carboxylate was important for activity, it was not important for binding to the enzyme. However, the aromatic groups were found to be essential for potency, and the binding site tolerated a wide range of functionalisations on the aromatic rings.^{16,19} Since the carboxylate was not essential for binding, research carried on until the discovery of Raltagevir **3** (figure 1.3).¹⁹

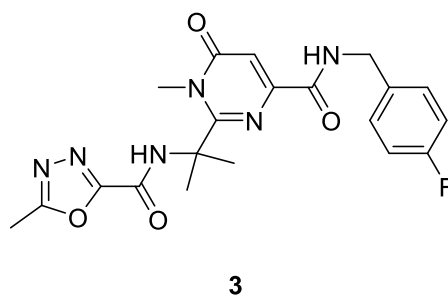


Figure 1.3: Raltagevir **3**

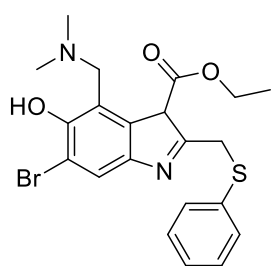
Although integrase strand inhibitors are excellent inhibitors of genome replication, resistance to DKA IIs has arisen quickly. Mutations coding for the integrase enzymes show that 6 amino acids have changed at the binding site to prevent DKAs from binding.^{20,21} Some of the amino acid mutations reduce the affinity of the integrase enzyme for Mg^{2+} .^{20,21} Since the metal cofactor is essential for DKA binding, this reduced affinity for the cofactor reduces the activity of DKA based drugs. Also, changes to the binding site amino acids changes the binding interactions and also reduce the binding interactions between the DKAs and the enzyme active site.^{16,19-21}

Though resistance of the integrase enzyme towards DKA based drugs is an issue, IIs also inhibit recombinases, RNAses, and other integrases. Therefore they are not selective for HIV-1 integrases. Since integration of the viral genome into the host genome is a multistep process, viral resistance can evolve to bypass IIs. A key problem with IIs is that they are required to act early in the viral lifecycle to prevent the viral genome being incorporated into the host genome. This means that late stage infections cannot be treated with IIs alone and require the use of other drugs in

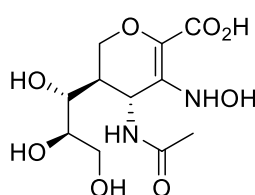
combination with them. Therefore, IIs cannot prevent replication of the viral genome directly, and so, act indirectly, limiting their utility.

1.2.2.2 Fusion Inhibitors/Co-receptor antagonists

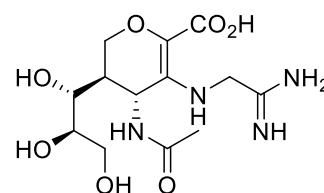
Fusion inhibitors and co-receptor antagonists prevent viruses from binding to host cell membranes. Either the compound blocks receptors on the host cell, or the compound blocks receptors on the viral envelope. In figure 1.4, three compounds are shown: Arbidol **4** a fusion inhibitor for influenza A and B, and Neu5Ac2en **5** and Zanamivir **6**, the co-receptor antagonists for the same indication.²²⁻²⁴



4
Arbidol



5
Neu5Ac2en



6
Zanamivir

Figure 1.4: Fusion inhibitors and co-receptor antagonists Arbidol, Neu5Ac2en and Zanamivir

Arbidol **4** is a fusion inhibitor that intercalates the host cell and prevents the virus from binding. It also occupies the viral receptors on the viral envelope disrupting the ability of the virus to bind to the host cell.²² Neu5Ac2en **5** and Zanamivir **6** are both co-receptor antagonists that mimic neuraminic acid. In influenza, the neuraminidase enzyme cleaves neuraminic acid residues in the mucin to allow the virus to bind to the host cells. Neuraminic acid inhibitors such as Zanamivir act as a competitive substrate for the viral enzyme and thus prevent viral binding by mimicking the host cell neuraminic acid residues.^{23,24} A major issue with both classes of these drugs is a result of their high specificity, which allows viral resistance to evolve rapidly.²²

In the case of the neuraminidase inhibitors, although they prevent the virus binding to the host cell, they cannot prevent initial infection unless given prophylactically. The initial stages of influenza are asymptomatic, therefore drugs administered after the initial infection will only reduce the duration of infection by 1-4 days.²⁴ Prophylactic administration of the drugs has been shown to reduce infections between people in close quarters by 70 – 90%. However, these drugs are unable to halt viral replication

directly which means the initial infection persists. Also, due to the high specificity of these drugs, resistance evolves very quickly.^{23,24}

1.2.2.3 Protease Inhibitors

Protease inhibitors (PIs) are an important class of anti-viral agent that inhibit the cleavage of viral polyproteins into mature viral proteins before the virion is assembled. Typically when the viral genome is replicated, the genome is translated into a viral polyprotein which is cleaved by host cell or viral proteases. The cleavage of the viral polyprotein into mature proteins happens before viral assembly. Inhibition of viral proteases therefore prevents assembly of the mature virion.^{7-11,25} In figure 1.5 boceprevir **8** and telaprevir **7** are shown, and both of these drugs are HCV protease inhibitors. PIs were first developed to counter HIV-1 infection.²⁶

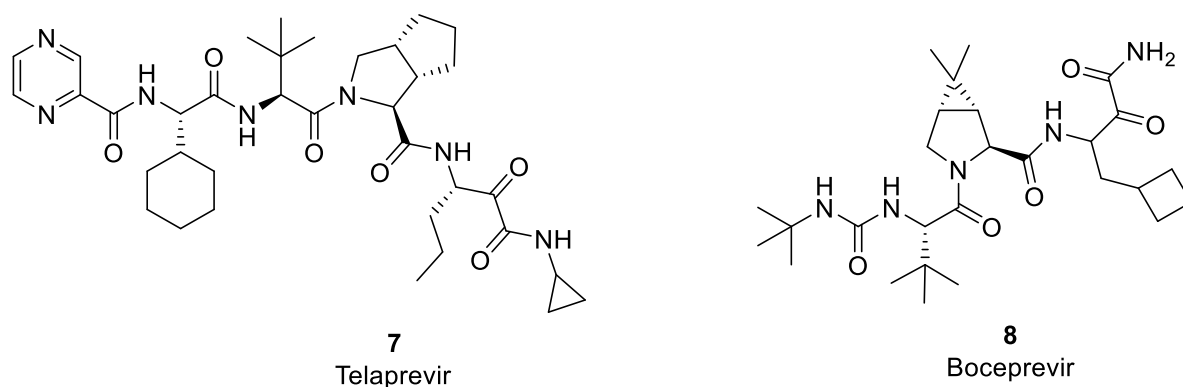


Figure 1.5: Telaprevir **7** and Boceprevir **8**

Telaprevir **7** and Boceprevir **8** are both NS3 PIs termed linear peptidomimetic ketoamide serine protease inhibitors and their mechanism of action is shown in figure 1.6.²⁷⁻²⁹

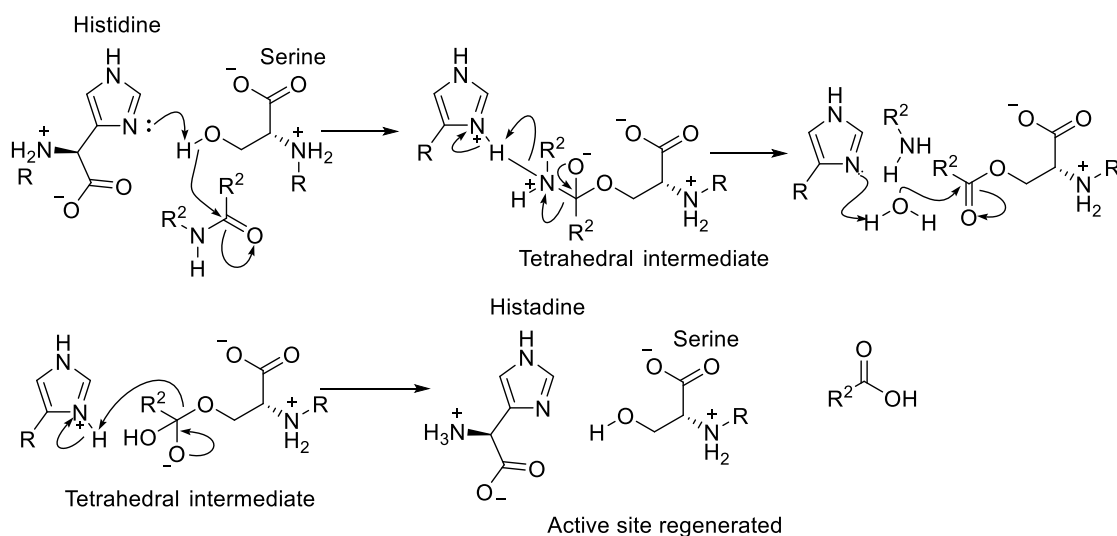


Figure 1.6: In the HCV protease active site, histidine and serine make up the catalytic core of the enzyme and cleaves the C-N bond.

In the NS3 active site, the incoming peptide is attacked by the serine residue at the carbonyl end which forms a tetrahedral intermediate. The histidine residue binds to the proton on the amine end which withdraws electron density from the C-N bond so that when the C=O bond is reformed, the C-N bond breaks. Water then enters the active site which reacts with the serine residue which forms another tetrahedral intermediate that acts as a leaving group to reform the catalytic core. Boceprevir uses a ketoamide to trap the catalytic serine residue, binding to it covalently (figure 1.7). The tetrahedral intermediate of boceprevir is stable however the reaction is reversible.²⁹

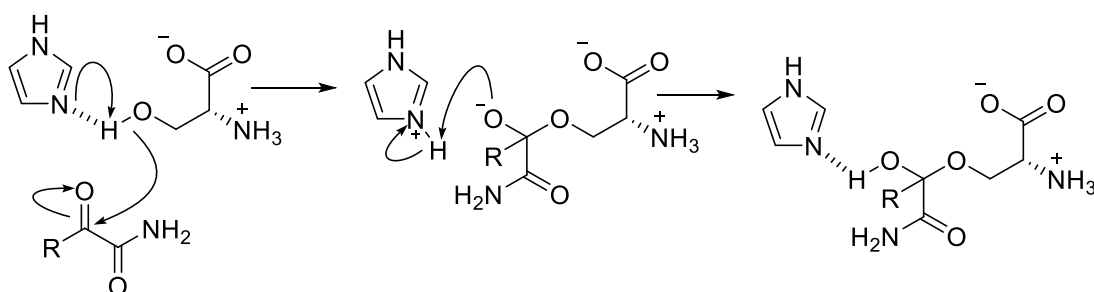


Figure 1.7: Mechanism of action of boceprevir ketoamide in NS3 HCV protease.

X ray diffraction data of boceprevir in the active site of the NS3 protease shows that it is covalently bound to the serine residue (figure 1.8).²⁹ This is consistent with the mechanism of action expected for the drug. In all PIs, the mechanism of action is similar.²⁹

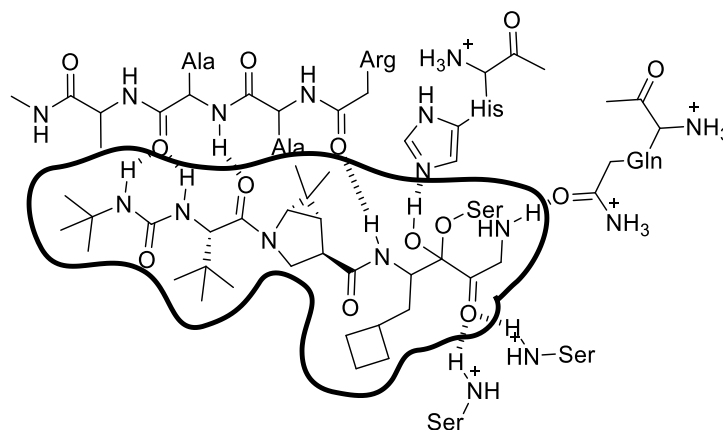


Figure 1.8: Binding interactions of boceprevir

In HCV, the protease is a serine protease and thus, boceprevir and telaprevir are serine protease inhibitors. In retroviruses such as HIV-1, the protease is an aspartyl protease.³⁰ The mechanism of action is similar serine and aspartyl proteases, with the nucleophilic attack occurring via the carboxylate in aspartic acid and the alcohol in serine. In figure 1.9, saquinavir, an aspartyl protease inhibitor for HIV-1 is shown.³⁰

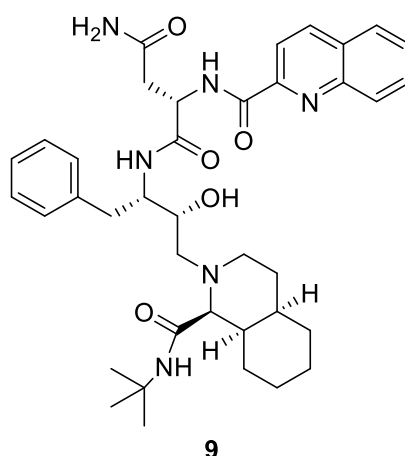


Figure 1.9: Saquinavir, an aspartyl protease inhibitor for HIV-1

In both serine and aspartyl proteases, the bound drug blocks the active site of the protease preventing cleavage of the viral polyprotein into the active mature proteins,

and thus prevents viral assembly in both HIV and HCV. However, because protease inhibitors are highly specific, they must be used in combination with other drugs as viral resistance to proteases evolves quickly.^{28,29} Protease inhibitors act indirectly to prevent viral replication, and as such, do not inhibit viral polymerases that allow for viral genome replication. Therefore, monotherapy with PIs is avoided.

1.2.2.4 Non-nucleoside Inhibitors

Non-nucleoside inhibitors bind to allosteric sites on viral polymerases.^{4,31} Two classes of these drugs exist: non-nucleoside reverse transcriptase inhibitors (NNRTI's) and non-nucleoside replicase inhibitors (NNRIs). The NNRTIs are active against HIV and the NNRIs are active against HCV.¹¹

1.2.2.4.1 Non-nucleoside Reverse Transcriptase Inhibitors

NNRTIs interact with allosteric sites on HIV reverse transcriptase that change the morphology of the binding site.¹¹ This change in morphology inhibits genome replication, therefore NNRTI's are an important class of drug. However, rapid resistance evolves against this class of drug and therefore they are used in combination therapy with DAAs. The use of combination therapy reduces the incidence of resistance from evolving.¹¹ Figure 1.10 shows a typical NNRTI used to treat HIV infection.¹¹

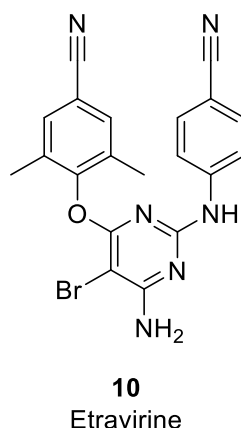


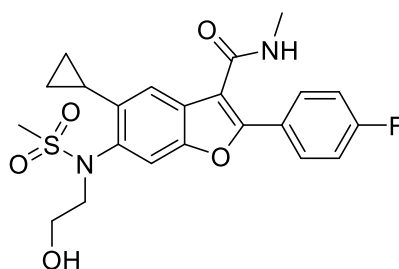
Figure 1.10: NNRTIs used to treat HIV infections: Etravirine **10**

These drugs bind to allosteric binding sites that affect the shape of the active site, preventing the natural substrate from binding. This then prevents the enzyme from functioning. Etravirine **10** (figure 1.10) has also been shown to block RNase H

function, preventing the reverse transcriptase enzyme from implanting viral DNA into the host DNA. This means that the viral genome cannot be replicated.¹¹

1.2.2.4.2 Non-nucleoside Replicase Inhibitors

NNRIs target the HCV NS5B polymerase, which has several allosteric binding sites. This has led to a significant number of different classes of NNRIs being developed.¹¹ However, despite the increased number of allosteric binding sites, cross mutations and resistance are still a major problem with this class of drug.³²



11
HCV-796

Figure 1.11: HCV-796 **11** non-nucleoside replicase inhibitor

Figure 1.11 shows the non-nucleoside replicase inhibitor of HCV NS5B polymerase. HCV-796 **11** was shown to bind to the palm site subdomain of the enzyme (the others being the finger subdomain and the thumb subdomain).³¹ It was shown that the major binding interactions occurred between arginine and cysteine residues of the palm subdomain. This interaction changes the shape of the active site, reducing the enzymes ability to replicate the viral genome. Rapid viral resistance evolved to this, and other candidate compounds.^{11,31} (Reference 33 gives an overview of the palm, finger and thumb domains. See references 34 - 40 for an overview of the biology of HCV polymerases, and some other papers dealing with NNRI's).

1.2.2.5 Nucleoside Inhibitors

Nucleoside inhibitors are a class of drug that act on the viral genome and prevent viral genome replication. They are the most important class of anti-viral drugs.^{7,14,19-22} These drugs mimic endogenous nucleotides but are chemically modified to prevent binding. These classes of drugs are called directly acting antiviral agents as they bind directly to the active site of a virus's replicase complex.^{7,14,19-22} Nucleoside drugs can

be phosphate modified, sugar modified or based modified in order to increase their activity.³³ These drugs act via two mechanisms: as obligate chain terminators and non-obligate chain terminators (figure 1.12).^{7,14,19-22}

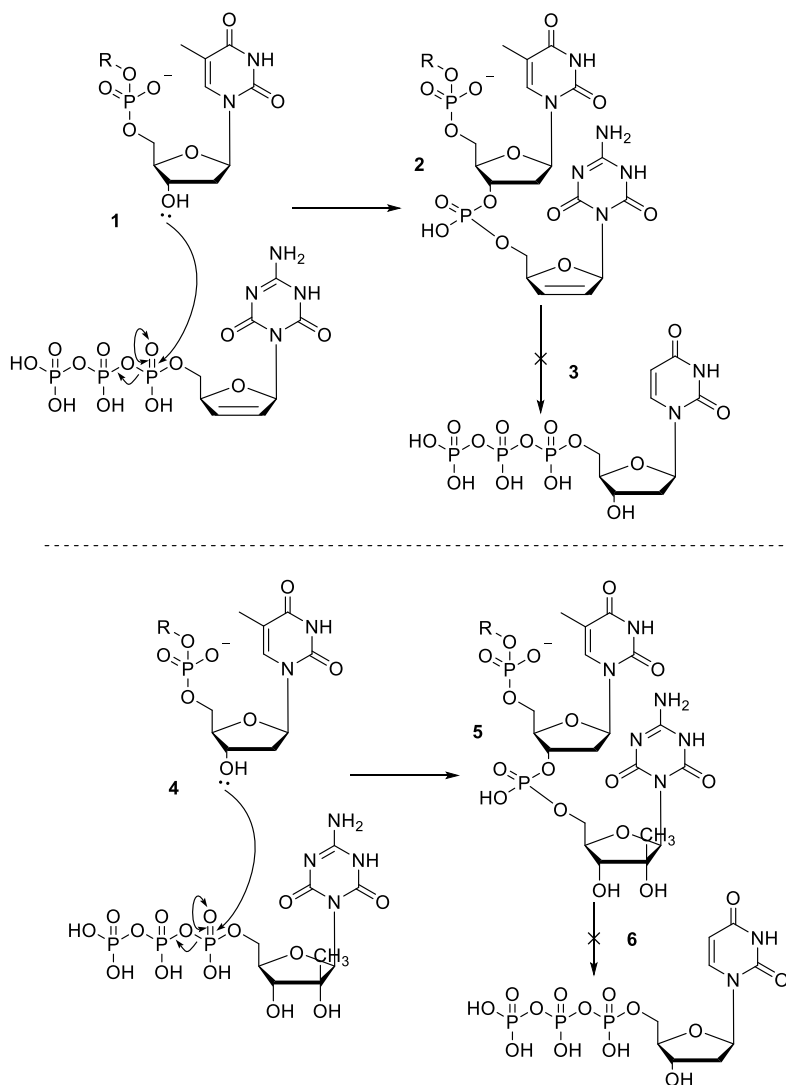


Figure 1.12: Top: obligate chain terminator. **1** the 3'-hydroxy group of the DNA or RNA bound nucleotide attacks the triphosphate of an incoming nucleotide, in this case, the drug molecule. **2** the phosphodiester bond is formed between the DNA or RNA chain and the drug molecule. **3** with no 3'-hydroxy group on the drug molecule, the incoming nucleotide cannot bind and chain elongation is halted. Bottom: non-obligate chain terminator. **4** and **5** are similar to steps **1** and **2**. In step **6** though the 3'-hydroxy group is present in the drug molecule, steric hindrance and conformational changes caused by the methyl group prevents binding of the incoming nucleotide

Obligate chain terminators (see example in figure 1.13) do not contain the 3'-OH group that is essential for the formation of the phosphodiester bonds. As such, the next incoming nucleotide is unable to react with the bound obligate chain terminator.

In non-obligate chain terminators the 3'-OH group is present, but steric and electronic effects prevent the formation of new phosphodiester bonds. The elongation of the viral genome is terminated and therefore viral replication is halted.^{6,11,34-37}

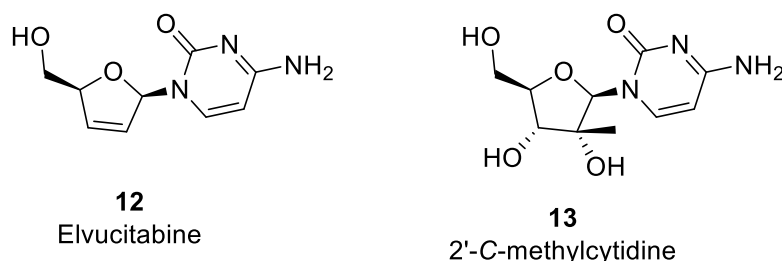


Figure 1.13: Example of an obligate and non-obligate chain terminating DAA. Elvucitabine an anti-HIV obligate chain terminator and 2'-C-methylcytidine an anti-HCV non-obligate chain terminator.

It can be seen therefore, that both types of prodrugs are used to exploit the metabolic pathways of endogenous nucleosides and nucleotides by acting as anti-metabolites. These drugs enter the cells through specific nucleoside transporter mechanisms and are phosphorylated by three kinases, the first step to the monophosphate by nucleoside phosphate kinase is rate limiting as this kinase is very discriminatory.^{6,31} This is a major cause of observed inactivity in DAAs. The next two kinases: nucleoside diphosphate kinase and either creatine kinase or 3-phosphoglycerate kinase make the di- and tri-phosphate of the DAA.⁶ Only the triphosphate is active, therefore, all unmodified DAAs are prodrugs since they require phosphorylation before activity is observed.^{4,6,11,31,35,38,39} As will be discussed, methods to mask the monophosphate groups have been successful in overcoming the rate limiting step of the first kinase.

1.2.2.5.1 Nucleoside Reverse Transcriptase Inhibitors

Nucleoside reverse transcriptase inhibitors are all obligate chain terminators. They lack the 3'-OH group necessary (figure 1.14) for the formation of the phosphodiester bond that must form for genome replication to occur.⁴⁰ These drugs are used to treat HIV patients, and throughout their clinical development, significant challenges had to be overcome.

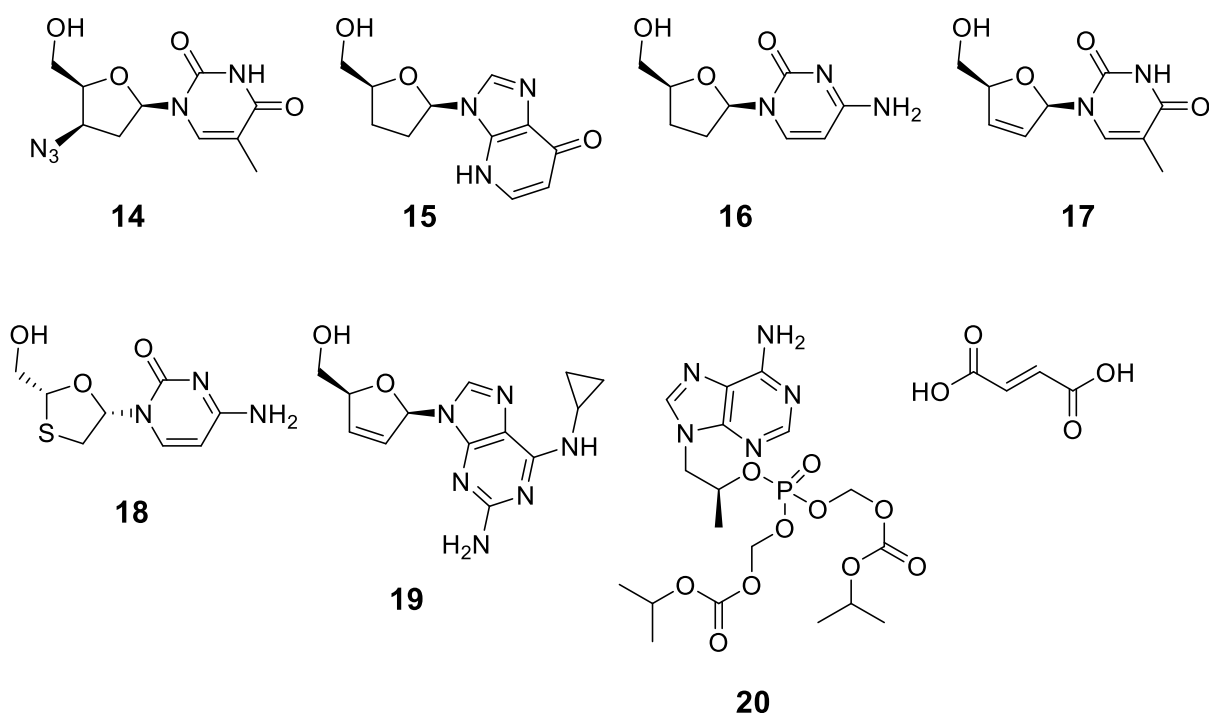


Figure 1.14: Current reverse transcriptase inhibitors in clinical use. All lack the 3'-OH group necessary for genome replication. Without this group, chain extension is not possible. **14:** Zidovudine (AZT) **15:** Didanosine **16:** Zalcitabine **17:** Stavudine **18:** Lamivudine **19:** Abacavir **20:** Tenofovir diisoproxil fumarate

In figure 1.14, seven nucleoside reverse transcriptase inhibitors are shown. All of these compounds are assumed to have the same mechanism of action as zidovudine **14**, in that they act as competitive metabolites.^{40,41} These compounds are converted to their active triphosphates at the 5'-OH end by endogenous kinases. Then, these compounds bind to the catalytic binding site of reverse transcriptase and are incorporated into the growing viral genome. Once these compounds are incorporated, chain elongation is terminated as the next nucleotide is unable to bind.^{11,35,40,42-46}

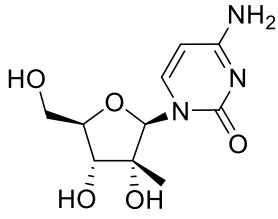
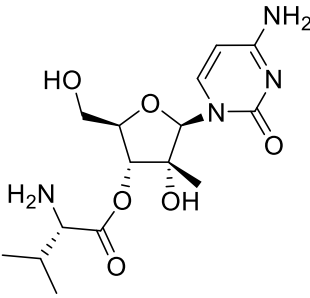
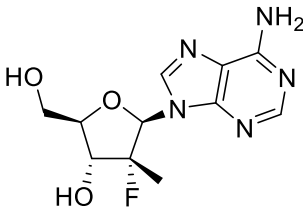
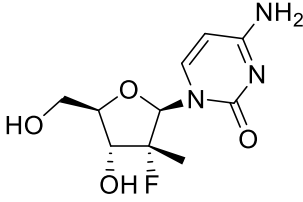
1.2.2.5.2 Nucleoside Polymerase Inhibitors

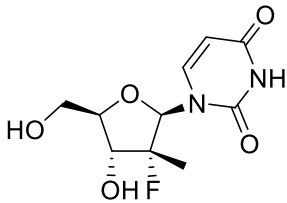
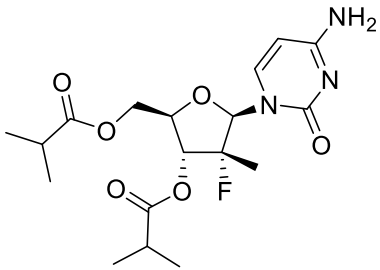
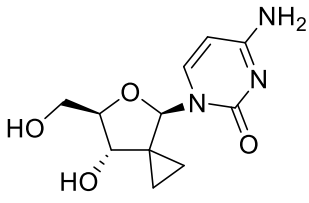
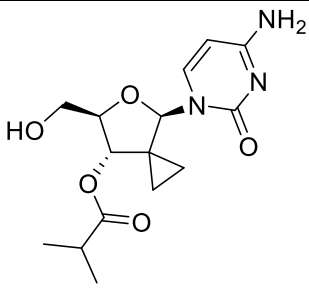
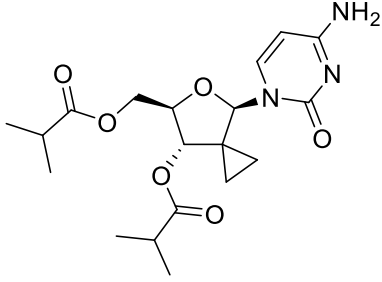
With the success of anti-HIV nucleosides, focus shifted towards HCV viral infection with research into nucleoside replicase inhibitors, known as DAAs coming to the forefront.

The 2'- β -C-methyl and 2'- α -OH compounds were the first class of inhibitors to be developed and has subsequently grown into a broad class which are potent and

devoid of cytotoxicity. The first compound discovered was NM107 **21** (table 1.1) and studies indicated that the 3'-OH in the alpha orientation was essential for activity without cytotoxicity.

Table 1.1: Biological data for 2'- α -fluoro compounds

Compound	IC ₅₀ (μ M)	EC ₅₀ (μ M)	Viral Load Reduction ($-\log_{10}$)
 <p>21 NM107</p>	-	1.23	-
 <p>22 NM283</p>	-	7.6	-1.2 monotherapy
 <p>23</p>	-	4.5	-
 <p>24 PSI6130</p>	1.19	-	-

 <p>25 PSI6206</p>	-	-	-2.7 monotherapy -5 combination therapy
 <p>26 RG7128 Mericitabine</p>	-	7.3	-
 <p>27 TMC647078</p>	-	-	-
 <p>28</p>	-	42.8	-
 <p>29</p>		20.3	

NM107 **21** had moderate potency ($EC_{50} = 1.23 \mu M$), though its triphosphate, acting as a non-obligate chain terminator, was much more active ($IC_{50} = 0.09 - 0.18 \mu M$) however studies revealed that resistance developed quickly.^{11,31,37,47-50} This led to the development of the 3-O-valinyl ester prodrug, NM283 **22** (figure 1.14, table 1.1) known as valopicitabine had an $EC_{50} = 7.6 \mu M$ with bioavailability in rats of 34%.^{31,37,47} NM283 **22** entered human clinical trials and showed modest reduction in viral load by $-1.2 \log_{10}$, however the trial was stopped at phase IIb due to significant gastrointestinal (GI) toxicity.^{11,31,37,49,50}

Replacement of the 2'- α -OH group with a 2'- α -F group resulted in the discovery of a new class of potent RNA dependant RNA polymerase (RdRp) HCV inhibitors. Base variations revealed that the cytosine analogues were the most potent.^{11,31} The adenosine, guanosine and uridine analogues had EC_{50} values greater than $50 \mu M$ and were weakly active or inactive with significant cytotoxicity. The inactivity was due to poor phosphorylation in the first step of triphosphate formation.^{34,51} The cytosine analogue, PSI 6130 **24** (table 1.1) has an EC_{50} of $4.5 \mu M$, however, this was metabolised to the inactive uradine analogue PSI 6206 **25** (table 1.1).^{34,39,51} The triphosphate of PSI 6206 was active with an IC_{50} of $1.19 \mu M$.³¹ In order to overcome the formation of the inactive metabolite, the 3',5'-diisobutyrate ester prodrug of PSI 6130 **24** was synthesised to yield RG7128, mericitabine **26**.^{11,27,31,50,52} In monotherapy RG7128 **26** resulted in a $-2.7 \log_{10}$ reduction in viral load and progressed to phase IIa clinical trials for genotypes 1, 2, and 3. The genotypes are differences in the genetic make-up of the same type of virus. HCV has 6 genotypes in its family. In phase IIa there was a response in 85 – 90% of patients with a $-5 \log_{10}$ reduction in viral load with no significant adverse effects observed. RG7128 in combination with two PI's: MK7009 vaniprevir and RG7227 danoprevir, in the absence of PEG IFN and RBV, showed -4.9 to -5.1 reductions in viral load and is expected to enter phase III trials.³¹

Further exploration of 2'-substituted nucleosides resulted in the identification of TMC 647078 **27** (table 1.1) with an EC_{50} of $7.3 \mu M$, no cytotoxicity, with broad genotype coverage.³¹ However, TMC 647078 **27** was metabolised to the inactive uridine metabolite with a low plasma concentration in rats.³¹ 3'-O-isobutyrate and 3',5'-O-

diisobutyrate prodrugs of TMC 647078 **27** to yield compounds **28** and **29** (table 1.1). The prodrugs had reduced activity ($EC_{50} = 42.8 \mu\text{M}$ and $20.3 \mu\text{M}$ for compounds **28** and **29** respectively) in bioassays but had increased exposure by 10 fold in compound **29** and 24 fold in compound **28**.

1.2.2.5.3 Development of Phosphoramidates

The nucleosides discussed thus far have been shown to be active potent inhibitors of HVC RdRp, however, as has been stated, the nucleosides must be converted to 5'-triphosphates by intracellular kinases to act as active inhibitors.³¹ Many potential compounds have failed to demonstrate activity in whole cell assays as they have been found to be poor substrates for one or more of the kinases in the phosphorylation cascade.³¹ Formation of the monophosphate is the most problematic step because the first kinase in the cascade is the most discriminatory of the three kinases, therefore bypassing the first kinase by delivering a 5'-monophosphate can result in higher levels of the active triphosphate in cells (figure 1.15).^{4,31,37-39,53} However, 5'-monophosphates are enzymatically dephosphorylated and are negatively charged (compound **33**, figure 1.15), the latter preventing entry to the cell, therefore making 5'-monophosphates poor drug candidates. However, 5'-monophosphate prodrugs have been synthesised to overcome this problem.^{31,37}

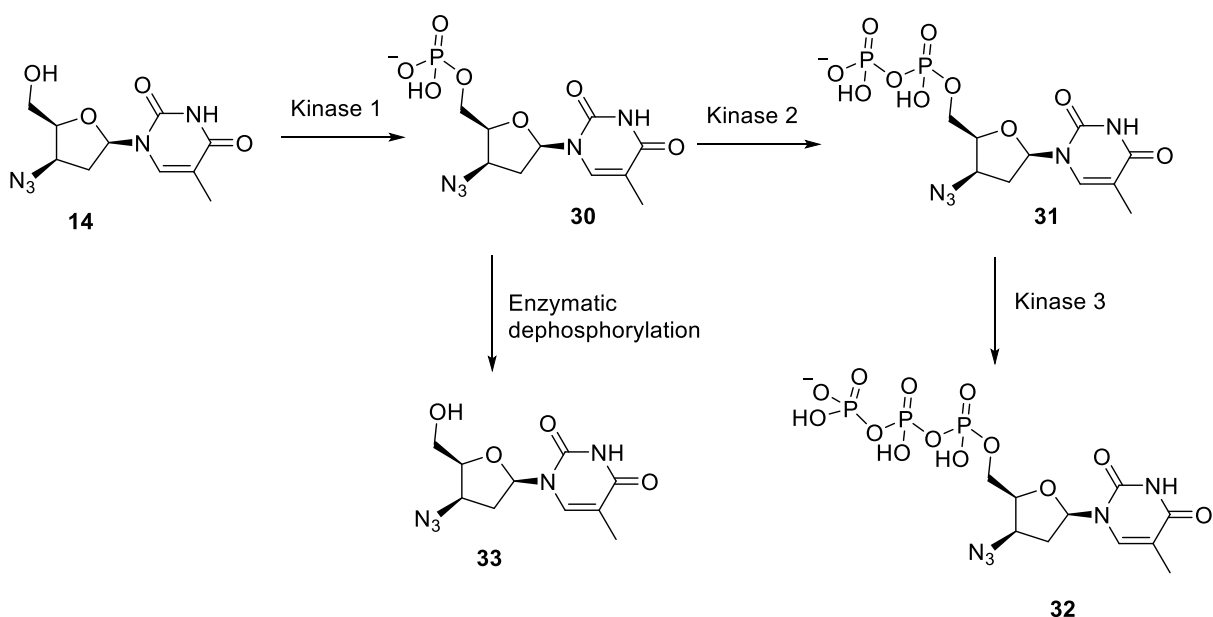


Figure 1.15: The phosphorylation steps of the three kinases to the active triphosphate using Zidovudine **14** as an example. Kinase 1 creates the nucleotide monophosphate (NMP) **30**, kinase 2 creates the nucleoside diphosphate (NDP) **32** and kinase 3 creates NTP **33**. As shown, the NMP can be enzymatically cleaved to an inactive form.

The 5'-monophosphates nucleoside prodrugs must have sufficient chemical stability for formulation into an orally administered drug and be stable to the gastrointestinal tract so as to reach the site of absorption. The prodrug must then be efficiently absorbed and reach the liver intact after which hepatic enzymes remove the 5'-monophosphate group allowing for the conversion to the active nucleotide triphosphate (NTP). Since HCV is a liver disease, this strategy allows for significantly improved liver targeting.^{31,37-39}

The phosphoramidate prodrugs are a class of 5-monophosphates that have excellent liver targeting and good potency. They exist as ProTides, HepDirect and SATE compounds.³¹ HepDirect compounds are prodrugs released by cytochrome P450 mediated mechanism and produce aryl vinyl ketone by products which are potentially cytotoxic. SATE compounds (bis(*S*-aryl-2-thioethyl) phosphate esters) are prodrugs which are released by initial ester hydrolysis followed by expulsion of the free 5'-hydroxy nucleoside by via liberation of an episulfide.³¹ ProTide compounds will only be discussed in this section as they have no associated toxicity that both HepDirect and SATE compounds do. For a review of HepDirect and SATE compounds, see reference 31. In the ProTide, HepDirect and SATE compounds, the phosphoramidate

group masks the negatively charged monophosphate thereby increasing lipophilicity and subsequently, cell permeability. However, a major setback for the phosphoramidate group is that the phosphorus atom is chiral and diastereomeric mixtures are always obtained upon synthesis. It has been shown in some cases that isolation and assessment of the anti-viral activity of each diastereomer shows different activities. One diastereomer may be significantly active and the other not active. In a mixture, the activity of the drug is diminished due to the presence of the inactive counterpart. Separation of the diastereomers is difficult and hampers their development.^{31,37,38}

NM107 **21** (table 1.1) has limitations such as poor conversion to the active NTP, it has only modest potency and some adverse clinical effects have been reported.^{31,37} When NM107 **21** was converted to the phosphoramidate prodrug **34** (figure 1.16), there was improvement in potency and increased levels of NTP conversion. When compared to NM283 **22**, phosphoramidate **35** had improved potency ($EC_{50} = 0.22 \mu M$) relative to NM283 **22** with increased levels of NTP observed in hepatocytes. Low oral bioavailability was assumed in hamster studies which showed only a 2 fold increase in hepatic NTP levels.^{31,37} In an attempt to increase liver NTP levels, the chain length of the ester moiety in phosphoramidate **35** was explored, which resulted in phosphoramidate **35** (figure 1.16). Although potency was the same ($EC_{50} = 0.24 \mu M$), there was no improvement in liver NTP levels. Further efforts to increase hepatic NTP levels resulted in phosphoramidate **35** (figure 1.16) which had inferior potency when compared to phosphoramidates **34** and **36**. It did have higher levels of the active NTP in human hepatocytes when dosed by subcutaneous IV. However, phosphoramidate **36** when dosed orally did not have the same level of hepatic NTP.³¹

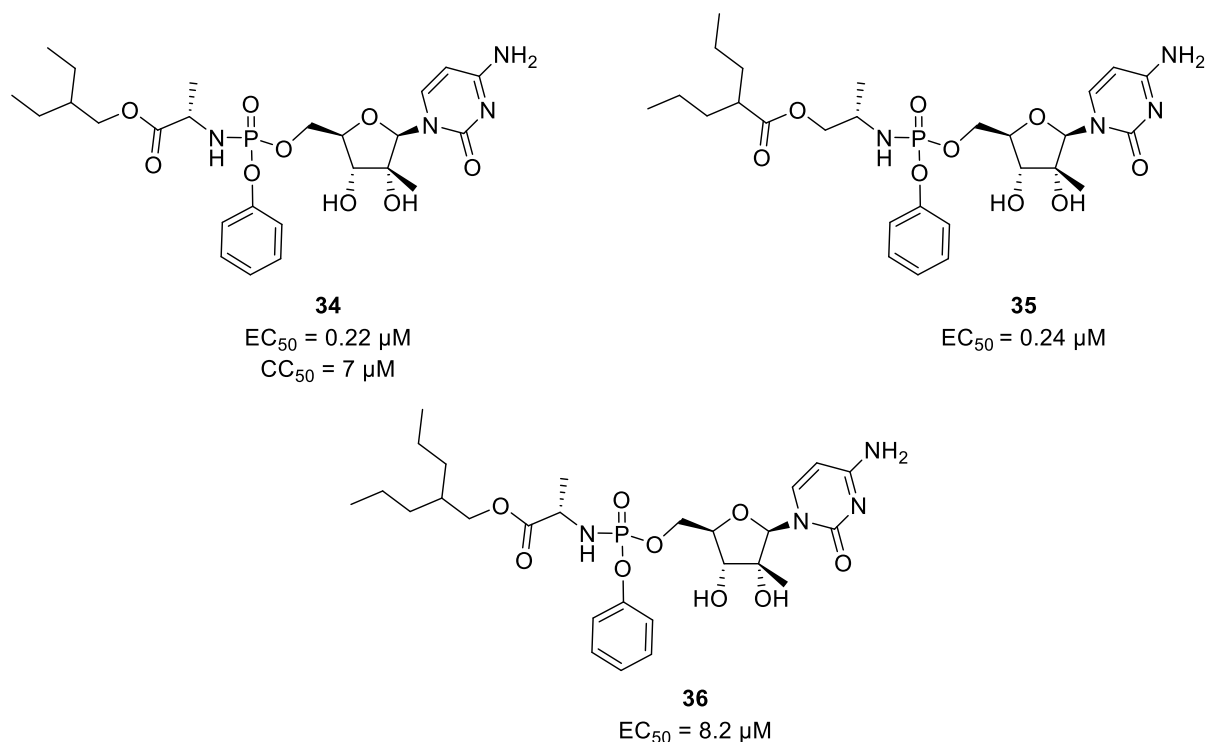


Figure 1.16: Phosphoramidate prodrugs of NM107 **21**

The uridine derivative PSI6206 **25** was found to be inactive, however its NTP was found to have significant activity (table 1.1), so phosphoramidate prodrugs of PSI6206 **25** were developed which yielded two highly potent compounds, PSI7851 **37** and PSI7977 **38** (figure 1.17).^{4,31,52}

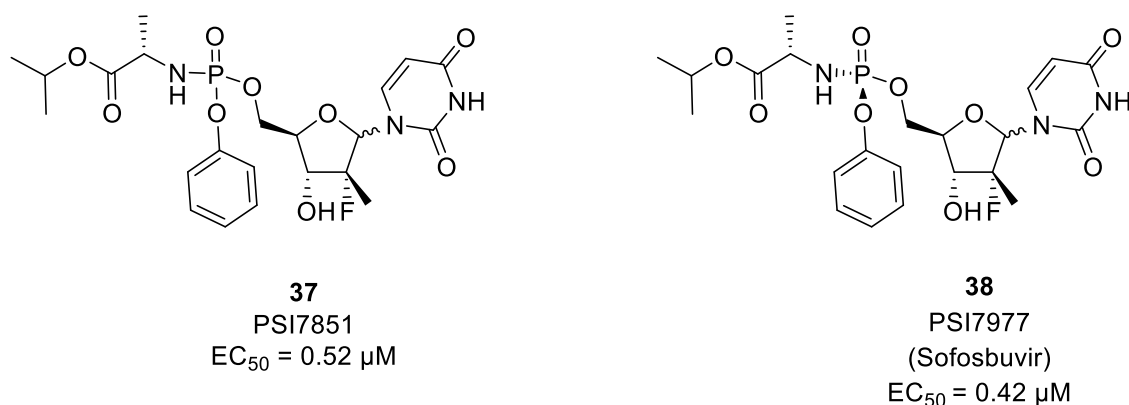


Figure 1.17: PSI7851 and PSI7977 (Sofosbuvir)

PSI7851 **37** was developed as a 1:1 diastereomeric mixture as a drug candidate. It was found to have synergistic effects with PEG IFN and RBV with a PI in quadruple therapy. No viral resistance or adverse effects were observed.³¹

PSI7977 **38** (sofosbuvir) was developed as a single isomer as it was tenfold more active than its diastereomer. In genotype 1 patients, the viral load was decreased by $-5 \log_{10}$ with between 85 – 90 % having no detectable viral RNA. In genotype 2 and 3 patients, 96% of patients achieved SVR in phase IIb trials. In 2014 it was approved as the first in class DAA nucleoside prodrug for the treatment of HCV infected patients.^{4,31}

Extending the work on guanosine analogues, PSI353661 **41** (figure 1.18) was found to be a very highly potent drug candidate for HCV genotype 1 and 2 patients with an EC_{90} of 0.008 μM and is currently entering clinical trials.^{31,38}

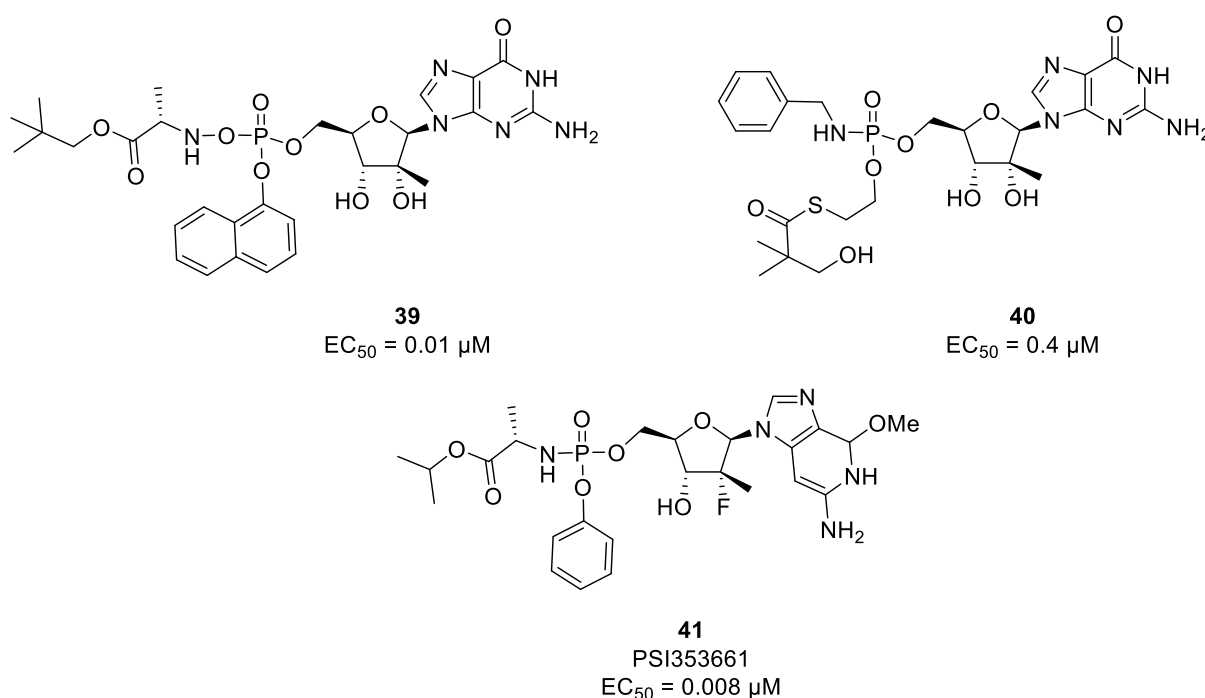


Figure 1.18: Guanosine based phosphoramidates

Although new developments in targeting HCV RdRp show promise, new drug candidates are hampered by poor bioavailability, toxicity issues, poor conversion to the active triphosphate, and have poor genotype coverage.^{4,11,31,54} Only one candidate TMC 647078 **27** (table 1.1) showed coverage for all six HCV genotypes, however was converted to the inactive uridine derivative and had low plasma concentrations.³¹ Synthesis of isobutyrate prodrug did not improve efficacy either. Phosphoramidate prodrugs show promise however; these are hampered by synthetic issues, are slow to develop, and are currently only able to target genotypes 1 to 3.³¹

As of 2014, sofosbuvir **38** the first in class phosphoramidate DAA nucleoside for treating HCV was approved for use. This means that current treatment regimes are combination therapy of sofosbuvir **38** with ribavirin and boceprevir **7** or telaprevir **8** (figure 1.5); or combination therapy without ribavirin. This does away with the significant side effects of ribavirin and IFN 2 α . However, due to the cost of sofosbuvir **38**, the limited genotype coverage, and the risk of evolving viral resistance occurring, newer DAAs are required.⁵⁵

A major setback for ProTide, HepDirect and SATE compounds is that to release the free nucleoside before conversion to the triphosphate is enzymatically controlled.⁵⁶ Efficient anabolism to the free nucleotide is limited by deamination or cleavage of the glycosidic bond, therefore the therapeutic utility of these phosphoramidates are limited.⁵⁶ Meier devised *cycloSal* pronucleotides which are chemical Trojan horses that are chemically cleaved, circumventing the problems with enzymatic cleavage of the phosphate bond.⁵⁶ Figure 1.19 shows the chemical cleavage of a Meier compound.

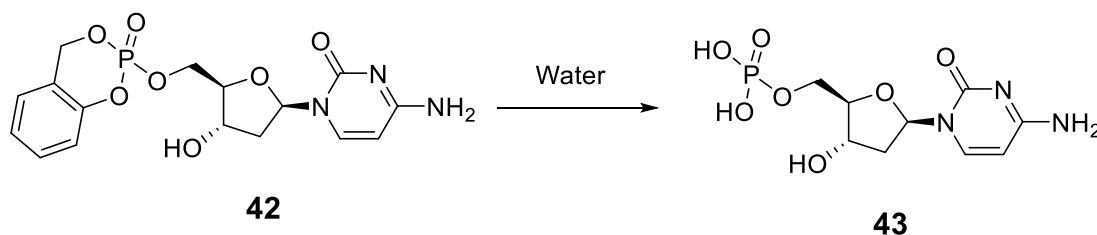


Figure 1.19: Chemical hydrolysis of Meier pronucleotides

1.2.2.5.4 Conformationally Restricted Nucleosides

A major issue in the activity of ribose and deoxyribose based nucleosides is the bias of cellular kinases and DNA and RNA polymerases towards the conformational structure of the sugar moiety (figure 1.20).^{57,58} It has been experimentally confirmed that kinases require south puckering nucleosides for phosphorylation to the active triphosphate, and the polymerases require north puckering nucleotides. Polymerases will not incorporate south puckered nucleotides into a replicating genome as the nucleotide will not be in the correct conformation to bind into the polymerase active site.⁵⁹ The energy expenditure to ring flip from the south pucker to the north pucker is large (about 17 KJ mol⁻¹).⁵⁷⁻⁶⁰ This must be overcome before incorporation of the

nucleotide into the replicating genome can occur. As such, this is the cause of observed inactivity, or lower than expected activity of ribose and deoxyribose anti-viral agents, even where there is a high level of the NTP present in the cells.⁵⁷⁻⁶⁰

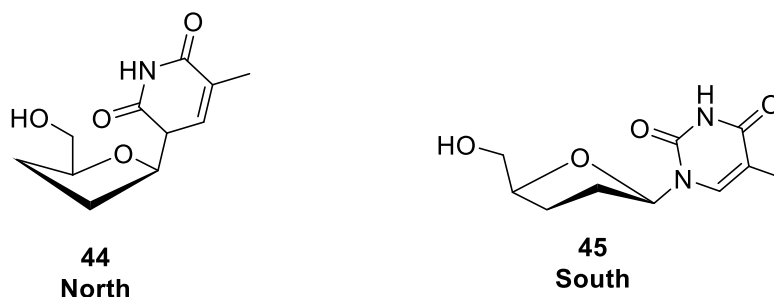
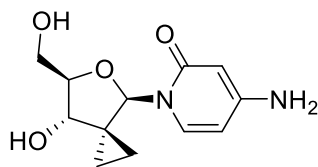


Figure 1.20: North and south puckered nucleotides

In order to overcome this problem, conformational locking of nucleotides into the north conformation has proven useful, but this is not the only method of avoiding this kinase-polymerase bias.⁶¹ A major issue with this method is that by locking the nucleoside into the north conformation, phosphorylation at kinases does not occur. Additional steps are required to phosphorylate or mask the 5'-OH group to avoid the kinases altogether (see section 1.2.3.5.3). Research into conformationally locked nucleosides is ongoing, though faces similar issues.⁵⁹⁻⁶³ Locking the nucleoside in the south conformation allows for phosphorylation, however, as stated north conformation nucleosides are required for incorporation into the viral genome.⁶¹ Spironucleosides are one such method of locking nucleosides in the preferred conformation as the anomeric carbon on the sugar and the base are shared, though variations in where the spiro-component is incorporated can also determine conformational locking.³³ Spironucleosides are able to enhance base stacking within the genome and increase the rate of backbone pre-organisation, ie, these types of nucleosides create stable interactions within the genome. However, the main pitfall is the fact that conformational locking affects phosphorylation and hence incorporation into the genome.³³ Figure 1.21 shows an example of a spironucleoside where compound **46** showed anti-HCV activity with the spiro component at C-2 forcing the nucleobase conformation into the south conformation. (Note: The review by Soengas *et al.*, goes into more detail on the topic of spironucleosides that is not within the remit of this thesis such as the differing mechanisms of action of C-1, C-2, C-3, and C-4 spironucleosides).³³



46

Figure 1.21: Typical C-2 Spironucleoside active against HCV infection

Nucleoside/nucleotide based drugs are the best class of anti-viral agent for the treatment of viral infection as they are able to prevent viral replication; and this in turn allows the immune system to fight the infection.^{8,10} Many modifications can be made to these nucleosides, such as phosphate modifications, sugar modifications, base modifications and conformational locking. These modifications are required to overcome the issues regarding kinase bias causing low levels of the active triphosphate, discrimination between kinases and polymerases, and solubility issues.³¹ Continued research in this area is necessary due to the ability of viruses to quickly evolve resistance against these drugs. Modifications to the polymerase active site can create less favourable binding interactions for these un-natural nucleosides.

1.3 Summary and Conclusions

The major classes of anti-viral agents include receptor antagonists, inhibitors and interferons.^{14,16,19,22,31,51} The drawback with interferons is that they do not act on the life cycle of the virus, with their mechanism of action being to induce an immune response to a viral infection.^{7,8} This means that the infection can persist, and relies on the the immune system being able to stave off infection.^{7,13} As such, interferon treatment is limited to viruses that do not harm the host immune system. Receptor antagonists are another class of drug where their utility is limited.^{22,23} This class of drug relies on prophylactic treatment; where the drug is administered before infection.²⁴ Like NNRTIs, IIs, PIs, and NNRTIs, which are all highly specific, resistance evolves very quickly limiting the utility of all these classes of drugs.¹

Nucleoside based drugs are the best class of drugs to target viral infections. This class of drug is able to directly prevent viral replication in all stages of the viral infection pathway whereas other classes of drug act only in a specific stage of infection.^{31,39,64} Nucleoside drugs do not work when the virus is latent and not

replicating, however, these drugs are able to prevent replication once the virus has entered the cell, or has started to replicate.^{11,31}

Typical drug regimens now utilise a DAA (nucleoside drug) a NNRI or NNRTI (usually two) and a PI. This type of combination therapy allows rapid treatment of viral infections. The DAA prevents genome replication along with the NNRI or NNRTI. The PI is used to prevent the protease from cleaving the viral polyprotein before a new virion is assembled. This method has been used successfully to treat HIV and HCV. However, much work is required for new DAAs, and therefore, the major aim of this project is to develop nucleoside based drugs to treat viral infections.

1.4 Aims and Objectives

Since DAAs have shown the greatest potential in treating viral infections, the major aim of this project is to develop new nucleoside based DAAs. However, the conformation of ribose nucleosides has been shown to be a major factor in inactivity. Therefore, 4-membered ring nucleosides will be assessed for their anti-viral activity. (See introduction to chapter 2). Thietane nucleosides and thioribose nucleosides have shown significant promise due to their stability against kinases and nucleases. The sulfur atom makes these compounds less susceptible to nucleases cleaving the glycosidic bond. (See chapters 2 and 4 introductions for a detailed explanation). Therefore the project aimed to develop three libraries of compounds.

Aims:

To develop and optimise synthetic routes toward target sulfur containing nucleosides by exploiting available chemistry to synthesise the target nucleosides. The chemical strategies are to be assessed to enable efficient synthesis of the target compounds.

Assess the anti-viral activity of the target thietane and 4'-thiohamamelose nucleosides in biological assays to determine SARs. Use this data to develop more potent nucleosides by varying the structure of the compounds in line with observations from the biological assays.

Objectives:

1. Library 1: thietane nucleosides as anti-viral agents. This will involve the design and synthesis of 3,3-bis(hydroxymethyl)-thietan-2-yl nucleosides to probe the SAR of the nucleobases. This will then lead to
2. Library 2: thietane nucleosides as anti-viral agents This will involve the design and synthesis of 4,4-bis(hydroxymethyl)-thietan-2-yl nucleosides. Here, the geminal hydroxyl groups position has been modified. The nucleobases are the same as those in library one, so that the SAR of the position of the hydroxyl methyl groups can be assessed.
3. Library 3: 4'-thiohamamelose nucleosides. This will involve the design and synthesise a library of 4'-thiohamamelose nucleosides as potentially active anti-HCV nucleosides.
4. Assessment of the anti-viral activity: The IC_{50} , and CC_{50} will be determined in an anti-viral assay. Prior to these assays, cell viability studies will be performed on selected nucleosides to assess whether these compounds affect cell viability before more stringent cytotoxicity assays are performed. The IC_{50} and CC_{50} data will be used to determine the SAR of these compounds
5. Once the SAR is determined, a final library of compounds will be synthesised based on the biological data with the intention of increasing potency and decreasing any observed cytotoxicity.

Objective 1 has been met with this programme and the cell viability of 4 candidate compounds, in line with the objective 4, has been determined with no significant loss in cell viability and is detailed in chapter 2.

Objectives 2 and 3 have been partially with the optimisation of the synthetic routes towards the key intermediates for the synthesis of the respective target nucleosides and are detailed in chapters 3 and 4.

1.5 References

- (1) Kharb, R.; Yar, M. S.; Sharma, P. C. *Mini-Rev Med Chem* **2011**, 11, 84.
- (2) Murray, C. J. L. *Lancet* **2015**, 384, 1005.
- (3) Du, J.; Chun, B. K.; Mosley, R. T. *et al. J Med Chem* **2014**, 57, 1826.
- (4) Sofia, M. J.; Bao, D.; Chang, W. *et al. J Med Chem* **2010**, 53, 7202.
- (5) *Hepatitis C Fact Sheet*, World Health Organisation, 2012.
- (6) Jordheim, L. P.; Durantel, D.; Zoulim, F. *et al. Nat Rev Drug Discov* **2013**, 12, 447.
- (7) Lawrence, C. M.; Menon, S.; Eilers, B. J. *et al. J Biol Chem* **2009**, 284, 12599.
- (8) Breitbart, M.; Rohwer, F. *Trends Microbiol* **2005**, 13, 278.
- (9) Koonin, E. V.; Senkevich, T. G.; Dolja, V. V. *Biol Direct* **2006**, 1, 29.
- (10) Edwards, R. A.; Rohwer, F. *Nat Rev Microbiol* **2005**, 3, 504.
- (11) De Clercq, E. *Nat Rev Drug Disc* **2007**, 6, 1001.
- (12) Razonable, R. R. *Mayo Clin Proc* **2011**, 86, 1009.
- (13) Anderson, J. P.; Daifuku, R.; Loeb, L. A. *Annu Rev Microbiol* **2004**, 58, 183.
- (14) Peska, S.; Krause, C. D.; Walter, M. R. *Immunological Reviews* **2004**, 202, 8.
- (15) Lauer, G. M.; Walker, B. D. *New Engl J Med* **2001**, 345, 41.
- (16) Pommier, Y.; Johnson, A. A.; Marchand, C. *Nat Rev Drug Discov* **2005**, 4, 236.
- (17) Casadella, M.; van Ham, P. M.; Noguera-Julian, M. *et al. J Antimicrob Chemother* **2015**, 70, 2885.
- (18) Summa, V.; Petrocchi, A.; Bonelli, F. *et al. J. Med. Chem* **2008**, 51, 5843.
- (19) Godwin, C. G.; Zhang, X.; Marchand, C. *et al. J Med Chem* **2002**, 45, 3184.
- (20) Goethals, O.; Clayton, R.; Van Ginderen, M. *et al. J Virol* **2008**, 82, 10366.
- (21) Hazuda, D. J.; Ferlock, P.; Witmer, M. R. *et al. Science* **2000**, 287, 646.
- (22) Boriskin, Y. S.; Leneva, I. A.; Pecheur, E. I. *et al. Curr Med Chem* **2008**, 15, 997.
- (23) Gubareva, L. V.; Kaiser, L.; Hayden, F. G. *The Lancet* **2000**, 355, 827.
- (24) Moscona, A. *N Eng J Med* **2005**, 353, 1363.
- (25) Sampath, A.; Padmanabhan, R. *Antiviral Res* **2009**, 81, 6.
- (26) Wood, J. J. A. *N Eng J Med* **1998**, 338, 1281.
- (27) Doyle, J. S.; Aspinall, E.; Liew, D. *et al. Br J Clin Pharmacol* **2013**, 75, 931.

- (28) Poordad, F.; McCone, J. J.; Bacon, B. R.*et al. New Engl J Med* **2011**, 364, 1195
- (29) Venkatraman S; Bogen, S. L.; Arasappan, A.*et al. J Med Chem* **2006**, 49, 6074
- (30) Kim, A. E.; Dintaman, J. M.; Waddell, D. S.*et al. J Pharmacol Exper Thera* **1998**, 286, 1439
- (31) Sofia, M. J.; Chang, W.; Furman, P. A.*et al. J Med Chem* **2012**, 55, 2481.
- (32) Gentles, R. G.; Ding, M.; Bender, J. A.*et al. J Med Chem* **2014**, 57, 1855.
- (33) Soengas, R. G.; Silva, S. *Mini Rev Med Chem* **2012**, 12, 1485.
- (34) Eldrup, A. B.; Allerson, C. R.; Bennett, C. F.*et al. J Med Chem* **2004**, 47, 2283.
- (35) De Clercq, E.; Field, H. J. *Br J Pharmacol* **2006**, 147, 1.
- (36) Migliaccio, G.; Tomassini, J. E.; Carroll, S. S.*et al. J Biol Chem* **2003**, 278, 49164.
- (37) Gardelli, C.; Attenni, B.; Donghi, M.*et al. J Med Chem* **2009**, 52, 5394.
- (38) Chang, W.; Bao, D.; Chun, B.*et al. ACS Med Chem Lett* **2011**, 2, 130
- (39) Murakami, E.; Niu, C.; Bao, H.*et al. Antimicrob Agents Chemother* **2008**, 52, 458.
- (40) De Clercq, E. *J Clin Virol* **2004**, 30, 115.
- (41) Cihlar, T.; Ray, A. S. *Antiviral Res* **2010**, 85, 39.
- (42) De Clercq, E. *Med Res Rev* **2008**, 28, 929.
- (43) De Clercq, E. *Med Res Rev* **2009**, 29, 571.
- (44) De Clercq, E. *Annu Rev Pharmacol Toxicol* **2011**, 51, 1.
- (45) De Clercq, E. *Antiviral Res* **2005**, 67, 56.
- (46) De Clercq, E. *Med Res Rev* **2015**, 35, 698.
- (47) Pierra, C.; Amador, A.; Benzaria, S.*et al. J Med Chem* **2006**, 49, 6614.
- (48) De Francesco, R.; Tomei, L.; Altamura, S.*et al. Antiviral Research* **2003**, 58, 1.
- (49) De Francesco, R.; Migliaccio, G. *Nature* **2005**, 436, 953.
- (50) Soriano, V.; Peters, M. G.; Zeuzem, S. *Clinical Infect Dis* **2009**, 48, 313.
- (51) Eldrup, A. B.; Prhavc, M.; Brooks, J.*et al. J Med Chem* **2004**, 47, 5284
- (52) Varshney, J.; Sharma, A.; Sharma, P. K. *Med Chem Res* **2013**, 22, 1043
- (53) Tomassini, J. E.; Getty, K.; Stahlhut, M. W.*et al. Antimicrob Agents Chemother* **2005**, 49, 2050.
- (54) Olsen, D. B.; Eldrup, A. B.; Bartholomew, L.*et al. Antimicrob Agents Chemother* **2004**, 48, 3944.

- (55) Phelan, M.; Cook, C. *BMC Infect Dis* **2014**, 14 Suppl 6, S5.
- (56) Meier, C. *Mini Rev Med Chem* **2002**, 2, 219.
- (57) Marquez, V. E.; Choi, Y.; Comin, M. J.*et al. J Am Chem Soc* **2005**, 127, 15145.
- (58) Marquez, V. E.; Ben-Kasus, T.; Barchi, J. J.*et al. J Am Chem Soc* **2004**, 126, 543.
- (59) Ketkar, A.; Zafar, M. K.; Banerjee, S.*et al. Biochemistry* **2012**, 51, 9234.
- (60) Mu, L.; Sarafianos, S. G.; Nicklaus, M. C.*et al. Biochemistry* **2000**, 39, 11205.
- (61) Dejmek, M.; Hrebabecky, H.; Sala, M.*et al. Bioorg Med Chem* **2014**, 22, 2974.
- (62) Boyer, P. L.; Julias, J. G.; Marquez, V. E.*et al. J Mol Biol* **2005**, 345, 441.
- (63) Dell'Isola, A.; McLachlan, M. M.; Neuman, B. W.*et al. Chem. Eur. J.* **2014**, 20, 11685.
- (64) Reddy, P. G.; Chun, B. K.; Zhang, H. R.*et al. J Org Chem* **2011**, 76, 3782.

Chapter 2:

**The Design and Synthesis of 3,3-
bis(hydroxymethyl)-thietan-2-yl
Nucleosides**

Chapter 2: Synthesis of 3,3 bis(hydroxymethyl) thietane nucleosides

2.1 Background

A major issue in the anti-viral activity of ribose and deoxyribose based nucleosides is the bias of cellular kinases and DNA and RNA polymerases towards the conformational structure of the sugar moiety (figure 2.1).^{1,2} It has been experimentally confirmed that kinases require south puckering nucleosides for phosphorylation to the active triphosphate, and the polymerases require north puckering nucleotides. Polymerases will not incorporate south puckered nucleotides into a replicating genome as the nucleotide will not be in the correct conformation to bind into the polymerase active site.³ The energy expenditure to ring flip from the south pucker to the north pucker is large (about 17 kJ mol⁻¹) and must be overcome before incorporation of the nucleotide into the replicating genome can occur, and as such, this is the cause of observed inactivity, or lower than expected activity, of ribose and deoxyribose anti-viral agents.¹⁻⁴

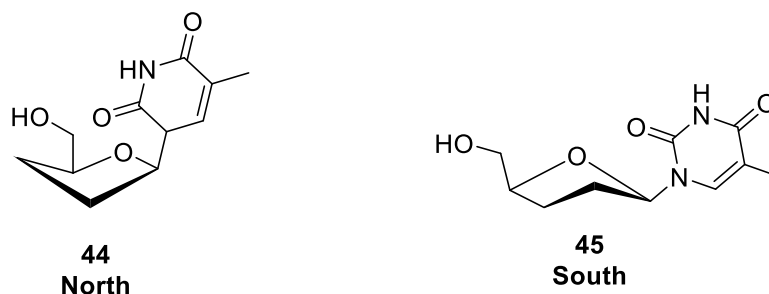


Figure 2.1: North and south puckered nucleotides **44** and **45**

In order to overcome this problem, conformational locking of nucleotides into the north conformation has proven useful, but this is not the only method of avoiding this kinase-polymerase bias.⁵ A major issue with this method is that by locking the nucleoside into the north conformation, phosphorylation by kinases does not occur. Additional steps are required to phosphorylate or mask the 5'-OH group to avoid the kinases altogether. As noted in chapter 1, the first kinase in the phosphorylation steps is the most discriminatory and hence the most important factor in inactivity of nucleosides is due to the first kinase in the phosphorylation step. In order to overcome this, several methods of masking the 5'-OH group as phosphonate esters

or phosphoramidates have been developed. These have been applied to north puckered conformationally locked nucleosides.^{6,7}

However, since this adds several steps, a more prudent method would be to change the sugar moiety altogether. Oxetane nucleosides have been extensively studied as alternative nucleoside analogues to ribose derivatives. In its unsubstituted form, the oxetane ring will flip between planar and two puckered forms (figure 2.2) with ease as the energy barrier is small (the total energy change for flipping through the planar state from either conformation is -1.2 kJ mol^{-1}).^{8,9}

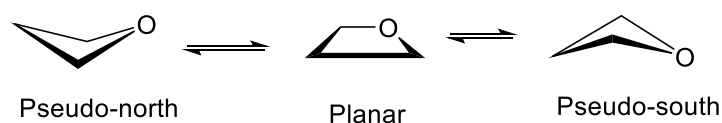


Figure 2.2: Conformations of oxetane

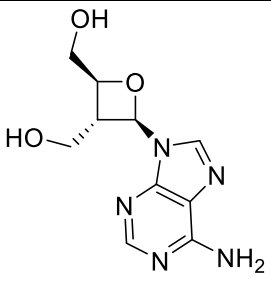
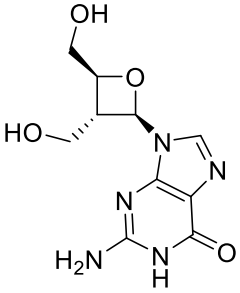
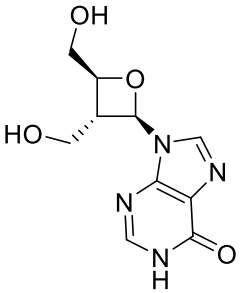
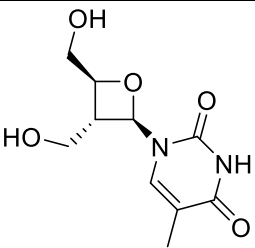
The ring flip between these forms in oxetane is prevented once they are substituted, locking in place the conformation of the ring. This conformational locking is due to the fact that 4 membered ring closing mechanisms favour 4-exo-tet reactions.^{8,9} This leads only to the pseudo-south puckered conformation as formation of the 4-endo-tet cyclisation is disfavoured by Baldwin's Rules.

It seems counterintuitive that kinases will recognise the pseudo-south conformation given that kinases only recognise south conformations. Further, it seems that polymerases should not recognise pseudo-north conformation since polymerases only recognise north conformations. It would be expected that conformationally locked pseudo-south oxetanes would not be recognised or be phosphorylated by kinases. However, kinases recognise them as substrates and will phosphorylate them as described below.¹⁰

2.1.1 Oxetane and Thietane Nucleosides

Oxetane nucleosides have been extensively studied and have shown anti-viral activity against VZV, HSV-1,2, HIV, HBV and CMV.¹⁰⁻¹⁶ Oxetanocin A was first isolated in 1986 and showed anti-viral, anti-bacterial, anti-tumour and anti-fungal activity.^{10-13,17,18} Shown in table 2.1 are the oxetane nucleosides that are active against HIV, HBV, HSV and VZV.

Table 2.1: Anti-viral activity of oxetane nucleosides

Nucleoside	Virus	(EC ₅₀ μM)	(CC ₅₀ μM)
 Oxetanocin A 47	HIV ¹⁵	1.4	11 ¹⁵
 Oxetanocin G 48	HIV ^{15,16} HBV ¹⁶	7.3 1.5	29 ¹⁵ -
 Oxetanocin H 49	HIV ¹⁵	2.2	28 ¹⁵
 Oxetanocin T 50	VZV ¹⁵ HSV-1 ¹⁵ HSV-2	0.003 0.05 1.0	>100 >100 >100

It was noted that the oxetanocin nucleosides were all converted to their active triphosphates hence their anti-viral activity.¹⁰ However, compound **47** did not

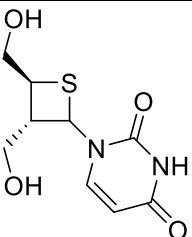
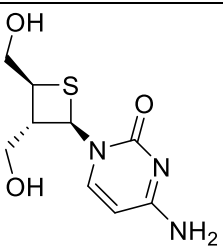
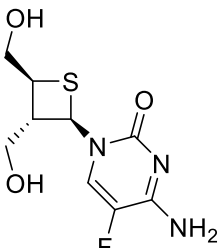
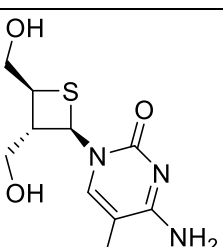
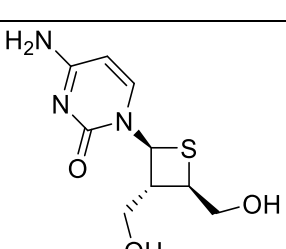
incorporate well into the DNA of HBV which would allow chain extension of the viral genome to occur even after nucleoside incorporation.¹⁶ Therefore, compound **47** is inefficient at inhibiting viral genome replication as it was not specific for the viral polymerase, with several host cell targets which resulted in some observed cytotoxicity. Cytotoxicity was observed in compounds **48** and **49** and was also due to the unspecific binding of these molecules.

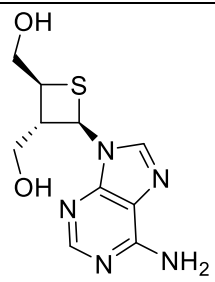
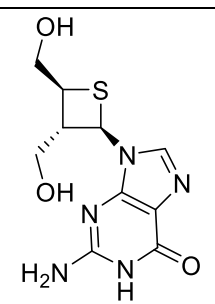
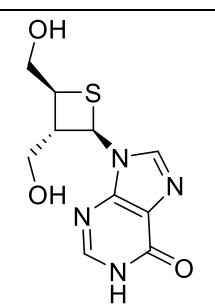
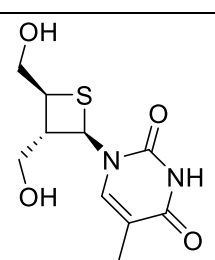
Through nucleobase modification, compound **50** was found to have a longer half-life than compound **47**, the half-life of compound **50** being three hours versus 1.7 hours for compound **47**.¹⁴ This was due to compound **47** being deaminated by adenine deaminase to form the inactive metabolite.^{11,16} The oxetane ring was found to be unstable toward cellular phosphorylases, which inactivates the nucleosides.^{10-13,19,20} A way to overcome the problem of adenine deaminase and hydrolysis of the glycosidic bond is to replace the oxygen with sulfur.^{11,21} This kind of replacement has been shown to increase the stability of nucleosides to acid hydrolysis since sulfur atoms do not protonate as easily as oxygen atoms.²⁰

Since thietane nucleosides are predicted to be more stable towards acid glycosidic hydrolysis and cellular phosphorylases than the oxetane counterparts; it is predicted that the thietane nucleosides will still retain activity or have increased activity over the oxetane counterparts. It is also predicted that the thietane nucleosides will be phosphorylated. The thietane nucleosides should behave in exactly the same manner as the oxetane nucleosides; that is although the thietanes are predicted to be conformationally locked in a pseudo-south conformation in much the same way as the oxetanes, this should not impede activity.

Choo *et al.*, have synthesised several thietane nucleosides, based on the oxetanocin A scaffold, that are active against HIV (table 2.2).¹¹

Table 2.2: Thietane nucleosides active against HIV

Nucleoside	(EC ₅₀ μM)	PBM (IC ₅₀ μM)	CEM (IC ₅₀ μM)
 <p>51</p>	6.9	8.5	4.9
 <p>52</p>	1.3	=1.0	4.3
 <p>53</p>	5.8	<1.0	19
 <p>54</p>	11.5	>100	1.8
 <p>55</p>	14.1	13.1	45.6

 <p>Thietanocin A 56</p>	>100	>100	>100
 <p>Thietanocin G 57</p>	>100	>100	>100
 <p>Thietanocin H 58</p>	>100	>100	>100
 <p>Thietanocin T 59</p>	>100	>100	>100

Compounds **51** – **55** showed anti-viral activity against HIV, however, cytotoxicity in peripheral blood mononuclear cells (PBM) and CEM-T4 cells was an issue (CC_{50} for CEM T4 cells were highest at 45.6 μ M and CC_{50} for PBM cells were highest at 13.1 μ M). The high CC_{50} values are problematic for these compounds as HIV-1

infects these blood cells, and death of these immune cells is a significant issue as this reduces the effectiveness of the host immune system at fighting infection. Addition of a halogen group to the 5-position of the pyrimidine ring reduced the cytotoxicity of these compounds, however, anti-viral activity was also reduced.¹¹ The activity of the thietane compounds are comparable to the oxetane counterparts, however, the thietane purine derivatives were not active despite molecular models showing thietanocin A **56** binding in the exact same manner as the active oxetanocin A **47**. The observed inactivity of thietanocin A **56** could be due to low levels of the active triphosphate being formed.¹¹ Despite this, the pyrimidine thietane nucleosides show excellent promise as anti-viral nucleosides. Though cytotoxicity may be an issue, this can be controlled by analysing structure activity relationships. By focusing on groups which favour binding to viral polymerases over host cell organelles, cytotoxicity may be reduced and anti-viral activity should increase as the compounds become more selective and potent.

The benefits of thietane nucleosides have been demonstrated (table 2.2). They are predicted to be more stable than the oxetane derivatives and may be more active when a more focused medicinal chemistry campaign is used to further develop them. These compounds have been shown to be recognised by kinases and to be incorporated into viral genomes. This suggests that thietane nucleosides are phosphorylated by kinases without discrimination of the ring conformation. It has been noted in the literature that the reason for the limited number of thietane nucleosides analysed thus far is due to the difficulty in synthesising the nucleosides.^{10-13,17-19,22} The key challenges to overcome are:

1. synthesising the thietane scaffolds of interest,
2. synthesising the nucleosides, of which two methods are known, one of which has low yields and reproducibility problems;^{10-13,17}
3. the lack of clinical data means that additional SAR studies are required to understand which components of the thietane scaffolds are important for activity. From this data, selectivity and potency could be fine-tuned toward the synthesis of a potent, active anti-viral thietane nucleoside.

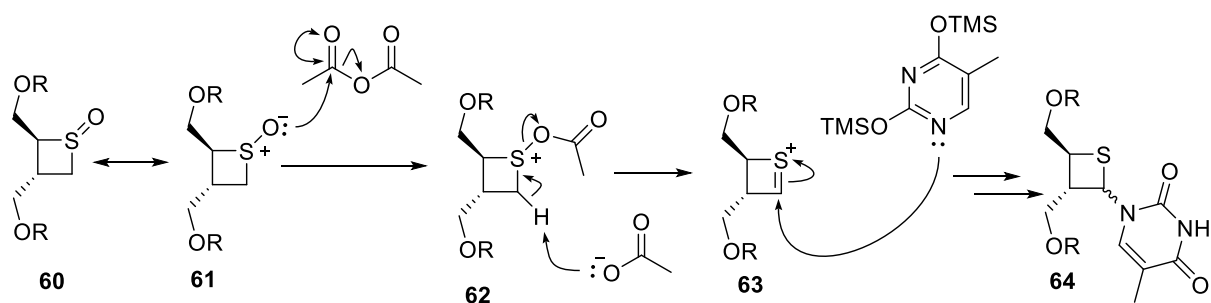
2.2 Aims and Objectives

Choo *et al.* have shown that thietane nucleosides have anti-viral activity and the major aim of the research described herein was therefore to determine the anti-viral activity of complementary 3,3-bis(hydroxymethyl) thietane nucleosides. In order to achieve this major aim several goals must be achieved first:

- Exploratory chemistry: There are two known methods toward the synthesis of thietane nucleosides (section 2.2.1), the Pummerer Reaction and Vorbrüggen conditions. Both of these methods will be explored.^{10,11,13}
- Build a library of thietane nucleosides using the literature as a guide to identify key nucleobases that have been shown to confer anti-viral activity.
- Determine the anti-proliferative profile: Pre-screening cell viability assays will be used to determine whether the nucleosides impact cell viability. Candidate compounds that are representative of the library will be screened to assess their impact on cell viability.
- Once cell viability assays have determined whether or not the compounds affect cell viability, the compounds will be screened against a library of viruses to determine CC₅₀ and their IC₅₀; which is the concentration required to halt viral replication by 50%.

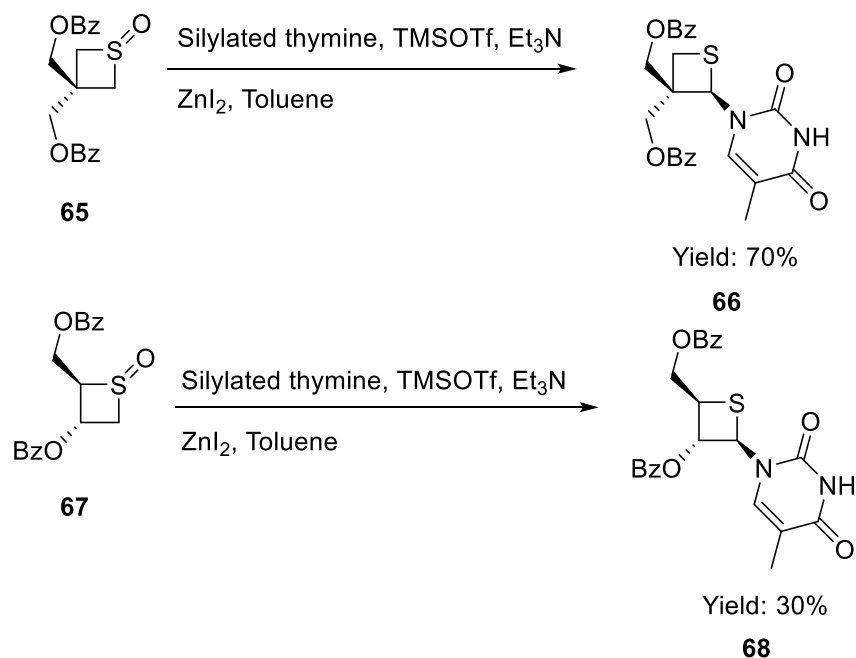
2.2.1 Formation of Thietane Nucleosides

Historically, thietane nucleosides were formed via the Pummerer reaction.^{10,17,22-25} A general mechanism is shown in scheme 2.1. Sulfoxide **60** and the sulfonium ylide **61** exist as resonant structures. Sulfonium ylide **61** attacks acetic anhydride. The resulting acetate **62** forms, which is deprotonated by the carboxylate ion. This forms the Pummerer intermediate **63** which undergoes a reaction with the silylated nucleobase to yield nucleoside **64**.



Scheme 2.1: General mechanism of the Pummerer reaction

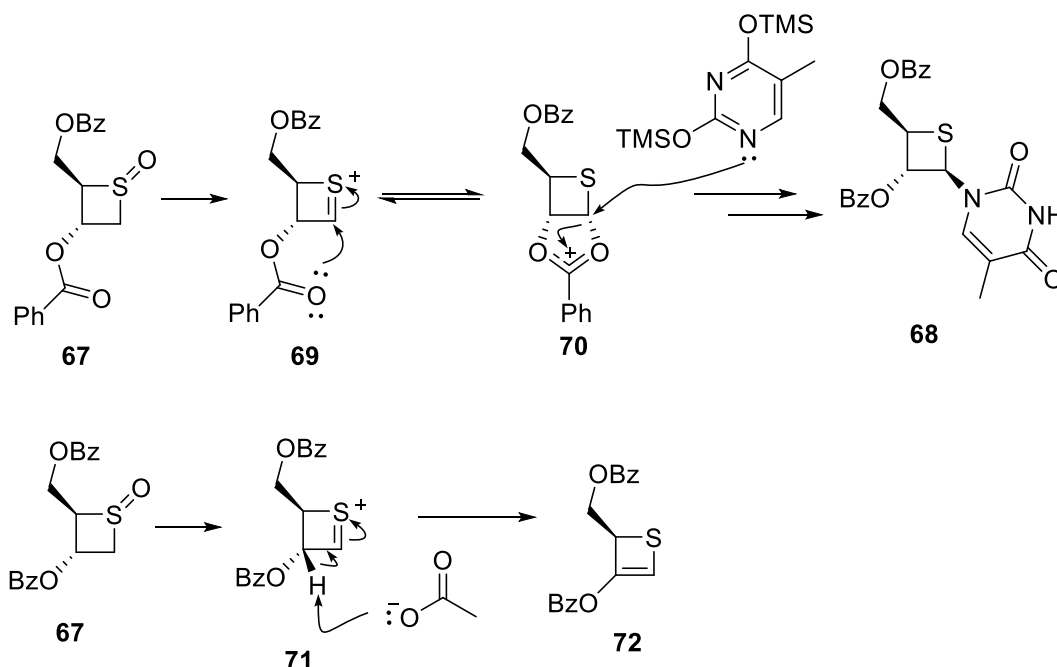
The yield of the Pummerer reaction depends upon the structure of the thietane precursor. Nishizono *et al.* first synthesised two sets of thietane nucleosides: one set with a 3,3-bis(hydroxymethyl)thietane core, compound **65**, and one set with a 3-hydroxy-4-hydroxymethyl thietane core compound **67**.¹⁰ It was observed that in the 3-hydroxy-4-hydroxymethyl thietane compounds, yields to the nucleoside were 30% overall, but for the 3,3-bis(hydroxymethyl)thietane compounds, the yield to the nucleoside was 70% under the same conditions (scheme 2.2). [Note, in this case, only the thymine derivatives were synthesised but showed no anti-viral activity against VSV for HSV-1,2].¹⁰



Scheme 2.2: Thietane core structure affects product yield.

The drop in yield was due to a major competing side reaction (scheme 2.3) which saw proton abstraction occurring at C-3 rather than at C-2 in thietane **67** (see

mechanism in scheme 2.1 for C-2 proton abstraction). Proton abstraction at C-3 in the 3-hydroxy-4-hydroxymethyl thietane compounds resulted in the unreactive product compound **72**.^{10,23}

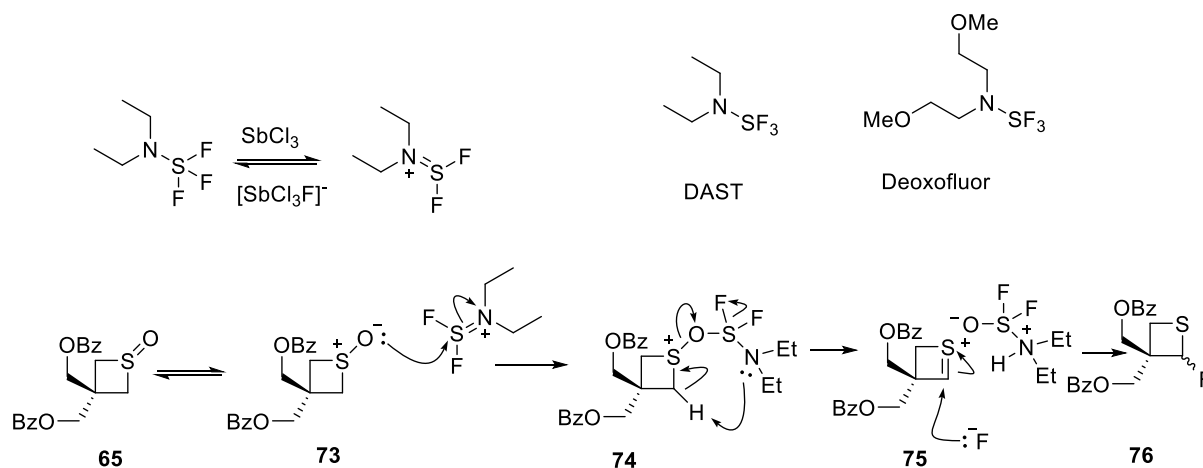


Scheme 2.3: Top: Pummerer rearrangement proceeds via neighbouring group participation of the –OBz group shown by **69** and **70**. The incoming nucleoside can only attack from the top face resulting in an diastereomerically pure product **68**. Bottom: Major competing reaction resulting in an unreactive intermediate that does not undergo Pummerer rearrangement.

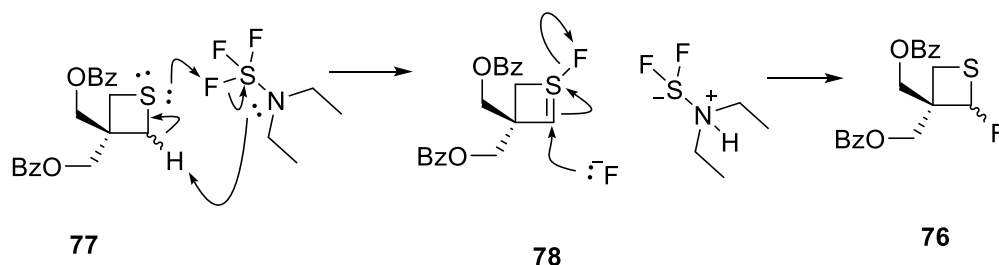
Choo *et al.* also noted low yields for the formation of the nucleosides (see table 2.2 for section 2.1.1) which were also attributed to proton abstraction at C-3 leading to the formation of the unreactive intermediate **72**.^{11,23} The yields for the Pummerer rearrangement for the Choo compounds ranged from 30-75% depending on the nucleobase used (30% for thymine versus 75% for cytosine). The difference in yield was due to the lower nucleophilicity of the cytosine moiety making it more selective toward attacking at the sulfur ylide, whereas the thymine moiety may be more nucleophilic and therefore prone to proton abstraction at C-3.¹¹

In order to improve the yields of thietane nucleoside formation newer methods of introducing the nucleobase onto the thietane ring have been developed. Standard nucleoside reactions consist of the use of a glycosyl halide and a silylated nucleobase to furnish nucleosides and are known as Vorbrüggen conditions.²⁶ Nishizono *et al.* devised two methods for the introduction of a halogen atom onto the

thietane ring so that the ring could act as the glycosyl halide.¹³ By introducing a fluorine atom to C-2 by using diethyaminosulfurtrifluoride (DAST) or deoxofluor, the glycosyl fluoride **76** could be furnished in high yield. The fluoride was chosen as it is more stable than typically used glycosyl chlorides or bromides. The reaction mechanism proceeds via the fluoro-pummerer reaction to give the glycosyl fluoride from a sulfoxide (scheme 2.4) with yields of 86% (DAST) and 22% (Deoxofluor), and from a sulfide with yields of 92% DAST and 83% deoxofluor (scheme 2.5).^{13,27}



Scheme 2.4: Fluoro-Pummerer reaction from a sulfoxide **65**

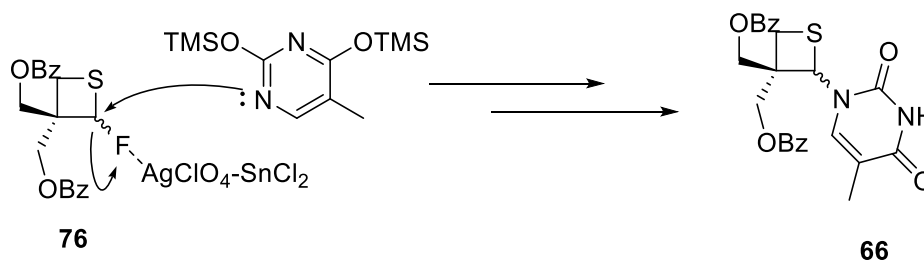


Scheme 2.5: fluoro-Pummerer reaction from a sulfide **77**. Note $[\text{SbCl}_3\text{F}]^-$ liberates fluoride ions as the reaction proceeds.

From sulfoxide **65**, fluorination proceeds via a standard Pummerer rearrangement, but from sulfide **77**, the fluoro-Pummerer rearrangement occurs via a six membered transition state to sulfur ylide **78**.^{24,25,27} Two processes occur in this reaction: SbCl_3 catalyses the formation of the initial fluoride ions that form the first set of 2-fluorothietane **76** molecules. Once the sulfur ylide **78** forms, the second process of liberating fluoride ions begins by reaction of fluoride ions at ylide **78**.^{24,25,27} This means a slight excess of the deoxofluor or DAST is required when using sulfides.

The use of sulfides for the fluoro-Pummerer reaction is advantageous as it removes a step: the oxidation of the thietane to sulfoxide **65**. Another advantage of using a sulfide is that the yields are comparable when DAST or deoxofluor are used (92% DAST and 86% deoxofluor).^{13,27}

Formation of the thietane nucleosides under the Pummerer reaction gave variable yields (scheme 2.2 page 41).²⁸ Under the Vorbrüggen conditions utilised by Nishizono *et al.*, using a fluorophilic activator complex of $\text{SnCl}_2\text{-AgClO}_4$ the thymine and 6-chloropurine derivatives were furnished with yields of 56% and 42% respectively.^{13,26} Though under the Pummerer reaction the 3,3-bis(hydroxymethyl) thietane nucleosides were furnished with a yield of 70%, the Pummerer reaction was only applied to one nucleobase (thymine).¹⁰ Choo *et al.* have shown utility of the Pummerer reaction, but yields were low and major competing reactions were an issue (see section 2.2.1).¹¹ It is clear that at the start of this project, both the Pummerer reaction and the Vorbrüggen conditions must be assessed to determine the most viable synthetic method toward target thietane nucleosides. However, it is predicted that, based on the evidence presented in this section, that the Vorbrüggen conditions may give the most reproducible reactions compared to the Pummerer reaction.



Scheme 2.6: Mechanism of thietane nucleoside formation under Vorbrüggen conditions

From the literature, the 3,3-bis(hydroxymethyl)thietane nucleosides have not been fully assessed for their anti-viral activity as only one nucleoside (the thymine derivative **66**) has been tested against VZV and HSV-1,2, which showed no activity.¹⁰ It has been shown in section 2.1 that thietane nucleosides are more stable and potentially more active than their oxetane counterparts, despite their higher cytotoxicity in blood cells.¹¹ Formation of the 3,3-bis(hydroxymethyl) thietane core will follow the synthesis of Nishizono *et al.*, and both the Pummerer reaction and

Vorbrüggen conditions will be investigated to assess which reaction gives access to the nucleosides in good yields.

The target compounds are shown in figure 2.3. The nucleobases chosen are based on the active compounds discovered by Choo *et al.*, along with all of the standard nucleobases.¹¹

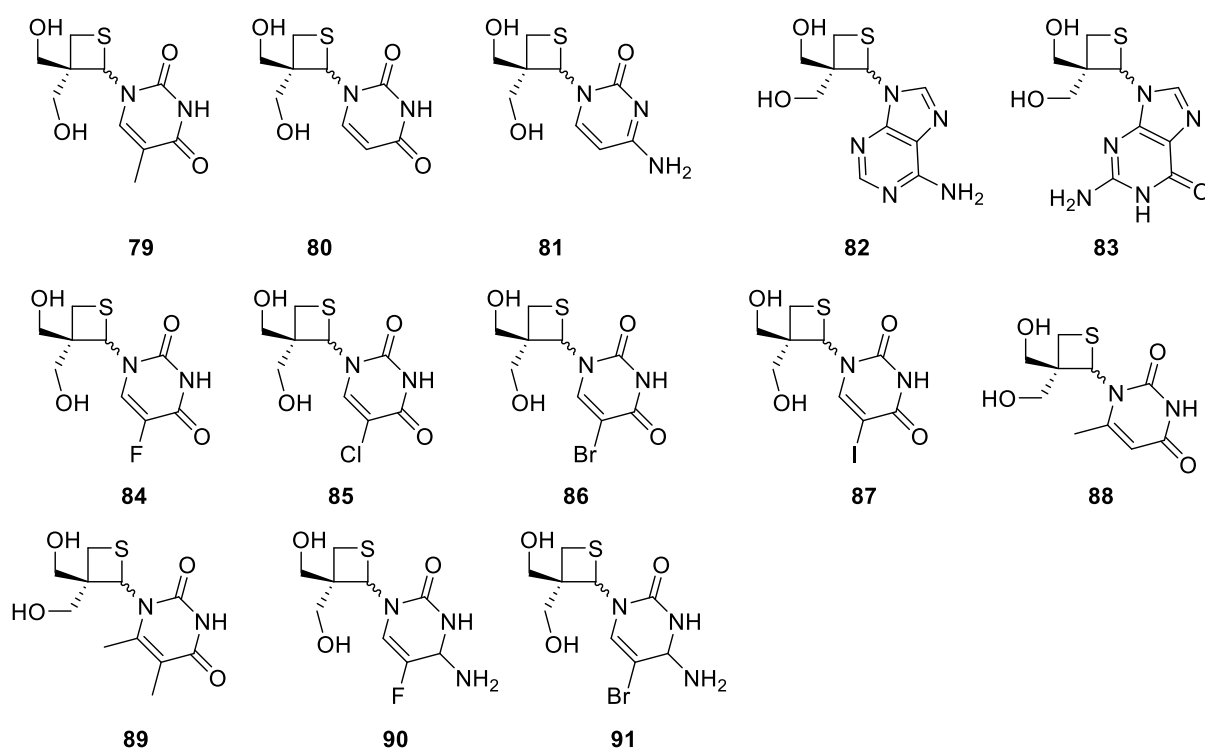
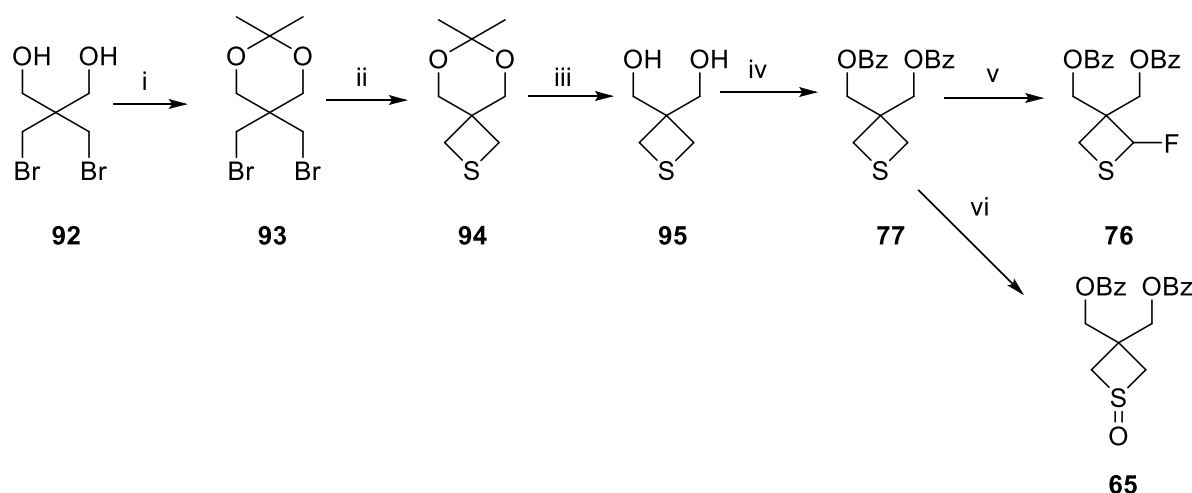


Figure 2.3: Target compounds

Further to the initial aims in section 2.2, the structure activity relationship of the pyrimidine bases will be assessed. This will be used to guide the synthesis of compounds in subsequent compound libraries with the overall aim of fully assessing the complete SAR of the geminal bis(hydroxymethyl) thietane core; and using this information to guide the synthesis of highly potent nucleosides. The halogenated variants, nucleosides **84-87** and **90-91**, have shown activity in several different anti-viral agents and the purine derivatives **82** and **83** expected to be inactive or minimally active.^{3,6,11,29-40}

2.3 Synthetic Strategy towards 3,3-bis(hydroxymethyl) thietane nucleosides

Synthesis of the 3,3-bis(hydroxymethyl) thietane core proceeded with ease (scheme 2.7) according to the synthesis reported by Nishizone *et al.*¹³ During the initial stages of the synthesis both the Pummerer reaction and the Vorbrüggen conditions were assessed for suitability to furnish the thietane nucleoside. Both fluoride **76** and sulfoxide **65** could be easily synthesised from the dibenzoate **77** with yields in excess of 80% on multi-gram scales.



Scheme 2.7: Conditions: i) *p*TSA, 1,2-DMP, Acetone, RT, 24 hrs, 91% ii) Na₂S·9H₂O, DMF, 110° C, 24 hrs, 94% iii) *p*TSA, MeOH, RT, 86% iv) BzCl, DMAP, DCM, RT, 24 hrs, 78% v) Deoxofluor, SbCl₃, DCM, RT, 86% vi) NaIO₄, MeOH, RT, 24 hrs, 64%

The synthesis began from commercially available 2,2-bis(bromomethyl)-1,3-propanediol **92** which was reacted with 2,2-dimethoxypropane to form the isopropylidene dibromide **93** on scales ranging from 1 g to 100 g from 2,2-bis(bromomethyl)-1,3-propanediol **92**. ¹H NMR spectroscopic analysis (figure 2.4) confirmed that the isopropylidene group was present with the methyl group protons present at 1.4 ppm with an integration of 6 protons. Two distinct CH₂ environments were evident at 3.6 and 3.8 ppm, both integrating to 4 protons each.

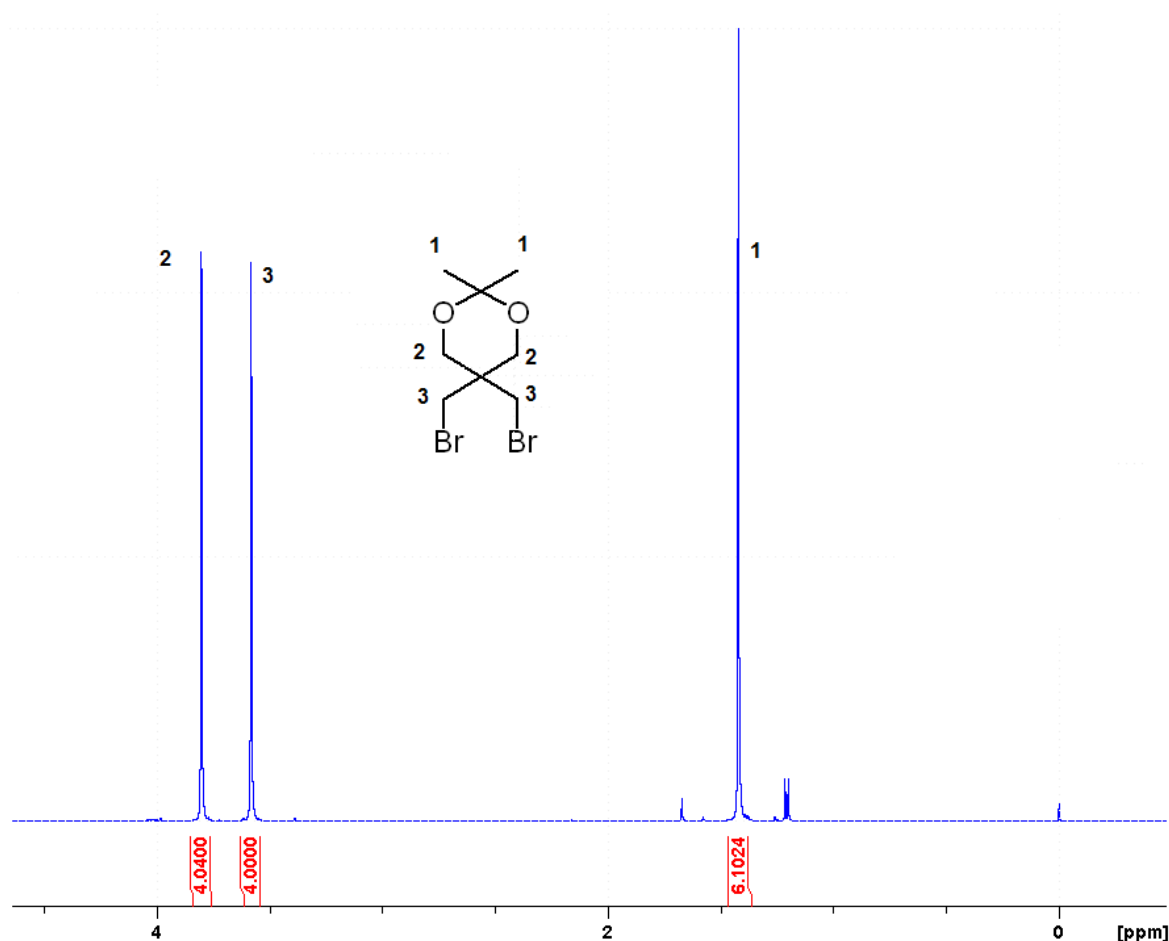


Figure 2.4: ^1H NMR spectrum of isopropylidene dibromide **93**

This result is as expected as the CH_2O methylene protons are more deshielded than the CH_2Br methylene protons. Mass spectrometry gave three peaks for the isopropylidene dibromide $\text{M}+\text{H}^+$ at 301, the $\text{M}+2+\text{H}^+$ at 303 and $\text{M}+4+\text{H}^+$ at 305, which are indicative of the bromine isotopic abundance ($\text{M}+\text{H}^+$ ^{79}Br - ^{79}Br , $\text{M}+2+\text{H}^+$ ^{79}Br - ^{81}Br and $\text{M}+4+\text{H}^+$ ^{81}Br - ^{81}Br).

Formation of the isopropylidene thietane **94** using $\text{Na}_2\text{S}\cdot 9\text{H}_2\text{O}$ proceeded in high yield, on scales ranging from 1 g to 50 g. ^1H NMR spectroscopic analysis (figure 2.5) showed the methylene peaks at 3.6 ppm shifting down to 3.0 for the CH_2SCH_2 methylene protons whilst the CH_2O protons shifted slightly to 3.9 ppm. These shifts are expected; the CH_2O methylene protons moving by 0.1 ppm could be indicative of changing electronic structure due to ring strain provided by the thietane ring. The smaller peaks either side of the main peaks seem to indicate that the reaction concentration was too high, and that there is possibility that the thiol compound **96**

has reacted with compound **93** to form a dimer. This can be avoided by reducing the concentration of the reactants. Low concentrations tend to favour intramolecular reactions, as this is entropically favoured.

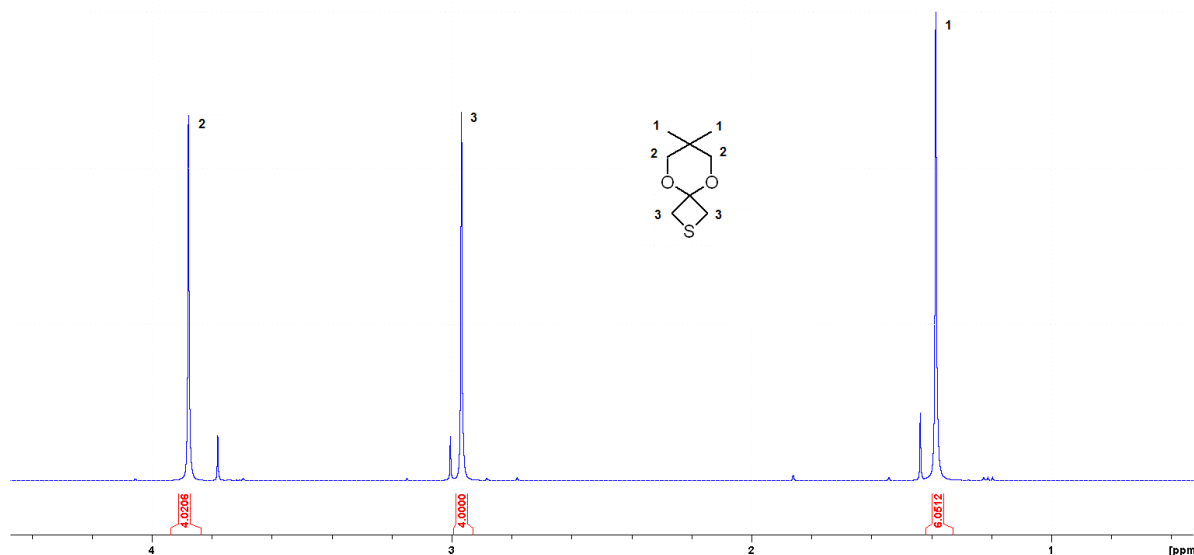
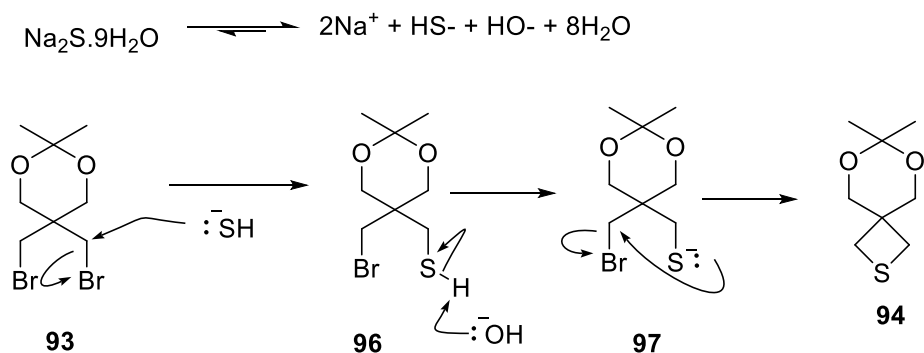


Figure 2.5: ^1H NMR spectrum of isopropylidene thietane **94**

The CH_2SCH_2 upfield shift is indicative of the lower electronegativity of the sulfur atom, and hence less deshielding of the CH_2 methylene protons occurred. However, due to the reaction mechanism, where $\text{S}_{\text{N}}2$ displacement of the bromine atoms occurs (scheme 2.8) there is a possibility that a dithiol could have formed. This would give the symmetric NMR spectrum that was obtained and the change in chemical shifts that were observed.⁴¹⁻⁴³



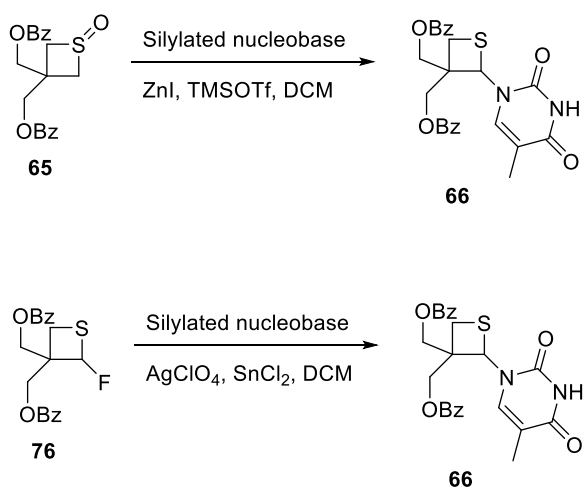
Scheme 2.8: Reaction mechanism of thietane formation

Mass spectrometry data gave the M+H for thietane **94** at 175.0788 Da which confirmed that the thietane compound had been synthesised and was in agreement with the literature.¹³

Deprotection of the isopropylidene thietane **94** to the diol **95** was achieved in quantitative yields using *p*TSA on scales ranging from 1 – 50 g from isopropylidene **94**. ¹H NMR spectroscopic analysis of the purified diol **95** showed no peaks for the isopropylidene acetal at 1.4 ppm, which is in agreement with the literature, and the IR spectrum showed a broad peak at 3300 cm⁻¹ for the diol.¹³ The CH₂OH methylene protons shifted to 3.9 ppm as expected due to the greater deshielding effect of the free hydroxyls over the isopropylidene acetal. A mass spectrum of the diol **95** gave an M+H⁺ of 135 Da as expected.

Next, diol **95** was reacted with benzoyl chloride on scales ranging from 10 – 20 g to furnish dibenzoate **77**. The proton NMR showed the CH₂OH methylene protons moving downfield from 3.9 ppm in diol **95** to 4.4 ppm. This is due to the greater deshielding effect of the benzoate protecting group. In diol **95** and dibenzoate **77** the CH₂SCH₂ methylene protons only moved by 0.2 ppm, which is attributed to the changing electronic structure at the CH₂O groups.

Once dibenzoate **77** had been synthesised, two potential routes to the thietane nucleosides were evident from the literature. From sulfoxide **65** a Pummerer reaction could be used to furnish the nucleosides, or from fluoride **76** the Vorbrüggen conditions could be used and hence both reactions were explored (scheme 2.9).



Scheme 2.9: Top: Pummerer reaction. Bottom: Vorbrüggen conditions.

From dibenzoate **77**, NaIO₄ was used to furnish the sulfoxide **65** which gave an interesting ¹H NMR spectrum (figure 2.6).

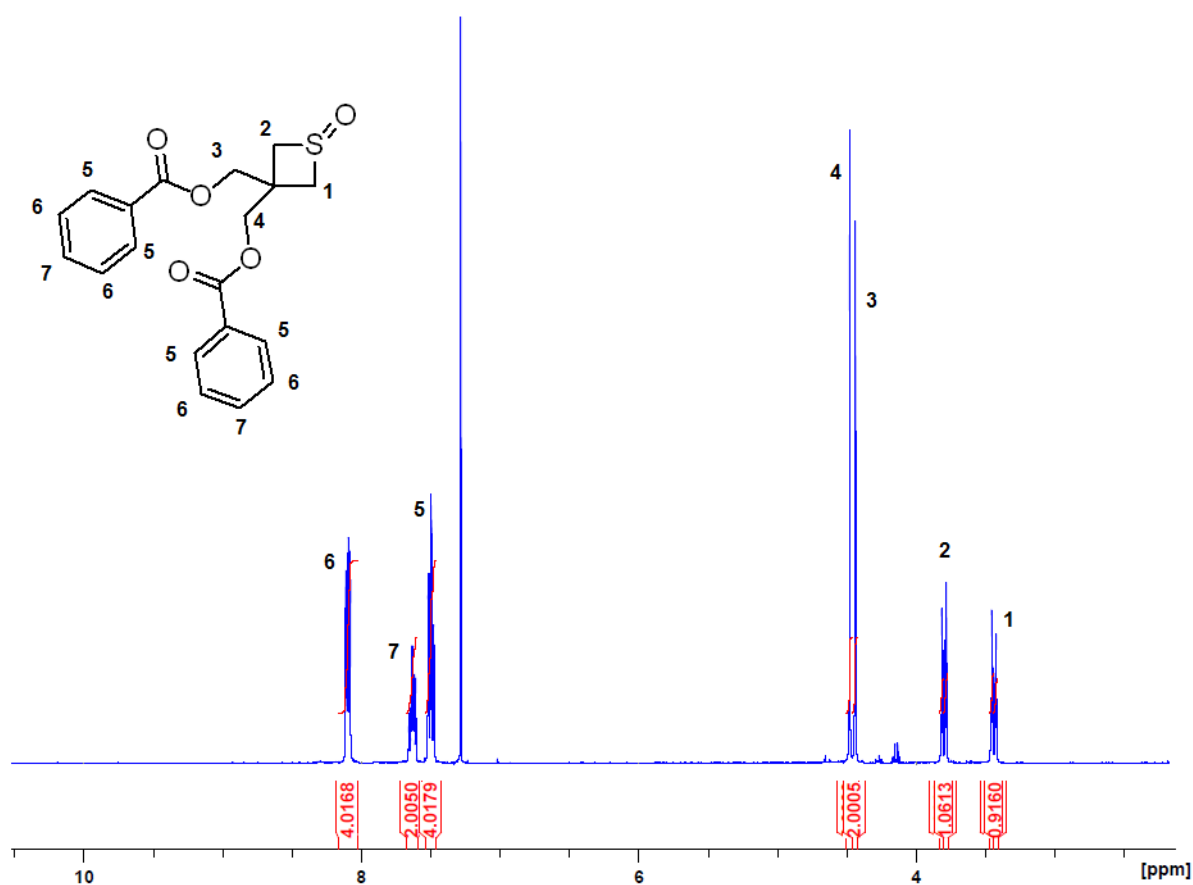


Figure 2.6: ¹H NMR spectrum of sulfoxide **65**

The CH₂S=OCH₂ protons were both doublets of doublets with *J* couplings of 3 Hz and 10.0 Hz respectively but the CH₂OBz protons remained unchanged as singlets integrating to 2H for each CH₂OBz group. This is due to the sulfoxide being chiral and hence the protons occupying slightly different chemical environments (figure 2.7). The coupling of 10.0 Hz is attributed to geminal coupling between two protons on the same carbon atom, and the coupling of 3.0 Hz is attributed to a through bond coupling effect via the CH₂S=OCH₂ group.^{43,44}

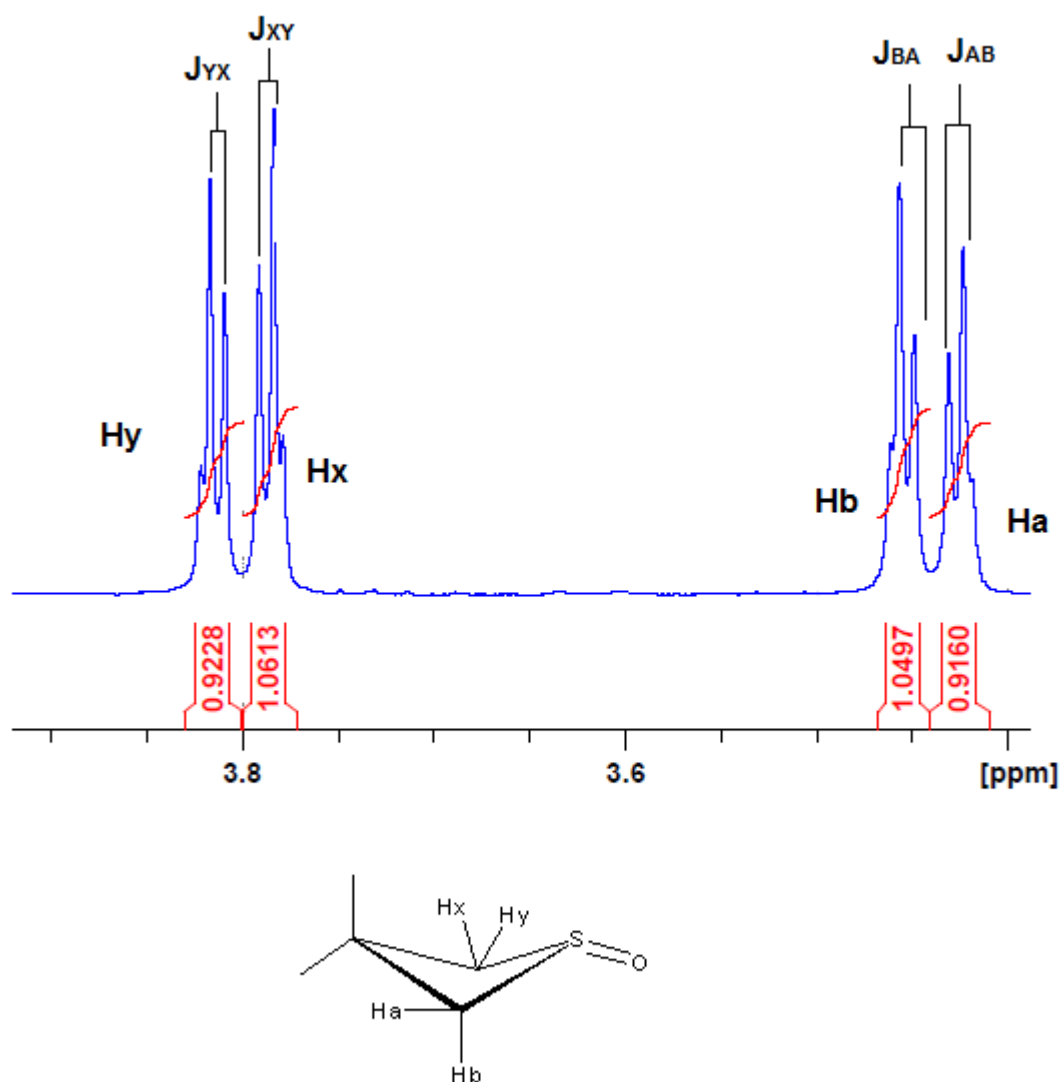


Figure 2.7: Sulfoxide **65** coupling patterns. Ha/Hb are conformationally non-equivalent to Hx/Hy

As can be seen from figure 2.7 both protons 1 and 2 are shown and can be seen as a pair of doublet of doublets. Fronza et al have shown that protons Ha and Hb are conformationally non-equivalent to Hx and Hy and are seen as separate doublets where Ha and Hb couple to each other as do Hx and Hy. This gives rise to a potential for an ABX system to arise, however, these doublets are not a true ABX system.⁴⁵⁻⁴⁷ In an ABX system, Ha and Hb couple strongly to each other, and weakly couple to Hx. In the sulfoxide, this is not specifically seen as H_{AB} and H_X are not seen separately as would be expected.^{46,47} In sulfoxide **65** Ha couples to Hb and Hb couples to Ha to give the two doublets. The same is true for Hx and Hy. However, analysis of the doublet shows that they are not true doublets, with spurs that indicate

an interaction between Ha/Hb with Hx/Hy as they are conformationally non-equivalent to each other. In order to resolve this, either temperature dependant NMR is required or a larger frequency spectrometer would be required to tease out the interaction between Ha/Hb with regards to Hx and vice versa. There is potentially an ABX interaction occurring, however, the J value for $J_{AX/BX}$ etc is not obvious from this data.

The extreme change in chemical shift of the methylene protons in CH_2SCH_2 to $\text{CH}_2\text{S}=\text{OCH}_2$ methylene protons from 2.9 ppm to 3.9 ppm is due to the charge on the sulfur ylide. This significantly deshields the $\text{CH}_2\text{S}=\text{OCH}_2$ methylene protons giving rise to the higher chemical shift as the proton can interact with the applied magnetic field.

Synthesis of glycosyl fluoride **76** from dibenzoate **77** (scheme 2.7) required optimisation as the fluorination reaction was very sensitive to air and moisture, the amount of SbCl_3 catalyst and to the reaction time. Though Nishizono *et al.* formed the glycosyl fluoride from both sulfoxide **65** and dibenzoate **77**, it was decided to only concentrate on fluoride formation from dibenzoate **77** as this removed one step from the synthesis allowing for quicker access to the fluoride. It must be noted that isopropylidene **93**, isopropylidene thietane **94** and dibenzoate **77** were purified by recrystallization from isopropyl alcohol (IPA). Only diol **95** and fluoride **76** required purification by column chromatography. On scale up from isopropylidene **93**, purification was avoided all the way to dibenzoate **77** and the yield of dibenzoate **77** was unaffected which meant that time scales for reaction scheme could be reduced from 8 days to 5 days which includes reaction times and purifications. However, glycosyl fluoride **76** required column chromatography for purification which led to increased time scales.

Initial small scale exploratory reactions using DAST and Deoxofluor gave mixed results (table 2.3). Two factors were found to be important to furnish glycosyl fluoride **76**: the amount of SbCl_3 catalyst and the equivalents of DAST or deoxofluor.

Table 2.3: Optimisation reactions to glycosyl fluoride **76**: Effect of catalyst

Reaction	Reagent	Equiv	SbCl ₃ (%)	Time (hrs)	Outcome	Yield (%)
1	DAST	1.5	1	24	13% mass recovery of total mass on column	-
2	DAST	1.5	1.5	24	37% mass recovery of total mass on column	-
3	DAST	1.5	10	24	Impure product	-
4	DAST	1.5	20	24	Degraded product	-
5	DeoxoFluor	1.5	1	24	Product isolated	15
6	DeoxoFluor	1.5	1.5	24	Product isolated	19
7	DeoxoFluor	1.5	10	24	Product isolated	46
8	DeoxoFluor	1.5	20	24	Product isolated	38

As table 2.3 shows, DAST was not an ideal reagent for furnishing fluoride **76** and it is thought that it generates fluoride ions quickly, resulting in excess HF in solution. The HF in solution would degrade the compound, and this was seen by analysis of the ¹H NMR spectrum, where no peaks associated with the products were observed. For DAST, increasing the catalytic loading did not give rise to any product, however, for DeoxoFluor, increasing the catalytic loading did increase the yield of the final product. It was found that 10% SbCl₃ was ideal for forming fluoride **76**; however, 20% SbCl₃ was found to lower the yield. Analysis of the ¹H NMR spectrum for reaction 8 showed some degradation of the product. This could be due to the fact that at 20% catalytic loading, fluoride ions are forming at a greater rate than the thietane can react with them. This then could form HF in solution, which would destroy some of the compound. Table 2.4 shows that increasing the reaction time increased the yield of the fluoride **76**.

Table 2.4: Effect of increased reaction time on the yield of fluoride **76**

Reaction	Reagent	Equiv	SbCl ₃ (%)	Time (hrs)	Outcome	Yield (%)
1	DeoxoFluor	1.5	10	24	Product isolated	46
2	DeoxoFluor	1.5	10	48	Product isolated	58
3	DeoxoFluor	1.5	10	72	Product isolated	86
4	DeoxoFluor	1.5	10	96	Product isolated	83

In general, table 2.4 shows that by increasing the reaction times increases in yields were observed. It was found that 72 hours was an optimal time for the reaction to go to completion. Any longer and no appreciable gains in yields were obtained, and at 96 hours, a yield of 83% for fluoride **76** was obtained. Therefore, it was found that 10% catalytic loading with 1.5 equivalents of deoxofluor reacting for 72 hours was the optimal reaction conditions. In order to try and bring the reaction time down, 2 equivalents of deoxofluor were trialed; however, di-fluorination of the thietane ring resulted after 48 hours. Although this indicated the reaction rate did increase, the end result was a di-fluorinated thietane ring as the product, which was unwanted.

An interesting feature of the NMR of glycosyl fluoride **76** is the doublet at 6.1 ppm (figure 2.8). This doublet has a coupling constant of 64 Hz which is the coupling between the H-1 and fluorine on C-1.

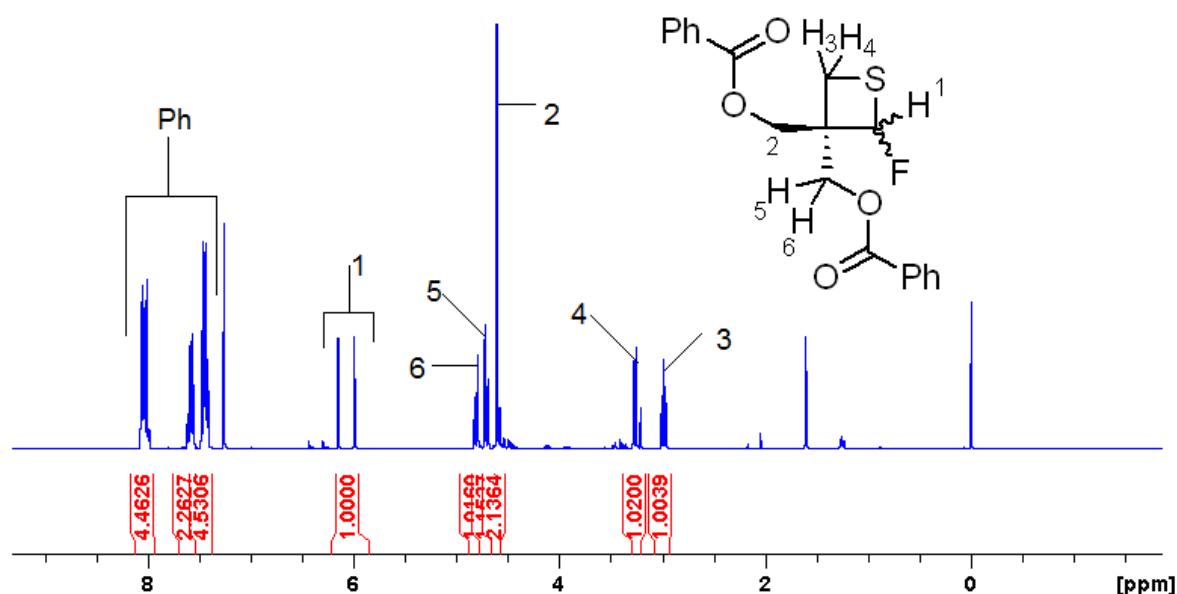


Figure 2.8: ^1H NMR spectrum of fluorothietane **76**

One of the CH_2O groups integrates to 2 and on the other CH_2O group, geminal coupling is observed with a coupling constant of 10 Hz. Protons 3 and 4 also show geminal coupling, one as a doublet and one as a triplet. The triplet is geminal coupled to the proton on the same carbon and W coupled to the proton on the SCHF carbon. It would be expected that both protons on C-3 should be double doublets but is observed as a triplet in the ^1H NMR spectrum due to the possibility that there is peak overlap (figure 2.9).

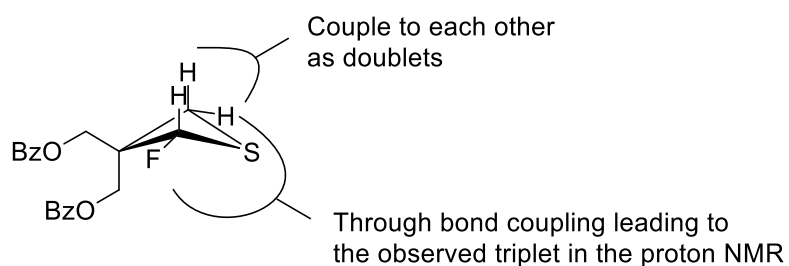


Figure 2.9: Coupling of C-3 protons to the SCHF bond. As can be seen, the protons on C-4 occupy different environments. One proton couples to its neighbour giving rise to the doublet and the other proton couples to the proton and the fluorine on C-1 as a through bond effect.

In the carbon NMR spectrum C-1 has a coupling of 248 Hz as expected since fluorine and carbon also couple. ^{19}F NMR spectroscopic analysis shows the fluorine

is present as a doublet at -157 ppm (63.5 Hz) and is within the expected range for this compound (figure 2.10).

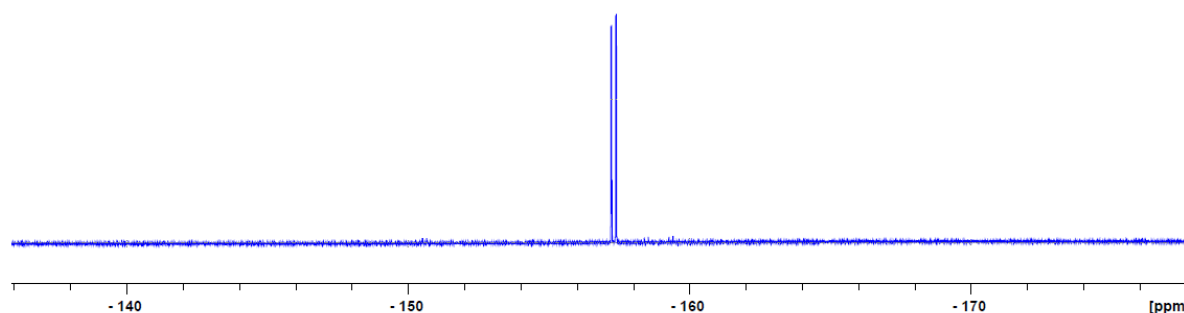
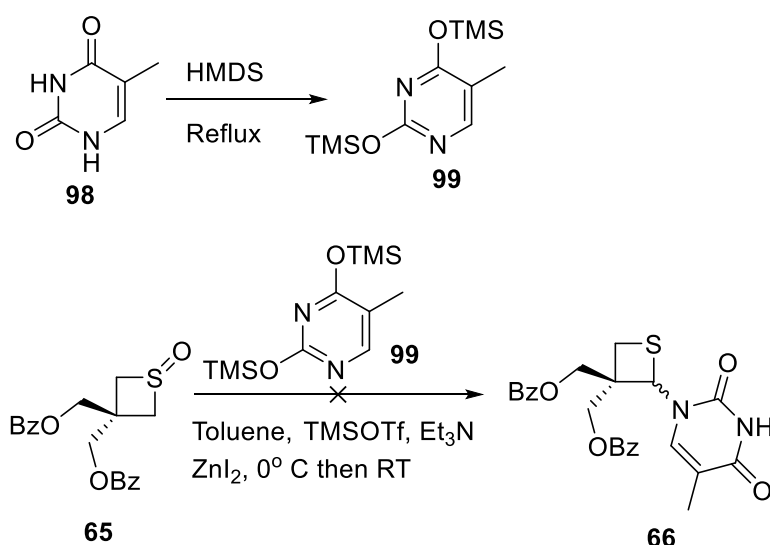


Figure 2.10: ^{19}F NMR of fluorothietane **76**

2.3.1 Synthesis of Thietane Nucleosides via the Pummerer Reaction

Two routes to thietane nucleosides were explored: one route using the Pummerer reaction and one route using Vorbrüggen conditions. The reaction conditions chosen were identical to the first synthesis published by Nishizono *et al.* in 1996.¹⁰ First, thymine was heated at reflux in hexamethyldisilazane (HMDS) to effect silylation (scheme 2.10). By doing so, the thymine is soluble in the reaction conditions and should be able to react with sulfoxide **65**. Once the HMDS is removed under reduced pressure, the silylated thymine is dissolved in toluene and the sulfoxide, triethylamine and TMSOTf are added followed by ZnI_2 . Two equivalents of the silylated thymine were used to one equivalent of sulfoxide **65** in all reactions.



Scheme 2.10: Pummerer reaction to thymine nucleoside

Nishizono *et al.* reported yields of 70% when the reaction was performed in toluene or DCM under the conditions in scheme 2.10, however, these results could not be replicated even after leaving the reaction for 48 hours. Analysis of the crude ^1H NMR spectrum showed only the presence of starting material peaks. Purification of the crude reaction material enabled starting material to be recovered and recycled with a yield of 90%. Table 2.5 shows the reaction conditions attempted.

Table 2.5: Pummerer reaction conditions

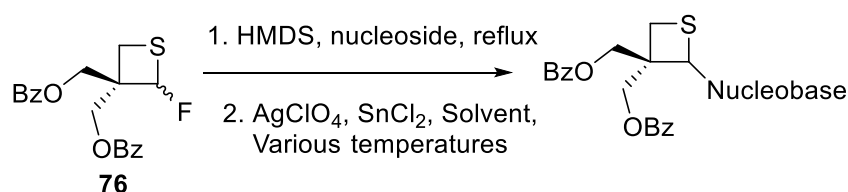
Reaction	Temperature ($^\circ\text{C}$)	Scale (mg)	Solvent	Time (hrs)	Result
1	0	100	Toluene	30	SM recovered
2	0	100	Toluene	48	SM recovered
3	25	100	Toluene	48	SM recovered
4	0	100	DCM	30	SM recovered
5	25	100	DCM	48	SM recovered

All reactions were stopped after 48 hours based on TLC analysis and analysis of the crude reaction by ^1H NMR spectroscopy. TLC analysis of the crude reaction showed no changes in R_f or the number of spots and analysis of the crude reaction mixture by ^1H NMR spectroscopy did not show product formation. Initially, it was thought that the reaction was not left for long enough, and so the reaction was left for 24 hours. However, no change was observed and thus the reaction temperature was raised as it was thought that raising the temperature would give favourable kinetics for product

formation. With no product forming, DCM was trialled as it was suspected that the silylated nucleobase was not dissolving adequately enough in toluene. However, as can be seen from table 2.4, no reaction was observed. It was also suspected that completely removing the HMDS (by azeotrope with toluene) could be causing deprotection of the trimethylsilyl groups on the silylated nucleobase. In subsequent reactions, the HMDS was removed under reduced pressure to leave an oily residue instead. In these reactions, no reactions were observed and it is highly likely that the TMSOTf was quenched by the residual HMDS left behind.

2.3.2 Synthesis of Thietane Nucleosides under Vorbrüggen Conditions

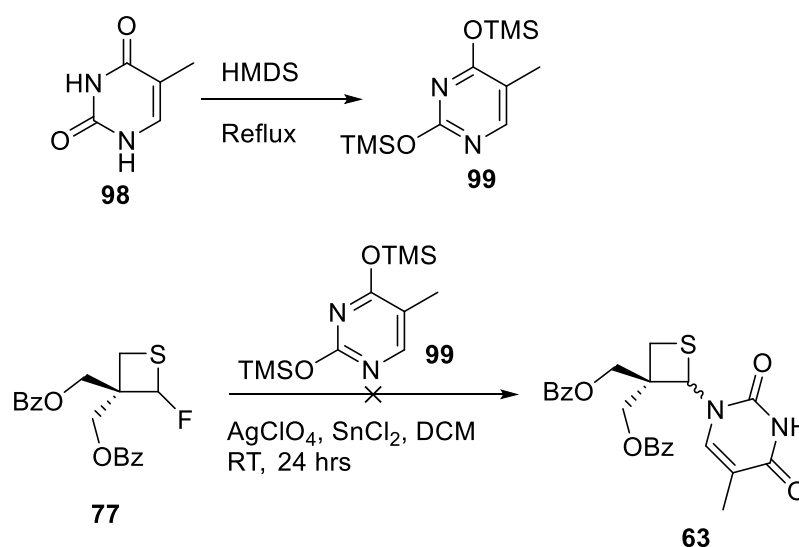
In parallel to the Pummerer reaction, the glycosyl fluoride **76** chemistry had been optimised and the Vorbrüggen conditions were trialled with great success.^{13,26} Following the Nishizono *et al.* conditions for the thymine nucleoside **66**, the nucleoside was furnished with a yield of 57% after reacting in DCM at room temperature for 18 hours.



Scheme 2.11: General reaction scheme toward thietane nucleosides

In all cases except for nucleoside **66**, the reaction conditions set out by Nishizono *et al.* required optimisation either for silylation of the nucleobases, or application of the Vorbrüggen conditions.

As with the Pummerer reaction for the synthesis of nucleoside **66**, thymine was first silylated with HMDS (scheme 2.12).



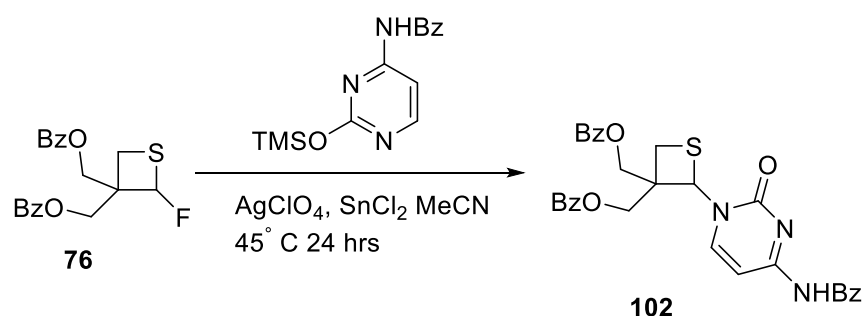
Scheme 2.12: General conditions for the Vorbrüggen synthesis

The HMDS was removed under reduced pressure before the silylated thymine was dissolved in DCM, then AgClO₄, SnCl₂ and glycosyl fluoride **76** were added. The reaction scales ranged from 100 mg exploratory reactions up to multi gram scale and the reaction mixtures were purified by flash column chromatography after optimisation of the column conditions were achieved. Nucleosides **66**, **100** – **107** were all synthesised and purified on these scales.

HMDS was used in all silylation reactions except for the uracil derivative and the 5-chloro, 5-bromo, and 5-iodo moieties. It was also noted that use of ammonium sulfate as a catalyst reduced the reaction times from 4- 24 hours to 1-4 hours. Initially, it was observed that silylation of uracil using HMDS worked well up until removal of the HMDS *in vacuo*, where loss of the TMS groups was observed. It is suspected that the TMS groups on uracil were labile under the conditions used for removing HMDS. No reaction between the fluorothietane and uracil was observed when HMDS was used as the silylating agent, further adding to suspicions that the TMS groups were labile. Instead, *N,O*-bis(trimethylsilyl) acetamide (*N,O*-BSA) was used.⁴⁸ The general procedure required suspending uracil in MeCN and injecting 1.1 equivalents of *N,O*-BSA under argon then heating to 70° C for an hour. Completion was determined when the solution became clear. At this point, the reaction was cooled to room temperature and the fluorothietane and Lewis acids were added *in situ*. The advantage here was that there was no need to remove the solvent or *N,O*-BSA under

vacuum. This prompted exploration of silylation methods that were quick and efficient and therefore both HMDS and *N,O*-BSA were assessed as silylating agents.

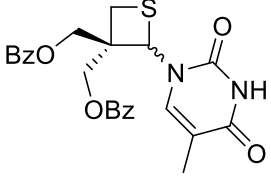
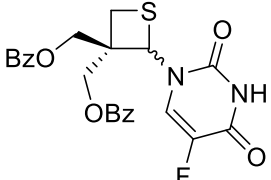
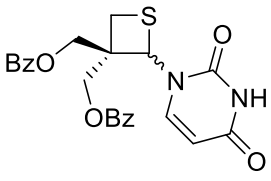
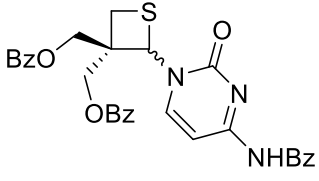
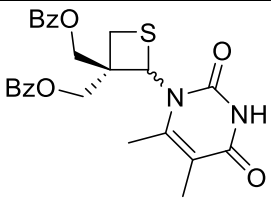
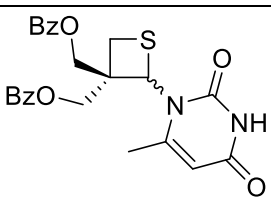
Synthesis of the cytosine moiety **102** proved difficult however. Initial attempts to synthesise the silyl protected cytosine nucleobase following the method reported by Schütz *et al.*, did not yield the silylated cytosine moiety even after heating to reflux in HMDS for 24 hours.⁴⁹ Instead, *N*⁴-benzoylcytosine was synthesised (later purchased from Sigma Aldrich) was heated to reflux in HMDS for 24 hours to afford the silylated cytosine moiety. After removal of HMDS *in vacuo*, the cytosine moiety was suspended in DCM and the fluorothietane and Lewis acids were added. However, at room temperature the reaction was not complete at 24 hours. This was due to the observed insolubility of the *N*⁴-benzoyl-6-(trimethylsilyl)-cytosine moiety in DCM. Repeating the reaction in MeCN at room temperature did not improve the outcome; the reaction was not complete within 24 hours and required 48 – 72 hours to reach completion. Heating to 45° C over 24 hours resulted in a yield of 47% for nucleoside **102** (scheme 2.13).

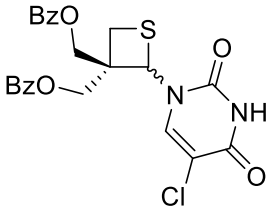
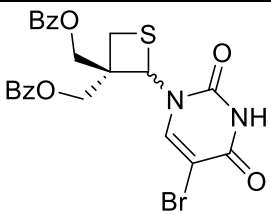
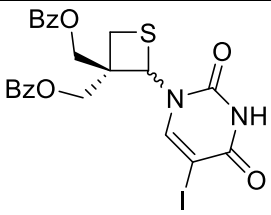


Scheme 2.13: Synthesis of cytosine nucleoside **102**

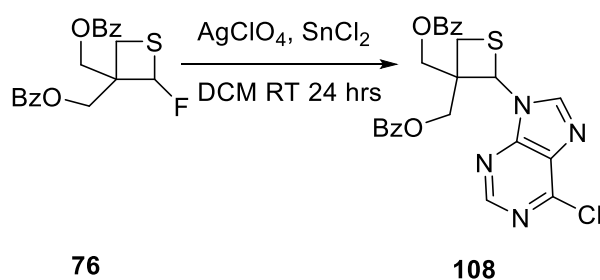
Table 2.6 shows yields and structures of the compounds synthesised along with the ¹H NMR spectroscopic data for the SCH-nucleoside bond and the expected and observed mass spectrometry data. The SCH-nucleoside bond chemical shifts are broadly similar for all compounds, ranging between 5.8 – 6.0 ppm. The mass spectrum data revealed several important features of the molecules. For instance, for compounds **105** and **106** two mass ion peaks are observed. For compound **105** both ³⁵Cl and ³⁷Cl are observed with a ratio of 3:1 as expected based on the natural abundance of ³⁵Cl relative to ³⁷Cl. Both ⁷⁹Br and ⁸¹Br mass ion peaks with a ratio of 1:1 are observed for compound **107** since both bromine isotopes exist in a 1:1 ratio in Nature.

Table 2.6: Thietane nucleosides synthesised using Vorbrüggen conditions

Structure	Yield (%)	Key ¹ H NMR	MS Expected	MS Observed
 66	57	5.9	467.1271	467.1265
 100	45	6.0	471.1021	471.1017
 101	64	5.8	453.1115	453.1118
 102	47	6.0	556.1537	556.1539
 103	45	5.9	481.1427	481.1428
 104	38	5.8	489.1089	489.1089

 <p>105</p>	51	5.9	487.0725 489.0693	487.0725 489.0696
 <p>106</p>	66	5.9	553.0039 555.0019	553.0044 555.0022
 <p>107</p>	37	5.9	579.0081	579.0082

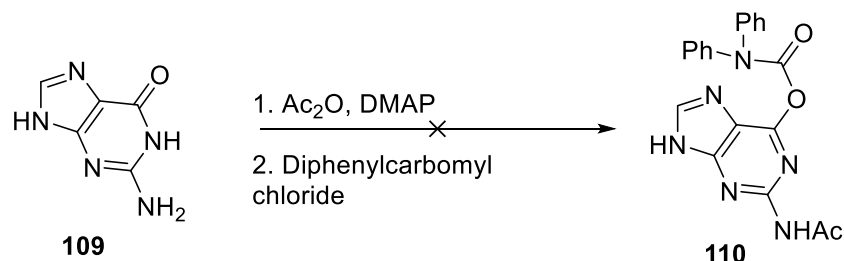
Attention was then turned to synthesis of the purine nucleosides. Attempts to synthesise the adenine and guanine moieties using Nishizono conditions were met with failure however. Nishizono *et al.* reported the synthesis of the 6-chloropurine substituted thietane **108**, however this reaction could not be reproduced (scheme 2.14).



Scheme 2.14: Nishizono synthesis of 6-chloropurine substituted thietane **108**

Although on small scales (100 mg) the compound could be observed by analysis of the crude reaction mixture by ^1H NMR spectroscopic analysis, with the key signal at 6.32 ppm being observed for the SCHN proton, purification via column chromatography proved difficult and the desired compound could not be isolated.

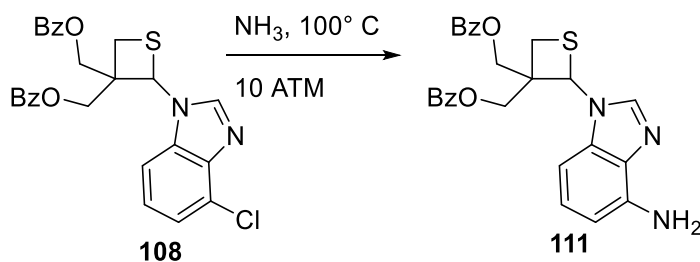
Attention was turned to alternative methods of synthesising the guanine derivative using diphenyl carbamoyl chloride to mask the ketone group and acetic anhydride to protect the -NH_2 group (scheme 2.15).⁵⁰



Scheme 2.15: Attempts to synthesise carbamoyl protected guanine **110**

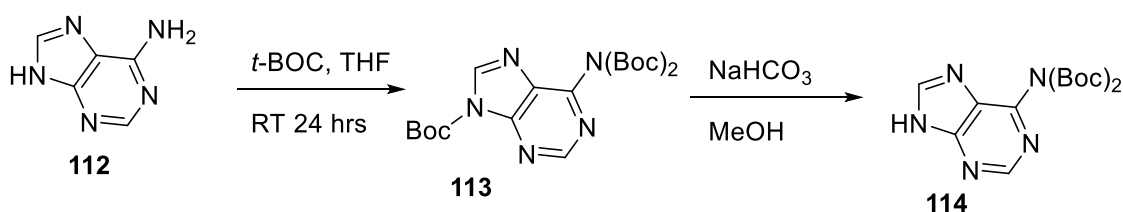
Though this literature method was attempted several times, the $^1\text{H-NMR}$ spectroscopic data did not match the reported data in any of the attempts.

Nishizono *et al.* also reported the synthesis of the adenine moiety **111** (scheme 2.16), via 6-chloropurine using gaseous ammonia at 100°C at 10 ATM.



Scheme 2.16: Nishizono synthesis of adenine **111** using gaseous ammonia.

A milder set of conditions could be used to achieve adenine **114** by suspending adenine **115** in THF and *t*-Boc to make the di-Boc adenine moiety (scheme 2.17).⁵¹



Scheme 2.17: Synthesis of diBoc adenine **114**

The di-Boc **114** adenine moiety was synthesised on a several gram scales. Initially, the tri-Boc **113** moiety is formed which is deprotected with sat NaHCO_3 in methanol to form the diBoc moiety as illustrated in scheme 2.17. Reaction with the fluorothietane and Lewis acids showed consumption of the fluorothietane over a 24 hour period however, purification was a problem. Although analysis of the crude reaction mixture by ^1H NMR spectroscopy showed product formation with the key signal at 6.5 ppm indicative of the proton on the same carbon as the bound nucleobase, TLC analysis showed several products were formed. Isolation of these individual components was not possible by column chromatography. Analysis by ^1H NMR showed the mixed fractions to contain varying amounts of product (36%), mono-Boc (36%) and free amine components (29%). At this stage, after many iterations of synthesis and attempts to isolate the diBoc adenine moiety, it was decided that after synthesis and purification through a plug of silica, the impure products would be globally deprotected.

Initial attempts with TFA in DCM to remove the Boc groups were successful, however, analysis of the crude reaction mixture by ^1H NMR spectroscopy showed that the adenine was no longer bound to the thietane ring. The key peak at 6.3 ppm for the SCHN proton was no longer observed. Use of formic acid in methanol and water gave the same result. Due to low yields, unreproducible reactions, and the instability toward acidic deprotection, the synthesis of the purine nucleosides was not pursued further.

2.3.2.1 Deprotection of the benzoate groups

Removal of the benzoate groups from compounds **66**, **101** – **107** was required prior to anti-viral screening as the free hydroxyl groups are required for anti-viral activity. These free hydroxyls covalently bond to phosphate groups on preceding nucleotides in the viral genome.

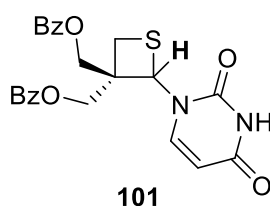
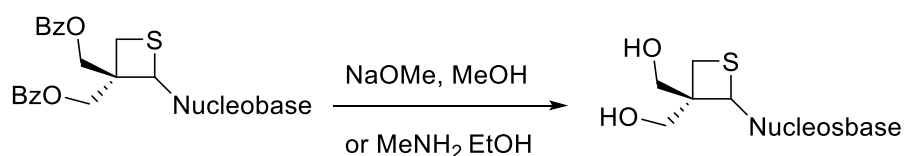


Figure 2.11: Structure showing the SCH bond that was indicative of product formation

Solubility of the products was the main driver behind the method of deprotection used. In all cases, MeNH₂ in EtOH was first used, the benefit being that the deprotection reactions took 2-6 hours, though purification was sometimes problematic. Compounds **66**, **100**, **102** - **107** were reacted for 2 hours, however, cytosine derivative **102** required 96 hours before completion was observed.

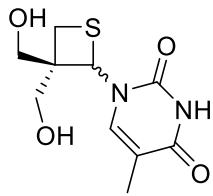
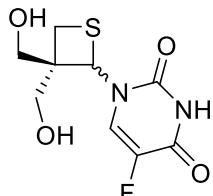
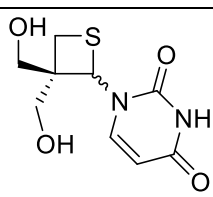
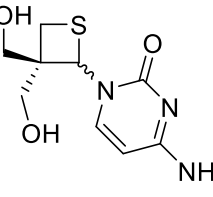
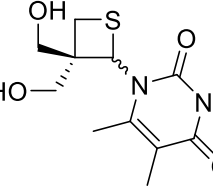
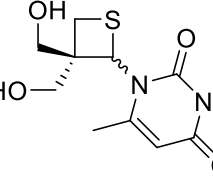
It was observed that reactions lasting more than 4 hours tended to cleave the nucleoside thietane bond, and the reason for this is unknown, but it is suspected that the methylamine is able to react as a nucleophile causing expulsion of the nucleobase. All that was observed by analysis of the ¹H NMR spectrum of the crude reaction mixtures were broadened peaks, masses of peaks that could be assigned to an elimination product nor could any peaks be found that could be associated with products. The low yield of cytosine derivative **102** is attributed to instability in the highly basic reaction conditions.

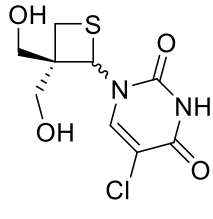
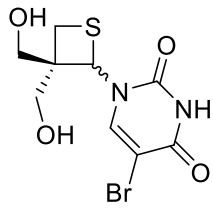
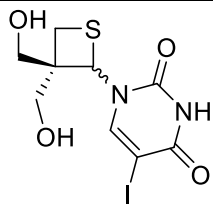
It was also noted that uracil derivative **101** did not react with methylamine in ethanol. It was suspected that this was due to a solubility issue so NaOMe was employed as the base in methanol. The reaction proceeded overnight and the product was isolated with a yield of 93%. NaOMe was used for the deprotection of all compounds **66**, **100** - **101** and **103** - **107** as NaOMe was milder and all compounds were found to be more stable to NaOMe over MeNH₂ for the reasons outlined above. Derivative **102** could not be reacted with NaOMe as this reagent was insufficiently basic to cleave the *N*⁴-Bz group. Table 2.7 shows the free hydroxyl thietane nucleosides including key ¹H NMR spectroscopic data (SCH-nucleobase bond), HPLC purity data and expected and observed MS data. The HPLC purity data was obtained using MeCN:water under gradient elution conditions. The expected purity for each compound was intended to equal or exceed 95%.



Scheme 2.18: General scheme for the removal of benzoate groups

Table 2.7: Free hydroxyl thietane nucleosides with key data. Reaction conditions: a = NaOMe in MeOH, RT, 24 hrs b = MeNH₂ in EtOH, RT, 2 hrs

Structure	Yield (%)	Key ¹ H NMR	HPLC Purity	MS Expected	MS Observed	Conditions
 <p>79</p>	98	5.86 ppm	98.6%	259.0747	259.0749	b
 <p>84</p>	77	5.9 ppm	94.5%	263.0496	263.0498	a
 <p>80</p>	93	5.86 ppm	97.9%	245.0591	245.0591	a
 <p>81</p>	96	5.81 ppm	75.1%	244.0750	244.0752	b
 <p>89</p>	95	5.91	96.4%	295.0723	298.0725	a
 <p>88</p>	98	5.86	47.1%	259.0746 281.0564	259.0747 281.0566	a

 <p>85</p>	88	5.9	98.5%	279.0200 281.0170	279.0201 281.0171	a
 <p>86</p>	96	5.9	95.6%	322.9696 324.9674	322.9698 324.9675	a
 <p>87</p>	90	5.9	97.7%	370.9557 245.0591	370.9557 245.9813	a

All ^1H NMR spectroscopic data gave similar chemical shifts for the SCH-nucleobase bond. The halogenated nucleobases tended to give chemical shifts of 5.9 ppm or greater and the non-halogenated nucleobases tended to give chemical shifts sub 5.9 ppm and this is attributable to the greater deshielding effect of the halogenated nucleobases on the SCH-nucleobase bond. In figure 2.12 the ^1H NMR spectroscopic data is shown for derivative **80**.

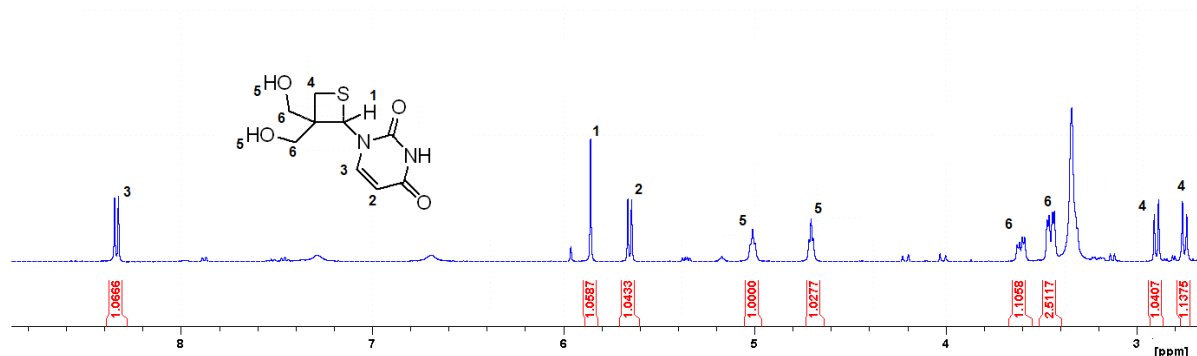


Figure 2.12: ^1H NMR spectrum of spectroscopic data for uracil **80**.

The mass spectrum for compound **87** confirmed the compound but also showed the presence of the uracil compound too. The mass ion peak for the sodium salt of

iodouracil ($m/z = 368.9422$ Da) was observed along with the uracil adduct (245.0593 Da). This suggests that the iodide is labile and along with the ^1H NMR spectroscopic data, it can be concluded that two compounds are present, the iodouracil moiety and the uracil moiety in a 1:1 ratio by ^1H NMR spectroscopic analysis after column chromatography. It is assumed that the iodide is labile under column conditions used and is hydrolysed on silica. Since the column conditions used 10% methanol in chloroform with 1% triethylamine, it is possible that the iodine was eliminated and a proton abstracted from the solvent to give rise to **80** from **87**.

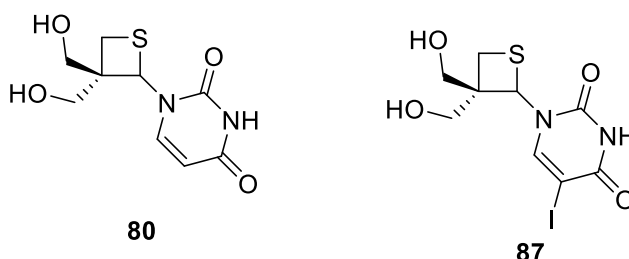


Figure 2.13 Mass spectrum and ^1H NMR spectroscopic data revealed two compounds present: uracil **80** and iodouracil **87**

No second mass ion peak was observed in the mass spectrum data for the benzoyl protected iodouracil moiety **87** lacking the iodine atom.

Compounds **79 – 81** and compounds **84 – 89** were tested for their purity by HPLC. A purity of 95% or greater was required for anti-viral testing and this purity level is the minimum level required for confidence that the compound is causing an observed outcome and not an impurity. All compounds bar cytosine **81** and 6-methyluracil **88** meet this standard.

2.4 ^1H NMR Features of Thietane Nucleosides

The ^1H NMR spectra selected thietane nucleosides are tabulated in table 2.8. The selected nucleosides were chosen based on their spectroscopic characteristics; where the spectroscopic data differed significantly from other nucleosides.

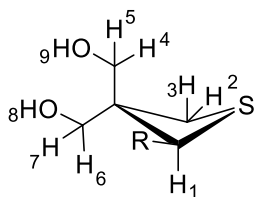


Table 2.8: Key ^1H NMR spectra for the thietane ring in thietane nucleosides. The ppm values are given first, followed by the signal type (s – singlet, d – doublet, t – triplet etc). The number of protons per signal is 1 proton as all the protons on the ring are non-equivalent.

R	H1	H2	H3	H4	H5	H6	H7	H8	H9
	5.86 s	2.80 d $J = 9$ Hz	2.88 d $J = 9$ Hz	3.34 d $J = 11$ Hz	3.48 m	3.60 d $J = 11$ Hz	3.48 m	4.66 t $J = 4$ Hz	5.00 t $J = 4$ Hz
	5.86 s	2.75 d $J = 9$ Hz	2.90 d $J = 9$ Hz	3.35 d $J = 11$ Hz	3.50 m	3.60 d $J = 11$ Hz	3.50 m	4.70 t $J = 4.5$ Hz	5.00 t $J = 4.5$ Hz
	5.81 s	2.77 d $J = 4$ Hz		3.17 d $J = 11$	3.39 d $J = 11$	3.44 d $J = 11$	3.70 d $J = 11$	4.60 d $J = 4$ Hz	4.91 d $J = 4$ Hz
	5.27 s	2.23 d $J = 9$ Hz	3.07 d $J = 9$ Hz	3.40 d $J = 5$ Hz	3.82 m	3.50 d $J = 5$ Hz	3.82 m	4.5 t $J = 5$ Hz	5.15 t $J = 5$ Hz
	5.90 s	2.80 d $J = 9$ Hz	2.88 d $J = 9$ Hz	3.31 d $J = 11$ Hz	3.42 d $J = 11$ Hz	3.53 d $J = 11$ Hz	3.61 d $J = 11$ Hz	4.90 s	5.10 s

X-ray crystallographic data by Nishizono and Choo separately has shown that the nucleobases are equatorial on thietane rings, hence the R group in the compound above table 2.8 being equatorial.^{10,52} This is intuitive as the nucleobase being equatorial reduces ring strain in the thietane ring by reducing diaxial interactions between the nucleobase and protons H3 and H4.

Table 2.8 shows some interesting features in the ^1H NMR spectroscopic data for the thietane nucleosides. In general, protons H2, H3, H4, H5, H6 and H7 are non-

equivalent. This is expected as these are conformationally non-equivalent with respect to the R group. Protons H4 and H6 are spatially facing the R group nucleobase, whilst protons H5 and H7 are facing away from the R group nucleobase. Protons H2 and H3 are conformationally non-equivalent as H3 is equatorial and H2 is axial, meaning that these protons are occupying different chemical environments with respect to the R group nucleobase.

The data shows that, in general, protons H2 and H3 are found at 2.80 and 2.88 ppm for thymine, 5-chloro, 5-bromo- and 5-iodo uracil nucleobases. The nucleobase 5,6-dimethyl uracil has a large ppm range between H2 and H3 at 2.23 ppm for H2 and 3.07 ppm for H3. This indicates that there is an interaction occurring between H3 and the methyl group on this nucleobase. A NOSEY spectrum should confirm whether an interaction is due to the methyl group interacting with H3. It is assumed that there is a diaxial interaction occurring between the 5,6-dimethyl uracil and proton H3, indicating the nucleobase may not be bound equatorially. If there the nucleobase is axially bonded, one of the methyl groups on 5,6-dimethyl uracil would interact strongly with proton H3.

Interestingly for the cytosine nucleobase, protons H2 and H3 are two closely spaced doublets integrating to two protons. This is very different to the rest of the nucleosides in the library, which are seen as a set of two doublets, spaced further apart by 0.8 ppm. Analysis of the COSY spectrum shows that H2 and H3 are only interacting with themselves, with no interaction with any other proton, ruling out a doublet of doublets interaction, which would require the interaction of a third non-equivalent proton. The small *J* value indicates an increase in ring strain for these protons. Pople and Bothner showed in 1965 that increased strain due to electronic effects in geminally coupled protons can affect the *J* coupling values. Pople showed that unstrained bonds in cyclic compounds typically have *J* values of 12 Hz, and increased strain (among other factors) can decrease the *J* value.⁵³ Therefore, it can be assumed that the lower than expected *J* value of 4 Hz for protons H2 and H3 is a result of ring strain

The OCH₂ protons H4, H5, H6 and H7 are non-equivalent and are observed as doublets. Where R is thymine, uracil, or 5,6-dimethyl uracil, protons H5 and H7 are seen as integrating to 2 as multiplets, whereas with the other nucleosides, these

protons integrate to 1. COSY spectra for nucleosides where R is thymine, uracil or 5,6-dimethyl uracil, the OCH₂ protons are observed as two sets of correlations, where one proton from each set overlaps. This indicates that one proton on each hydroxyl methyl group is equivalent to a proton on the other hydroxymethyl group. This explains why the integration pattern is 1:2:1 for the four protons of the dihydroxymethyl groups on the thietane ring for nucleosides where R is thymine, uracil, or 5,6-dimethyl uracil. For the rest of the nucleosides, each proton correlation in the COSY is seen as independent projections that correlate only to the proton on the same hydroxymethyl group. Thus, in these nucleosides, H4, H5, H6, and H7 are truly non-equivalent. Typically, the *J* values for these protons are 11 Hz, however, where R is 5,6-dimethyl uracil, the *J* value is 5 Hz. This implies an increase in the strain in these bonds. As stated previously, Pople and Bothner showed that increased ring strain due to electronic effects in geminally coupled protons can affect the *J* coupling values of these protons. It can be assumed therefore, that the nucleobase bound to the thietane ring has a direct effect on the bond angle of the substituents bound to the ring. In the case of 5,6-dimethyl uracil, the interaction seems to only affect one of the hydroxymethyl groups.

H1 also varied significantly depending on the nucleobase bonded to the thietane ring. Most nucleobases had a chemical shift of 5.86 ppm for H1. However, the largest chemical shift was 5.9 ppm and the lowest was 5.27 ppm. This is due to the shielding/de-shielding effect of the R group nucleobase. The effect of the applied magnetic field depends on how shielded H1 is. If H1 is not shielded, the proton interacts with the applied magnetic field strongly, and H1 is observed more downfield. If H1 is shielded, it is observed more upfield. The nucleobase 5-fluorouracil decreases electron density on H1 via the inductive effect, resulting in the chemical shift moving downfield to 5.90 ppm. However, 5,6-dimethyl uracil increases electron density via the inductive effect, onto H1, resulting in an upfield chemical shift to 5.27 ppm.

It can be seen therefore, that the type of nucleobase bound to the thietane ring can affect ring strain of the thietane ring and the inductive effect of the nucleobases can affect the chemical shift of H1. Inductive effects from the attached nucleobase could affect ring strain due to increased electron density around some bonds, as could be the case with the observed decrease in the *J* values for protons H2 and H3 in the

cytosine nucleoside moiety. Spatial and steric effects of the nucleobases is not fully known, however, it is assumed that 5,6-dimethyl uracil interacts diaxially with H3. To further probe these effects, temperature variable NMR and NOSEY experiments could give further insights into the NMR features of thietane nucleosides. These insights could be further elucidation of the conformational structure of the thietane ring, and the effect that the nucleobases have on ring conformation.

2.5 Assessment of Cellular Viability

The 11 thietane nucleosides that have been synthesised require preliminary cell viability testing to be performed prior to full anti-viral screening in order to potentially eliminate compounds that may cause cytotoxicity before an anti-viral response can be measured. A representative sample of 4 thietane nucleosides were chosen from the library for testing in an XTT assay, and the compounds were chosen based on structural considerations (figure 2.14).

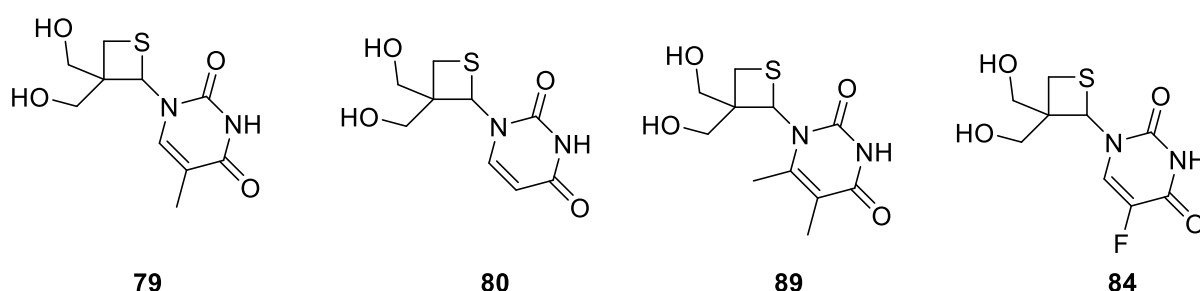


Figure 2.14: Candidate compounds chosen for cell viability assays.

Thymine **79** was tested against HSV-1, HSV-2 and VZV by Nishizono *et al*, but it did not exhibit any anti-viral activity in an *in vitro* anti-viral assay.¹⁰ This could either be due to the nucleoside being inactive, or that the nucleoside was unable to enter the cell to exhibit anti-viral activity. However, neither cell viability nor cytotoxicity data is available for the compound. Both thymine **79** and uracil **80** were included in the initial screen as they represent the traditional nucleobases used in anti-viral therapies and can easily be compared to other active anti-viral thietane nucleosides shown by Choo *et al* (see section 2.1). 5,6-dimethyluracil **89** (DMU) was included in the screen since the effect of the 6-methyl substituent is unknown. The 5-fluorouracil moiety **84** (5FU) was included in the screen as it is representative of the halogenated class of

nucleosides in the library. 5-Fluorouracil itself used to be used as an anti-cancer agent for various cancers and it is predicted to show cytotoxicity or loss in cell viability.^{54,55} 5-Fluorouracil is very polar and is used as a topical treatment and its route of entry is by diffusion into the skin. It is predicted that 5FU **84** will have significant cytotoxicity since the additional thietane ring may increase its solubility into the cell.

2.5.1 The XTT Assay

The XTT (2,3-bis-(2-methoxy-4-nitro-5-sulfophenyl)-2*H*-tetrazolium-5-carboxanilide) assay measures cell viability, and indirectly, cytotoxicity, by measuring cellular respiration.⁵⁶ The assay measures the activity of NADPH oxidoreductase enzymes in mitochondria and therefore measures ATP synthesis. It is assumed that viable cells will be undergoing respiration and therefore, the cell will be constantly producing ATP via the mitochondrial enzyme NADPH oxidase.⁵⁶ In general, a known concentration of cells are plated into a 96 well plate in cell culture media and incubated for 24 hours to allow them to reach confluence.^{57,58} The cell culture media is removed and known concentrations of the drugs being tested are added to the 96 wells and incubated for 24 hours further. XTT is mixed with phenazine methasulfate (PMS) in known concentrations and added to the 96 well plate and incubated for a further 4 hours. PMS is an activator reagent that acts as an intermediate electron acceptor that aids in the reduction of XTT to the active formazan derivative that is detected.⁵⁹ The XTT assay is a colorimetric assay that determines cell viability by measuring the concentration of the XTT formazan derivative that is only present in respiring cells. The mitochondria reduce the XTT to give the yellow-brown formazan derivative that is able to be assessed by a spectrophotometer. The concentration of the formazan derivative gives an approximation of the number of respiring cells, therefore, cell viability can be assessed by the absorbance of a specific wavelength of light at 475 nm.^{56,59}

A colour change to yellow-brown indicates viable cells, and no colour change indicates total cell death or the presence of non-viable cells. However, the major limitation of this assay is that it is highly susceptible to metabolic interference.⁵⁶ An increase in cellular respiration can give false positives by indicating the cells are more viable than would be expected. In some cases, cell viability figures in excess of

100% can be observed, and this is due to an increase in cellular metabolism.⁵⁶ The XTT assay is very useful to obtain preliminary information on cell viability prior to anti-viral screening as it can be used to eliminate compounds that may cause potential problems in anti-viral activity studies as any compound that affects cell viability may reduce or eliminate any anti-viral activity observed. This is due to the fact that viruses require viable cells to replicate, and a compound that reduces cell viability will reduce the cellular responses measured for viral activity.

2.5.2 Results and Discussion: General Background

With the 4 candidate compounds chosen cell viability testing could begin. The cell line used was the SH-SY5Y cell line which are neuroblastoma cells and these were chosen because the exponential growth phase lasted 32 hours versus 44 hours for fibroblast like cells.⁶⁰ This means that the saturation density of neuroblastoma cells versus fibroblast cells is greater in a short period of time. Bieder *et al.* found that the SH-SY5Y cell line had on average 115×10^4 cells per cm^2 versus 9×10^4 cells per cm^2 .⁶⁰ This means that SH-SY5Y cells will give a more intense signal in the cell based assay versus fibroblast cells as there are more of the SH-SY5Y cells per cm^2 .⁶⁰

2.5.2.1 Results and Discussion

In figures 2.15, 2.16, 2.17, and 2.18 the cell viability results for thymine **79**, uracil **80**, 5,6-dimethyluracil (5,6-DMU) **89**, and 5-fluorouracil (5FU) **84** are shown. The results shown are of the biological triplicates of the assay and the individual assay data along with the raw data can be found in the appendix.

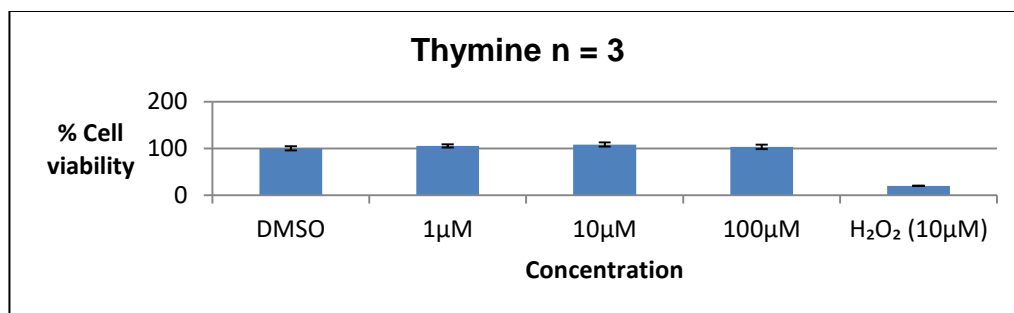


Figure 2.15: Cell viability data for thymine **79**

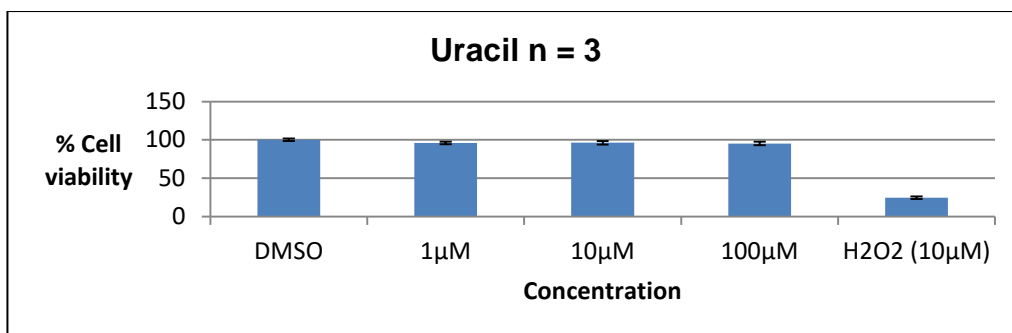


Figure 2.16: Cell viability data for uracil **80**

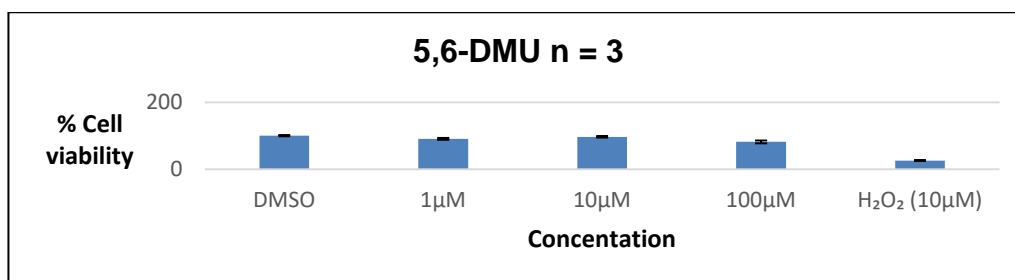


Figure 2.17: Cell viability data for DMU **89**

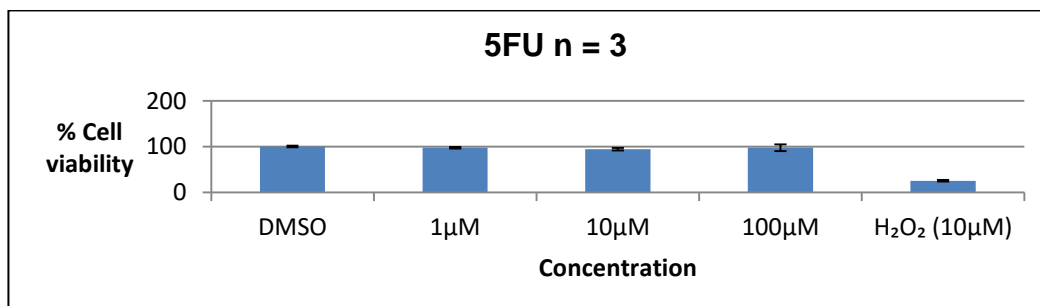


Figure 2.18: Cell viability data for 5FU **84**

Over the three biological replicates the data for thymine **79** suggests that the compound does not affect cell viability at any concentration. At 1 µM the cell viability is 105%, at 10 µM it is 108% and at 100 µM it is 103% with standard error means (SEM) of $\pm 3.4\%$, $\pm 4.4\%$ and $\pm 4.9\%$ respectively. Though this data may suggest that cell viability has increased, the limitation of this assay is that the reduction of XTT to the is affected by cellular respiration, and therefore, any increase in cellular respiration, for whatever reason, will be detected by this assay. The higher than expected SEM for each concentration is due to this limitation and therefore it cannot be concluded that cell viability has been affected. The positive control of H₂O₂ shows

a decrease in cell viability to $20\% \pm 0.52\%$ and confirms cell viability is being measured.

The biological replicates for uracil **80** show $96\% \pm 1.6\%$ cell viability at $1\ \mu\text{M}$, at $10\ \mu\text{M}$ the data shows $96\% \pm 2.2\%$ cell viability and at $100\ \mu\text{M}$ the data shows $95\% \pm 2.3\%$ cell viability. This data does not suggest that uracil **80** is affecting cell viability as there does not seem to be a correlation between the observed decrease in cell viability and the concentrations used. The observed decrease in the number of viable cells by 4 – 5% at each concentration ($\pm 2\%$) could be attributed to experimental error, or, 5% of the cells are viable but not actively respiring, which the XTT assay would detect as non-viable.

The data for 5,6-DMU **89** at $1\ \mu\text{M}$ shows the cell viability is $91\% \pm 2.9\%$ and increases to $97\% \pm 2.3\%$ at $10\ \mu\text{M}$, but at $100\ \mu\text{M}$, the cell viability decreases to $82\% \pm 4.1\%$. Therefore, the data shows at least 80% cell viability up to $100\ \mu\text{M}$.

It was predicted that 5FU **84** would be cytotoxic due to the fact that 5-fluorouracil on its own is used as a cancer treatment, and since 5FU **84** is less polar than 5-fluorouracil alone, it was predicted that 5FU **84** would be able to cross the cell membrane much easier than 5-fluorouracil. Though the mechanism of action of 5FU **84** is not as yet known, 5-fluorouracil causes thymineless death of cells. It was assumed that 5FU **84** would exert a similar cytotoxic response by preventing cellular replication.^{60,61} If cellular replication was halted, the assay would show significantly lower numbers of viable cells than expected. However, as can be seen from figure 2.4, the expected inhibition of cellular replication was not observed. At $1\ \mu\text{M}$ the cell viability was observed to be $98\% \pm 1.7\%$, at $10\ \mu\text{M}$ it was observed to be $94\% \pm 2.9\%$ and at $100\ \mu\text{M}$ the cell viability was observed to be $98\% \pm 7.5\%$. It can therefore be concluded that 5FU **84** does not affect cell viability at any concentration up to $100\ \mu\text{M}$ of compound.

2.6 Conclusions

In all, a library of 9 thietane nucleosides, 7 of which are novel, has been synthesised via key intermediate fluorothietane **76** using Vorbrüggen conditions. An optimised route has been established for quick access to thietane nucleosides that can be

applied to any pyrimidine nucleobases. Further optimisation toward purine nucleobases is required as the purines have been shown to be unreactive or unstable to the employed reaction conditions for their formation and/or deprotection. Thymine **79**, uracil **80** and 5FU **84** did not show any appreciable loss of cell viability. However, the limitation of this assay is that it measures the number of viable cells as a product of their respiration. This means that if the cells are alive but not actively respiring, the assay is unable to determine whether these cells are viable. Also, if an external stressor increases the rate of respiration in the cells, the assay will detect this increased respiration and thus the number of viable cells will be higher than expected. 5FU **84** did not show the expected decrease in cell viability and the hypothesis that it would be the most cytotoxic was shown not to be true. In the case of 5,6-DMU **89**, the data suggests that at least 80% cell viability is observed up to 100 μ M.

2.7 References

- (1) Marquez, V. E.; Choi, Y.; Comin, M. J.*et al. J Am Chem Soc* **2005**, 127, 15145.
- (2) Marquez, V. E.; Ben-Kasus, T.; Barchi, J. J.*et al. J Am Chem Soc* **2004**, 126, 543.
- (3) Ketkar, A.; Zafar, M. K.; Banerjee, S.*et al. Biochemistry* **2012**, 51, 9234.
- (4) Mu, L.; Sarafianos, S. G.; Nicklaus, M. C.*et al. Biochemistry* **2000**, 39, 11205.
- (5) Dejmek, M.; Hrebabecky, H.; Sala, M.*et al. Bioorg Med Chem* **2014**, 22, 2974.
- (6) Sofia, M. J.; Chang, W.; Furman, P. A.*et al. J Med Chem* **2012**, 55, 2481.
- (7) Du, J.; Chun, B. K.; Mosley, R. T.*et al. J Med Chem* **2014**, 57, 1826.
- (8) Balsamo, A.; Ceccarelli, G.; Crotti, P.*et al. J Org Chem* **1975**, 40, 473
- (9) Rode, J. E.; Dobrowolski, J.Cz. *Chem Phys Lett* **2002**, 360, 123.
- (10) Nishizono, N.; Kioke, N.; Yamagata, Y.*et al. Tet Lett* **1996**, 37, 7569.
- (11) Choo, H.; Chen, X.; Yadav, V.*et al. J Med Chem* **2006**, 49, 1635
- (12) Nishizono, N.; Akama, Y.; Agata, M.*et al. Tetrahedron* **2011**, 67, 358.
- (13) Nishizono, N.; Sugo, M.; Machida, M.*et al. Tetrahedron* **2007**, 63, 11622.
- (14) Alder, J.; Mitten, M.; Norbeck, D.*et al. Antimicrob Agents Chemother* **1994**, 93.
- (15) Seki, J. S., N; Takahashi, K; Takita, T; Takeuchi, T; Hoshino, H *Antimicrob Agents Chemother* **1989**, 33, 773.
- (16) Nagahata, T. K., M; Matsubara, K *Antimicrob Agents Chemother* **1994**, 38, 707.
- (17) Ichikawa, E.; Yamamura, S.; Kato, K. *Nucleic Acids Symposium* **1999**, 42, 5.
- (18) Ichikawa, E. K., K *Synthesis* **2002**, 1, 1.
- (19) Masuda, A.; Kitigawa, M.; Tanaka, A.*et al. J antibiotics* **1993**, 46, 1034.
- (20) Parks, R. E. J. S., J.D; Cambor, C; Saverse, T.M; Crabtree, G.W; Chu, S.H 5'-methylthioadenosine phosphorylases: Targets of chemotherapeutic agents; Academic Press: New York, 1981.
- (21) Toyohara, J.; Kumata, K.; Fukushi, K.*et al. J Nucl Med* **2006**, 47, 1717.
- (22) Ichikawa, E. Y., S; Kato, K *Tett Lett* **1999**, 40, 7385.
- (23) Ichikawa, E. K., K *Curr Med Chem* **2001**, 385.
- (24) Feldman, K. S. *Tetrahedron* **2006**, 62, 5003.
- (25) Smith, L. H.; Coote, S. C.; Sneddon, H. F.*et al. Angew Chem Int Ed Engl* **2010**, 49, 5832.

- (26) Vorbrüggen, H. R.-P. *C Org React* **2000**, 55.
- (27) Hugenberg, V.; Haufe, G. *J Fluor Chem* **2012**, 143, 238.
- (28) Choo, H.; Chen, X.; Yadav, V. *et al. J Med Chem* **2006**, 49, 1635.
- (29) De Clercq, E. *Nat Rev Drug Disc* **2007**, 6, 1001.
- (30) De Clercq, E. *Med Res Rev* **2008**, 28, 929.
- (31) De Clercq, E. *Med Res Rev* **2009**, 29, 571.
- (32) De Clercq, E. *Annu Rev Pharmacol Toxicol* **2011**, 51, 1.
- (33) De Clercq, E. *J Clin Virol* **2004**, 30, 115.
- (34) De Clercq, E. *Antiviral Res* **2005**, 67, 56.
- (35) De Clercq, E. *Med Res Rev* **2015**, 35, 698.
- (36) De Clercq, E.; Field, H. J. *Br J Pharmacol* **2006**, 147, 1.
- (37) Jonckers, T. H.; Vandyck, K.; Vandekerckhove, L. *et al. J Med Chem* **2014**, 57, 1836.
- (38) Razonable, R. R. *Mayo Clin Proc* **2011**, 86, 1009.
- (39) Elion, G. B.; Furman, P. A. *Proceedings of the National Academy of Sciences USA* **1974**, 74, 5716.
- (40) Weller, S. B., M.R. *Clin Pharmacol Ther* **1993**, 54, 595.
- (41) Bordwell, F. G.; Hewett, W. A. *J Org Chem* **1957**, 23, 636.
- (42) Etienne, Y.; Soulas, R.; Lumbroso, H. In *Chemistry of Heterocyclic Compounds*; Weissberger, A., Ed.; Wiley: 1964.
- (43) Sander, M. *Chem Rev* **1966**, 6, 297.
- (44) Buza, M.; Andersen, K. K.; Pazdon, M. D. *J Org Chem* **1978**, 43, 3827.
- (45) Fronza, G. *J Mag Res* **1979**, 36, 343
- (46) Bain, A. D. *J Mag Res* **1980**, 37, 209
- (47) Slomp, G. *Applied Spectroscopy Reviews* **1969**, 2, 263.
- (48) Wang, Z.; Tang, J.; Salomon, C. E. *et al. Bioorg Med Chem* **2010**, 18, 4202.
- (49) Schütz, A. P.; Osawa, S.; Mathis, J. *et al. Eur J Org Chem* **2012**, 2012, 3278.
- (50) Dalpozzo, R.; De Nino, A.; Maiuolo, L. *et al. Tetrahedron* **2001**, 57, 4035.
- (51) Michel, B. Y.; Strazewski, P. *Tetrahedron* **2007**, 63, 9836.
- (52) Choo, H.; Chen, X.; Yadav, V. *et al. J Med Chem* **2006**, 49, 1635.
- (53) Pople, J. A.; Bothner, B. A. A. *J Chem Phys* **1965**, 42, 1339.
- (54) Kim, Y. H.; Shin, S. W.; Kim, J. H. *et al. Cancer* **1999**, 85, 295.
- (55) Salim, A.; Leman, J. A.; McColl, J. H. *et al. Br J Dermatol* **2003**, 148, 539.
- (56) Kepp, O.; Galluzzi, L.; Lipinski, M. *et al. Nat Rev Drug Discov* **2011**, 10, 221.

- (57) Pahlman, S.; Hoener, J. C.; Nanberg, E.*et al. Eur J Cancer* **1995**, 31, 453.
- (58) Alfredsson, C. F.; Ding, M.; Liang, Q. L.*et al. Biomed Pharmacother* **2014**, 68, 129.
- (59) Tominaga, H.; Ishiyama, M.; Ohseto, F.*et al. Anal. Commun* **1999**, 36, 47.
- (60) Bieder, J. L.; Helson, L.; Spengler, B. A. *Cancer Res* **1973**, 33, 2643.
- (61) Crump, K. S.; Hoel, D. G.; Langle, C. H.*et al. Cancer Res*, 36, 2973.

Chapter 3:

**The Design and Synthesis of 4,4-
bis(hydroxymethyl)-thietan-2-yl
Nucleosides**

Chapter 3: Synthesis of 4,4-bis(hydroxymethyl) thietane

Nucleosides

3.1 Background

The intention of the work in chapter 2 was to explore the SAR of the nucleobases and to determine the anti-viral activity of the 3,3-bis(hydroxymethyl) thietane core. In this chapter, derivatives were selected for synthesis in order to allow further SAR data to be established, by moving the hydroxymethyl groups around the ring. To allow conclusions to be made about the effect of this transformation, the nucleobases were kept constant and both of the hydroxymethyl groups are moved around by one carbon bond on the thietane ring (figure 3.1).

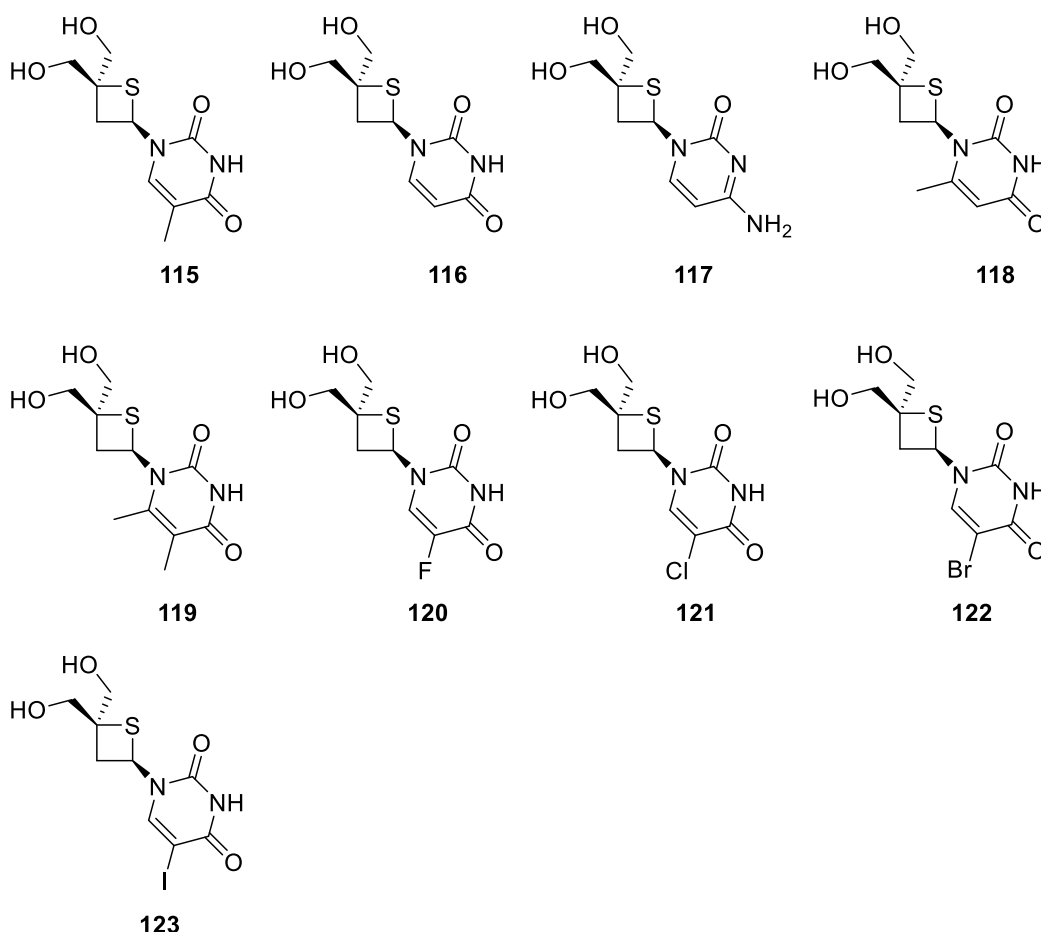


Figure 3.1: Target thietane nucleosides for the 4,4-bis(hydroxymethyl) thietane core compounds

By comparing and contrasting the biological data between the 3,3-dihydroxymethyl series and the 4,4-dihydroxymethyl series, it was anticipated that the SAR of the

molecules can be assessed in detail. This information can then be used as a guide to design and synthesise a highly active thietane nucleoside.

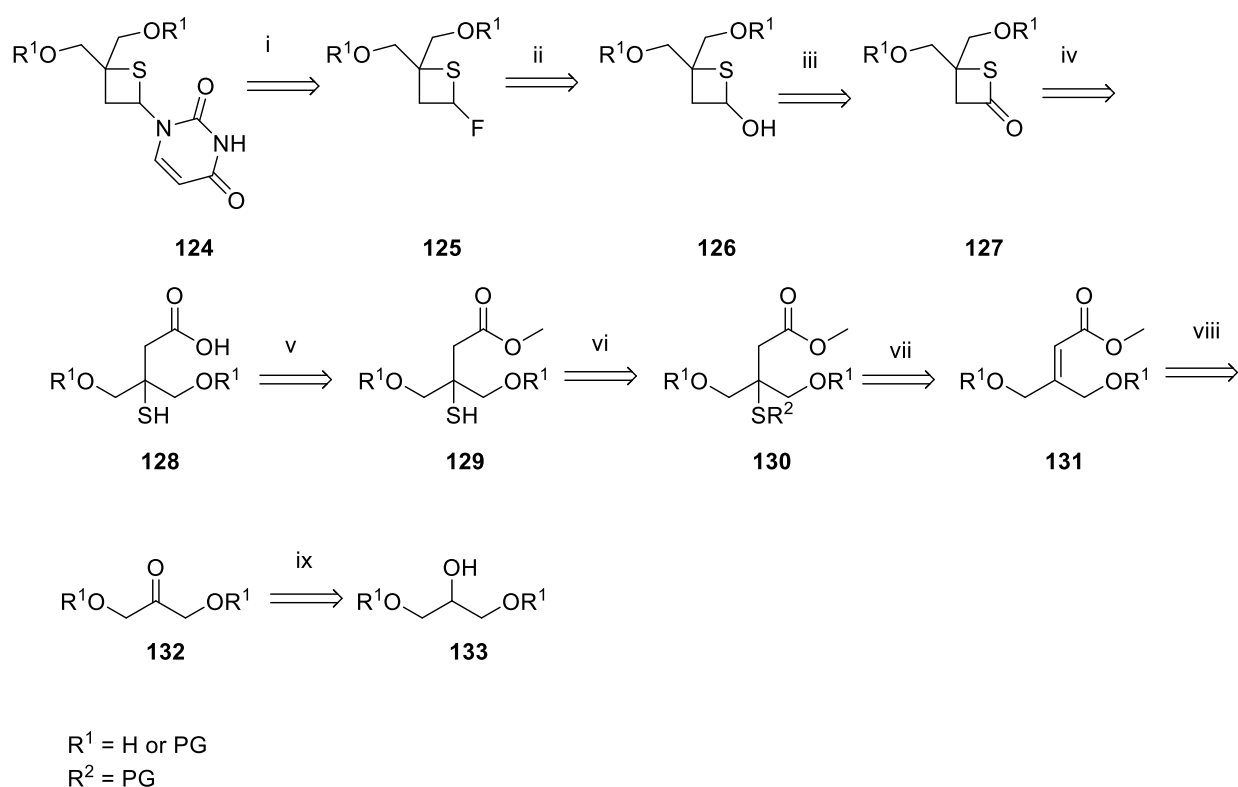
3.1.1: Aims and Objectives

The following aims and objectives are detailed and are similar to the aims in chapter 2:

- Explore potential chemical methods toward the 4,4-bis(hydroxymethyl) thietane core. Since the substitution pattern on the thietane is novel, several synthetic strategies are to be explored.
- Build a library of thietane nucleosides with the same nucleobases as the previous library in chapter 2. This will enable more direct comparisons to be made between these two libraries.
- Assess anti-viral activity by measuring CC_{50} and IC_{50} in biological assays.
- Determination of a structure activity relationship based on the biological data between both nucleoside libraries. This information will be used to guide the synthesis of a final set of compounds with the intent that these compounds will have a better anti-viral profile.

3.2 Synthetic Strategies towards 4,4-bis(hydroxymethyl) thietane nucleosides

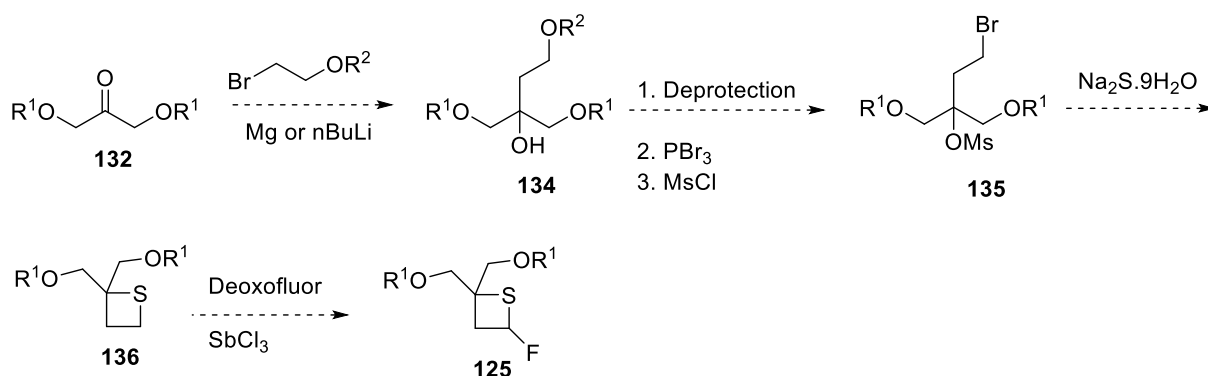
In scheme 3.1 the retrosynthetic steps to potentially allow synthesis of the 4,4-bis(hydroxymethyl) thietane nucleosides is shown.



Scheme 3.1: Retrosynthetic steps toward 4,4-bis(hydroxymethyl) thietane nucleosides

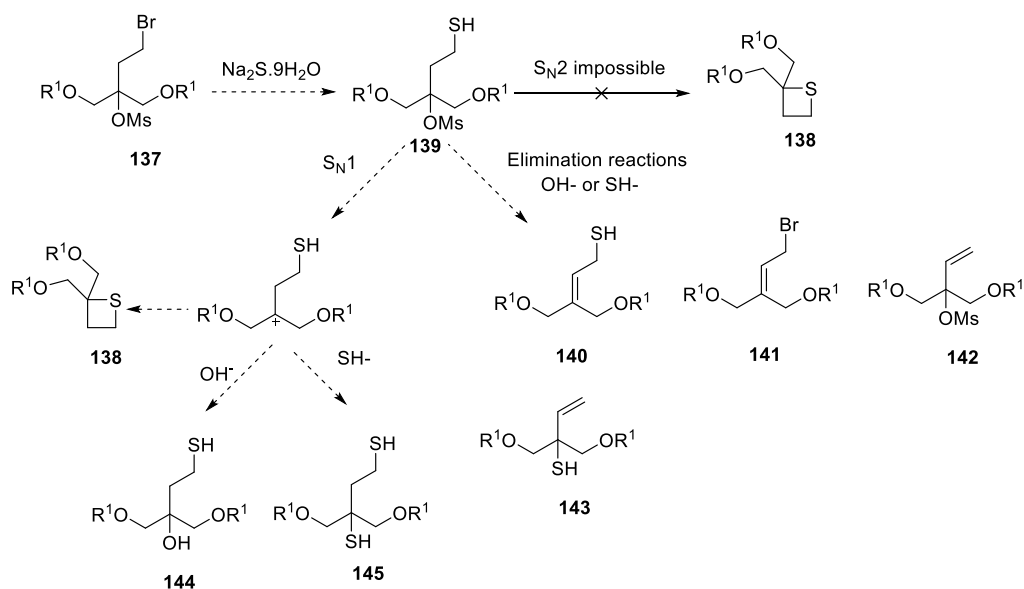
Formation of nucleoside **124** in step i) requires fluoride **125** to be formed harnessing the chemistry developed in chapter 2. Next, a functional group interconversion (FGI) to alcohol **126** in step iii) is required and another FGI to ketone **132** allows for a cyclisation reaction to furnish thietane **127** from carboxylic acid **128** in steps iv) and v). A thia-Michael addition to allyl methyl ester **131** allows for the incorporation of the sulfur moiety, and a further FGI reveals ketone **132** with which a Wittig reaction can be performed in steps vi), vii) and viii). Reduction of the ketone to triol **133** reveals the readily available starting material glycerol in step ix).

Synthesis from ketone **132** can begin with Grignard reagents, or lithium salts of ethanol derivatives could potentially be used to form the thietane ring by use of $\text{Na}_2\text{S} \cdot 9\text{H}_2\text{O}$ as per the chemistry in chapter 2 (scheme 3.2).



Scheme 3.2: Potential chemistry toward the thietane target using already established chemistry

Despite the appeal of the chemistry in scheme 3.2, with the already established chemistry of thietane formation using $\text{Na}_2\text{S}\cdot 9\text{H}_2\text{O}$, several problems persist with this route.¹ In solution, $\text{Na}_2\text{S}\cdot 9\text{H}_2\text{O}$ produces sodium sulfide, sodium hydroxide and water (see chapter 2 for detailed chemistry), and as such is highly basic. Under these basic conditions, both the bromide and mesylate in compound **135** are susceptible to elimination. Several potential side reactions could occur using these conditions to furnish the thietane (scheme 3.3).



Scheme 3.3: Potential side reactions that could occur by using $\text{Na}_2\text{S}\cdot 9\text{H}_2\text{O}$ to furnish thietane **142** from compound **143**.

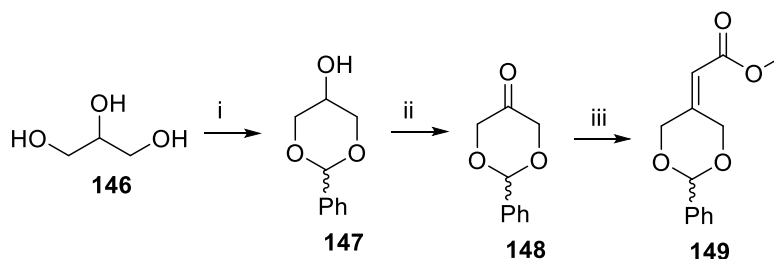
As can be seen from scheme 3.3, if the HS^- ion is able to undergo an $\text{S}_{\text{N}}2$ reaction with the bromide in compound **137** to form compound **139**, several competing reactions are possible from compound **139**. It can be seen that the intramolecular

S_N2 reaction of the sulfur in compound **139** with the mesylate group is not favourable as the mesylate carbon is tertiary and tertiary compounds do not undergo S_N2 reactions. Backside attack of a nucleophile is impossible and hence this reaction cannot occur. For the reaction to thietane **138** to be plausible, the reaction must undergo an S_N1 reaction, ie, the mesylate must leave first to form the carbocation, which is a stable intermediate as hyperconjugation stabilises the ion. This then allows intramolecular attack of the thiol group in compound **139** to yield thietane **138**. However, the carbocation could react with hydroxide or sulfide ions in solution to give compounds **144** and **145** respectively.

Since the reaction is run in basic conditions with $\text{Na}_2\text{S} \cdot 9\text{H}_2\text{O}$, several elimination reactions from compound **139** are possible and the compounds **140** – **143** are the possible elimination products that could form. Therefore it can be concluded that the use of the optimised reaction conditions in chapter 2 for the formation of thietane rings is not feasible for accessing the 4,4-bis(hydroxymethyl) thietane core. Therefore, the set of reaction conditions in scheme 3.1 shows more promise as the potential for side reactions is significantly minimised.

3.3 Initial Synthetic Steps Toward 4,4-bis(hydroxymethyl) thietane nucleosides

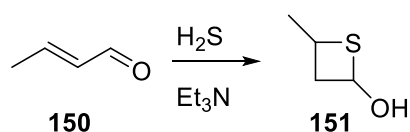
From the retrosynthetic strategy in scheme 3.1 it was revealed that the synthesis of the target thietane could begin from the cheap, commercially available compound glycerol **146**. Scheme 3.4 shows the initial synthetic strategy toward the target thietane molecule.



Scheme 3.4: Initial synthetic strategy toward 4,4-bis(hydroxymethyl) thietane nucleosides i) glycerol, *p*TSA, Toluene, 40° C, 6 hrs, 62% ii) DMP, DCM, 0° C, 4 hrs, 82% iii) NaH, methyl diethylphosphonoacetate, THF, RT, overnight, 61%

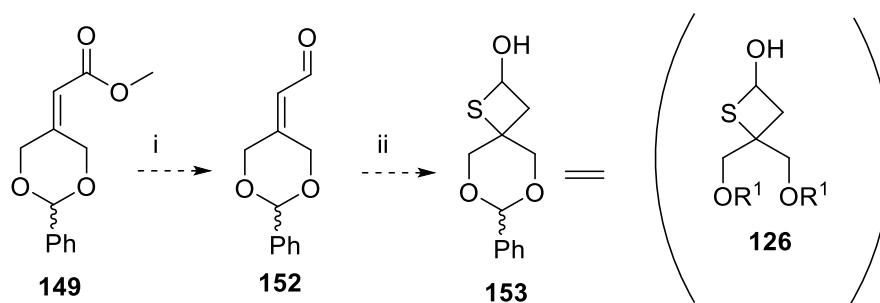
The acetal protecting group was chosen for the protection of glycerol **146** to afford acetal **147**, as the acetal is easy to install and it was expected to be stable to the first six steps of the synthesis based on literature precedent.² Also, since the introduction of the acetal in chapter 2 gave high, reproducible yields, the acetal protecting group was thought to be an effective protecting group for this synthesis.² Oxidation of acetal **147** to ketone **148** has been achieved using mild oxidation reactions (see section 3.3.3.1) and incorporation of the allyl methyl ester **149** was also achieved using the Horner-Wadsworth-Emmons (HWE) reaction (section 3.3.3.1).³⁻⁶ From methyl ester **149**, two possible methods exist for the formation of the target thietane core: use of hydrogen sulfide or use of benzyl mercaptan on derivatives of ester **149** have been shown.^{7,8}

Givaudan *et al.* have shown that 4-methyl-thietan-2-ol **151** can be synthesised from crotonaldehyde **150** by reacting it with hydrogen sulfide in excess triethylamine at -10° C (scheme 3.5).⁷



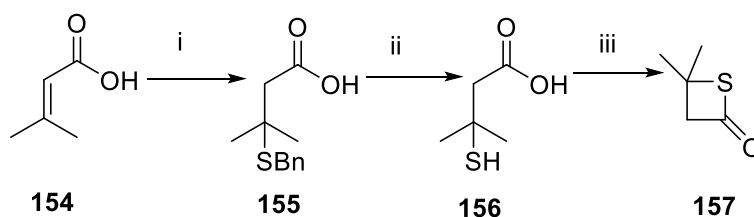
Scheme 3.5: Givaudan synthesis of 4-methyl-thietan-2-ol using crotonaldehyde and H₂S

Applying the Givaudan synthesis to the synthesis of target thietane **126** in scheme 3.1 would first require reduction of methyl ester **149** to aldehyde **152** by use of diisobutyl aluminium hydride (DIBAL-H) prior to formation of thietane **153** shown in scheme 3.6. (Here, the target thietane number has changed from **126** in scheme 3.1 to **153** in scheme 3.6 to highlight the acetal protecting group versus the R group).



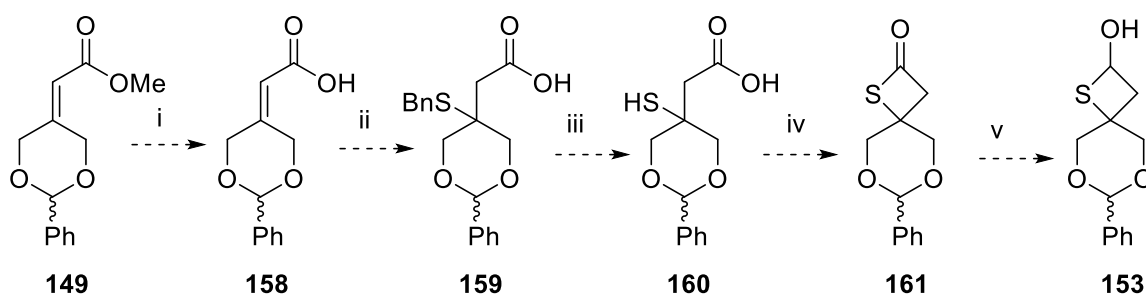
Scheme 3.6: Application of the Givaudan synthesis to methyl ester **149** to give target thietane **153** i) DIBAL-H, THF, -78°C , 3 hrs ii) H_2S , Et_3N , -10°C , 6 hrs.

Pattenden *et al.* showed that α,β -unsaturated carboxylic acids could be used to form thietanone compounds: 2-methyl-buten-oic acid **154** was heated at reflux in excess piperidine with benzylmercaptan (BnSH) to afford 2-thiobenzyl-2-methyl-butanoic acid **155**.⁸ From here, use of sodium in liquid ammonia furnished 2-thio-2-methylbutanoic acid **156** which was then cyclised to thietanone **157** (scheme 3.7).



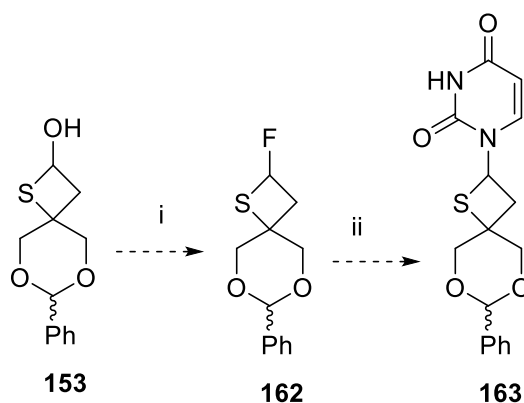
Scheme 3.7: Pattenden synthesis of thietanone compounds i) BnSH , piperidine, reflux, 24 hrs ii) Na , NH_3 , -78°C , 2 hrs iii) Isobutyl chloroformate, Et_3N , DCM, -10°C , 20 mins

The Pattenden synthesis would require incorporation of two additional steps for the synthesis of target thietane **153** from ester **149**; which would have to be hydrolysed to carboxylic acid **159** prior to use of the Pattenden conditions. Once thietanone **161** is successfully cyclised, thietanol **153** can be synthesised by reduction of thietanone **161** with DIBAL-H (scheme 3.8)



Scheme 3.8: Proposed conditions to methyl ester **149** i) NaOH or LiOH, IPA, water ii) Na, NH₃, -78° C, 2 hrs iii) Isobutyl chloroformate, Et₃N, DCM, -10° C, 20 mins iv) DIBAL-H, THF, -78° C, 3 hrs.

From thietane **153**, incorporation of the fluorine atom to fluorothietane **162** can be achieved using already established chemistry from chapter 2. Use of deoxofluor will give key intermediate **162** and the nucleosides can be furnished using the already established chemistry from chapter 2 (scheme 3.9).¹

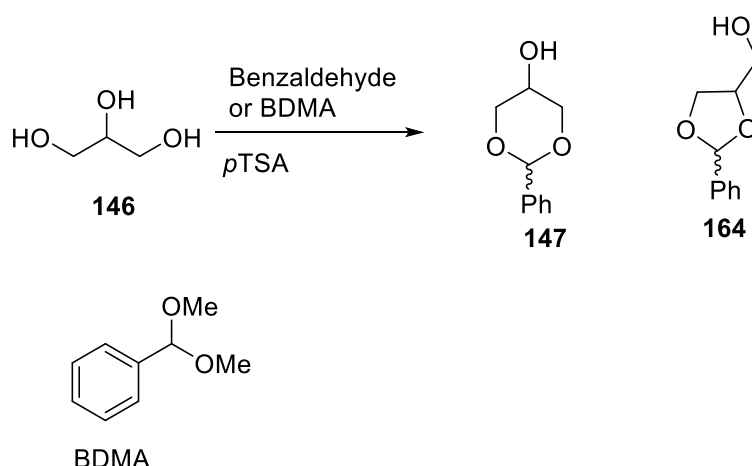


Scheme 3.9: Proposed condition: (this chemistry was established in chapter 2 i) deoxofluor, SbCl₃, DCM, RT, 24 hrs ii) silylated nucleobase, AgClO₄, SnCl₂.

The Givaudan thietane synthesis will be used to furnish thietane **153** as there are fewer steps to the target than with the Pattenden synthesis.

3.3.1 Results and Discussion: Initial Synthesis and Optimisation of Synthetic Route Toward 4,4-bis(hydroxymethyl) thietane Nucleosides

The literature synthesis of acetal **147** was optimised by acetal protection of glycerol **146** to acetal **147** (scheme 3.10) using *p*TSA and benzylidene dimethyl acetal (BDMA).



Scheme 3.10: General synthesis of acetal **147** using either benzaldehyde or BDMA to furnish acetal **147**.

Reproduction of the literature synthesis of acetal **147** used excess benzaldehyde and the reaction was heated at reflux for a minimum of 12 hours and typically gave low yields of the acetal **147** with yields ranging from 5 – 15%, which was lower than the reported yield of 46%.⁹ The solvent was switched to DMF and 1.1 equivalents of benzaldehyde were used. The yields improved to 50%. Toluene was then used as a solvent with a Dean-Stark apparatus to remove the water. It was suspected that any water formed during the reaction would shift the equilibrium away from product formation (table 3.1) using the reaction conditions set out by Patwardhan *et al.* where the reaction was heated at reflux for 5 hours.²

Table 3.1: Reaction conditions attempted for the synthesis of acetal **147**

Reaction	Conditions	Yield
1	Glycerol, pTSA (0.01 equiv), benzaldehyde (excess), RT, 48 hrs	5%
2	Glycerol, pTSA (0.02 equiv), benzaldehyde (excess), RT, 48 hrs	15%
3	Glycerol, pTSA (0.02 equiv), benzaldehyde, toluene, 130° C, 24 hrs	29%
4	Glycerol, , pTSA (0.1 equiv), BDMA DMF, 65° C, 5 hrs	40%
5	Glycerol, pTSA (0.1 equiv), BDMA, DMF, 50° C, 5 hrs	50%
6	Glycerol, pTSA (0.1 equiv), , BDMA, toluene, RT 5 hrs	62%

Although yields were slightly improved to 50%, the decision to move to BDMA was taken as it was a) more reactive than benzaldehyde and b) more moderate reaction conditions could be used. The use of BDMA gave acetal **147** as a 1:1 mixture of the 6 membered ring acetal and the 5 membered ring acetal **164** (table 3.2 for key ¹H

NMR spectroscopic data). Toluene was then used as a solvent due to the fact that the reaction could be performed at ambient temperature, whereas with DMF, the reaction had to be heated before it would occur. The reason for this could be that DMF is too polar to favour product formation at low temperatures and as such, the activation energy for the reaction is higher in DMF than in toluene.¹⁰ This could be because the solvent interaction with the product in DMF is disfavoured as it is relatively non-polar with respect to DMF, but in toluene, the phenyl ring in the product and the BDMA starting material may have more favourable solvent-reagent interactions.¹⁰

It was observed that the reaction to afford acetal **147** gave both the cis and trans isomers of both the 6 membered ring acetal **147** and its 5 membered ring counterpart acetal **164**, which were observed in a 1:1 mixture for each ring. The ¹H NMR spectroscopic data of the crude reaction mixture showed 4 singlet peaks at 5.38 and 5.54 ppm, which corresponded to the benzyldiene proton in the cis and trans isomer of the 6 membered acetal **147**; and 5.83 and 5.91 for the benzyldiene proton for the 5 membered acetal **164** (table 3.2). Attempts to purify the reaction mixture using column chromatography were unable to resolve acetal **147** from the 5 membered ring acetal **164**. The crude reaction mixture was dissolved in minimal chloroform and the 6 membered ring product, acetal **147**, was precipitated out of solution using petroleum ether.² Table 3.2 and figure 3.2 shows the key ¹ H NMR spectroscopic data for both the 5 membered ring acetal **164** and the 6 membered ring acetal **147**.

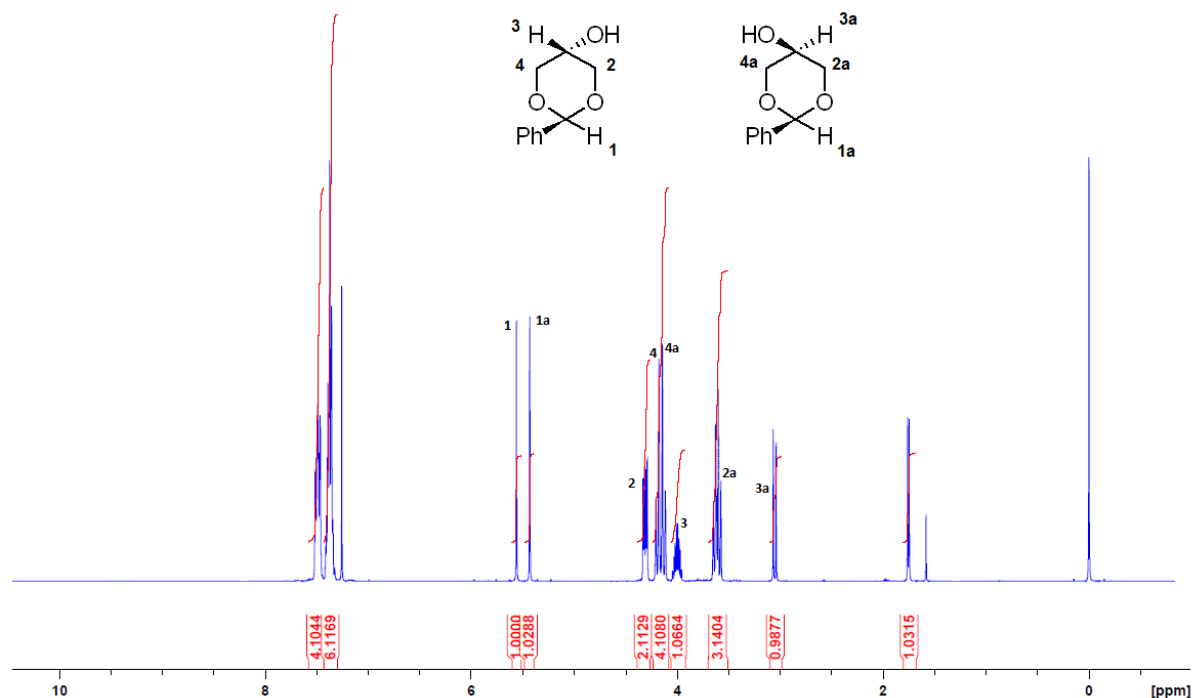
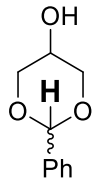
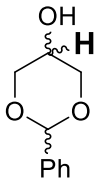


Figure 3.2: ^1H NMR spectrum for acetal **147** which shows both cis and trans isomers are present

Table 3.2: Key ^1H NMR spectroscopic data for both acetal **147** and the 5 membered ring acetal. The bold protons are the protons of interest and uses acetal **147** as the reference compound. (d) doublet, (s) singlet, (m) multiplet (t) triplet (q) quartet

Fragment	Acetal 147 chemical shift	Acetal 164 chemical shift
	Cis isomer: 5.54 ppm (s) Trans isomer: 5.38 ppm (s)	Cis isomer: 5.91 ppm (s) Trans isomer: 5.83 ppm (s)
	Cis isomer: 3.61 ppm (t) Trans isomer: 3.01 (t)	Cis/trans isomer: 3.52 ppm (m)
OCH_2	Cis isomer: 4.63 ppm (m) Trans isomer 4.00 ppm (m)	Cis/trans isomer: 4.92 ppm (m)

Despite the very different ^1H NMR spectroscopic data for the cis and trans isomers of acetal **147**, the cis and trans isomers were not resolved as the next step to ketone

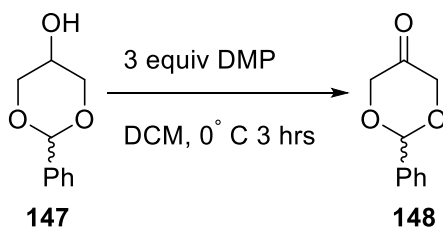
148 would create symmetry in the molecule, and as such any isomerism would cease to exist.

The low yields ascribed to formation of acetal **147** only account for the yield of the 6 membered ring acetal **147**. The total yields for both the 5 and 6 membered rings of acetal **147** and **164** were 70 - 75% after work up and drying of the crude reaction material. Although analysis of the crude reaction mixture by ^1H NMR spectroscopy revealed a 1:1 mixture of the 5 and 6 membered rings of acetal **147** and **164**, recrystallization gave only the acetal **147**, but the total yield dropped to around 28%.

^1H NMR spectroscopic analysis revealed that the product had formed, IR spectroscopy confirmed the presence of the hydroxyl group on at 3347 cm^{-1} . MS data gave the mass ion peak at 180.0859 which corresponds to the mass ion peak of acetal **147** which is in the expected range as the calculated value for acetal **147** was 180.0786 Da. All of this data confirmed the successful synthesis of acetal **147** and matched literature data for this compound.^{2,9}

3.3.1.1 Oxidation Reactions toward 2-phenyl-1,3-dioxan-5-one **148**

After optimisation of the reaction toward acetal **148**, oxidation of the hydroxyl group was required prior to installation of the allyl ester **149** via the HWE reaction. Classical oxidation reactions using acidified dichromate could not be used due to the sensitivity of the acetal group toward acids. A review of the literature revealed three potentially useful, mild oxidation reactions for the synthesis of ketones from secondary alcohols: Dess Martin Periodinane oxidation (DMP), Swern oxidation and the Parikh-Doering oxidation reactions.³⁻⁶ In scheme 3.11 the optimised conditions toward ketone **148** are shown with DMP.



Scheme 3.11: Optimised reaction conditions for the oxidation of acetal **147** to ketone **148** using DMP

In table 3.3 the optimisation data is shown for this reaction.

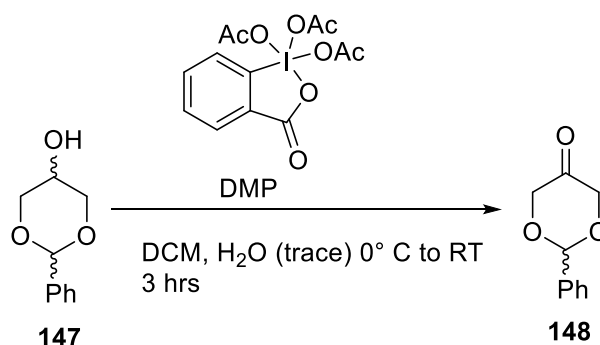
Table 3.3: Optimised reaction conditions using DMP toward the synthesis of ketone **148**

Reaction	Conditions	Yield (%)
1	1.1 equiv DMP, anhydrous DCM, 0°C 3 hrs	15
2	1.5 equiv DMP, anhydrous DCM, 0° C 3 hrs	50
3	1.5 equiv DMP, standard non-dried DCM, 0° C 3 hrs	80
4	1.5 equiv DMP, standard non-dried DCM, 0° C 3 hrs	45
5 - 7	1.5 equiv DMP, 0.5 equiv water, DCM, 0.5 equiv water, 0° C 3 hrs	6.4
8	As reaction 4, dry DCM, 6 hrs	-
9	2 equiv DMP, standard non dry DCM, 0° C, 6 hrs	40
10	3 equiv DMP, standard non dry DCM, 0° C, 6 hrs	32
11 - 12	As reaction 10	8
13	1.5 equiv DMP, standard non-dried DCM, 0° C 4 hrs increased to 2 equiv DMP react further 2 hrs	49
14	1.5 equiv DMP, standard non-dried DCM, 0° C 4 hrs increased to 2 equiv DMP react further 2 hrs	52
15	1.5 equiv DMP, standard non-dried DCM, 0° C 6 hrs increased to 2 equiv DMP react further 2 hrs	10

As can be seen from table 3.3, the initial reactions gave the product in good yield, though the high yield of 80% in reaction 3 was never reproduced. In the first reaction, although product was isolated, analysis of the crude reaction mixture by ^1H NMR spectroscopy implied the acetal group might be unstable. This was determined by loss of the singlet peaks at 5.3 ppm. Purification by column chromatography gave 15% yield of the product and analysis of the remaining fractions revealed some benzaldehyde was present, implying loss of the acetal group either during the reaction, during work up, or during column chromatography. However, the silica was neutralised with 1% triethylamine. This, coupled with the analysis of the crude material by ^1H NMR spectroscopy, implies that the acetal group was unstable to the reaction conditions.

The equivalents of DMP were increased to 1.5 equivalents and gave a yield of 50% in reaction 2. However, as with reaction 1, some acetal deprotection was observed, though less so than in reaction 1.

Reaction 3 showed the largest yield obtained with DMP at 80% and this is attributed to the use of standard DCM rather than anhydrous DCM. It is suspected that trace amounts of water aid this reaction and it has been shown in the literature that this reaction can be accelerated with the addition of water due to the fact that the water molecule is able to displace the acetate ligand from the iodo moiety in the DMP compound (scheme 3.12).



Scheme 3.12: Oxidation reaction using DMP

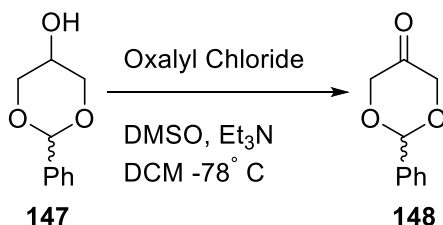
Therefore, the partially hydrated periodinane is far more reactive toward oxidation.¹¹ However, as reaction 5 showed, the direct addition of water reduced the yield significantly and it is suspected that this allowed the acetic acid to act as an acid rather than a nucleophile in the reaction, causing significant deprotection of the acetal group. From then on, non-anhydrous DCM was used for these reactions.

In further reactions, no direct addition of water was used, but the reaction of DMP with acetal **147** became increasingly less reproducible and the acetal group was found to be unstable to these reaction conditions. As can be seen from reactions 6-8 sometimes no product was seen by TLC analysis and analysis of the crude reaction by ¹H NMR spectroscopy revealed no peaks that were consistent with the product (see section 3.2.2.3 for NMR data for ketone **148**). Due to the unreproducible nature of the reactions and the instability of the acetal group towards the reagent meant that other oxidation reaction conditions were required. This variability in yields meant the reactions could not be optimised efficiently.

3.3.1.2 Swern Oxidation Reactions toward Ketone 148

The Swern oxidation is a useful oxidation reaction for secondary alcohols to ketones as it is relatively mild. Although the reaction is performed at -78° C, the reaction is

relatively quick and the products are easily isolated and purified. Scheme 3.13 shows the optimised reaction conditions used for this reaction.



Scheme 3.13: Optimised reaction conditions for the Swern oxidation reaction toward ketone **148**

The Swern oxidation reactions were typically more reproducible than the reactions using DMP, but acetal stability was still an issue.⁶ The Swern oxidation reactions had isolated yields of 15 – 61% versus 6% - 80% for the DMP reactions.

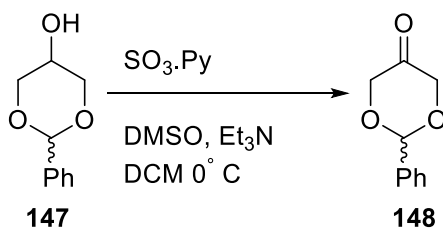
Analysis of the crude reaction material by ¹H NMR spectroscopy did reveal that the acetal group was labile. It was suspected that order of addition was the issue, in that the reaction requires addition of oxalyl chloride and DMSO in solution followed by the alcohol starting material, and after 1 hour, addition of triethylamine. Since the reaction generates HCl as a by-product, it was suspected that addition of the triethylamine was occurring too late in the reaction to avoid acetal deprotection. To overcome this issue, the alcohol was dissolved in minimal DCM and the triethylamine added to it. However, yields remained low and lability of the acetal group was still observed by ¹H NMR spectroscopic analysis. The benzyldiene proton at 5.54 ppm and 5.83 ppm were no longer present which indicated the loss of the acetal group.

However, the isolated yields remained consistent at 25% for the formation of ketone **148**, but this was problematic for the synthesis as at this early stage, low yielding reactions would result in significant mass loss. This would result in negligible amounts of the final product being synthesised. Coupled to this fact, the reproducibility of, and yields of, proceeding reactions in this synthesis were unknown and therefore, the Parikh-Doering oxidation reaction was screened as a potential mild oxidation reaction to overcome the issue of acetal lability and low yields. At this stage the ketone is a key intermediate as it will be used to create allyl ester **145** via the HWE reaction (scheme 3.4). From here, the thietane can be furnished. Without

reliable oxidation reactions to ketone **148**, the rest of the synthesis becomes significantly more difficult to achieve.

3.3.1.3 Parikh-Doering Oxidation Reactions toward Ketone **148**

The Parikh-Doering oxidation reaction is a very mild reaction for the oxidation of alcohols into aldehydes or ketones using a sulfur trioxide pyridine complex in DMSO and triethylamine. The reaction is analogous to the Swern reaction in that the DMSO forms a sulfur ylid and reacts as a nucleophile with the sulfur trioxide.⁴ Scheme 3.9 shows the standard Parikh-Doering oxidation method used ($\text{SO}_3\cdot\text{Py}$ is the sulfur trioxide pyridine complex).



Scheme 3.14: Parikh-Doering oxidation

As shown in table 3.4, the Parikh-Doering reaction was not consistently reproducible. Either the yields were low or no reaction took place and the reason for this is unknown. No acetal deprotection was observed when the crude reaction mixture was analysed by ^1H NMR spectroscopy.

Table 3.4: Parikh-Doering Reaction toward the synthesis of ketone **148**

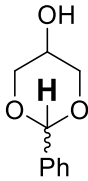
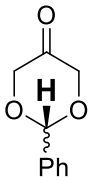
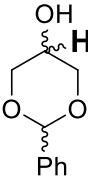
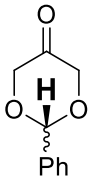
Reaction	Conditions	Yield (%)
1	2.5 equiv $\text{SO}_3\cdot\text{Py}$ 3 equiv Et_3N , 0°C , 4 hrs, 1 g SM	26% product, 16% SM recovered
2	2.5 equiv $\text{SO}_3\cdot\text{Py}$ 3 equiv Et_3N , 0°C , 5 hrs, 1g SM	No reaction, SM recovered
3	2.5 equiv $\text{SO}_3\cdot\text{Py}$ 3 equiv Et_3N , 0°C , 6 hrs, 2.5 g SM	52%
4	2.5 equiv $\text{SO}_3\cdot\text{Py}$ 3 equiv Et_3N , 0°C , Overnight, 2.5g SM	No reaction

The low yields and variability in the reaction outcome indicated that the reactions were not reproducible. In reactions 2, at 6 hours TLC analysis showed that no product had formed. A further 2.5 equivalents of the $\text{SO}_3\cdot\text{Py}$ complex and 3 equivalents of triethylamine were added and the reaction left overnight. The next day,

the starting acetal **147** was recovered. This implied that the SO₃.Py complex was not undergoing a reaction. However, upon scale up in reaction 3 a yield of 52% was observed, but repeating the reaction for reaction 4 showed the reaction no longer worked. At 6 hours TLC analysis did not show any product formation so more of the SO₃.pyridine complex and base was added to the reaction and left overnight. All the starting material was recovered at this point and a new direction for the synthesis was chosen (see section 3.2.3).

Despite the unreproducible reactions, the lability of the acetal group and generally low yields of the reaction, the ¹H NMR spectrum of ketone **148** was indicative of its formation. Striking differences were observed between acetal **147** and ketone **148** as seen in table 3.5. In figure 3.3 the ¹H NMR spectra for acetal **147** and ketone **148** are shown for a side by side comparison.

Table 3.5: Comparisons between the ¹H NMR spectra of hydroxyl acetal **147** and keto acetal **148**

Acetal 147	Acetal 147 chemical shift (ppm)	Ketone 148	Ketone 148 chemical shift (ppm)
	Cis 5.54 (s) Trans 5.38 (s)		5.9 (s)
	Cis 3.61 (t) Trans 3.01 (t)		N/A
OCH ₂	Cis 3.61 (m) Trans 3.01 (m)	OCH ₂	4.50 (2xd)

As can be seen in the ¹H NMR spectra for both compounds, the chemical shift of the benzylidene proton increases markedly between hydroxyl acetal **147** and keto acetal **148**, and this is due to the electron withdrawing effect of the ketone on the ring. This proton becomes increasingly deshielded in ketone **148** which increases its chemical shift. This also affects the protons bound to positions 2 and 4 on the 1,3-dioxane ring. These protons are also deshielded in ketone **148** and are seen at a higher chemical shift than those in acetal **147**. Also, it is noted that proton 3 in hydroxyl acetal **147** in

figure 3.3 is no longer present in ketone **148** (see figure 3.2 for the ^1H NMR spectrum of acetal **147**).

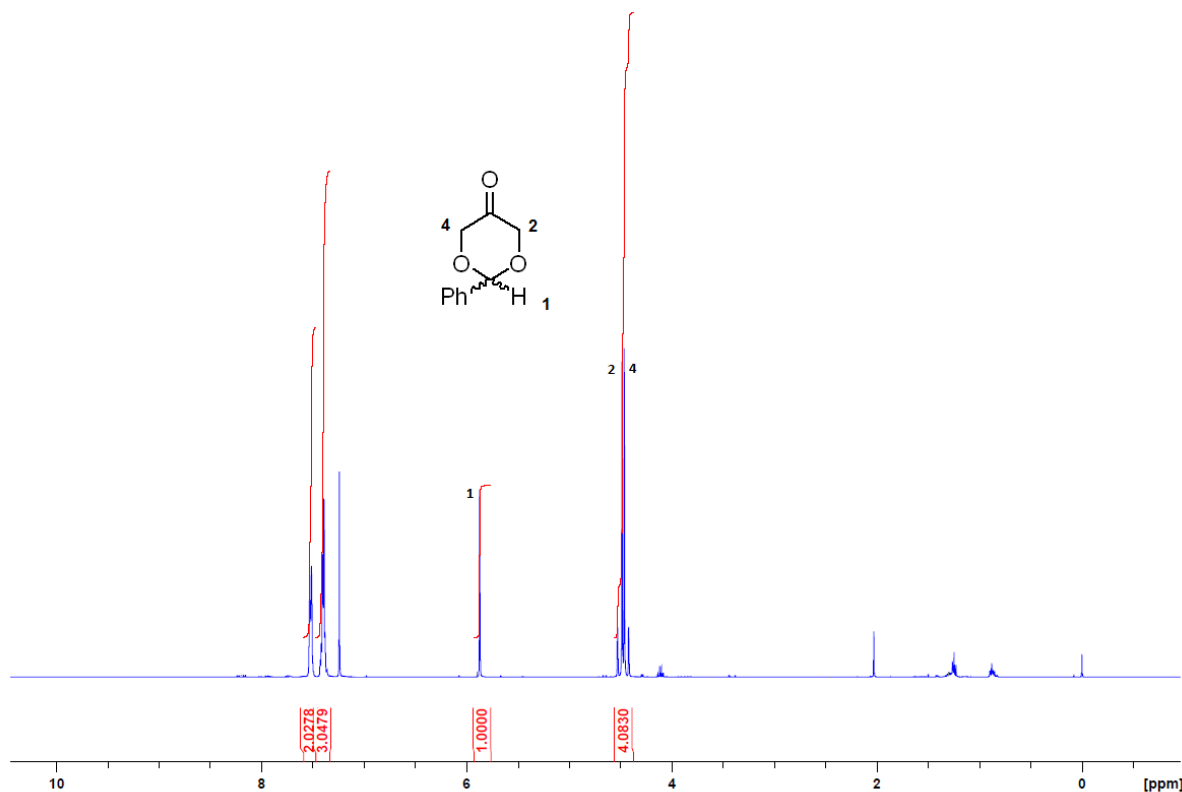


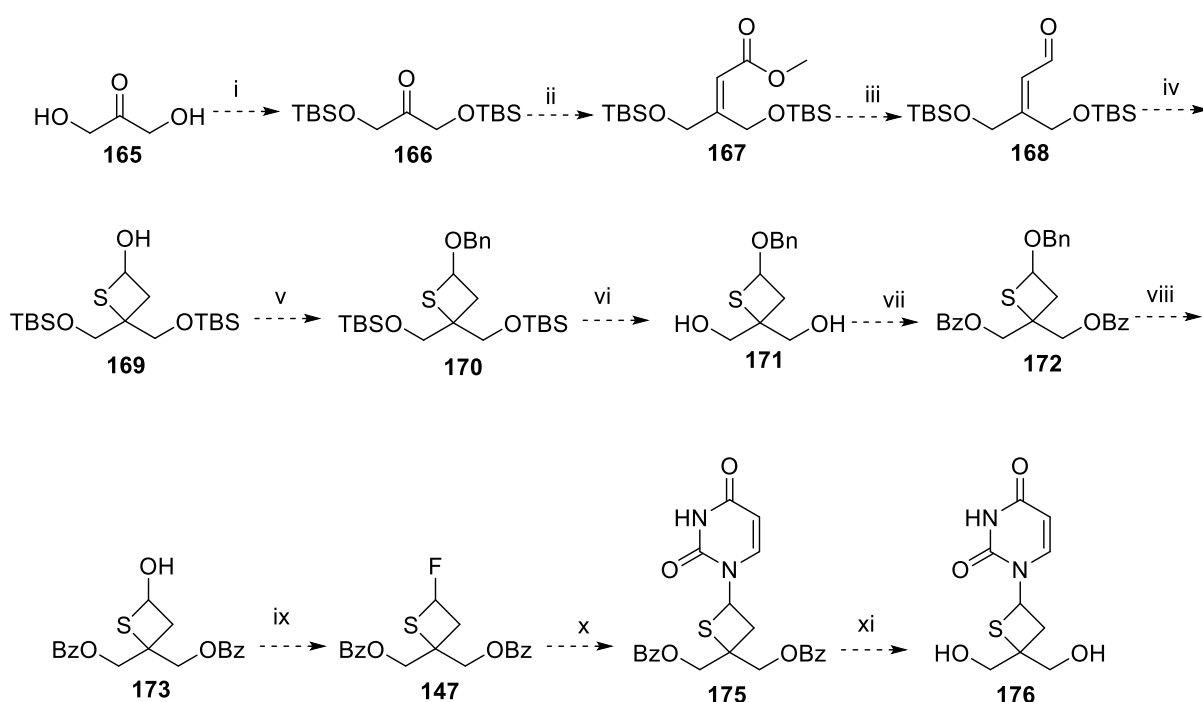
Figure 3.3: ^1H NMR spectrum of ketone **148**

The conversion of the hydroxyl group in acetal **147** to the ketone group in ketone **148** was confirmed by comparisons between the IR spectra for these two compounds. Acetal **147** shows a clear broad peak at 3348 cm^{-1} which is not observed in ketone **148** and is indicative of the hydroxyl group. The IR spectrum for ketone **148** does show a very sharp peak at 1740 cm^{-1} that is not present in acetal **147** and is indicative of the ketone group. Mass spectrometry data found the mass ion peak for ketone **148** at 178.0444 Da and confirmed that the ketone had been synthesised which is consistent with the expected mass ion peak of 178.0630 Da .

3.3.2 Results and Discussion: Modification of the Protecting Group

Although the acetal protecting group can be a versatile and resilient protecting group, it was found to be unsuitable for this synthesis. Although the oxidation reactions were mild, the acetal group was found to be unstable toward these reactions, the yields

were often low and the major problem was that these reactions were not reproducible. Two solutions to these problems were identified: the first solution was to remove the oxidation reaction altogether and the second solution was to change the protecting group. In scheme 3.15 a new approach to thietane **174** is shown, the key intermediate toward the target nucleosides. The *tert*-butyldimethylsilyl (TBS) group was chosen as it is stable to a pH range of 3-12, high temperatures and almost every stage of the synthesis except for the addition of fluorine. This would require a change in protecting group to the benzoyl protecting group as was used in the synthesis of thietane nucleosides in chapter 2.

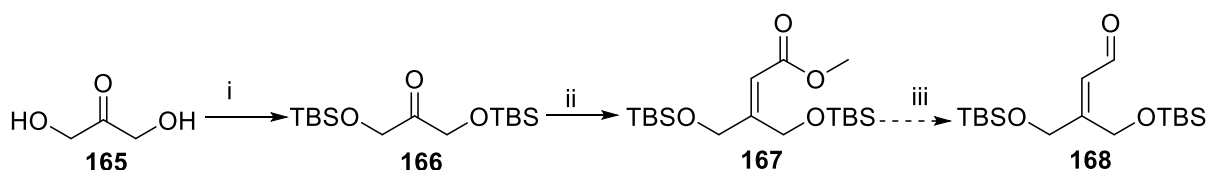


Scheme 3.15: Proposed synthetic strategy toward 4,4-bis(hydroxymethyl)-thietane nucleosides i) TBS-Cl, imidazole, DCM, RT ii) NaH, Methyl diethylphosphonoacetate, THF, RT iii) DIBAL-H, THF, -78° C iv) H₂S, Et₃N, -10° C v) BnBr, DMF, RT vi) nBu₄NF, THF vii) BzCl, Et₃N, DMAP, DCM, RT viii) H₂ Pd/C, MeOH ix) Deoxofluor, SbCl₃, DCM, RT x) silylated nucleobase AgClO₄, SnCl₂ various solvents and conditions (see chapter 2) xi) NaOMe, MeOH, RT

The reaction starts from 1,3-dihydroxyacetone **165** (DHA) a cheap starting material that is also the simplest keto-sugar known. Starting from DHA **165** removes the problematic oxidation reaction and allows for the installation of the TBS protecting group immediately and from here, the reactions generally follow the reaction conditions in scheme 3.4.

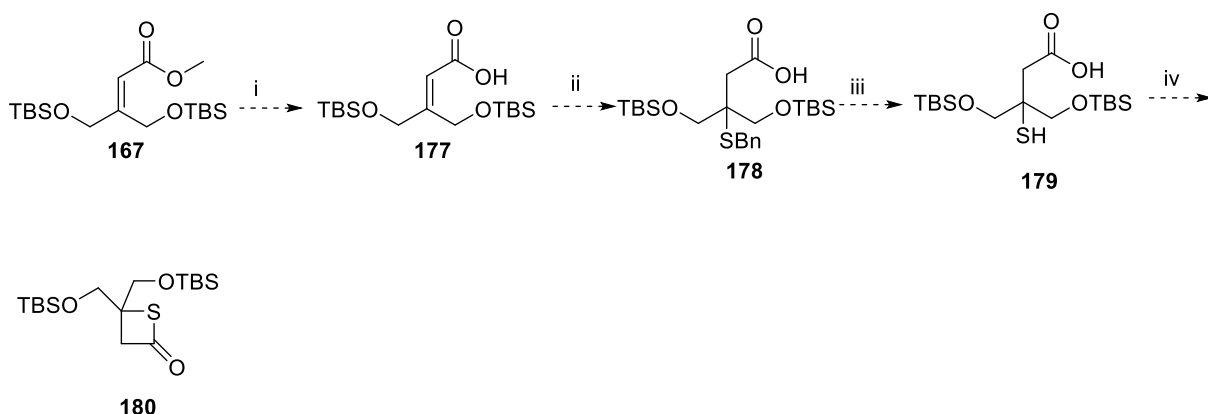
3.3.2.1 Results and Discussion: Synthesis of the Allyl Aldehyde

In scheme 3.16, the reaction conditions and yields of the first three steps are shown.



Scheme 3.16: Proposed synthetic steps to the allyl aldehyde: i) TBS-Cl, imidazole, DCM, RT, 18 hrs, quantitative yield ii) NaH, Methyl diethylphosphonoacetate, THF, 1 hr then ketone **171**, RT, overnight, 61% iii) DIBAL-H, THF -78° C product not observed, however, compound **181** was (see text) isolated

From aldehyde **168**, H₂S can be used to synthesise the thietane from methyl ester **167**, but, as seen in scheme 3.17, methyl ester **167** can also be used to furnish the thietane using the steps developed by Pattenden *et al.* should the former scheme fail to yield usable results.^{8,12}



Scheme 3.17: Modification of the Pattenden synthetic steps toward thietanes: i) LiOH or NaOH ii) BnSH, piperidine, 116° C iii) Na/NH₃, THF, -78° C iv) Isobutyl chloroformate, Et₃N, DCM, -10° C

The synthesis of TBS ketone **166** from DHA **165** proceeded with ease after reacting overnight. The initial reaction conditions of 4 – 6 hours were too short to force the reaction to completion and this was due to the solubility of DHA **165**, it was poorly soluble in DCM. However, after 24 hours, TLC analysis coupled with analysis of the crude reaction mixture by ¹H NMR spectroscopy revealed that the reaction had gone to completion with a quantitative yield after purification. The quantitative yield was

comparable to the 98% yield obtained by Weissflock *et al.*¹³ The ^1H NMR spectrum of ketone **166** is shown in figure 3.4

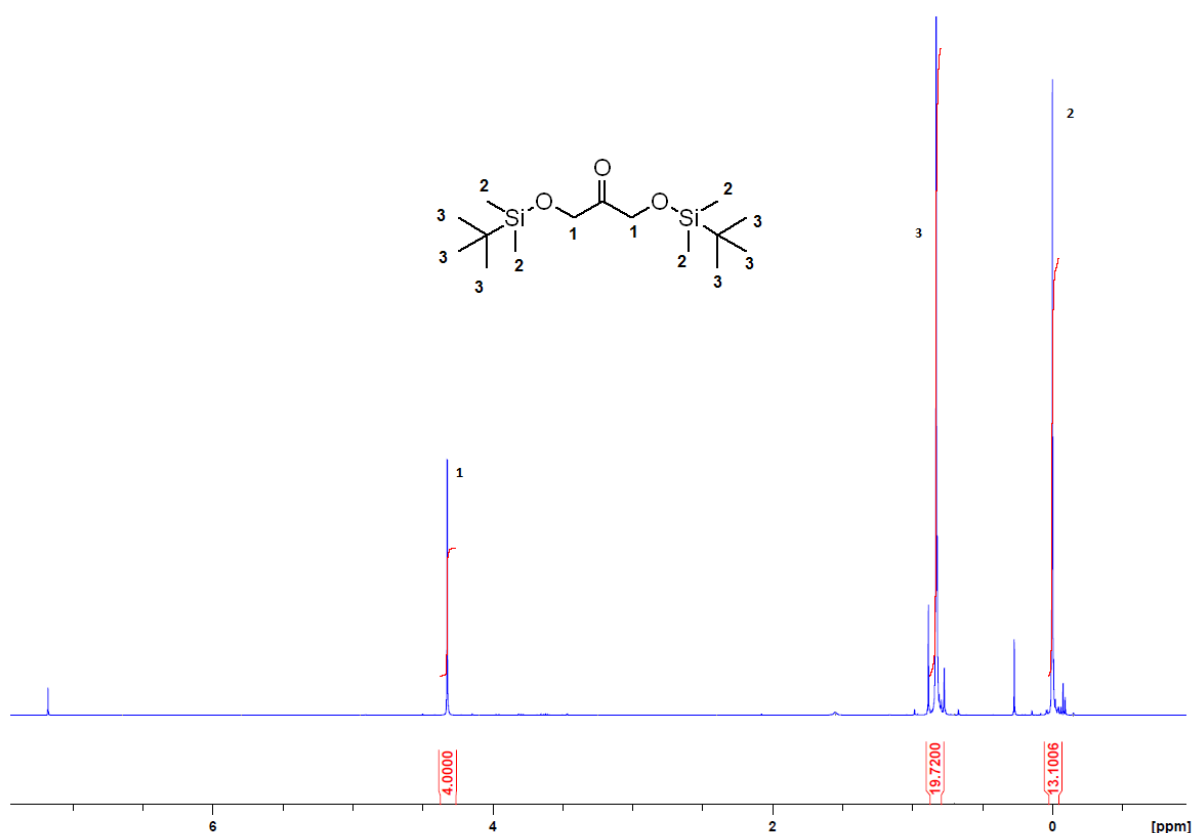


Figure 3.4: ^1H NMR spectrum of TBS Ketone **166**

The spectrum in figure 3.4 clearly shows the TBS groups are present with the CH_2 groups shown as a sharp singlet at 4.3 ppm. The IR spectrum for ketone **166** confirmed the presence of the ketone group as a sharp peak at 1738 cm^{-1} , and mass spectrometry data gave an m/z of 341.2000 Da which was found to be the sodium adduct of ketone **166**. The expected m/z for this compound was 341.1994 Da for the sodium adduct. With small scale synthesis of ketone **166** successful, several 50 g batches were subsequently synthesised and all were purified through a plug of silica to give quantitative yields of ketone **166**.

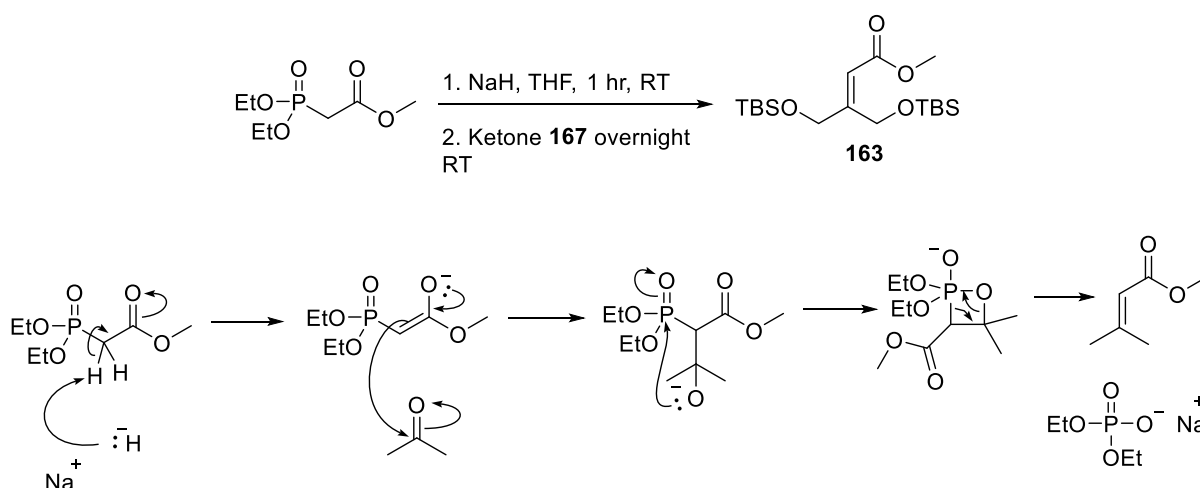
Optimisation of the reaction conditions towards methyl ester **167** were required as table 3.6 shows. Initial reaction conditions showed incomplete reactions and this was suspected to be due to the first step of the reaction where sodium hydride in THF was used as a base to deprotonate the phosphonate (see scheme 3.18 for the

overall scheme and the reaction mechanism). Increasing the equivalents of sodium hydride significantly increased the yields.

Table 3.6: Optimisation of reaction conditions toward methyl ester **167**

Reaction	Conditions	Yield (%)
1	1.1 equiv NaH, 1 equiv phosphonate, THF, RT, overnight	17
2	1.1 equiv NaH, 1 equiv phosphonate, THF, RT, overnight	39
3	1.5 equiv NaH, 1 equiv phosphonate, THF, RT, overnight	43
4	1.5 equiv NaH, 1 equiv phosphonate, THF, RT, overnight	43
5	1.5 equiv NaH, 1 equiv phosphonate, THF, RT, overnight	56
6	1.5 equiv NaH, 1 equiv phosphonate, THF, RT, overnight	61

Initial reactions showed that 1.1 equivalents of NaH did not satisfactorily deprotonate the phosphonate. Increasing the equivalents of NaH to 1.5 showed an increase in yield and the reaction gave more reproducible yields such that upon scale up (reactions 4 – 6) 25 g scale reactions could be performed with good to moderate yields. All reactions were quenched by cooling to 0° C by dropwise addition of ice cold water, and then extracted with DCM. The reactions were then purified by flash column chromatography and the column was optimised by using a gradient elution (100% petroleum ether to 95:5 petroleum ether:ethyl acetate) to give an isolated yield of 70% of methyl ester **167**.



Scheme 3.18: Synthetic scheme and reaction mechanism toward methyl ester **167**

As can be seen from the ^1H NMR spectrum (figure 3.5) for methyl ester **167**, the singlet at 4.3 ppm which is indicative of the CH_2 groups for ketone **166**, is now observed as two singlets for the same CH_2 groups in methyl ester **167** (figure 3.5).

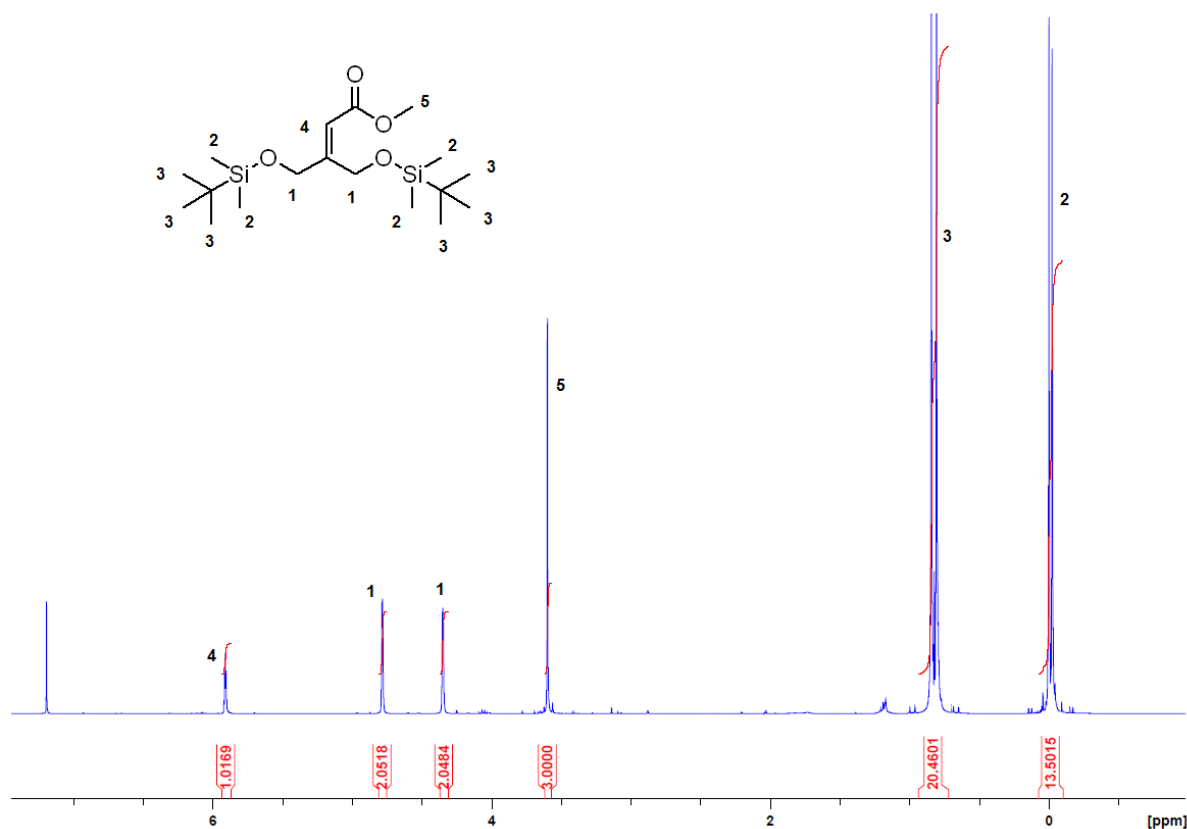


Figure 3.5 ^1H NMR spectrum of methyl ester **167**

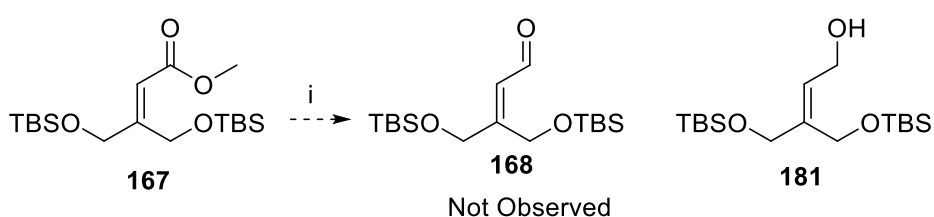
The key peak that determined whether the alkene had formed was the peak at 5.9 ppm which is indicative of the $\text{C}=\text{CH}$ proton. HMBC confirmed that the $\text{C}=\text{CH}$ proton was 4 bonds away from the CH_2OSi protons. IR spectroscopy data showed a sharp peak at 1718 cm^{-1} , a drop of 20 cm^{-1} versus the peak observed in ketone **166**. A C-O stretch at 1100 cm^{-1} which is indicative of the C-OMe bond stretch was also observed. Mass spectrometry data confirmed the compound had been successfully synthesised with the m/z of 375.2384 Da which was close to the expected m/z value of 375.2309 Da.

3.3.2.2 Divergence of the Synthetic Scheme

As shown in schemes 3.6 (section 3.3), two methods were identified as plausible synthetic schemes toward thietane nucleosides: The Givaudan synthesis which uses

an aldehyde and hydrogen sulfide to form the thietane, and the Pattenden synthesis, which uses a carboxylic acid, benzyl mercaptan and two additional steps to cyclise the thietane (see section 3.3).

The Givaudan synthesis of the thietane was first attempted as it allows quicker access to the target compound with only a reduction of methyl ester **167** to aldehyde **168**. The Pattenden synthesis requires ester hydrolysis followed by several steps prior to cyclising the thietane ring. However, use of DIBAL-H did not give the aldehyde, instead as table 3.7 and scheme 3.19 show, the reaction conditions were not conducive toward the aldehyde, and instead, alcohol **181** was isolated.¹⁴



Scheme 3.19: DIBAL-H reduction of methyl ester **167** did not give aldehyde **168**, but instead gave allyl alcohol **181** i) DIBAL-H, THF, -78° C, 80% for **181**.

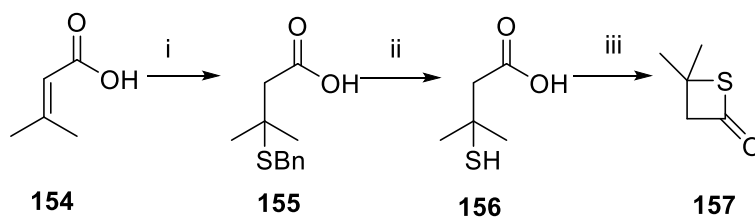
Table 3.7: Optimisation of the DIBAL-H reduction reaction of methyl ester **167** to allyl alcohol **181**. All reactions performed at -78° C in anhydrous THF

Reaction	Conditions	Outcome
1	250 mg 167 , 2 equiv DIBAL-H react 3 hrs. Further 1 equiv DIBAL-H added and reacted for 1 additional hour.	TLC showed no change at 3 hrs. After additional 1 equiv DIBAL-H, consumption of SM was observed. 28% yield of 181
2	250 mg 167 , 3 equiv DIBAL-H react 3 hrs	22% yield of 181
3	500 mg 167 , 3 equiv DIBAL-H react 3 hrs	26% yield of 181
4	1 g 167 , 3 equiv DIBAL-H react 3 hrs	80% yield of 181

Optimisation of the reaction toward allyl aldehyde **168** could not be achieved, though careful control of the number of equivalents of DIBAL-H is known to give the aldehyde over the alcohol. No change by TLC analysis was observed for this reaction when less than 3 equivalents of DIBAL-H were used. Increments of 0.5 equivalents of DIBAL-H were added to the vessel in reaction 1 every 3 hours and no reaction was observed until 3 equivalents were reached. Increasing the number of equivalents of

DIBAL-H had the potential to increase the reaction rate as concentration of a reagent is tied to reaction rates. However, increasing the number of equivalents also increases the likelihood of allyl alcohol **181** forming. Analysis of the crude reaction mixture by ^1H NMR spectroscopy revealed only ester **167** was present after 3 hours in the presence of DIBAL-H in reaction 1 which prompted the addition of more DIBAL-H as discussed. Subsequent reactions used 3 equivalents of DIBAL-H and in all cases allyl alcohol **181** was isolated. Failure to form aldehyde **168** is due to the fact that DIBAL-H is known to reduce α,β -unsaturated esters to the corresponding allyl alcohol. It could still be possible to synthesise aldehyde **168** by using 2 – 2.5 equivalents of DIBAL-H over much longer periods of time.

At this juncture, oxidation of allyl alcohol **181** to aldehyde **168** was considered as a means to access the aldehyde **168**, and the Swern oxidation reaction was chosen as the easiest method to use as it showed greater reproducibility than the DMP and Parikh-Doering reactions for the oxidation of acetal **147** to ketone **148**. However, using the Swern oxidation conditions from the synthesis of ketone **148** for the conversion of allyl alcohol **181** to aldehyde **168** did not work and was not optimised for this system because success was being had with the reproduction of the Pattenden synthesis of thietanones using benzyl mercaptan to access 4,4-dimethyl thietanes (scheme 3.20).⁸



Scheme 3.20: i) Benzyl mercaptan, piperidine, reflux, 24 hrs, quant ii) Na, NH_3 , THF, -78°C , quant iii) Isobutyl chloroformate, Et_3N , DCM, -10°C , 20 minutes

Heating acid **154** in the presence of BnSH and piperidine gave thioether **155** with a quantitative yield. ^1H NMR spectroscopic data for thioether **155** matched the literature data.⁸ The methyl groups were observed at 1.46 ppm which is close to the literature value of 1.50 ppm. Allyl acid **154** contains a singlet at 5.7 ppm which is the alkene proton. This is not observed in thioether **155**, instead a CH_2 singlet is observed at 2.65 ppm, which matches the literature value. Thiol **156** was obtained after

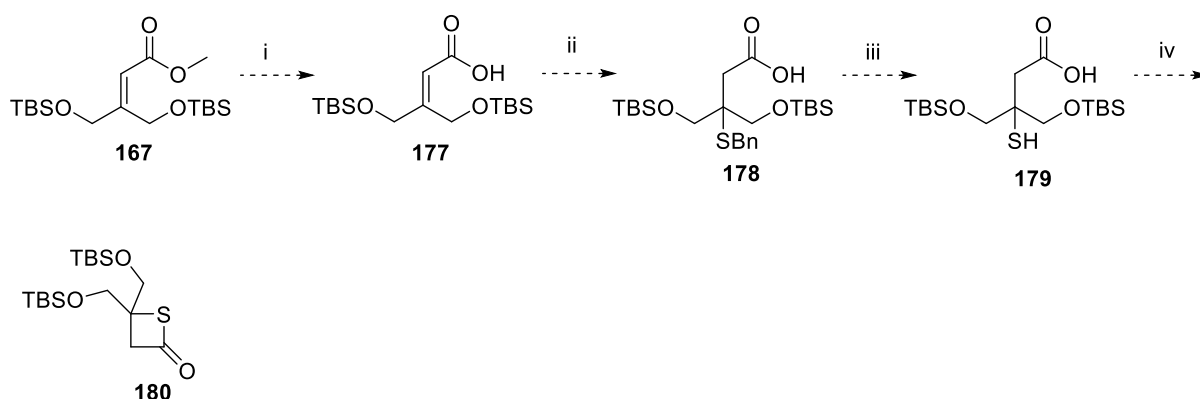
optimisation of the thea reaction between thioether **155** and sodium in liquid ammonia. Reproduction of the Pattenden reaction conditions were followed gave a thick gel, and in subsequent reactions, the starting material was dissolved in THF before the liquid ammonia was condensed, which overcame this problem.

The ^1H NMR spectroscopic data again matched the literature for thiol **156**. The methyl groups were observed at 1.46 ppm which exactly matched the literature data. The SH proton was observed at 2.68 ppm, which again, matched the literature.

Cyclisation toward thietanone **157** was achieved after optimisation of the reaction conditions with isobutyl chloroformate. The Pattenden conditions called for 1 equivalent of triethylamine and 2 equivalents of isobutyl chloroformate. However, attempts to replicate this method were met with failure as a solid white mass was formed. Analysis of the white solid revealed that the reaction did not go to completion and contained starting materials. The optimised reaction used 2 equivalents of triethylamine and 2.2 equivalents of isobutylchloroformate for 1 hour. TLC analysis of the crude reaction mixture showed that the reaction had reached completion. However, due to the high volatility of thietanone **157**, purification was not achieved and instead the ^1H NMR spectroscopic data of the crude reaction mixture was obtained which showed peaks consistent with the product. The methyl groups were observed at 1.44 and 1.45 ppm with literature values of 1.31 and 1.38 ppm. The CH_2 group was observed at 3.74 ppm with a literature value of 3.72 ppm.

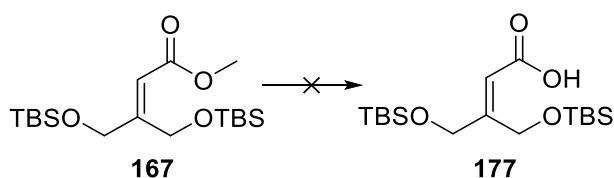
3.3.3 Ester Hydrolysis Reactions

With successful replication of the Pattenden reaction conditions, the synthetic strategy toward the target thietane was modified in order to successfully synthesise the novel thietane core (scheme 3.21). As stated in section 3.3, the Pattenden synthesis introduces two additional steps into the synthetic strategy when using methyl ester **167**. Ester hydrolysis is required prior to incorporation of the thiobenzyl moiety toward thioether **178**, and deprotection of thioether **178** to thiol **179** must occur prior to cyclisation to thietanone **180**.



Scheme 3.21: Modification of the synthetic route toward the target thietane i) LiOH or NaOH, various solvents, ii) BnSH, piperidine, 116° C, overnight iii) Na/NH₃, THF, -78° C 2-3 hrs iv) isobutyl chloroformate, Et₃N, DCM, -10° C, 1-2 hrs

Several methods were attempted to hydrolyse methyl ester **167** to acid **177** using mineral bases as the TBS group is reported to be stable up to pH 12 and the TBS group was stable at pH 12 with 5% NaOH in MeOH for 24 hours.^{15,16} A literature search for hydrolysis of conjugated methyl esters with TBS protecting groups revealed two methods for the hydrolysis reaction and implied that the TBS groups were indeed stable to base: One where six equivalents of LiOH are used and is heated to 60° C for one hour and another reaction where 10 equivalents of LiOH are used at room temperature for 8 hours.^{17,18} Neither reaction was conducive to hydrolysing the methyl group of methyl ester **167**, and analysis of the reaction by ¹H NMR spectroscopy revealed significant deprotection of the TBS groups. Table 3.8 summaries each reaction attempt and variations of solvents and equivalents of base used. Scheme 3.22 shows the general reaction scheme for this hydrolysis.



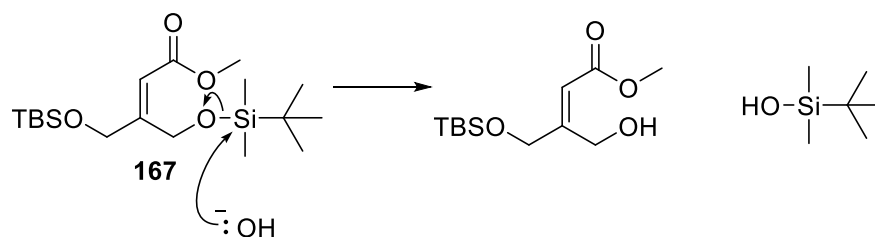
Scheme 3.22: General hydrolysis reaction of methyl ester **167** with mineral bases

Table 3.8: Mineral base hydrolysis of methyl ester **167** to acid **177**

Reaction	Base	Conditions	Outcome
1	LiOH	6 equiv base 4:1 IPA:Water 60° C 1 hr	TBS group deprotection
2	LiOH	10 equiv base 8:1:1 THF:MeOH:Water RT, overnight	TBS group deprotection

3	NaOH	1 equiv base, 1:1 THF:Water RT, overnight	No reaction
4	NaOH	1.5 equiv base, 1:1 THF:Water RT, overnight	No reaction
5	KOH	1.5 equiv base, 1:1 THF:Water RT, overnight	TBS group deprotection
6	LiOH	1.5 equiv base 2:1 MeOH:Water 6 hrs	No reaction
7	LiOH	6 equiv base 4:1 IPA:Water, RT, 6 hrs	TBS group deprotection
8	LiOH	3 equiv base, IPA, RT, overnight	No reaction
9	LiOH	3 equiv base, 4:1 IPA:Water dropwise addition of base over 8 hrs, RT, overnight	No SM, some TBS deprotection
10	LiOH	10 equiv base, dropwise addition over 8 hrs, 8:1:1 THF:MeOH:Water, RT, overnight	Hydrolysis observed by TLC analysis and ¹ H NMR spectroscopy. Still observed TBS group deprotection
11	LiOH	2.5 equiv base, dropwise addition over 8 hrs, 8:1:1 THF:MeOH:Water, RT, overnight	No reaction
12	LiOH	2.5 equiv base, dropwise addition over 8 hrs, 8:1:1 THF:MeOH:Water, 45° C, overnight	TBS group deprotection and some product isolated

The literature reaction conditions failed to yield the desired product (reactions 1 and 2). Initially LiOH was trialled as it is the least soluble of the mineral bases. The slow release of the hydroxide ion means that the reaction kinetics could be controlled. The low concentration of hydroxide in solution would allow selective reaction at the methyl ester rather than the silyl protecting groups. The number of equivalents was changed to further aid reaction kinetics. The base was changed to NaOH and KOH as these were stronger bases and as such would react more readily than LiOH. This was in order to bring down reaction times by increasing reaction rates. Analysis of each reaction by TLC analysis showed consumption of the starting material, however, after work up, analysis by ¹H NMR spectroscopy revealed multiple peaks around 0 ppm and 1.5 ppm where the TBS groups are present. Here, instead of the expected doublets, several peaks were observed which indicated that the TBS groups were hydrolysing. This implied that the hydroxide ion was acting as a nucleophile at TBS groups (see scheme 3.23).



Scheme 3.23: Suspected hydrolysis reaction at the TBS group.

Since hydrolysis of the TBS group was a significant problem with the use of mineral bases, more mild conditions were sought. A literature search revealed three mild reaction conditions: the use of potassium trimethylsilanolate, trimethyltin hydroxide or lithium iodide in pyridine as potential mild reagents for this hydrolysis.¹⁹⁻²¹

3.3.3.1 Use of Potassium Trimethylsilanolate

Potassium trimethylsilanolate (KOSiMe_3) is a mild nucleophilic reagent that is useful for the hydrolysis of a wide range esters.²⁰ It has been shown that potassium trimethylsilanolate does not act as a base and therefore can be used to hydrolyse esters where there could be potential for elimination reactions or where abstraction of a proton is possible.^{19,20} Since potassium trimethylsilanolate is soluble in a multitude of organic solvents, esters that cannot be hydrolysed using mineral bases in alcohol/water solvent systems can be hydrolysed with this reagent in THF, diethyl ether, or toluene.^{19,20}

A model reaction with methyl benzoate and 1.2 equivalents of KOSiMe_3 was performed in THF and after 4 hours the benzoic acid was recovered with a quantitative yield. The method followed the report by Laganis *et al* for the use of KOSiMe_3 .²⁰ With successful synthesis of the literature method toward benzoic acid, the hydrolysis reaction with this reagent and methyl ester **167** was attempted several times and the reactions are summarised in table 3.9.

Table 3.9: Hydrolysis reactions with KOSiMe_3

Reaction	Equivalents of KOSiMe_3	Solvent and Temperature	Outcome
1	1	THF, RT	No reaction after 24 hrs, SM recovered
2	1.5	THF, heated at reflux	No reaction after 48 hrs, SM recovered

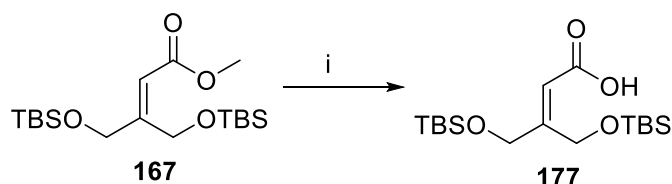
3	1.5	Toluene, heated at reflux	No reaction after 72 hrs, SM recovered
4	2	Toluene, heated at reflux	No reaction after 168 hours, SM recovered
5	10	Toluene, heated at reflux	¹ H NMR analysis did not show peaks consistent with SM or products

Although the model reaction was successful, the use of KOSiMe₃ for the hydrolysis of methyl ester **167** was not. Initial reaction conditions followed the paper but no reaction was observed. In reaction 2, 1.5 equivalents of KOSiMe₃ was then tried but no reaction was observed at room temperature in the first 24 hours. The reaction was heated at reflux for a further 24 hours to increase the rate of reaction. The solvent was changed to toluene to aid solubility of the starting materials, however, no reactions were observed when the number of equivalents were increased or when the reaction time was increased. The ¹H NMR spectrum of each crude reaction showed some lability of the TBS groups but this is suspected to be due to the 10% KOH that is present in the silanolate reagent due to the manufacturing method. However, in all but one reaction, no methyl ester hydrolysis was observed. In reaction 5, 10 equivalents of the silanolate reagent was used and heated to reflux but by the next day the ¹H NMR spectrum revealed complete hydrolysis of the compound. No peaks consistent with the starting material or the product were observed.

The use of anhydrous LiI in pyridine that is heated to reflux has been used to hydrolyse methyl esters.²¹ However, use of these conditions on methyl ester **167** did not yield any product and the starting material was totally recovered.

3.3.3.2 Trimethyltin Hydroxide Hydrolysis of Esters

Trimethyltin hydroxide (Me₃SnOH) has been used as a mild reagent for the selective hydrolysis of methyl and ethyl esters in sensitive substrates.²² Scheme 3.24 shows the optimised reaction conditions for the hydrolysis of methyl ester **167**.



Scheme 3.24: Optimised reaction conditions toward acid **177** i) 8 equivalents of Me₃SnOH, 1,2-DCE, 80° C, 96 hrs, 93% yield

Initially, 6 equivalents of the tin reagent were used but after 72 hours the reaction had not proceeded to completion. A further 2 equivalents of the tin reagent were used and after an additional 24 hours completion was observed and acid **177** was isolated pure with a yield of 93%. The number of equivalents were increased as the increased concentration of the tin reagent would have increased the likelihood of successful reactions occurring, and hence, an increase in reaction rate. No purification methods other than mildly acidic (pH 4) extractions were used. The ¹H NMR spectrum of acid **177** is shown in figure 3.6.

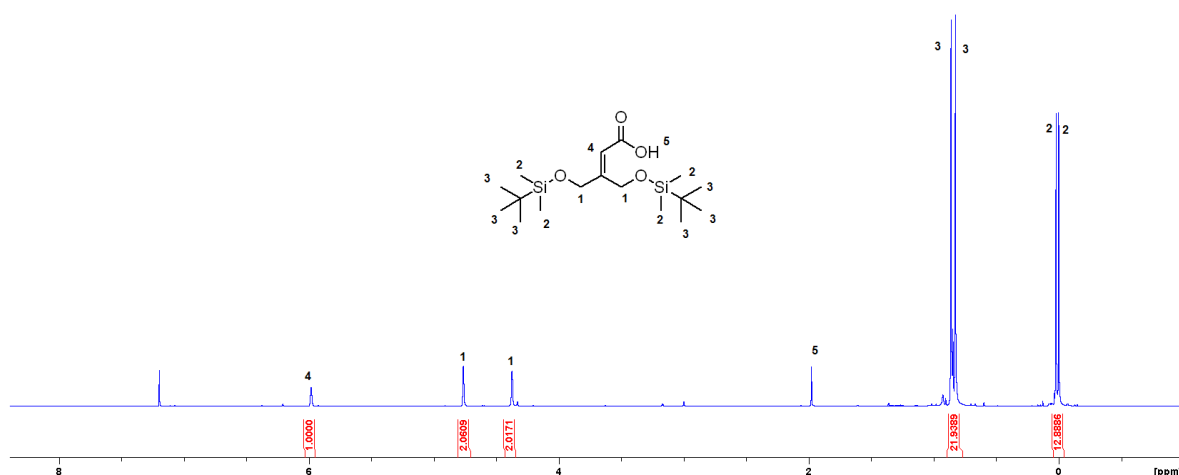
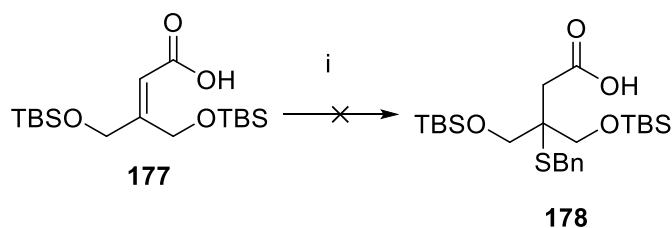


Figure 3.6: ¹H NMR spectrum of acid **177**. No methyl ester protons are present at 3.6 ppm.

The IR spectrum shows a sharp peak at 1682 cm⁻¹ which is indicative of an α,β-unsaturated carboxylic acid. The MS spectrum gives a mass charge ratio of 361.2225 Da which was close to the expected value of 361.2230 Da.

The synthesis continued with attempts to synthesise thioether **178** using BnSH and piperidine in a reaction analogous to the Pattenden reaction.⁸ The reaction shown in scheme 3.25 did not work and could not be optimised.

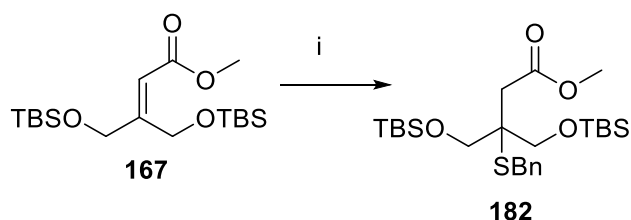


Scheme 3.25: Attempts to synthesis thioether **178** from acid **177** i) 1.1 equiv BnSH, piperidine (base and solvent), 116° C, 48 hrs no reaction

TLC analysis of the crude reaction mixture showed a reaction was occurring but after 24 hours there was still starting material present. Additional BnSH was introduced to the reaction to force it to completion but after 48 hours no change had been detected by TLC analysis in the proceeding 24 hours. Analysis of the crude reaction mixture by ^1H NMR spectroscopy was inconclusive as to whether the reaction had worked or not. Work up involved slow addition of ice cold dilute HCl. Though the Pattenden synthesis used concentrated acid, the acid sensitive TBS groups in compound **177** meant that milder conditions would need to be used. The aqueous phase was removed and dilute sodium carbonate was added, which deprotonated acid **177**. Chloroform was used to wash the basic phase to remove any organic impurities. The basic phase was slowly brought to pH 5 to re-protonate acid **177** which was extracted with chloroform. TLC analysis showed a number of products present in the organic phase. Attempts to purify the resulting residue using column chromatography could not resolve the compounds observed from the TLC plate. Analysis of the ^1H NMR spectrum for this reaction showed a multitude of peaks that could not be assigned to acid **177**. This indicated that the work up procedure was not suitable for extracting acid **177**. Though milder conditions were attempted, such as using dilute acetic acid, and milder bases such as sodium bicarbonate, extraction and purification of acid **177** was not achieved. In order to proceed with this reaction, changing the protecting groups from TBS groups to acid and base stable groups such as benzyl groups, would be advantageous. However, as benzyl mercaptan is used to introduce the sulfur atom later, and sodium in liquid ammonia is used to remove the benzyl group from the sulfur, a protecting group change would be required again before the use of benzyl mercaptan. This introduces further steps, reducing the efficiency of the synthesis.

3.3.3.3 Steps Toward the Target Thietane Molecule

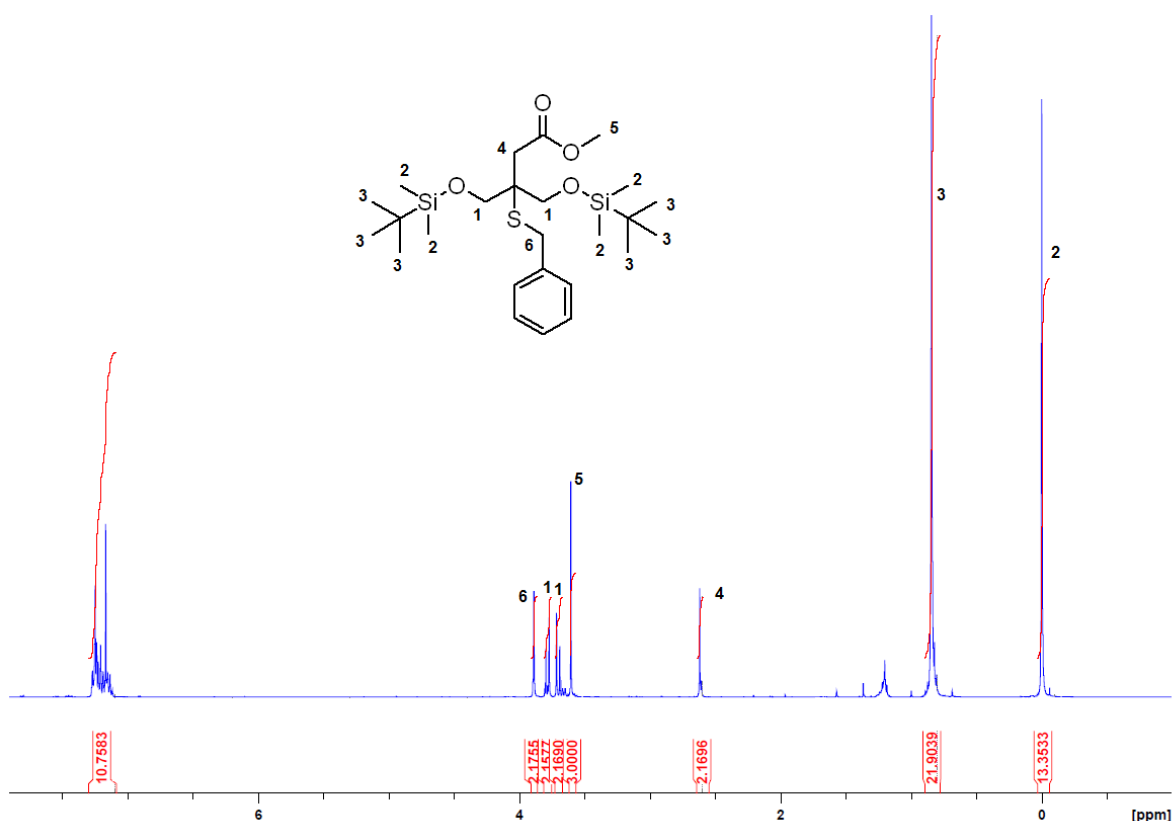
The synthesis of thioether **178** was neither optimised nor repeated because in parallel to this reaction, methyl ester **167** was also reacted with BnSH in piperidine to give thioether **182** (scheme 3.26) with a yield of 82%.



Scheme 3.26: Synthesis of thioether **182** i) 1.1 equiv BnSH in piperidine, heating to reflux over 24 hours.

The reaction did not require an acid work up because neither the starting material nor the product contains a carboxylic acid that requires re-protonation, and the piperidine could be washed out in the aqueous phase easily. However, purification of the product was difficult as a slight excess of BnSH was required to push this reaction to completion after 24 hours, the BnSH had a tendency to co-elute with the product.

Despite the problems with purification, thioether **182** was isolated and batch reactions allowed enough material to be synthesised to proceed to the next stages. In figure 3.7 the ^1H NMR spectrum is shown for thioether **182**. The most significant differences between this spectrum and that of methyl ester **167** is that the alkene proton at 5.9ppm is no longer present (as expected) and a new CH_2 group is present which is indicative of the SBn group.



IR spectroscopy showed peaks around 2952 cm^{-1} which are indicative of the benzene ring and the carbonyl stretch was observed at 1739 cm^{-1} which was not significantly different for the carbonyl stretch observed for methyl ester **167** which was observed at 1738 cm^{-1} . Mass spectrometry data confirmed that thioether **182** had formed with the mass ion peak observed with a mass of 521.2542 Da which was the sodium adduct, and was close to the expected value of the sodium adduct of 521.2553 Da .

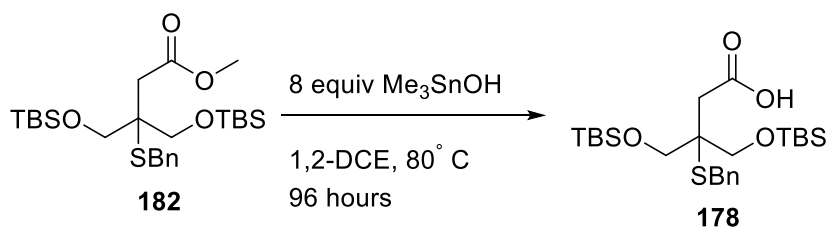
3.3.4 Ester Hydrolysis reactions of Thioether 178

With successful synthesis of thioether **182**, hydrolysis reactions were performed in an attempt to synthesise acid **178** (scheme 3.27).



Although KOSiMe_3 did not hydrolyse methyl ester **167**, the small scale exploratory reactions were performed on thioether **182** as it was suspected that the conjugated nature of methyl ester **167** was resistant to hydrolysis with this mild reagent. However, as table 3.11 shows, KOSiMe_3 as a reagent did not work adequately for this conversion. Elimination was observed in these reactions in almost all cases. According to Laganis and Lovric, KOSiMe_3 does not act like a base and behaves only as a nucleophile.^{19,20} The reagent has been used on compounds where elimination is a risk; therefore it is a good reagent for sensitive compounds. However, since the reagent contains up to 10% KOH, the observed elimination reaction could be due to the presence of this strong base. As shown in table 3.11, the elimination product was found to be allyl ester **167** with the ^1H NMR spectroscopic data revealing the indicative singlet at 5.9 ppm for the alkenic proton. In both reactions, the ^1H NMR spectroscopic data revealed a mixture of thioether **182** and allyl ester **167**.

Although only two reactions were performed, the reactions were attempted because the equivalents of reagent used were low for the conversion of methyl benzoate to benzoic acid (1.2 equivalents), versus Me_3SnOH which required 8 equivalents, significantly longer reactions times, and a significant work up protocol. However, immediate success was had with the tin reagent as seen in scheme 3.28.



Scheme 3.28: Ester hydrolysis using trimethyltin hydroxide

Since immediate success was had with the tin reagent for this hydrolysis, it was used in subsequent reactions, including large scale (10 g) synthesis of acid **178** with yields ranging from 61 – 88%. Figure 3.8 shows the ^1H NMR spectrum for acid **178** which shows no methyl ester peak at 3.9 ppm (figure 3.8).

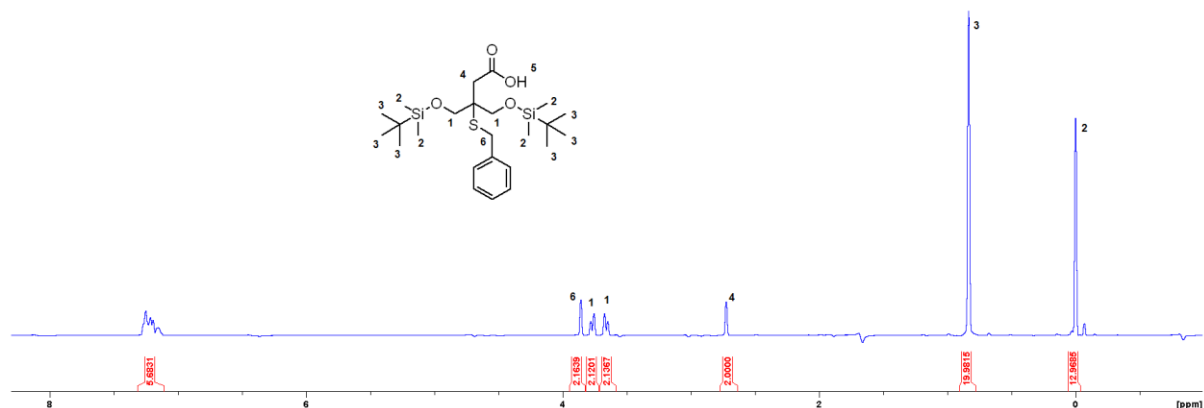
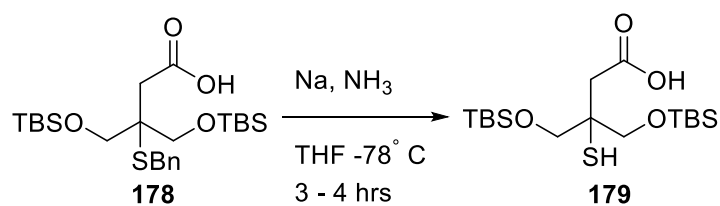


Figure 3.8: ^1H NMR spectrum of acid **178**

The IR data showed a change in the wavenumber for the carbonyl stretch which was at 1739 cm^{-1} in thioether **182** and in acid **178**, the carbonyl stretch is at 1707 cm^{-1} . Mass spectrometry data gave the mass ion peak 507.2391 Da which was the sodium adduct. The expected mass for the sodium adduct was calculated to be 507.2397 Da.

With successful reproduction and optimisation of the benzyl group deprotection reaction for the Pattenden synthesis of 4,4-dimethylthietan-2-one (see scheme 3.7 section 3.3) with sodium in liquid ammonia, the reaction optimised reaction conditions were trialled on thioether **178** to give thiol **179** (scheme 3.29).



Scheme 3.29: The synthesis of thiol **179** using sodium in liquid ammonia

Initial reactions with thioether **178** did not go to completion in the same time frame as the Pattenden synthesis (scheme 3.7) (1 – 2 hours versus 3 – 4) and an end point was hard to determine because TLC analysis was impossible due to liquid ammonia evaporation. However, small (0.1 ml) aliquots were removed from the crude reaction mixture, worked up and analysed by ¹H NMR spectroscopy which revealed the reaction had reached completion after 4 hours. After purification by mild acid work up, thiol **179** was fully characterised. Figure 3.9 shows the ¹H NMR spectrum for this compound.

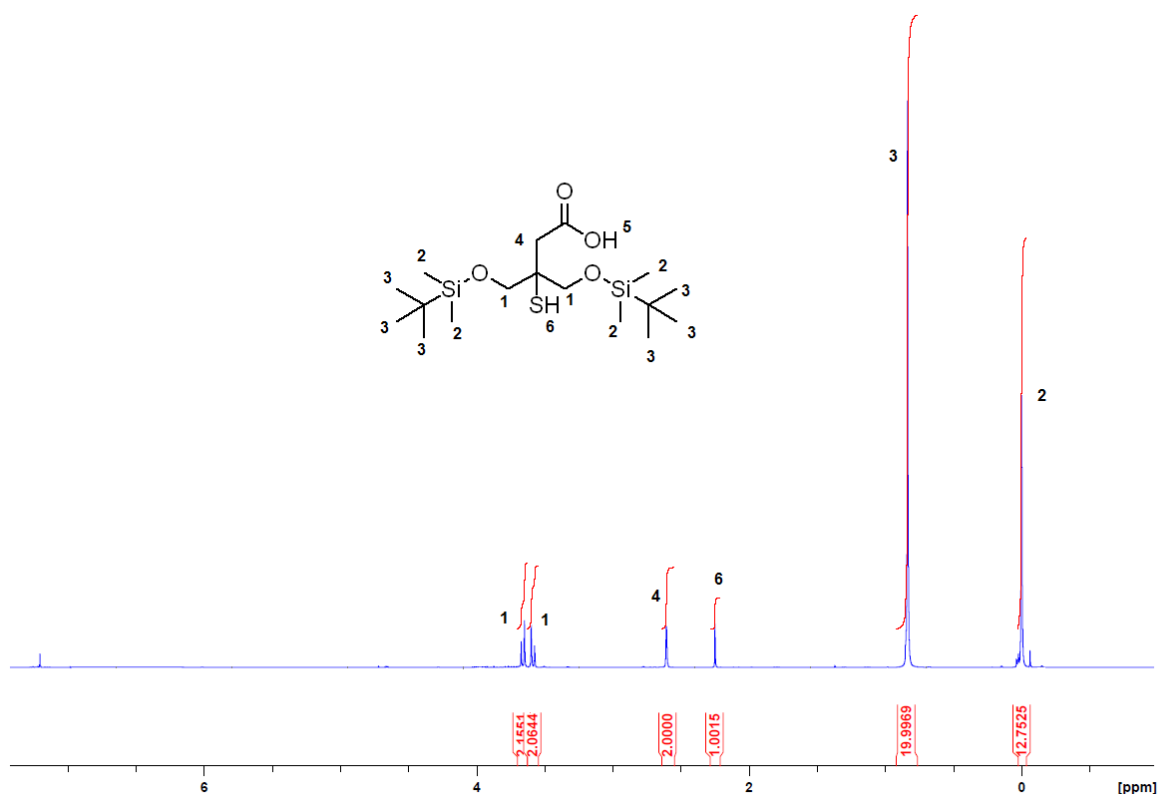
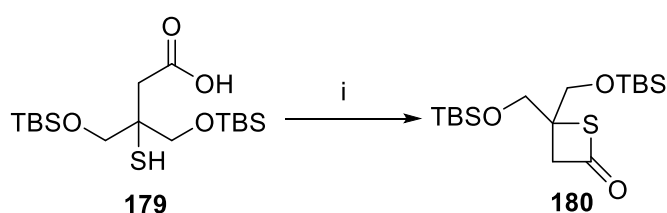


Figure 3.9: ¹H NMR spectrum of thiol **179**

The ¹H NMR spectrum shows clearly the thiol proton at 2.5 ppm which is the key indicative peak for this compound. The IR spectrum for this compounds shows

several signals: 3345 cm^{-1} as a sharp peak for the --OH stretch, 2857 cm^{-1} for the --SH stretch, and three sharp peaks at 1732 cm^{-1} , 1687 cm^{-1} and 1645 cm^{-1} which are indicative of the carbonyl C=O stretches. The mass spectrum data revealed the mass ion peak $+\text{H}^+$ at 395.2103 Da and the sodium adduct at 417.1922 Da with both corresponding to the calculated values of 395.2108 Da and 417.1927 Da .

With optimised reaction conditions from the model reaction for the synthesis of 4,4-dimethylthietan-2-one established, the synthesis of thietanone **180** was achieved with a yield of 37% after reacting for 4 hours (scheme 3.30). Figure 3.10 shows the ^1H NMR spectrum for thietanone **180**.



Scheme 3.30: Synthesis of thietanone **180** i) isobutylchloroformate, triethylamine, DCM, -10°C , 4 hours, 37%

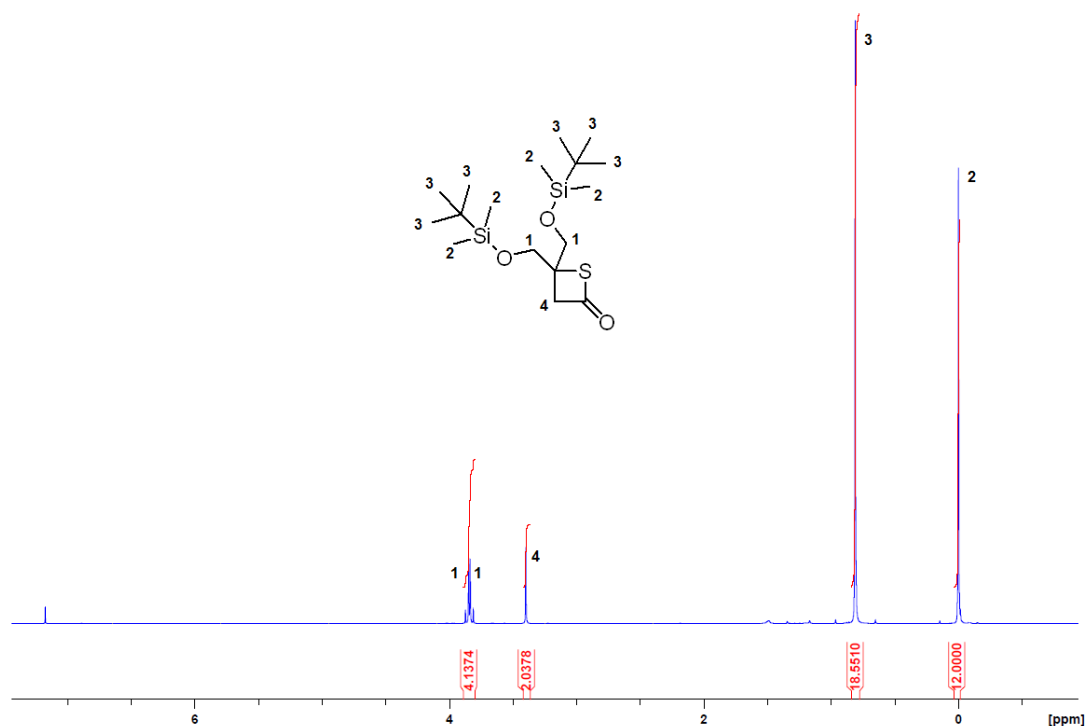


Figure 3.10: ^1H NMR spectrum of thietanone **180**

Interestingly, the IR spectrum of thietanone **180** was sufficiently different to the IR spectrum of thiol **179** that it was possible to distinguish between these compounds based by IR spectroscopy, as shown in figure 3.11.

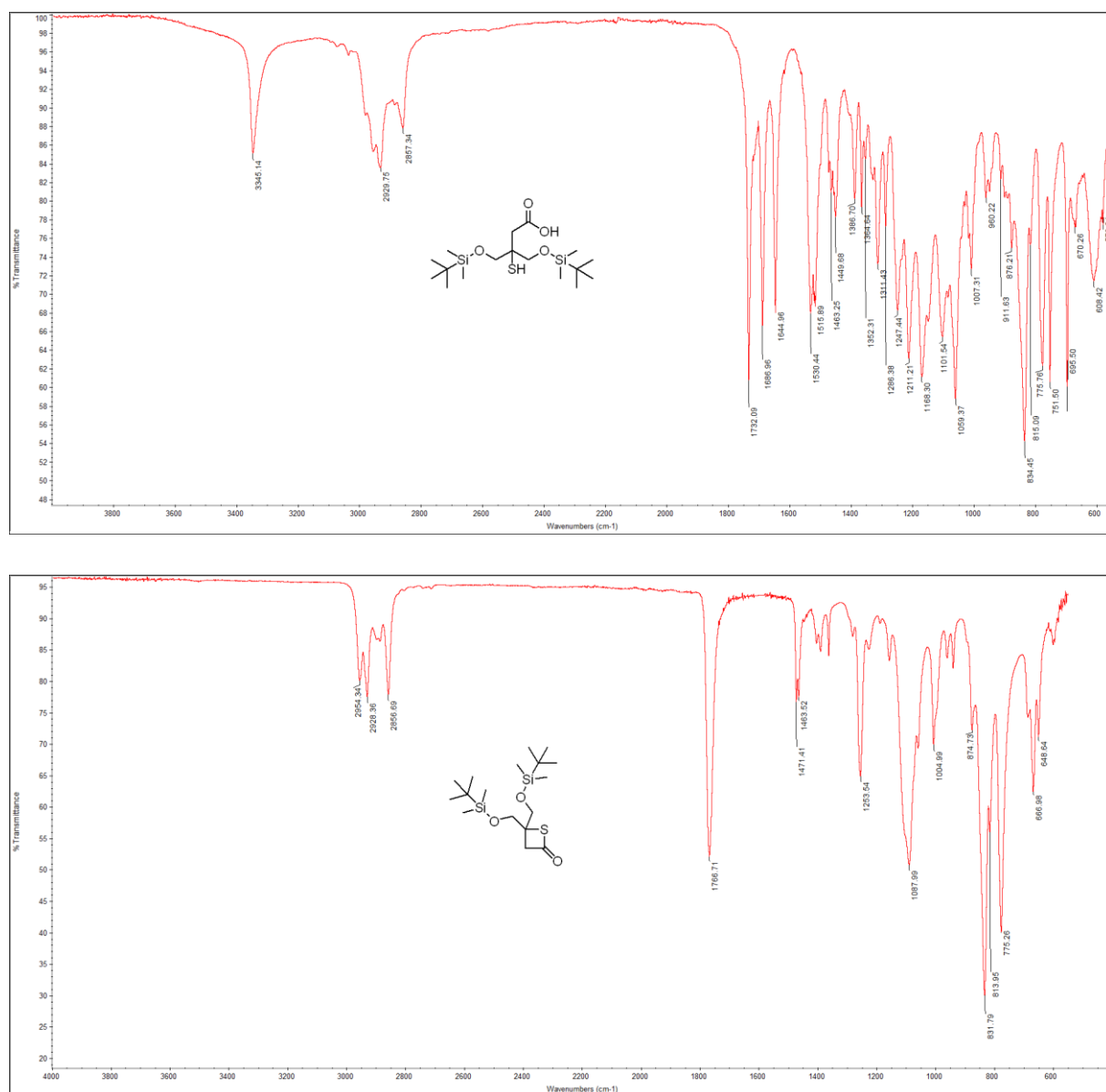


Figure 3.11: Top: The IR spectrum for thiol **179** and bottom: The IR spectrum for thietanone **180**

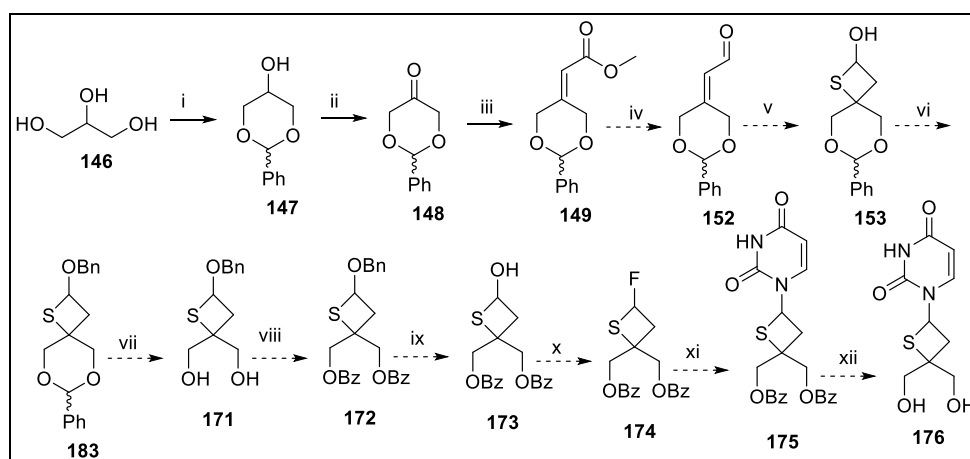
As can be seen from the IR spectrum for thietanone **180**, only one band for the ketone is present at 1767 cm⁻¹. This is rather high for a C=O stretch and is possibly due to ring strain, and is in the expected range for thietanone **180** as Pattenden *et al.* found that the C=O stretch for thietanone **180** was 1748 cm⁻¹.⁸

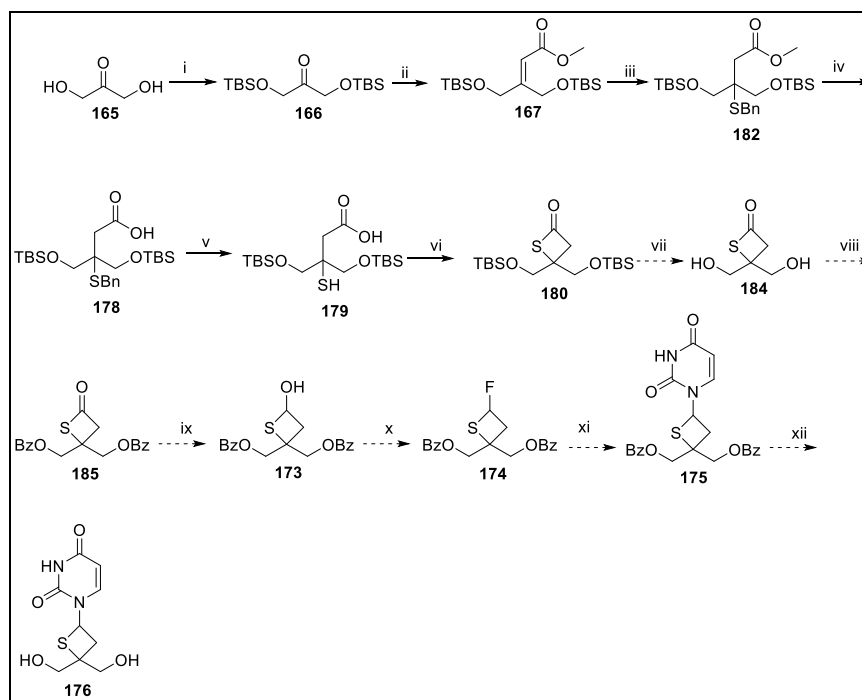
Immediate differences between the two spectra are: thietanone **180** does not contain the peak at 3345 cm⁻¹ and confirms that cyclisation has occurred because the

carboxylic –OH stretch is no longer present. The shift in the vibrational frequency toward a higher wavenumber for the ketone in thietanone **180** confirms cyclisation has occurred as the frequency is within the range of 4 member ring ketones.^{8,23} The mass spectrometry data showed the mass ion peak for thietanone **180** was 399.1817 Da as the sodium adduct and confirmed that the thietane had been made. The mass spectrum also showed a smaller peak at 377.1997 Da, which is the mass ion peak. The mass spectrum data closely matched the calculated values for the mass ion peak and the sodium adduct at 377.2002 Da and 399.1821 Da.

With successful synthesis of thietanone **180** achieved, future work involves changing the protecting groups to benzoyl groups, reducing the ketone to the alcohol, converting the alcohol to the fluorine and then using already established chemistry from chapter two to furnish the nucleosides.

Although the synthesis toward thietanone **180** was achieved, several key synthetic strategies required optimisation. The best approach toward this thietane ring at the moment is to form the benzyl thioether from ester **167** as it is far easier to achieve than reducing the ester to an aldehyde and converting to the thietane. The method where the benzyl thioether is formed removes the protecting group steps from the aldehyde method. A summary of the approach is presented in scheme 3.31.





Scheme 3.31: Top: Aldehyde method which requires additional protecting group chemistry and bottom: Optimised route toward thietanone **180** which was achieved after significant optimisation of the each step i) TBS-Cl, imidazole, DCM, RT, 24 hrs, quant ii) Methyl diethylphosphonoacetate, THF, NaH, RT, 24 hrs, 61% iii) BnSH, piperidine, 116° C, 24 hrs, 82% iv) 8 equiv Me₃SnOH, 1,2-DCE, 80° C, 96 hrs, 88% v) Na, NH₃, THF, -78° C, 2 – 3 hrs, 93% vi) Isobutylchloroformate, Et₃N, DCM, -10° C, 37% vii) nBu₄NF, THF viii) BzCl, DMAP, Et₃N, DCM, RT ix) NaBH₄, THF x) Deoxofluor, SbCl₃, DCM, RT xi) silylated nucleobase, AgClO₄, SnCl₂ various solvents and temperatures (see chapter 2) xii) NaOMe, MeOH, RT

The exploratory chemistry objective has been met and has shown that the Givaudan synthesis of thietane rings could not be easily applied to the synthetic strategy due to the difficulty in synthesising aldehyde **168**. Without this aldehyde the utility of the Givaudan synthesis could not be established. However, reproduction and optimisation of the Pattenden reaction conditions toward thietanones gave usable and productive results which led to the successful synthesis of thietanone **180** after some modification. Although the Pattenden conditions used a carboxylic acid as a starting material, conversion of **177** to thioether **178** could not be achieved. However, conversion of thioether **182** to acid **178** was achieved after significant optimisation of the reaction conditions. These modifications enabled the successful synthesis of thietanone **180**, a novel thietanone precursor to the key intermediate fluorothietane **174**.

3.4 References

- (1) Nishizono, N.; Sugo, M.; Machida, M.*et al. Tetrahedron* **2007**, 63, 11622.
- (2) Patwardhan, A. P.; Thompson, D. H. *Langmuir* **2000**, 16, 10340
- (3) Takahashi, S.; Nakata, T. *J Org Chem* **2002**, 67, 5739.
- (4) Parikh, J. R.; Doering, W. V. E. *J Am Chem Soc* **1967**, 89, 5505
- (5) Tewes, B.; Frehland, B.; Schepmann, D.*et al. Bioorg Med Chem* **2010**, 18, 8005.
- (6) Yin, J.; Gallis, C. E.; Chisholm, J. D. *J Org Chem* **2007**, 72, 7054.
- (7) Givaudan, L.; The Patent Office, L., Ed. Switzerland, 1972; Vol. 1379379, p 5.
- (8) Pattenden, G.; Shiker, A. J. *J Chem Soc Perkin Trans 1* **1992**, 1215.
- (9) Kim, Y.-A.; Park, M.-S.; Kim, Y. H.*et al. Tetrahedron* **2003**, 59, 2921.
- (10) Tomasi, J.; Persico, M. *Chem Rev* **1994**, 94, 2027.
- (11) Meyer, S. D.; Schreiber, S. L. *J Org Chem* **1994**, 59, 7549.
- (12) Beaulieu, P. L.; Organisation, W. I. P., Ed. 2009; Vol. WO/2009/076747 A1.
- (13) Weissfloch, A. N. E.; Kazlauskas, R. J. *J Org Chem* **1995**, 60, 6959.
- (14) Jogireddy, R.; Maier, M. E. *J Org Chem Soc* **2006**, 71, 6999.
- (15) Greene, T. W.; Wuts, P. G. M. *Greene's Protective Groups in Organic Synthesis*; John Wiley and Sons, 2007.
- (16) Davies, J. S.; Higginbotham, C. L.; Tremeer, E. J.*et al. J Chem Soc Perkin Trans 1* **1992**, 22, 3043.
- (17) Raji Reddy, C.; Rao, N. N.; Sujitha, P.*et al. Euro J Org Chem* **2012**, 2012, 1819.
- (18) Kuzniewski, C.; Gertsch, J.; Wartmann, M.*et al. J Org Lett* **2008**, 10, 1183.
- (19) Lovric, M.; Cepanec, I.; Litvic, M.*et al. Croatica Chemica Acta* **2007**, 80, 109.
- (20) Laganis, E. D.; Chenard, B. L. *Tet Lett* **1984**, 25, 5831.
- (21) Lepage, O.; Kattnig, E.; Fürstner, A. *J Am Chem Soc* **2004**, 126, 15970.
- (22) Nicolaou, K. C.; Estrada, A. A.; Zak, M.*et al. Angew Chem Int Ed Engl* **2005**, 44, 1378.
- (23) Stevens, S. J.; Berube, A.; Wood, J. L. *Tetrahedron* **2011**, 67, 6479.

Chapter 4:

The Design and Synthesis of 4'- Thiohamamelose Nucleosides

Chapter 4: The Design and Synthesis of 4'-Thio-D-Hamamelose Nucleosides as Anti-Viral Agents

Ribose nucleosides are ubiquitous as scaffolds for DAAs as the ribose sugar moiety is present in the sugar backbone of DNA and RNA. Since viral replication requires replication of the viral genome, drugs that mimic endogenous nucleosides/nucleotides are an excellent method of halting viral replication.¹⁻⁶ For a detailed explanation of how these drugs work see section 1.2.2.5.

Nucleoside based drugs can be modified in several different ways; phosphate modification, sugar modification or base modification.⁷ The types of modifications used depend on several factors:

- Susceptibility of the nucleoside to cellular kinases. Modification of the phosphate group can allow increased permeability of the drug through the cell membrane and also bypass kinases that may not phosphorylate the unmodified nucleoside (See section 1.2.2.5.3 for a detailed analysis).^{1,8-18}
- Binding interactions in the biological target. Modification of the sugar ring may be required to increase the binding interactions in the biological target, or to increase binding affinity in a pocket that the drug may not be binding to. Other factors such as ring conformation and ring size can be modified to overcome associated problems in these areas (see section 1.2.2.5.4).¹⁹⁻²²
- Base modifications are required as some nucleobases have better inhibitory characteristics than others. It is documented that purine nucleobases are typically inactive compared to the pyrimidine nucleobases (see chapter 1 section 1.2.2.5).

4.1 The 4'-Thioribose Nucleosides and their Derivatives

A major factor in the inactivity of ribose based nucleosides is their susceptibility to cleavage by a variety of nucleases.²³⁻²⁶ Thioribose nucleosides and their derivatives have been found to resist enzymatic cleavage of the glycosyl bond by nucleases. Blood degradation studies via HPLC analysis by Toyohara *et al* found that thymidine **184** was 50% degraded at 1 hour and fully degraded at 20 hours; whereas 4'-thiothymidine **185** was only 3% degraded at 1 hour and only 25% degradation was

observed at 20 hours (figure 4.1).²³ Ideally, the drug would be stable for at least 24 hours as once a day dosing is the gold standard for patient compliance as this minimises missed doses.

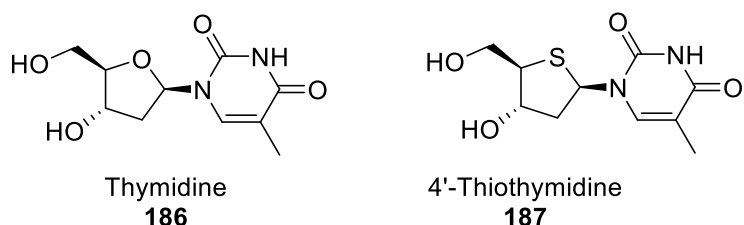


Figure 4.1: Thymidine and 4'-thiothymidine differ by the sulfur atom at the 4'-position

The study by Toyohara *et al.* indicated that the 4'-thioribose nucleosides resist catabolism and are stable to nucleases (see table 4.1).^{23,25,26} Further to this, (*E*)-5-(2-bromovinyl)-2'-deoxyuridine (BVDU) **188** and the 4'-thio derivative **189** also showed increased stability to pyrimidine phosphorylases. Dyson *et al.* showed (based on the work by Desgranges *et al* who measured the effect of pyrimidine phosphorylases in blood and showed that the nuclease was able to detach the uracil from the sugar ring in BVDU) that BDVU **188** was metabolised to the inactive metabolite (*E*)-5-(2-bromovinyl) uracil moiety **190** and 2-deoxyribose-1-phosphate **191** by pyrimidine nucleoside phosphorylase (figure 4.2).²⁶⁻²⁹ The 4'-thio moiety **189** was found to be more stable and no (*E*)-5-(2-bromovinyl) uracil residue was observed indicating that the 4'-thio moiety **189** is stable to nucleases. When comparing the plasma half-lives of BDVU **188** and the 4'-thio moiety **189**, there is 1.5 times more of the 4'-thio moiety **189** at 2 hours than there is of BDVU **188** when both are dosed at 40 mg/kg. At 2 hours BVDU **3** is found at a concentration of 35 μ M versus 50 μ M for 4'-thio moiety **189**. At 3 hours, no BDVU is measured, the concentration of the 4'-thio moiety **189** remains constant.^{28,30}

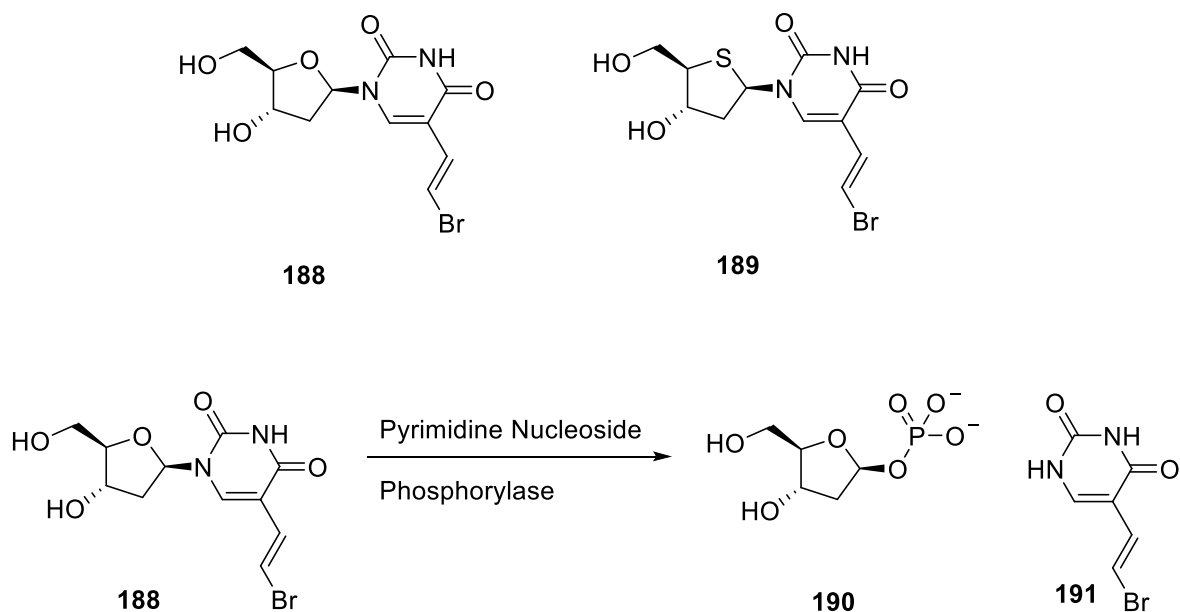
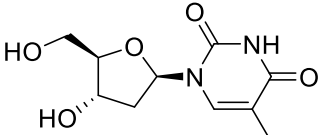
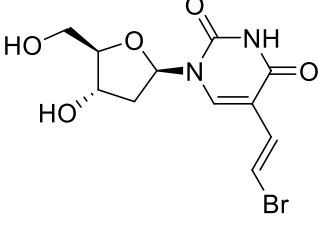
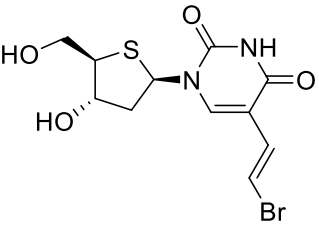
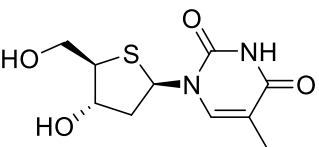
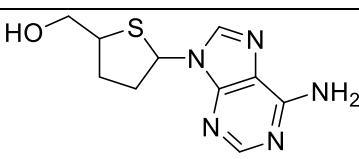
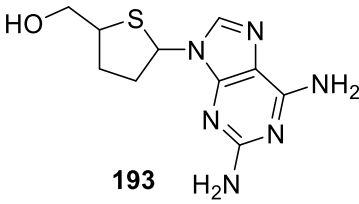
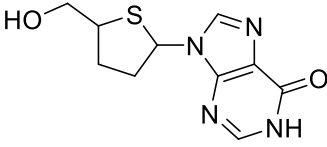
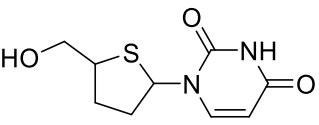


Figure 4.2: Action of pyrimidine nucleoside phosphorylase. No degradation was observed for the 4'-thioribose moiety.

Table 4.1 summarises the known 4'-thioribose nucleosides, their potency and therapeutic index.

Table 4.1: Known 4'-thioribose nucleosides (only active nucleosides have been shown with compounds **186** and **187** shown as the ribose counterparts with their associated activity).

Compound	IC ₅₀	Stability (%)	Therapeutic Index
 <p style="text-align: center;">186</p>	N/A	50% at 1 hour 100% at 20 hours	-
 <p style="text-align: center;">188</p>	0.02 μM	50% at 2 hours	10 000

 <p>189</p>	0.08 μ M	50% at 3 hours	62 500
 <p>187</p>	0.15 μ M	3% at 1 hour 25% at 20 hours	-
 <p>192</p>	0.32 μ M	-	-
 <p>193</p>	0.14 μ M	-	-
 <p>194</p>	0.37 μ M	-	-
 <p>195</p>	4.38 nM	-	-

Note: L-series 4-thionucleosides have been synthesised as anti-cancer agents but these compounds are not included as they are outside the scope of this thesis.³¹

It has been shown that as well as resisting nucleases, the 4'-thioribose moieties are more thermally stable; generally have higher binding affinities, and a higher chemotherapeutic index than the ribose counterparts that make them an attractive anti-viral target.^{24,25,27,32} Table 4.1 shows that nanomolar ranges of activity can be

achieved for 4'-thioribose nucleosides, and this is important as it reduces the chances of off target effects when drug concentrations are high.^{23,25-28,33}

4.2 Hamamelose Nucleosides

Hamamelose **196** is a 5 membered ring sugar with a 2'-C-hydroxymethyl group (figure 4.3). No 4'-thiohamamelose nucleosides are known but 4'-thioribose nucleosides have shown promise as nucleosides due to factors outlined in the previous paragraph. The intention with this piece of work was to explore the anti-viral properties of 4'-thiohamamelose nucleosides. It is hypothesised that similar to the 4'-thioribose counterparts, the 4'-thiohamamelose nucleosides will be more thermally stable and more biologically stable than their hamamelose counterparts.

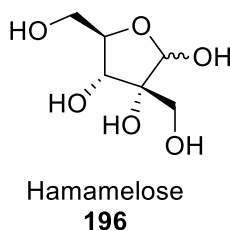


Figure 4.3: Hamamelose

Although hamamelose nucleosides are known to be active against HCV infection, initial research into anti-HCV compounds found that 2-C'-methyl and 2-F' groups were essential for activity. This was attributed to steric bulk preventing subsequent incoming nucleotides from binding into the HCV replicase complex and thus preventing genome replication.^{1,15-17,34-40} (See section 1.2.2.5.2 for a detailed description). Figure 4.4 shows the key compounds along with their anti-HCV activity.

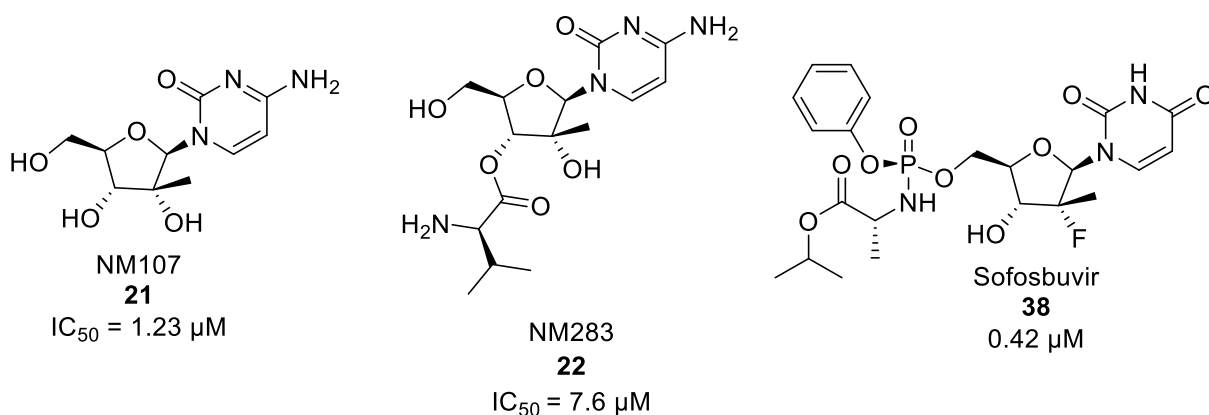


Figure 4.4: Key anti-HCV compounds

Both Yoo and Jeong separately hypothesised that the hamamelose 2-C'-hydroxymethyl group would have favourable electronic and steric effects that would increase interactions in the HCV replicase complex.^{41,42} The increased bulk was hypothesised to be better at preventing incoming nucleotides from binding into the replicase complex, and the hydroxymethyl group is hypothesised to have binding affinity to the polymerase.^{41,42} It was observed by Yoo *et al* that the hydroxymethyl group in derivative **197** was essential to binding, and along with Jeong *et al*, both derivative **197** and derivative **198** (figure 4.4) were shown to inhibit viral replication by 2% at 1μM and derivative **197** inhibited viral replication by 50% at 10μM. However, based on the low inhibitory values observed it cannot be concluded that the increased steric bulk of the hydroxymethyl group is essential for binding.

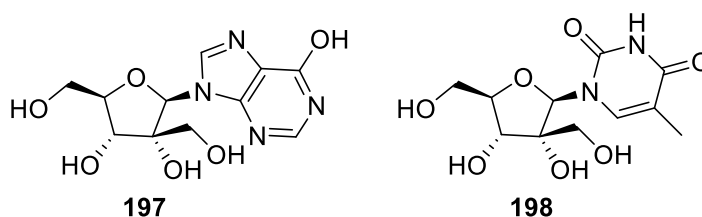


Figure 4.5: Hamamelose nucleosides active against HCV

However, despite these compounds being active against the HCV replicase complex, the inhibitory concentration was low and therefore significant research is required to optimise the activity of this class of compound.⁴¹

4.3 Aims

As has been shown, the 4'-thioribose nucleoside derivatives are more thermally and metabolically stable than their ribose counterparts, as well as having generally higher binding affinities than their ribose counterparts. Therefore, the major aim of this piece of work is to design and synthesise a range of 4'-thiohamamelose nucleosides that are hypothesised to be more metabolically stable than their hamamelose counterparts. The main objectives are listed below:

- Design and synthesise a series of 4'-thiohamamelose nucleoside libraries.
- Perform anti-viral testing to determine the IC_{50} , and CC_{50} values of the compounds.
- Modify the structure of the nucleosides to gain a full understanding of the SAR.
- Using the biological data, design and synthesise a new library of compounds with the aim of producing a highly potent, non-toxic nucleoside.

No 4'-thiohamamelose nucleosides are currently known therefore it would be valuable to prepare a large and varied number of derivatives to explore the SAR of these nucleosides.

4.3.1 SAR of 4'-thiohamamelose nucleosides

In order to explore the SAR of the 4'-hamamelose nucleosides, several modifications will need to be explored. Figure 4.6 shows the potential areas where chemical modifications can be made.

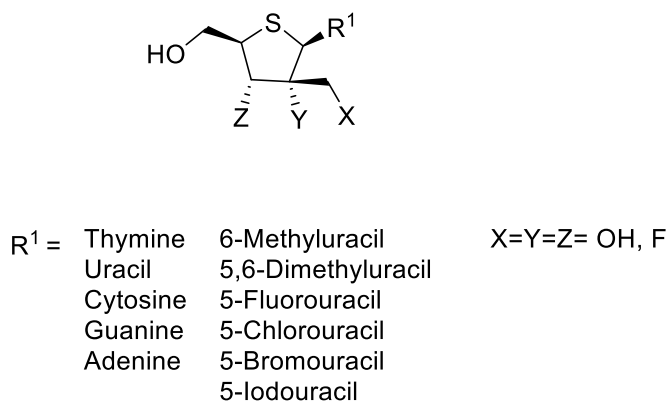


Figure 4.6: 4'-thiohamamelose showing potential areas of chemical modification

Since it has been shown that the 2'-C-hydroxymethyl group is essential to binding, and it has been shown that fluorine at C-2 is also essential for activity in the HCV replicase complex, figure 4.5 shows that several series of compounds can be synthesised to assess the importance of the C-3 OH, C-2 OH, and the 2'-CH₂OH groups for binding by varying where the fluorine atom or hydroxyl group is bound.

In the first series, X, Y, Z are all OH groups and the SAR of the nucleobases can be assessed. This first library was planned to have 11 members within it to give a comprehensive overview of how varying the nucleobases affects activity. Table 4.2 shows the potential number of compounds that can be synthesised to assess the SAR of the 4'-thiohamamelose nucleosides.

Table 4.2: Variations to sugar ring groups for assessment of SAR in 4'-thiohamamelose nucleosides

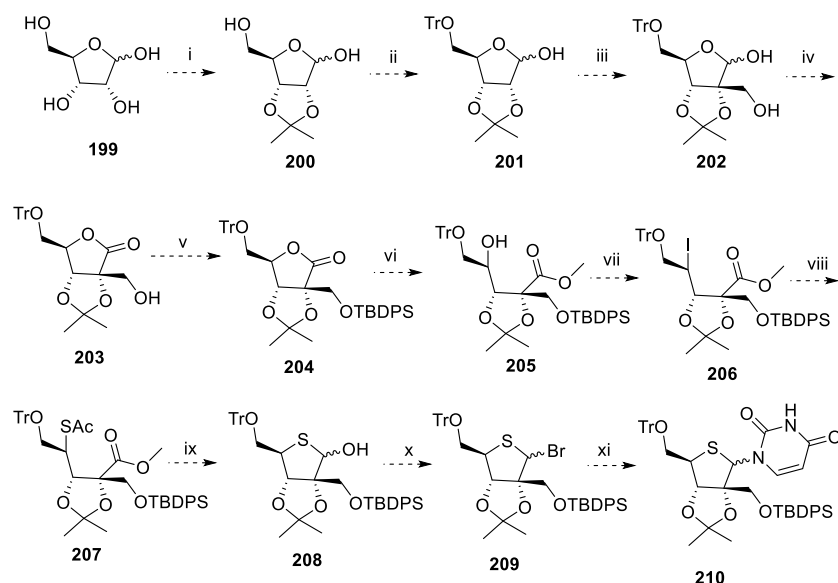
Series	X	Y	Z	N° of compounds
1	OH	OH	OH	11
2	OH	OH	F	11
3	OH	F	OH	11
4	F	OH	OH	11
5	OH	F	F	11
6	F	OH	F	11
7	F	F	OH	11
8	F	F	F	11

The table shows that 8 series of compounds can be synthesised to assess the SAR of the 4'-thiohamamelose moiety for a total of 88 potential compounds since each series can have up to 11 nucleobases attached to the hamamelose ring. The nucleobases have been chosen to keep the libraries consistent with the thietane libraries in chapter 2. This way comparison between the libraries and each series can be made.

In addition to the series shown in table 4.3, the L-4-thiohamamelose moieties can also be explored as L-series ribose based nucleosides have shown anti-HIV and anti-HBV activity.^{11,14} Not only does this increase the number of compounds that can be potentially synthesised, but it also broadens to scope of potential viruses that these compounds can target, and therefore, a greater chance that a hit compound can be found.

4.3.2 Synthetic strategy towards the 4'-thiohamamelose nucleosides

In scheme 4.1 the proposed synthetic route for potential entry to the 4'-thiohamamelose nucleosides is shown.



Scheme 4.1: Proposed synthetic steps to 4'-thiohamamelose nucleosides i) Acetone, H_2SO_4 RT 3 hrs ii) TrCl , Pyridine, RT, 20 hrs iii) Formaldehyde, Methanol, K_2CO_3 , 70°C , 20 hrs iv) Br_2 , K_2CO_3 , DCM, RT, 3 hrs v) TBDPS-Cl, Imidazole, DCM, RT, 12 hrs vi) NaOH , Me_2SO_4 , DMSO, RT, 3 hrs vii) PPh_3 , Imidazole, I_2 , DCM, 120°C , 6 hrs viii) AcSH , TBA-OH, toluene, RT, 18 hrs ix) DIBAL-H, toluene, 2 hrs x) CBr_4 , PPh_3 , DCM, -25°C , 1 hr xi) AgOTf , 135°C , μwave , DCE/MeCN, 30 mins

Synthesis of the 4'-thiohamamelose nucleosides can potentially be achieved using the Pummerer reaction by first converting thiohamamelose derivative **208** to the sulfoxide **212** (figure 4.7) using NaIO_4 .⁴³

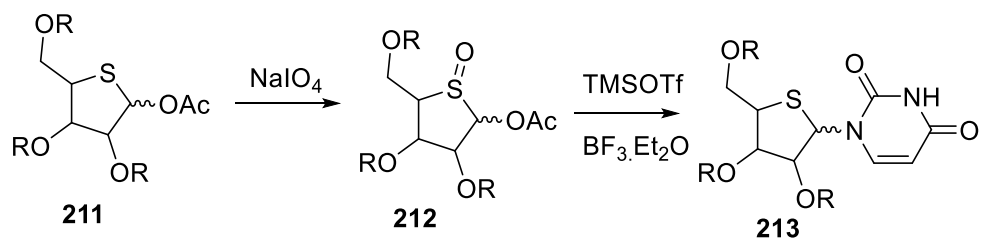


Figure 4.7: Pummerer Reaction for the formation of nucleosides

However, due to problems using the Pummerer reaction for the synthesis of the thietane nucleosides as described in chapter 2, and the success of using Vorbrüggen

conditions for the thietane nucleosides in the same chapter, it was decided that conversion of thiohamamelose derivative **208** to bromide **209** would allow access to the nucleoside derivatives of compound **210** using AgOTf.⁴⁴

The synthetic plan utilises known chemistry. Conversion of ribose **199** to acetonide **200** can be achieved using acetone and sulfuric acid.⁴⁵ Protection using a trityl group is necessary and a large group such as the trityl group will favour protection of the primary C-5 hydroxy group over the anomeric hydroxyl group allowing for selectivity between them, to furnish the literature compound trityl **201**.⁴⁶ Adding the hydroxymethyl group to C-2 can be achieved by use of formaldehyde in methanol and potassium carbonate to furnish hamamelose **202**.^{47,48} Oxidation of hamamelose **202** to ribolactone **203** can be achieved using bromine oxidation which is useful as it is mild and selective for oxidation of the anomeric hydroxyl group.⁴⁹ Next, protection of the 2'-C-hydroxymethyl group with a TBDPS group to afford ribolactone **204** will allow for selectivity toward deprotection as it can be removed with Bu₄NF, whilst the acetonide and trityl group can be removed with acid or other means.⁵⁰ Also, the TBDPS group is stable toward NaOH as are the acetonide and trityl group which allows for the formation of methyl ester **205**.⁵¹ The next series of reactions form the 4'-thiohamamelose sugar. First the ring is cleaved open with NaOH and then reacted with Me₂SO₄ to furnish methyl ester **205**, which is then converted to the iodo moiety **206** and cyclisation is achieved with thioacetic acid to yield **207** and DIBAL-H to give 4,-thiohamamelose derivative **208**.^{32,44,52,53}

4.4 Results and Discussion: Steps Toward the Synthesis of 4'-thiohamamelose Nucleosides

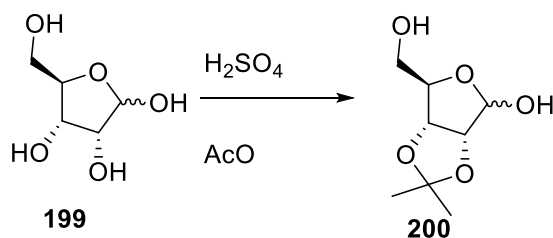
Two methods were trialled for the synthesis of acetonide **200** from ribose **199**; the initial method used 0.01 equivalents of *p*TSA, acetone as a solvent and a reagent, and 2,2-dimethoxypropane to furnish acetonide **200** with a yield of 69% after purification by column chromatography using ethyl acetate as the eluent. The second method utilised ribose **199**, acetone as a solvent and dropwise addition of concentrated sulfuric acid to furnish acetonide **200** with a yield of 85% after purification by column chromatography. The sulfuric acid method gave consistently more reproducible yields than the *p*TSA method (table 4.3) and as such the sulfuric acid method was used on subsequent scale up.

Table 4.3: Comparison of yields between the *p*TSA method and the sulfuric acid method

Reaction	Scale (g)	<i>p</i> TSA yield (%)	Sulfuric acid yield (%)
1	2	62	85
2	5	44	Quant
3	10	69	Quant
4	150	44	Quant
5	200	-	Quant

The *p*TSA method showed more variation in total yield after purification by column chromatography than the sulfuric acid method. This variation in yield for the *p*TSA reaction could be accounted for by the production of the pyranose form of ribose being. There was some indication of the pyranose form of ribose being formed after ^{13}C NMR spectroscopic analysis of the reaction products. The data showed two peaks at 94 ppm which are indicative of the C5 carbon in the pyranose form (these two peaks are the α and β anomers). These peaks were not observed in the furanose form of ribose, with the C5 carbon for the CH_2OH group being observed at 63 ppm. Comparison of the ^1H NMR spectroscopic data of the crude reaction material and the purified material for the sulfuric acid method showed no real differences post work up, whereas the ^1H NMR spectroscopic data for the *p*TSA crude reaction material did show differences, further indicating that the pyranose form was present. Since the sulfuric acid reactions did not show formation of a pyranose form in the crude or the pure proton and carbon NMR spectroscopic data, reactions 2 – 5, the organic phase was washed to remove any residual salts (NaHCO_3 was used to neutralise the acids) and the crude material flushed through a plug of silica under vacuum and was used crude in subsequent steps. Though both 5 and 6 membered rings are thermodynamically stable, with 6 membered rings being more stable than 5 membered rings, it would be expected to see more pyranose forms than furanose forms of ribose for both reactions. However, formation of the furanose form may be kinetically more favourable than the pyranose form. Therefore, with shorter reaction times (1 – 2 hours) using sulfuric acid, versus overnight for the *p*TSA reaction, it would be expected that the pyranose form of ribose would be seen using *p*TSA. The rate of formation of the pyranose form may be slower than the rate of formation of the

furnose form when using either acid, so longer reaction times would allow more time for an equilibrium to be established, allowing for the pyranose form of ribose to form.



Scheme 4.2: Large scale synthesis of acetonide **200** using acetone and sulfuric acid

The ^1H NMR spectroscopic data for acetonide **200** confirmed the presence of the acetonide methyl groups as two singlets at 1.3 and 1.5 ppm. The data also showed that the anomeric proton existed as 1:1 ratio of the α and β anomers, of which the α anomeric proton was observed at 5.4 ppm and the β anomeric proton was observed at 4.5 ppm (figure 4.8). This data matched the known literature values within 0.1 ppm.⁵⁰

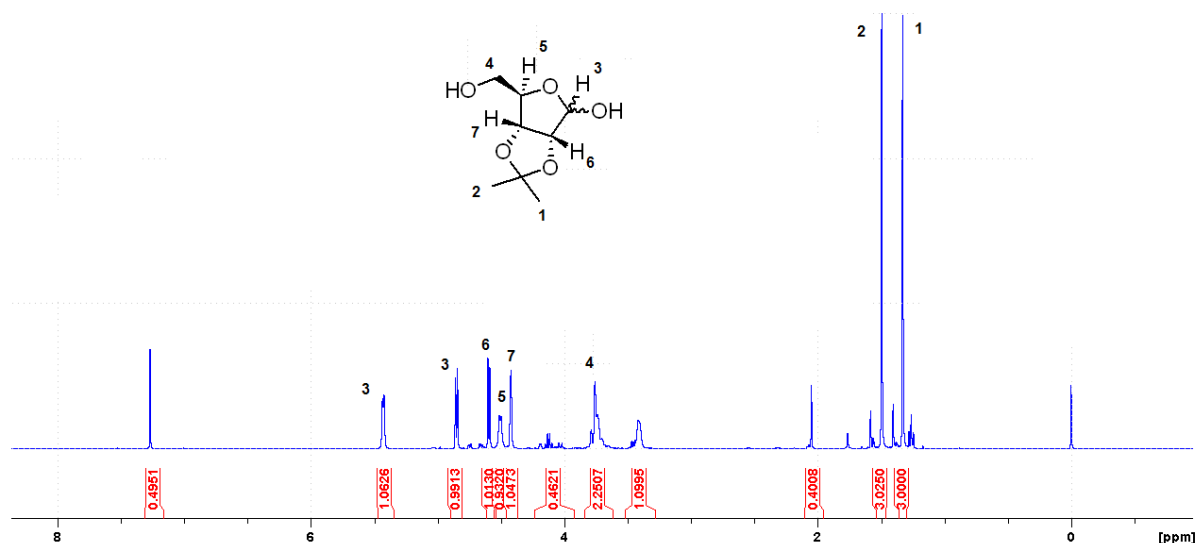
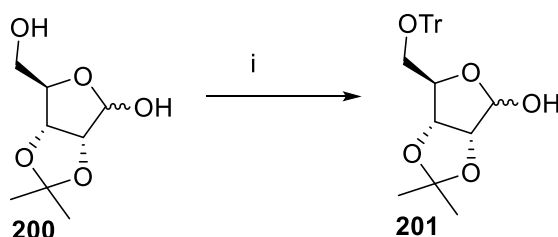


Figure 4.8: ^1H NMR spectrum of acetonide **200**

The methylene protons were observed at 3.8 ppm. The characteristic doublets of the three remaining CH bonds on the ribose ring were also observed with J coupling constants of 6 Hz. This data matched closely with the literature values of 1.3 and 1.5 ppm for the acetonide methyl groups, 3.8 ppm for the methylene protons and the expected CH protons were also observed with a coupling constant of 6 Hz.⁵⁰ IR spectroscopy data confirmed the presence of the hydroxyl group at 3400 cm^{-1} and

the mass spectrum data gave the mass ion peak of the sodium adduct at 213.0744 Da with the expected value at 213.0740 Da.

Next, trityl protected moiety **201** was synthesised in several small batches ranging from 5 – 15 g (scheme 4.3). In initial reaction conditions where 1 equivalent of trityl chloride were used, the reaction failed to go to completion and thus the reaction was optimised (table 4.4).



Scheme 4.3: Synthesis of trityl moiety **201** i) trityl chloride, pyridine, RT, 48 hrs, 82%

Table 4.4: Optimisation reactions for the protection of the 5'-OH group using trityl chloride

Reaction	Trityl Chloride Equivs	Outcome
1	1	Reaction did not go to completion after 48 hours
2	1.1	Reaction did not go to completion after 48 hours
3	1.5	Reaction did not go to completion after 48 hours
4	2	Isolated yield: 82% after 48 hours

Reactions 1 – 4 are the same reaction with each equivalent added after 48 hours total reaction time. In the first 48 hours, analysis of the crude reaction mixture by TLC revealed starting material and product was still present. 0.1 equivalents was then added and reacted for a further 48 hours and this was repeated until a total of 2 equivalents of trityl chloride was added and TLC analysis of the crude reaction mixture revealed total consumption of the starting material. After purification by column chromatography, the yield was found to be 61%. The reaction was repeated with 2 equivalents of trityl chloride and stirred at room temperature for 48 hours to give trityl moiety **201** with a yield of 82%. Since the reaction is an S_N1 reaction where the chlorine atom must leave before formation of the trityl cation, increasing the number of equivalent should not increase the rate of reaction. However, increasing the number of equivalents of trityl chloride did improve the yield of the reaction, and this is possibly due to the trityl chloride hydrolysing in the reaction. Though

glassware, reagents and solvents were dry, the ribose **200** used may have absorbed water as it was weighed. (Ribose **200** was dried under high vacuum to remove water, but as it was a thick gel, it may have had residual water and would have absorbed water as it was weighed). Any water present in the ribose would have hydrolysed the trityl chloride to trityl hydroxide. By increasing the number of equivalents of trityl chloride, the effects of hydrolysis on reaction yields could be overcome. Significant optimisation of the column chromatography conditions were required to isolate trityl **201** and this was due to the problem of trityl hydroxide co-eluting with the product.

Analysis of the purified product by ^1H NMR spectroscopy revealed the $\alpha:\beta$ ratio to be 1:5 and this was found by comparing the α proton signal at 5.75 ppm to the β proton signal at 5.32 ppm and finding the ratio between them (figure 4.9).

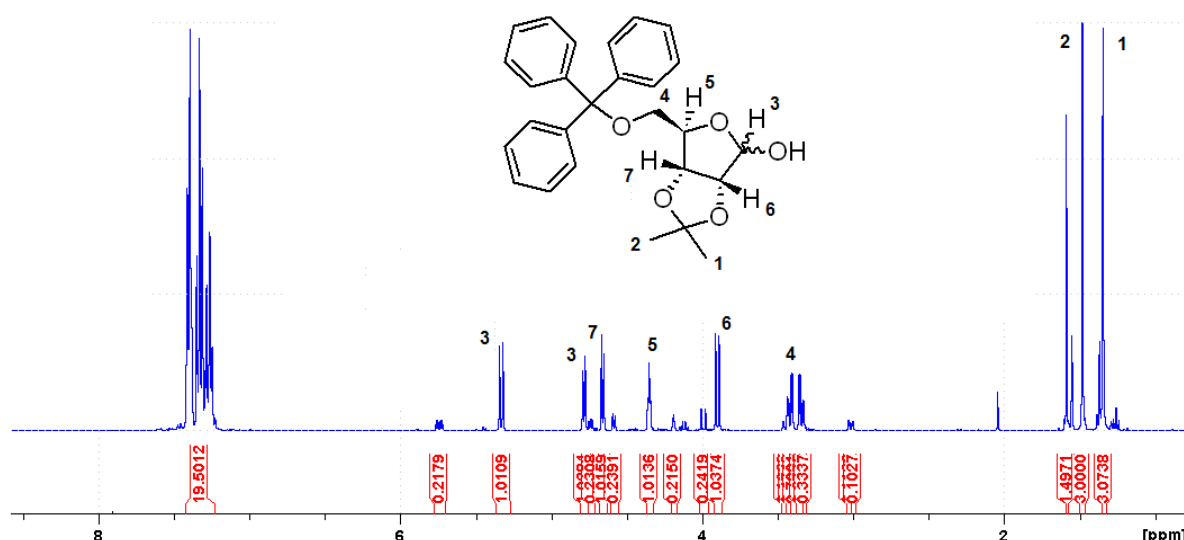
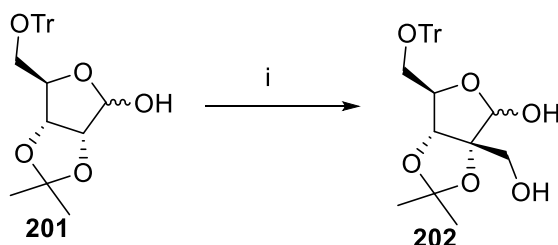


Figure 4.9: Proton NMR spectroscopic data for trityl moiety **201**

The methylene protons indicated by 4 in figure 4.8 are found as two doublets each integrating to 1. The anomeric protons, of which there are two, are the α and β anomeric protons giving the compound in a 1:1 $\alpha:\beta$ ratio. The IR spectroscopic data gave the anomeric hydroxyl group at 3308 cm^{-1} and the phenyl groups were observed at 2963 cm^{-1} . Mass spectrometry data for the sodium adduct found the mass ion peak to be 455.1829 Da with the calculated mass found to be 455.1826 Da for the sodium adduct.

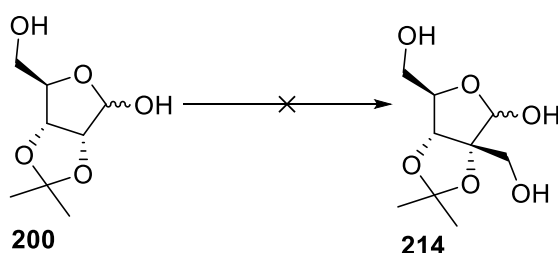
4.4.1 Model Formylation Reactions

Prior to the formylation reaction to form hamamelose **202** from trityl **201** (scheme 4.4), the formylation reaction was optimised using a model compound, using known chemistry.^{47,48}



Scheme 4.4: Synthesis of hamamelose **202** i) formaldehyde, methanol, K₂CO₃, 66° C, 97% (crude yield)

Ho *et al*/ published a reaction in 1978 that showed synthesis of hamamelose **214** from acetonide **200** (scheme 4.5). However, as table 4.5 shows, this reaction could not be reproduced.⁴⁸



Scheme 4.5: Synthesis of hamamelose by Ho *et al*⁴⁸

Table 4.5: Formylation reaction conditions

Reaction	Conditions	Outcome
1	8 equiv CH ₂ O 1.1 equiv K ₂ CO ₃ , methanol, Reflux 20 hrs	No reaction
2	8 equiv CH ₂ O 1.1 equiv K ₂ CO ₃ , methanol, 66° C 20 hrs	No reaction
3	8 equiv CH ₂ O 1.5 equiv K ₂ CO ₃ , methanol, 66° C 24 hrs	No reaction
4	8 equiv CH ₂ O 1.5 equiv K ₂ CO ₃ , methanol, 66° C 20 hrs	No reaction- Acetonide peaks were not seen at their expected chemical shift by

		¹ H NMR spectroscopic analysis
5	2 equiv CH ₂ O 1.1 equiv K ₂ CO ₃ , methanol, 66° C 20 hrs	No reaction
6	2 equiv CH ₂ O 1.5 equiv K ₂ CO ₃ , methanol, 66° C 24 hrs	No Reaction
7	8 equiv CH ₂ O 1.1 equiv K ₂ CO ₃ , methanol, 75° C 20 hrs	No reaction- Acetonide peaks were not seen at their expected chemical shift by ¹ H NMR spectroscopic analysis
8	2 equiv CH ₂ O 1.5 equiv K ₂ CO ₃ , methanol, 65° C 20 hrs	¹ H NMR spectroscopic analysis on isolated material (97.5:2.5 CHCl ₃ :EtOH column) revealed an impure product. Subsequent attempts to purify the material could not isolate the product.

Reaction 1 shows the conditions used by Ho *et al.*, and these conditions could not be reproduced. (The reaction used 39% w/w CH₂O in water as the reagent and solvent). No reaction was observed, and ¹H NMR spectroscopic analysis of the crude reaction mixture post work-up showed only ribose **200** was present. Increasing the temperature and increasing the number of equivalents of potassium carbonate did not aid in a reaction occurring.

In reactions 4 and 7, the acetonide methyl group peaks were observed as moving from 1.3 and 1.5 ppm to 1.5 and 2 ppm. However, the 2'-C-hydroxymethyl group protons were not observed. This indicates that what was observed was a side product; potentially due to a deprotonation at C-2 and subsequent reaction with water resulting in a hydroxyl group at C-2. Since chloroform was used as the solvent for the ¹H NMR spectroscopic data, this hydroxyl group may not have been observed. Changing the NMR solvent to DMSO and then utilising a D₂O shake could have confirmed if this occurred for reactions 4 and 7.

Reaction 8 did show that a reaction had occurred, however, the products could not be isolated. Spectroscopic analysis of reaction 8 using ^{13}C NMR was inconclusive as to whether the resulting impure product contained the pyranose and furanose forms of hamamelose **214** as there were multiple peaks at 94 ppm, which is indicative of the CH_2 group in the pyranose form of ribose. From this data, it can be assumed that excess formaldehyde may have a negative impact on the rate of reaction.

Although the reaction conditions by Ho *et al.* could not be reproduced, and optimisation of the reaction could not be achieved, the model reaction allowed confirmation that the 5'-OH group required protection prior to the formylation reaction being used.⁴⁸

Beigelman *et al.* showed that trityl hamamelose **202** could be synthesised from trityl ribose **201** using the same reactions conditions as Ho *et al.*^{47,48} The difference being that under Beigelman *et al.* reaction conditions, 30 equivalents of formaldehyde were required for the reaction (scheme 4.4) versus only 8 equivalents under the reaction conditions by Ho *et al.*^{47,48} Table 4.6 shows optimisation data for the conversion of trityl ribose **201** to trityl hamamelose **202**.

Table 4.6: Optimisation of the formylation reaction towards 5'-O-trityl-hamamelose

Reaction	Conditions	Outcome
1	30 equiv CH_2O 1.1 equiv K_2CO_3 65° C 20 hrs	Crude product 29% mass recovery
2	30 equiv CH_2O 1.5 equiv K_2CO_3 Reflux 20 hrs	Crude product 33% mass recovery
3	30 equiv CH_2O 1.1 equiv K_2CO_3 65° C 24 hrs	Crude product 46% mass recovery
4	30 equiv CH_2O 1.1 equiv K_2CO_3 65° C 24 hrs	Crude product 71% mass recovery
5	30 equiv CH_2O 1.1 equiv K_2CO_3 65° C 20 hrs	Crude product 82% mass recovery

Initially the yields for the reaction were low and required optimisation. Although Beigelman *et al.* reported that the potassium carbonate and formaldehyde solution were to be added to the sugar in methanol, and reported a 72% yield; it was observed that following this method of addition resulted in low yields. In reactions 4

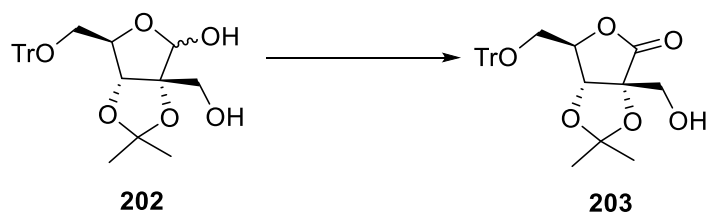
and 5, the potassium carbonate and methanol were allowed to reach 65° C first, and then trityl ribose **201** was added. Then the formaldehyde was injected dropwise. This gave the high yields for reactions 4 and 5 and was done because it was suspected that if the formaldehyde was added all at once, in the reaction conditions, it could possibly oxidise to formic acid and thus deprotect the acetonide group.

Attempts to purify the hamamelose **202** using 2.5% ethanol in chloroform could not adequately give a pure sample. However, comparing the ¹H NMR spectrum of the crude reaction material to the post-column ¹H NMR spectrum did show that some of the impurities had been removed. The crude material was found to have a purity of 60 – 70% after analysis of the ¹H NMR spectrum. Therefore, hamamelose **202** was used in its crude form in the next step after analysis of the ¹H NMR spectrum revealed the additional CH₂ methylene group at 3.7 ppm as a multiplet, and the CH proton at C-2 in trityl moiety **201** at 3.9 ppm is no longer present in hamamelose **205**. The mass spectrum data for the crude material revealed the expected mass ion peak for the sodium adduct at 485.1935 Da which was calculated to be 485.1931 Da. This gave enough confidence to use the material in the next step.

The attempted synthesis of hamamelose **202** shows that excess formaldehyde may be problematic, and is concordant with the data from the Ho model reactions. In both of these sets of reactions, excess formaldehyde either did not result in a reaction, or had a negative effect on product formation. Therefore, further reactions would involve optimising the number of equivalents of formaldehyde for the most efficient conversion to hamamelose, as it is suspected that formic acid may form with longer reaction times. To combat this, the number of equivalents of base would need to be optimised also as excess base may neutralise any formic acid present, and thus limiting the impact it potentially has on the reaction.

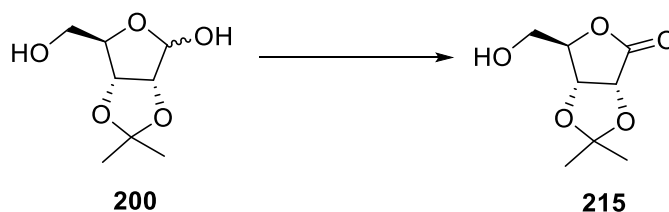
4.4.2 Optimisation of the Oxidation Reactions

The next reaction to be modelled was the bromine oxidation of hamamelose **202** to hamamelolactone **203** (scheme 4.6).



Scheme 4.6: Synthesis of hamamelolactone **203**

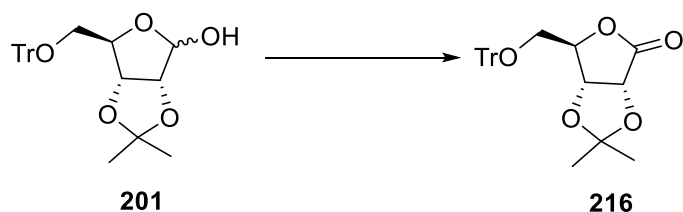
The reaction conditions by Stewart *et al* used water as the solvent for ribose, and DCM for any protected carbohydrate.⁴⁹ Before using hamamelose **202** as the reactant, ribose **200** was used for the model reaction for the synthesis of ribolactone **215** (scheme 4.7).



Scheme 4.7: Synthesis of ribolactone **215**. 1 equivalent bromine 1.1 equivalent K_2CO_3 in water, 98%.

Ribose **200** was dissolved in water and the potassium carbonate was added in one portion and the reaction cooled to 0° C with an ice water bath. Bromine was added dropwise and the reaction stirred for several hours until completion was observed by TLC analysis (100% ethyl acetate as eluent). Excess bromine was removed using sodium thiosulfate solution and then ethyl acetate was added. The crude reaction was boiled in ethyl acetate momentarily and then cooled back to 0° C and the product was precipitated by the addition of hexane.^{45,49} Ribolactone **215** was successfully synthesised with a yield of 98%. However, though the oxidation reaction worked for the model compound, synthesis of the trityl protected hamamelolactone **203** would be difficult if not impossible in water as it is not soluble.

The synthesis of hamamelolactone **203** was optimised using DCM using protocols established by Stewart *et al* by first optimising the reaction with trityl ribose **201** in DCM (scheme 4.8).⁴⁹



Scheme 4.8: Optimisation of the bromine oxidation reaction toward ribolactone **216** from trityl ribose

201. 1 equivalent of bromine, 1.5 equivalents of K_2CO_3 in DCM

As table 4.7 shows, it was possible to optimise the reaction. Initially, use of 1.1 equivalents of potassium carbonate was insufficient for the reaction to proceed well. Analysis of column fractions using 1H NMR spectroscopic analysis revealed that the acetonide and the trityl group were labile. This could be due to the bromine forming HBr in solution in a greater excess than the 0.1 equivalent excess of potassium carbonate. When the equivalents of potassium carbonate were increased to 1.5 equivalents, ribolactone **216** was isolated pure with a yield of 43%. The crude reaction mixture was analysed by 1H NMR spectroscopy which revealed the acetonide and trityl group were still labile, but not to such a great extent, and as such, the crude could be purified and the product isolated.

Table 4.7: Optimisation of the bromine oxidation reaction in DCM shown in scheme 4.8

Reaction	Conditions	Outcome
1	0° C, 3hrs, 1.1 equiv K_2CO_3 DCM	Unknown purity product 12%
2	0° C, 3hrs, 1.1 equiv K_2CO_3 DCM	Unknown purity product 9%
3	0° C, 3 hrs, 1.5 equiv K_2CO_3 DCM	Isolated pure 43%

Since the bromine oxidation reaction was selective for the anomeric hydroxyl group (as seen in the oxidation of acetonide **200**, no oxidation of the 5'-OH group was observed), and the reaction was optimised for the synthesis of ribolactone **216**, synthesis of hamamelolactone **203** could proceed (scheme 4.6).

Despite optimisation toward ribolactone **216**, formation of hamamelolactone **203** required further optimisation (table 4.8).

Table 4.8: Optimisation of the bromine oxidation toward 5'-O-tritylhamamelolactone **203** shown in scheme 4.8

Reaction	Conditions	Outcome
1	0° C, 3hrs, 1.5 equiv K ₂ CO ₃ DCM	No observed reaction: Acetonide and trityl group no longer bound when the reaction mixture was analysed by ¹ H NMR spectroscopy
2	0° C, 3hrs, 1.5 equiv K ₂ CO ₃ DCM	No observed reaction: Acetonide and trityl group no longer bound when the reaction mixture was analysed by ¹ H NMR spectroscopy
3	0° C, 3 hrs, 1.5 equiv K ₂ CO ₃ DCM	12% of an impure product. Some peaks could be assigned to the product when ¹ H NMR spectroscopic data was analysed
4	RT, 3 hrs, 1.5 equiv K ₂ CO ₃ DCM	27% of an impure product.
5	RT, 24 hrs, 1.5 equiv K ₂ CO ₃ DCM	19% of an impure product

Unfortunately the optimised conditions for the synthesis of ribolactone **216** did not work; therefore some further optimisation was required for the synthesis of hamamelolactone **203**. For reasons that are as of yet unknown, keeping the reaction at 0° C did not yield any product that could be isolated. Though a reaction occurred in the first 3 reactions in table 4.6, analysis of the crude reaction mixtures and the impure column fractions by ¹H NMR spectroscopic analysis revealed some peaks that could be assigned to the product, and a significant number of peaks that could not be easily assigned. Also, the ¹H NMR spectroscopic data showed that the acetonide and trityl groups were labile under these reaction conditions, which means that an acid was forming or had formed in solution. This acid could have also been introduced from the bromine, as it can contain some HBr naturally.

The reactions were repeated at room temperature and better yields were obtained. Initially, a 27% yield of crude hamamelolactone **203** was obtained, and in order to improve this yield, the reaction was left to react for 24 hours; however, this did not improve the yield. In fact, the yield dropped to 19%. Analysis of the crude reaction mixture by TLC analysis did show consumption of starting material, but several spots were identified therefore the end point was hard to judge. ¹H NMR spectroscopic

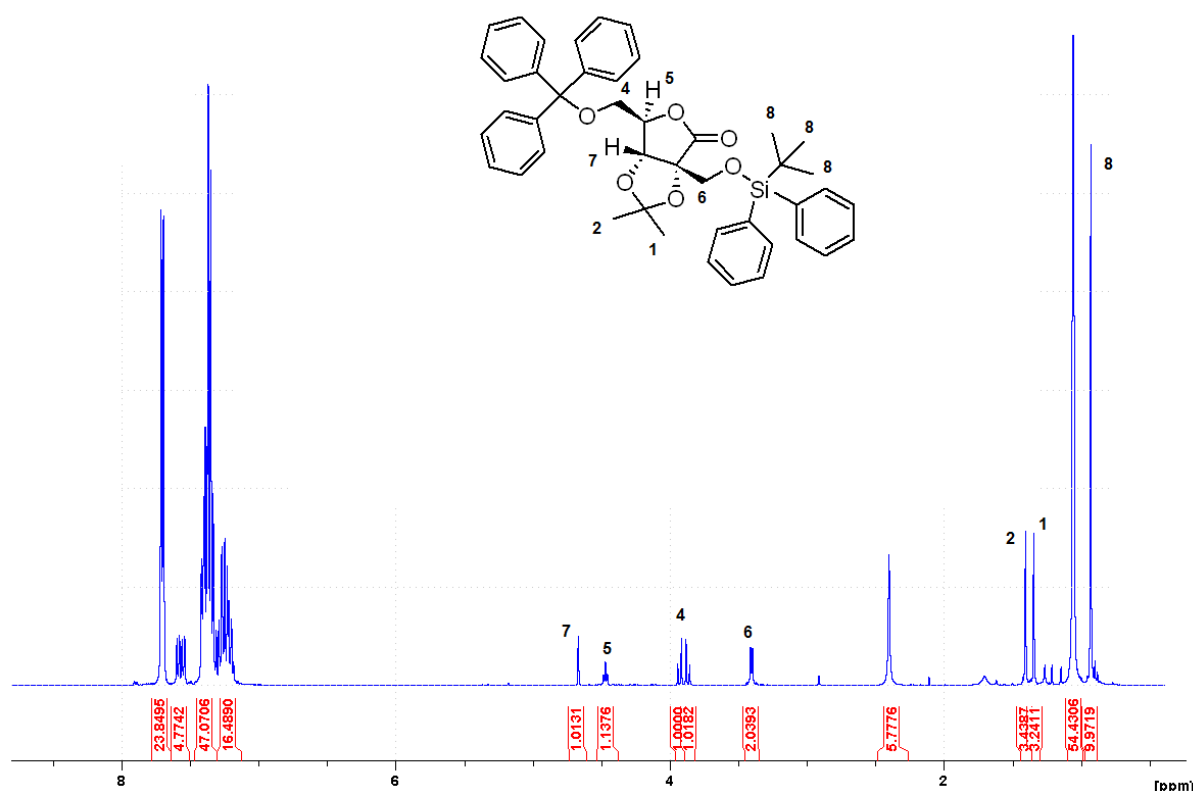
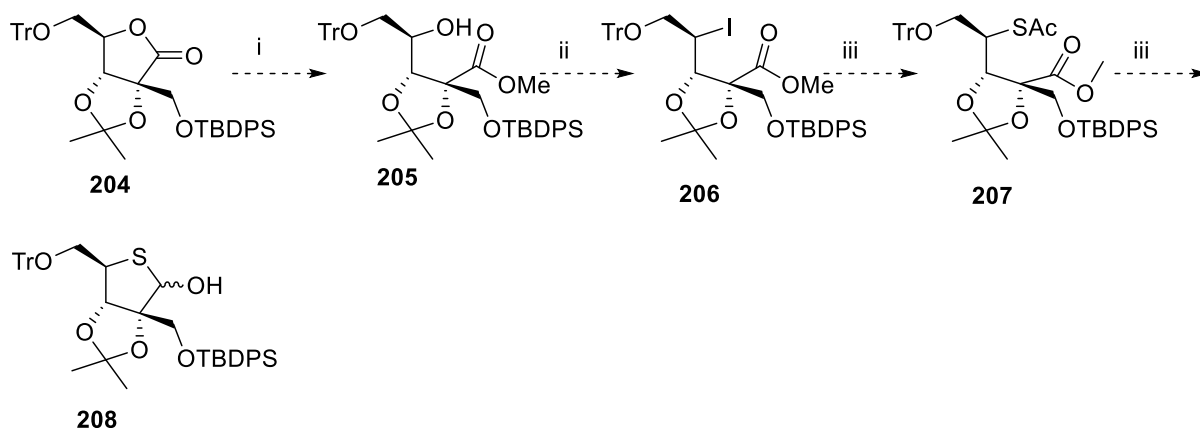


Figure 4.10: ^1H NMR spectrum of TBDPS moiety **204**

As can be seen from the spectrum in figure 4.9, there are still significant levels of TBDPS impurity in the post column fractions that could not be removed as it co-eluted with the product. The impurities in spectrum shown in figure 4.9 are at 1.5 ppm for the *tert*-butyl groups and at 7.5 and 7.9 ppm for the phenyl groups of the TBDPS-OH impurity. However, protons 5 and 7 are present as the two CH groups which integrate to 1 and the two methylene groups are also present and are shown as protons 4 and 6. The mass spectrum data for TBDPS moiety **204** was found to be 721.3115 Da for the sodium adduct and the calculated mass was 721.2961 Da. This gave confidence that the compound had been successfully synthesised despite the large impurities present in the product. The impurities are the 1.2 ppm and 7.5 ppm and at 7.8 ppm for the *tert*-butyldiphenylsilyl hydroxide impurity that co-eluted with the product, TBDPS moiety **204**.

4.4.3 Hydrolysis Reactions Toward Methyl Ester **205**

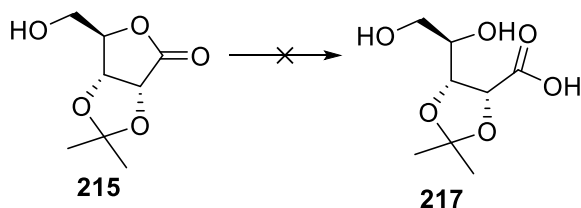
In order to synthesise the 4'-thiohamamelose **206**, the following transformations from TBDPS moiety **202** are required (scheme 4.10)



Scheme 4.10: Proposed synthetic steps toward 4'-thiohamamelose **208** i) NaOH, Me₂SO₄, DMSO, RT, 3 hrs ii) PPh₃, Imidazole, I₂, DCM, 120°C, 6 hrs iii) AcSH, TBA-OH, toluene, RT, 18 hrs iv) DIBAL-H, toluene, 2 hrs

In order to incorporate the sulfur atom, the proposed synthetic scheme in scheme 4.10 utilises the reaction conditions used by Secrist *et al.* to furnish 4'-thio-2',3'-dideoxyribose nucleosides.³² In the first step, TBDPS **204** is hydrolysed to a carboxylic acid using NaOH and then dimethyl sulfate is added to furnish methyl ester **205**. Then iodine is introduced to the compound to form the iodo derivative **206** which is reacted with thioacetic acid to form thioether **207** which is cyclised to 4'-thiohamamelose moiety **208**.

Before subjecting TBDPS moiety **204** to basic conditions, the hydrolysis reaction was first trialled with ribolactone **215** with the expectation of first isolating acid **217** (scheme 4.11).



Scheme 4.11: Model hydrolysis reaction toward acid **217** using NaOH

Replication of the Secrist reaction conditions using 1 equivalent of NaOH in water did not yield any product. Analysis of the reaction mixture by TLC showed only the starting ribolactone **215** was present even after 24 hours. Table 4.9 shows the attempts to optimise the hydrolysis reactions.

Table 4.9: Attempted optimisation for the model hydrolysis reactions

Reaction	NaOH (equiv)	Outcome
1	1	No reaction
2	1.5	No reaction
3	2	No reaction
4	5	No reaction

In all cases, no reaction was observed by TLC analysis of the crude reaction mixture. The ^1H NMR spectroscopic data also confirmed that no reaction had occurred in any of the reactions as the data matched that of the starting material, ribolactone **215** (figure 4.11). Each reaction was first reacted at room temperature and initially for 1 hour as per the conditions set out by Secrist. The reactions were left to react for 24 hours at room temperature, and no reactions were observed. Increasing the number of equivalents was trialled as this could increase the rate of reaction, but this had no effect. The failure of the reactions to proceed could be due to room temperature (25 °C) was not adequate enough to initiate the reaction, as this reaction may have a higher than expected activation energy. Increasing the reaction temperature would be the logical next step to assess whether this reaction is feasible. However, this was not done in this line of research as there were concerns for the stability of the TBDPS group towards mineral base for the formation of ester **205**. The TBDPS group is stable to base up to pH 12 at room temperature, and heating ester **205** in base will lead to deprotection of the TBDPS group.

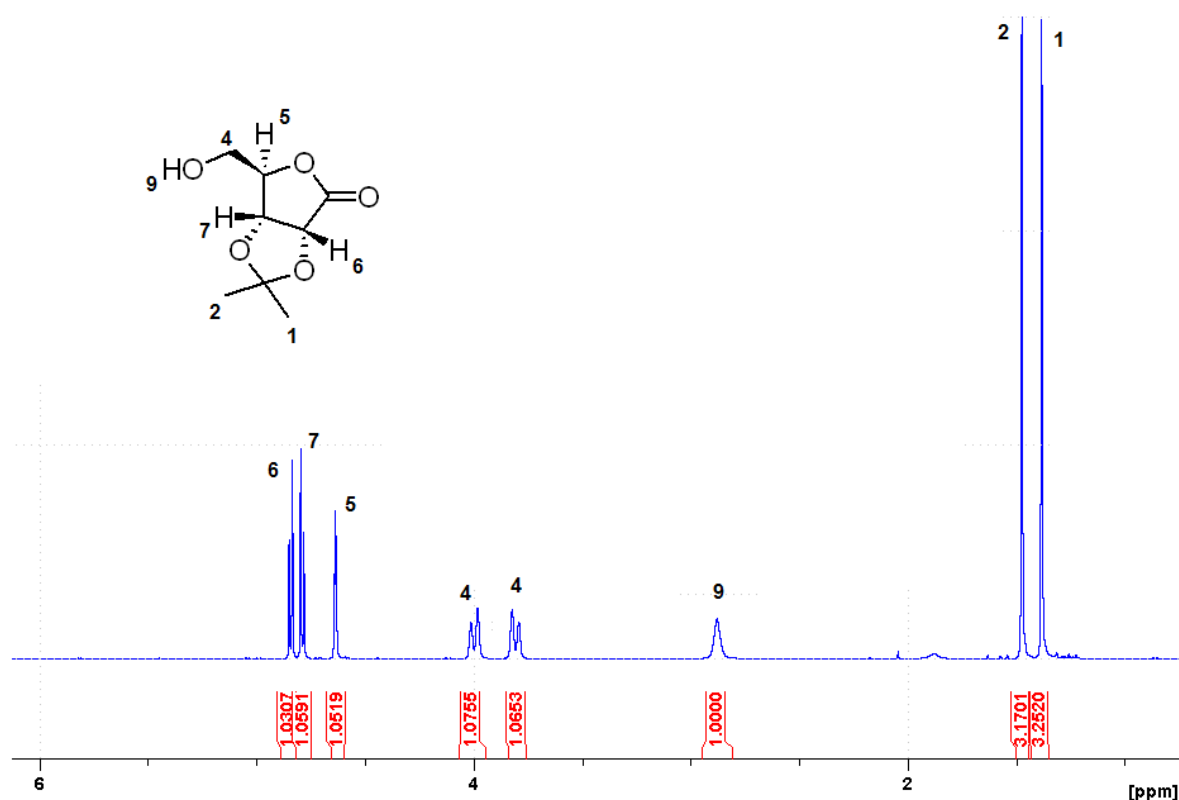


Figure 4.11: ^1H NMR spectrum of ribolactone **215**

As can be seen, the methyl groups on the acetonide are present as are the CH protons on the ribose ring. If hydrolysis had occurred, an extra $-\text{OH}$ peak at around 3 – 4 ppm should be observed and a broad peak at 11 – 12 ppm should also be observed which would be indicative of the carboxylic acid. This ^1H NMR spectroscopic data coupled with TLC analysis that showed no product formation confirmed that the hydrolysis reactions for the model compound were not working.

Since the Secrist method for the hydrolysis of ribose **215** could not be replicated and were deemed inappropriate to use for the formation of ester **205**, other methods were sought but a literature search did not reveal methods that were deemed acceptable to use for the hydrolysis of TBDPS moiety **204** such as boiling methanol with base as it was suspected that global deprotection would occur. Therefore, work toward the hydrolysis of TBDPS moiety **204** was stopped and further evaluation of the synthetic route is required.

In general, the current synthetic scheme has shown several other areas where optimisation is still required. Although the formylation reaction was optimised towards

hamamelose **202**, purification of this compound proved difficult and as such mass spectrometry and ^1H NMR spectroscopic data of the crude product had to be used to determine if the reaction had indeed been successful. Further, oxidation to hamamelolactone **203** requires further optimisation of the purification reactions as this compound could not be isolated in its pure form either, though this is compounded by the fact that the starting material was not pure. This, however, did not hamper the synthesis of TBDPS moiety **204** as attempts to purify the product by column chromatography was sufficiently successful to remove the impurities from the previous two steps. However, the TBDPS-OH impurity did co-elute with the TBDPS moiety **204**, therefore the purification step still requires optimisation. Therefore, coupled with the need to optimise the hydrolysis reaction toward methyl ester **205**, significant work is required to optimise the purification and reaction conditions of the preceding steps in this synthetic plan.

4.5 References

- (1) De Clercq, E. *Nat Rev Drug Disc* **2007**, 6, 1001.
- (2) Godwin, C. G.; Zhang, X.; Marchand, C.*et al. J Med Chem* **2002**, 45, 3184.
- (3) Pommier, Y.; Johnson, A. A.; Marchand, C. *Nat Rev Drug Discov* **2005**, 4, 236.
- (4) Casadella, M.; van Ham, P. M.; Noguera-Julian, M.*et al. J Antimicrob Chemother* **2015**, 70, 2885.
- (5) Summa, V.; Ludmerer, S. W.; McCauley, J. A.*et al. Antimicrob Agents Chemother* **2012**, 56, 4161.
- (6) Summa, V.; Petrocchi, A.; Bonelli, F.*et al. J. Med. Chem* **2008**, 51, 5843.
- (7) Soengas, R. G.; Silva, S. *Mini Rev Med Chem* **2012**, 12, 1485.
- (8) De Clercq, E. *Med Res Rev* **2008**, 28, 929.
- (9) De Clercq, E. *Med Res Rev* **2009**, 29, 571.
- (10) De Clercq, E. *Annu Rev Pharmacol Toxicol* **2011**, 51, 1.
- (11) De Clercq, E. *J Clin Virol* **2004**, 30, 115.
- (12) De Clercq, E. *Antiviral Res* **2005**, 67, 56.
- (13) De Clercq, E. *Med Res Rev* **2015**, 35, 698.
- (14) De Clercq, E.; Field, H. J. *Br J Pharmacol* **2006**, 147, 1.
- (15) Eldrup, A. B.; Allerson, C. R.; Bennett, C. F.*et al. J Med Chem* **2004**, 47, 2283.
- (16) Eldrup, A. B.; Prhavc, M.; Brooks, J.*et al. J Med Chem* **2004**, 47, 5284
- (17) Sofia, M. J.; Chang, W.; Furman, P. A.*et al. J Med Chem* **2012**, 55, 2481.
- (18) Murakami, E.; Niu, C.; Bao, H.*et al. Antimicrob Agents Chemother* **2008**, 52, 458.
- (19) Ketkar, A.; Zafar, M. K.; Banerjee, S.*et al. Biochemistry* **2012**, 51, 9234.
- (20) Kim, T.; Barchi, J. J., Jr.; Marquez, V. E.*et al. J Mol Graph Model* **2011**, 29, 624.
- (21) Marquez, V. E.; Choi, Y.; Comin, M. J.*et al. J Am Chem Soc* **2005**, 127, 15145.
- (22) Marquez, V. E.; Ben-Kasus, T.; Barchi, J. J.*et al. J Am Chem Soc* **2004**, 126, 543.
- (23) Toyohara, J.; Kumata, K.; Fukushi, K.*et al. J Nucl Med* **2006**, 47, 1717.
- (24) Haeberli, P.; Berger, I.; Pallan, P. S.*et al. Nucleic Acids Res* **2005**, 33, 3965.
- (25) Inoue, N.; Kaga, D.; Minakawa, N.*et al. J Org Chem* **2005**, 70, 8597.

- (26) Naka, T.; Minakawa, N.; Abe, H.*et al. J Am Chem Soc* **2000**, 122, 7233.
- (27) Secrist, J. A.; Tiwari, K. N.; Riordan, J. M.*et al. J Med Chem* **1991**, 34, 2361.
- (28) Dyson, M. R.; Coe, P. L.; Walker, R. T. *J Med Chem* **1991**, 34, 2782.
- (29) Desgranges, C.; Rabaud, G. R. M.; Bricaud, H.*et al. Biochem Pharmacol* **1983**, 32, 3583.
- (30) De Clercq, E. *Biochem Pharmacol* **2004**, 68, 2301.
- (31) Pejanović, V.; Stokić, Z.; Stojanović, B.*et al. Bioorg Med Chem Lett* **2003**, 13, 1849.
- (32) Secrist, J. A.; Riggs, R. M.; Tiwari, K. N.*et al. J Med Chem* **1992**, 35, 533.
- (33) Yokoyama, M. *Synthesis* **2000**, 1637.
- (34) Sofia, M. J.; Bao, D.; Chang, W.*et al. J Med Chem* **2010**, 53, 7202.
- (35) De Francesco, R.; Migliaccio, G. *Nature* **2005**, 436, 953.
- (36) Klumpp, K.; Leveque, V.; Le Pogam, S.*et al. J Biol Chem* **2006**, 281, 3793.
- (37) Gardelli, C.; Attenni, B.; Donghi, M.*et al. J Med Chem* **2009**, 52, 5394.
- (38) Carroll, S. S.; Tomassini, J. E.; Bosserman, M.*et al. J Biol Chem* **2003**, 278, 11979.
- (39) Olsen, D. B.; Eldrup, A. B.; Bartholomew, L.*et al. Antimicrob Agents Chemother* **2004**, 48, 3944.
- (40) Tomassini, J. E.; Getty, K.; Stahlhut, M. W.*et al. Antimicrob Agents Chemother* **2005**, 49, 2050.
- (41) Jeong, L. S.; Yoo, B. N.; Kim, H. O.*et al. Nucleosides Nucleotides Nucleic Acids* **2007**, 26, 725.
- (42) Yoo, B. N.; Kim, H. O.; Moon, H. R.*et al. Bioorg Med Chem Lett* **2006**, 16, 4190.
- (43) Haraguchi, K.; Matsui, H.; Takami, S.*et al. J Org Chem* **2008**, 74, 2616.
- (44) Mish, M. R.; Cho, A.; Kirschberg, T.*et al. Bioorg Med Chem Lett* **2014**, 24, 3092.
- (45) Booth, K. V.; da Cruz, F. P.; Hotchkiss, D. J.*et al. Tet Asymm* **2008**, 19, 2417.
- (46) Choi, W. J.; Moon, H. R.; Kim, H. O.*et al. J Org Chem* **2004**, 69, 2634.
- (47) Beigelman, L.; Ermolinsky, B. S.; Gurskaya, G. V.*et al. Carbohydr Res* **1987**, 166, 219.
- (48) Ho, P. T. *Tet Lett* **1978**, 19, 1623.
- (49) Stewart, A. J.; Evans, R. M.; Weymouth-Wilson, A. C.*et al. Tet Asymm* **2002**, 13, 2667.

- (50) Jin, Y. H.; Liu, P.; Wang, J.*et al. J Org Chem* **2003**, 68, 9012.
- (51) Beaulieu, P. L.; Organisation, W. I. P., Ed. 2009; Vol. WO/2009/076747 A1.
- (52) Garegg, P. J.; Samuelsson, B. *J Chem Soc Perkin Trans 1* **1980**, 2866.
- (53) Reddy, P. G.; Chun, B. K.; Zhang, H. R.*et al. J Org Chem* **2011**, 76, 3782.

Chapter 5:

Conclusions and Future Work

Chapter 5: Conclusions and Future Work

Viral infections are a common cause of illness and death in humans, but due to the rapid rate at which viruses are able to replicate, resistance to current drugs evolves quickly.¹ Nucleoside drugs are the most powerful types of compounds for treating viral infections as they are able to completely halt viral genome replication.²⁻⁴ Without a fully functioning genome, the virus is unable to replicate and the infection is stalled. Practically all of the currently available nucleoside drugs available on the market are based upon ribose so as to closely resemble endogenous nucleosides. This ensures that the host and viral enzymes and transport proteins are able to utilize these drugs. However, inactivity of nucleoside drugs based on ribose is still a problem. The most prominent issue is the discrimination between kinases and polymerases. In order to be incorporated into a genome, the nucleoside must first be phosphorylated.^{5,6} Ribose nucleosides exist in north and south conformations, but kinases only recognise south conformations and polymerases only recognise north conformations of the nucleoside.^{5,6} This means that the ribose nucleosides must be in the correct conformation to be phosphorylated, and then change conformation prior to entering the polymerase and being incorporated into the genome. This is a significant reason why potentially active ribose based nucleosides have low NTP concentrations in the cell.

A further issue that compounds the problem of kinase-polymerase bias is that the first kinase in the phosphorylation step is discriminatory.⁷⁻¹² This means that even if the conformation of the nucleoside is correct, the first kinase in the phosphorylation step may not recognise the nucleoside, and not phosphorylate it. This further reduces the NTP concentration in the cell. Both of these problems have been overcome by research into phosphoramidate chemistry. By masking the 5'-OH group with a phosphoramidate, the primary kinase could be bypassed.^{7,8} This led to higher levels of NTP in cells, and for nucleosides that were previously inactive, creating their phosphoramidate derivatives made the previously inactive drug, active.

Despite overcoming the major problem of phosphorylation and kinase-polymerase bias, ribose based nucleoside drugs were also found to be prone to the action of PNPs.¹³⁻¹⁵ This is a class of enzymes that hydrolyse the glycosidic bond between the ribose and the nucleobase. This too is a significant cause of inactivity. A major

method to overcome this involves replacing the oxygen in the ribose ring with sulfur to make 4'-thioribose nucleosides. It was found that these were less susceptible to PNPs, with longer half-lives than their ribose counterparts, and stronger binding affinities.

Another way to overcome conformational discrimination by kinases was to use alternative sugars. Oxetane nucleosides were shown to be phosphorylated by kinases, despite existing in pseudo-north and pseudo-south conformations, and were shown to be active, which meant that these compounds were being incorporated into viral genomes by polymerases. However, oxetane nucleosides were still susceptible to PNPs.¹⁶⁻²⁷

5.1 General Conclusions

Thietane nucleosides have previously been shown to be active against HIV-1 and it is hypothesised that they will be resistant to PNPs. It is also assumed that these drugs will be phosphorylated and overcome kinase-polymerase bias as already active anti-HIV thietane nucleosides are known.²⁵⁻²⁷ The 3,3-bis(hydroxymethyl)-thietan-2-yl nucleosides were explored in this programme as potential anti-viral compounds for the reasons outlined above. Although the thymine derivative for this scaffold is known, its anti-viral activity has not been explored. A library of nine nucleosides, seven of which are novel, were synthesised with the aim of exploring their anti-viral activity.

The 4,4-bis(hydroxymethyl)-thietane scaffold is completely novel and the intention was to explore how modifications to the thietane ring would affect the anti-viral properties of the thietanes. This would have been achieved by creating analogous compounds to those in the 3,3-bis(hydroxymethyl)-thietan-2-yl nucleosides, and comparing their activity.

The 4'-thiohamamelose nucleosides were of interest as hamamelose nucleosides were shown to be active against HCV, despite having low IC₅₀ values due to metabolic instability. As already shown, converting ribose to 4'-thioribose increased the half-life of the nucleoside drug, meaning that its bioavailability increased. Exploration of the 4'-thiohamamelose nucleosides as a way to increase their

metabolic stability could have beneficial effects on the anti-viral properties of this class of compound.

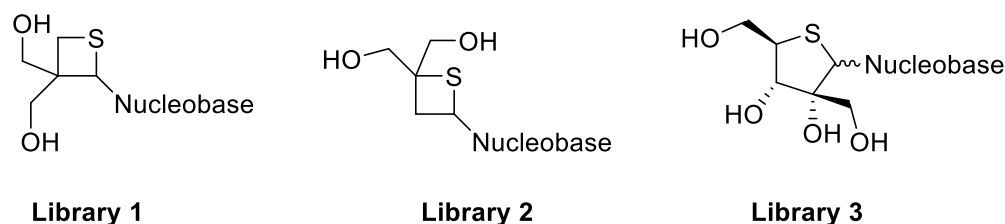


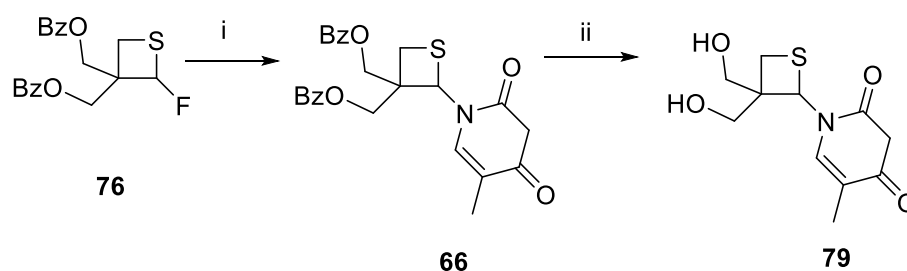
Figure 5.1: The two thietane scaffolds and the 4'-thiohamamelose scaffolds are shown. The scaffolds for the 3,3-bis(hydroxymethyl) (library 1) and 4,4-bis(hydroxymethyl)-thietane (library 2) nucleosides vary by the position of the hydroxymethyl groups. In library 1, nucleosides are varied. The biological activity of each nucleoside will give an indication of the SAR for this library. In library 2, the hydroxymethyl group position is altered. By using the same nucleobases as those in library 1, the effect of the hydroxymethyl group on the SAR can be determined. Library 3, the 4'-thiohamamelose nucleosides will also use the same nucleobases as the first two libraries, however, the SAR will determine whether 4'-thiohamamelose nucleosides have better anti-viral properties versus hamamelose nucleosides in the literature. From each library, the biological data will be used to determine the SAR with the intent of designing and synthesising more potent compounds for each scaffold.

5.2 Future Work

Detailed below is the intended work to determine the SAR of each scaffold discussed previously in section 5.1. In order to meet these requirements, the following scheme of work is proposed.

5.2.1 Synthesis of 3,3-bis(hydroxymethyl) thietane nucleosides

The synthetic route to 3,3-bis(hydroxymethyl)-thietan-2-yl nucleosides required efficient synthesis of key precursor fluorothietane **76**. It was found that the Pummerer reaction towards the synthesis of the nucleosides was not reproducible, and did not yield the desired nucleosides. However, from fluorothietane **76** it was found that the 3,3-bis(benzoylmethoxy)-thietan-2-yl nucleosides could be synthesised with yields ranging from 39 – 75%. Deprotection reactions toward the target nucleosides using NaOMe or MeNH₂ were achieved with yields in excess of 80 – 90% from the benzoyl protected moieties (scheme 5.1). This furnished nine thietane nucleosides, seven of which are novel.



Scheme 5.1: General synthetic scheme to target nucleosides from fluorothietane **76** i) silylated nucleobase, AgClO_4 , SnCl_2 , DCM, RT, 18 hrs, 57% ii) MeNH_2 , EtOH, RT, 2 hrs, 98%

With the nine nucleosides synthesised determination of their anti-viral activities is now possible. Prior to an anti-viral screen, the cytotoxic effects of the nucleosides require assessment. The desired outcome would be that no cytotoxicity would be observed. Four candidate compounds that best represented the library were chosen for cell viability testing. The cell viability assay used SH-SY5Y neuroblastoma cells, since the density of the cells meant that a more intense signal could be detected. This was important as it meant that assessing cell viability could be attributed to the compounds and not to any other biological reasons. XTT was used as the agent to determine the number of viable cells by measuring the optical density. The XTT assay relies on cellular respiration, therefore, only measures respiring cells as viable. In cells that have long exponential growth phases, some of the cells may not be actively respiring, which the assay would determine as non-viable.

The XTT assay was used to establish if the thietane nucleosides were affecting cell viability. If any compounds were shown to negatively affect cell viability, they would not proceed to the broad anti-viral screen. Therefore, the XTT assay was used as a pre-screening method to determine whether compounds proceeded to an anti-viral screen. Cytotoxic compounds would not be ideal candidates for the anti-viral screen as their anti-viral activities would be hard to determine if the cells were dead.

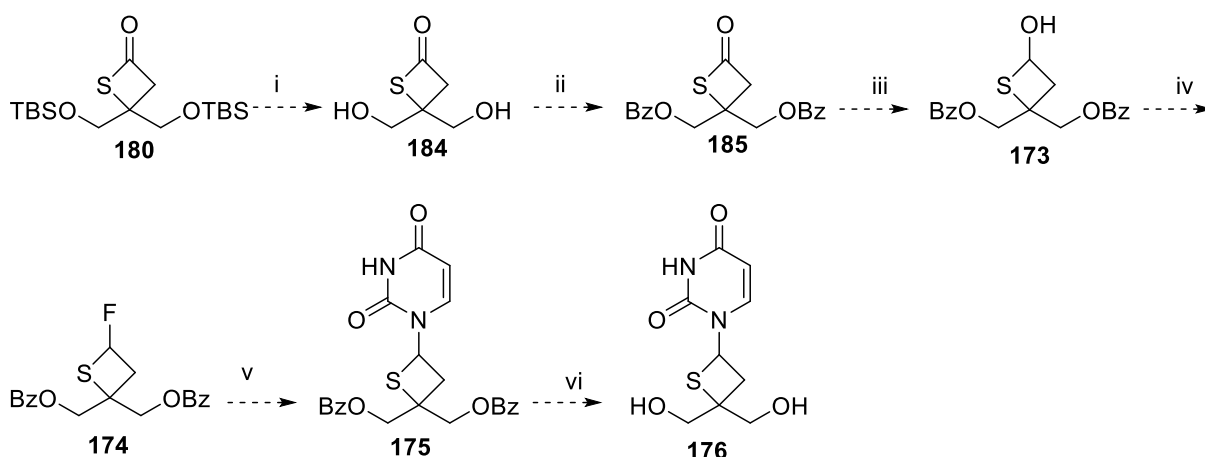
The cell viabilities were established for four candidate compounds. In three compounds, thymine **79**, uracil **80**, and 5-fluorouracil **84**, no significant cytotoxicity was observed at 100 μM , with the 5,6-dimethyluracil derivate **89** showing an 18% decrease in cell viability at 100 μM . Since the dose-response curve for biological systems is non-linear; a logarithmic scale can easily be used to drawn direct

comparisons between a biological response and the dose. If no response is observed at a very high concentration such as 100 μ M, this shows that the compound does not elicit a cytotoxic event. With the four candidate compounds being a representative sample of the nine compounds in the library, each compound can now be progressed to a broad anti-viral screen to assess the inhibitory concentration (IC_{50}) of the compounds and their cytotoxicity (CC_{50}). This will allow SAR of the compounds to be determined. Viruses of interest include HIV, HCV, VZV, HSV and HBV since HIV, HCV and HBV currently infects more than 200 million people combined and they evolve resistance to drugs quickly.³ This broad viral screen will allow multiple viruses to be assessed and a more targeted medicinal chemistry approach can be developed towards any potential viruses that show a response.

5.2.2 Synthesis of 4,4-bis(hydroxymethyl) thietan-2-yl nucleosides

The synthetic method for entry to the novel thietane core was significantly modified and the chemistry optimised to give 4,4-bis(*tert*-butyldimethylsilylmethoxy)-thietan-2-one **180** with a yield of 37% from thiol **179**. The introduction of the sulfur moiety via benzyl mercaptan was found to be a superior method than the Givaudan synthesis using H_2S and an aldehyde.

The 4,4-bis(hydroxymethyl)-thietan-2-yl nucleosides are of interest since the effect of the geminal hydroxyl groups on anti-viral activities are not known, therefore, comparing the anti-viral activities of the 3,3- and 4,4-bis(hydroxymethyl)-thietan-2-yl nucleosides could give potential insights into how these structures affect anti-viral activities. In order to assess the anti-viral activities of the 4,4-bis(hydroxymethyl) thietane nucleosides, thietanone **179** must first be reduced to alcohol **173**. Scheme 5.2 shows the proposed synthetic method required to achieve the intended nucleosides.



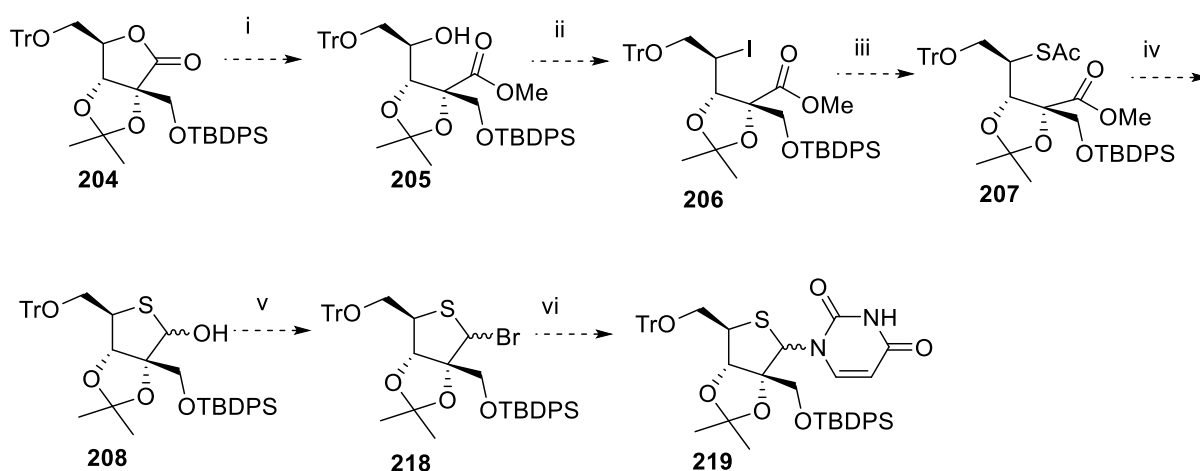
Scheme 5.2: Proposed synthesis of 4,4-bis(hydroxymethyl)-thietan-2-yl nucleosides i) $n\text{Bu}_4\text{NF}$, THF ii) BzCl , DMAP, Et_3N , DCM, RT iii) NaBH_4 , THF iv) Deoxofluor, SbCl_3 , DCM, RT v) silylated nucleobase, AgClO_4 , SnCl_2 various solvents and temperatures (see chapter 2) vi) NaOMe , MeOH , RT

The proposed synthesis first requires removal of the TBS groups and incorporation of benzoyl groups the chemistry of which is described in chapter 2 for the synthesis of fluorothietane **76**. In this proposed synthesis, the already optimised Vorbrüggen conditions from chapter 2 will be applied to this synthesis. As per the library in chapter 2, a library of nine nucleosides would be afforded (see introduction to chapter 3 for the complete list of proposed compounds) so that a direct comparison of the anti-viral activity can be made.

5.2.3 Synthesis of 4'-thiohamamelose Nucleosides

The synthetic strategy towards 4'-thiohamamelose was optimised to TBDPS **207**, and it was found that synthesis of hamamelose **205** first required trityl protection of the 5'-OH group prior to formylation of ribose **204**. The purification processes for the compounds requires significant optimisation as some reactions could not be purified adequately, and carrying through crude material to the next step in the synthetic plan may have adversely affected yields.

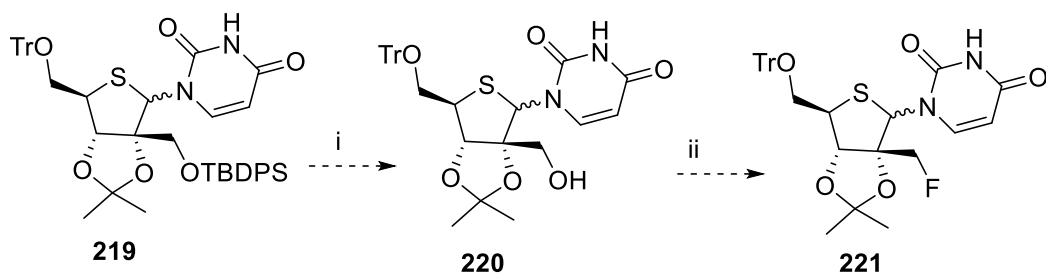
Despite the low yields and optimisation problems with the proposed synthesis, the synthetic scheme was successful in preparing TBDPS **204** as an important potential precursor to 4'-thiohamamelose. In scheme 5.3, the proposed synthesis towards the 4'-thiohamamelose nucleosides is shown. The reaction conditions proposed uses chemistry established by Secrist *et al.*^{28,29}



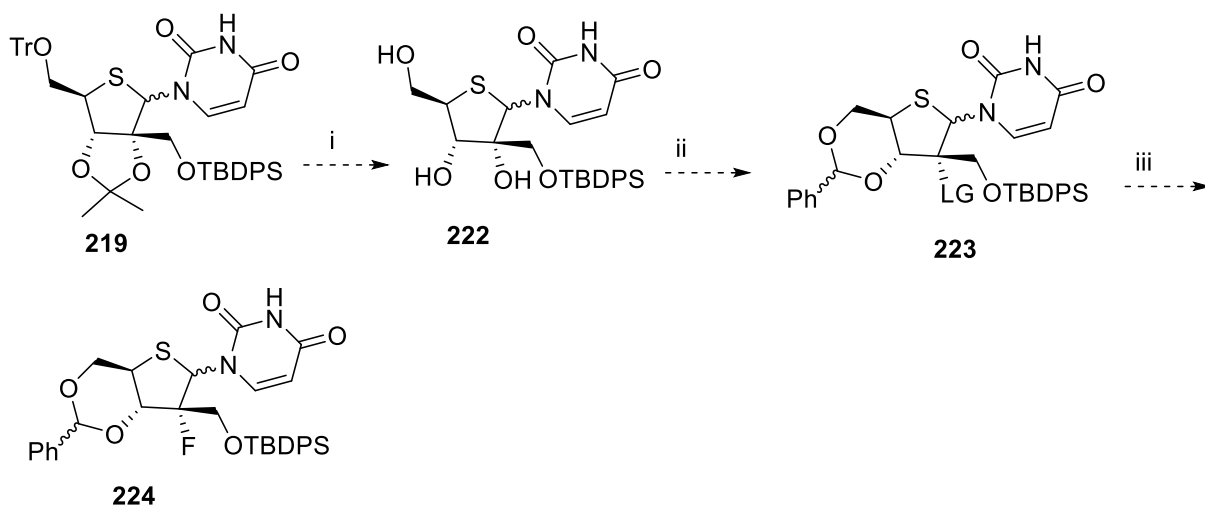
Scheme 5.3 Proposed synthetic method toward 4'-thiohamamelose nucleosides i) NaOH, Me₂SO₄ ii) PPh₃, Imidazole, I₂, DCM, 120°C, 6 hrs iii) AcSH, TBA-OH, toluene, RT, 18 hrs iv) DIBAL-H, toluene, 2 hrs v) CBr₄, PPh₃, DCM, -25° C, 1 hr vi) AgOTf, 135°C, μ wave, DCE/MeCN, 30 mins

As stated in chapter 4 section 4.5.3, the hydrolysis step shown in scheme 5.2 using the Secrist conditions could not be replicated, therefore, further optimisation of the reaction conditions are required. Potential conditions could require using a strong nucleophile such as NaOMe to create the methyl ester, though no literature syntheses are known for ribolactone ring opening using NaOMe. Formation of the 4'-thiohamamelose requires converting methyl ester **205** to iodide **206** using established chemistry with PPh₃ and I₂.³⁰ Conversion of iodide **206** to 4'-thiohamamelose **208** first requires synthesis of the thioether intermediate **207**, which is deprotected with DIBAL-H and cyclises to 4'-thiohamamelose **208** in an intramolecular cyclisation reaction.

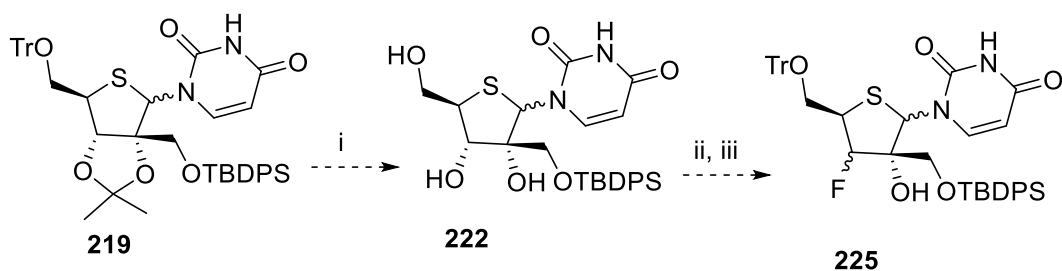
The protecting group strategy was chosen as it allows for selective deprotection of the hydroxyl group that requires conversion to the fluoride. Below are the planned synthetic steps toward 5'-OH, 3'-OH, 2'-OH and 2'-CH₂OH substitutions from thiohamamelose nucleosides (schemes 5.4, figure 5.5, figure 5.6).



Scheme 5.4: Synthetic strategy for the conversion of the 2'-C-methylhydroxy group to the fluoromethyl group: i) $n\text{Bu}_4\text{NF}$, THF, ii) Deoxofluor, SbCl_3 , DCM



Scheme 5.5: Conversion of the 2'-OH group to the 2'-Fluoro group first requires removal of the acetonide and formation of the benzylidene acetal. The 2'-OH group is converted to a leaving group (LG= Mesylate or tosylate or equivalent) and then deoxofluor is used to add the fluoride in an $\text{S}_{\text{N}}1$ fashion: i) H^+ eg $p\text{TSA}$ ii) Benzaldehyde dimethyl acetal then a Mesylate or tosylate added iii) Deoxofluor, SbCl_3 , DCM



Scheme 5.6: Conversion of the 3'-OH group to the fluoride requires removal of the acetonide and re-protection of the trityl group. Since the 3'-OH is a secondary hydroxide, the reaction mechanism of deoxofluor allows displacement by the $\text{S}_{\text{N}}2$ mechanism. The tertiary hydroxyl group will not react readily: i) $p\text{TSA}$ ii) TrCl , pyridine iii) deoxofluor SbCl_3

These derivatisations will allow access to a significant number of compounds that can be screened, giving a broader, more in depth analysis of how structure affects the anti-viral activity of these compounds.

5.2.4 HPLC Stability Studies

As has been stated in previous chapters, it has been predicted, and in some cases shown, that 4'-thioribose nucleosides are more stable toward nucleases and acidic conditions than ribose nucleosides.^{14,15,25,26,31} Thymidine **186** has a half-life of 1 hour versus the 4'-thioribose moiety **187**, which has a half-life 40 hours (figure 5.2).

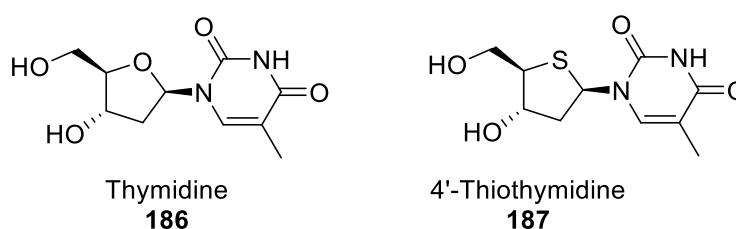


Figure 5.2: Thymidine and 4'-thiothymidine

Based on this and the data in chapter 4 section 4.1 (see table 4.1), it is proposed that the acid stability of 3,3- and 4,4-bis(hydroxymethyl)-thietan-2-yl nucleosides, and the 4'-thiohamamelose nucleosides should be determined by HPLC. It is hypothesised that these compounds are more stable than their oxetane or hamamelose counterparts. In figure 5.3 the control compounds are shown versus the thiethane and 4'-thiohamamelose counterparts. The structures are similar allowing for direct comparison between them.

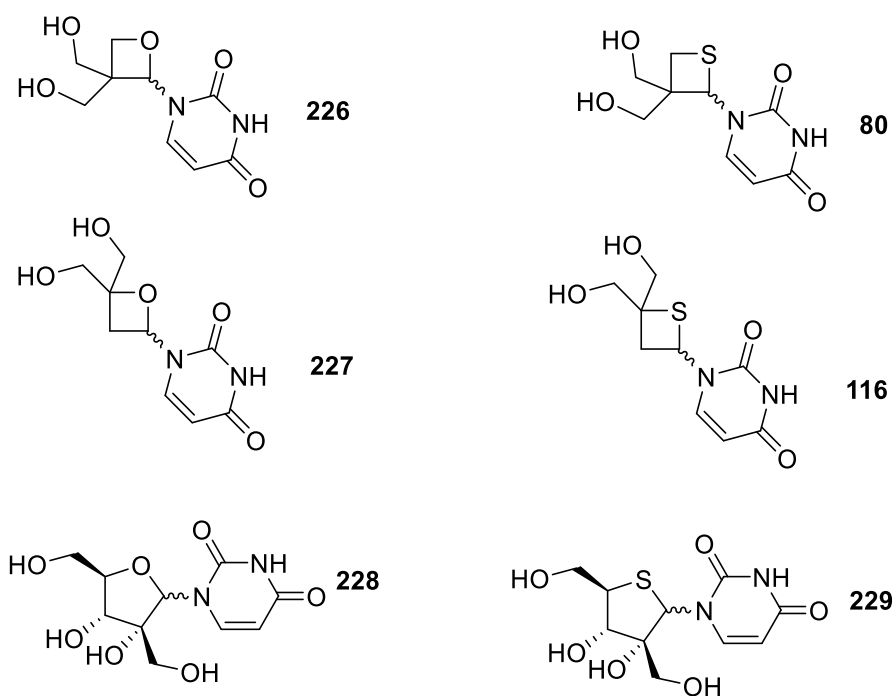


Figure 5.3: The control compounds (left) and the target compounds (right)

The half-lives of oxetanes **226** and **227**, and hamamelose **228** are unknown and would need to be determined prior to testing the candidate compounds from each library.

Acid stability would be tested by HPLC using known methods.³² The acid stability of oxetane **226** would be assessed in triplicate to give a mean half-life for its stability under acidic conditions. The thietanes would then be assessed using this method. Time points for measuring stability or degradation products can be done per hour over 24 hours to determine a half-life for each compound. Next, cell culture media would be used with and without serum to determine stability of the thietane and oxetane nucleosides in the cell culture assay that was used.

Further to HPLC stability studies being performed, assays would be performed to assess the stability of the thietane and hamamelose nucleosides toward pyrimidine nucleoside phosphorylases (PNPs), which have been shown to be a significant factor in inactivating oxygen containing ribose and oxetane nucleosides (see chapters 2 and 4).^{15-18,31} A basic method to assess the stability of the compounds to PNPs would involve incubating the samples of oxetane nucleoside **226** with PNP at 1 hour, 2 hours etc up to 24 hours to determine a half-life. The process would be repeated with each nucleoside and if the hypothesis that the sulfur containing nucleosides are more

stable to PNPs than the oxetanes or hamaleose nucleosides is true, a longer half-life for the thietanes should be observed. The ideal half-life would be close to 24 hours as this would limit the number of times a drug would have to be administered. Ideally, once a day administration of these drugs would combat patient compliance issues where doses are missed.

5.2.5 Synthesis of Phosphoramidates

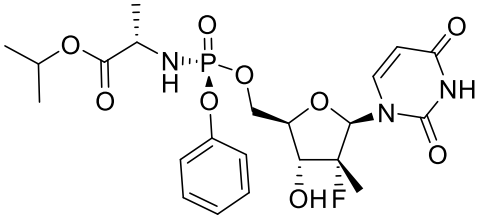
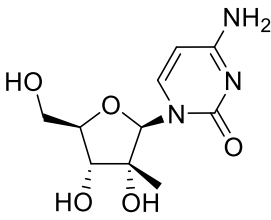
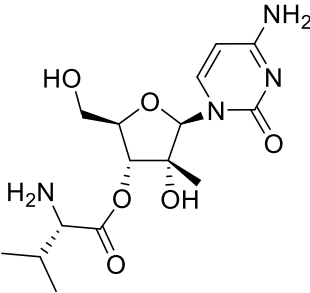
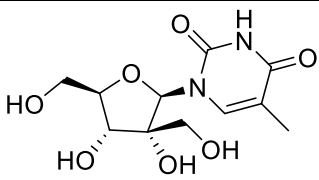
As shown in chapter 1, the triphosphate of the nucleoside drug is the active compound; however, of the three kinases involved in phosphorylation, the first kinase is discriminatory. This leads to low levels of active NTP in the cell and is a key factor in inactivity for this class of compound. Phosphoramidate prodrugs of nucleosides have been shown to increase anti-viral activity by virtue of the increased levels of NTP.

The solubility and therefore the ability of the nucleoside to cross the cell membrane (relying on transport proteins rather than diffusion across the cell membrane) means that in cases where the nucleoside has a large negative log P, low levels of active NTP in the cell are also observed. This therefore affects the activity of the compound in that if the compound is unable to enter the cell, it cannot elicit a response. Phosphoramidates increase the solubility of nucleosides as well as circumvent the primary kinase in the phosphorylation chain that is known to be a source of nucleoside inactivity.

It is proposed that synthesising phosphoramidate versions of the 3,3- and 4,4-bis(hydroxymethyl)-thietan-2-yl nucleosides, and the 4'-thiohamamelose nucleosides, will improve their anti-viral profiles. Shown in table 5.1 are three drugs with experimentally determined log P values, along with their calculated log P values of known compounds active against HCV. The clog P values were calculated herein using ChemDraw and compared to the known log P value where available. The log P or clog P values were compared to IC₅₀ values to give an indication of how improvement to bioavailability of the drug improves the anti-viral properties. However, this does not mean that improving log P values will improve the anti-viral activity of the compound class. However, it means that where low levels of NTP in cells are present along with no or low anti-viral activity, if the cellular NTP levels can be

improved by making the drug more available, low activity can be attributed to the drug and not the low cellular NTP levels.

Table 5.1: cLog P data for thietane nucleosides compared to known nucleosides

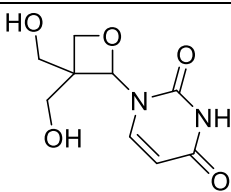
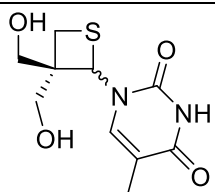
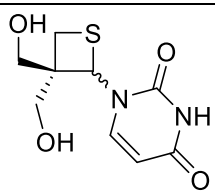
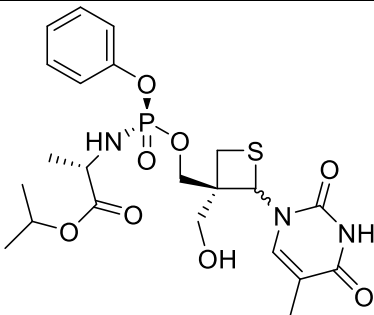
Compound	Log P	cLog P	IC ₅₀
 <p>Sofosbuvir 38</p>	1.6	0.84	0.42 μ M
 <p>NM107 21</p>	-0.97	-1.68	7.6 μ M
 <p>NM283 22</p>	-1.34	-1.17	1.23 μ M
 <p>230</p>	-2.56	10 μ M	

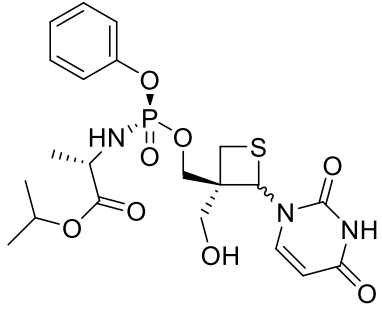
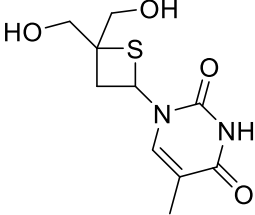
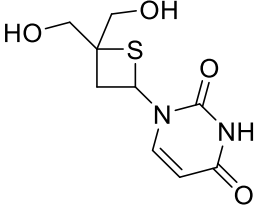
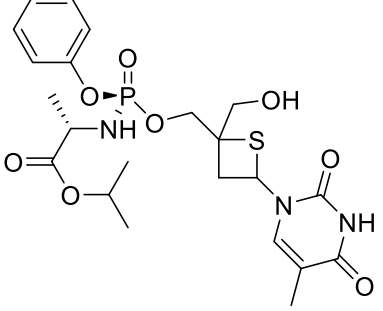
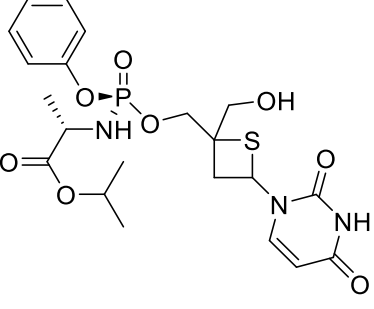
NM107 **21** and NM283 **22** have log P values of -0.97 and -1.34, and Sofosbuvir (trade name Sovaldi) **38** has a log P of 1.6. It is interesting to note that the IC₅₀ values for these compounds vary greatly, with the most active compound, Sofosbuvir **38** being the most active at 0.42 μ M and NM107 **21** being the least active at 1.23 μ M. It can be reasonably assumed that increasing the solubility of the compounds

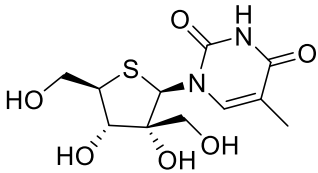
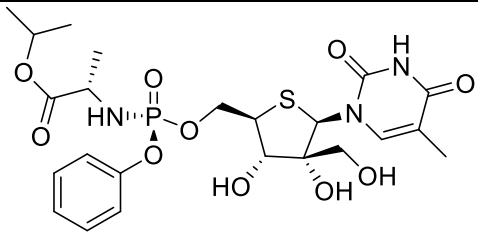
improves the level of active NTP in the cell. This therefore leads to greater potential for an anti-viral response to occur.

Table 5.2 shows the calculated log P values for the 3,3-, and 4,4-bis(hydroxymethyl)-thietan-2-yl nucleosides, and the 4'-thiohamamelose nucleosides. Also shown is the calculated log P data for the phosphoramidate derivatives of these classes of compounds.

Table 5.2: Calculated log P values for 3,3-, 4,4-bis(hydroxymethyl)-thietan-2-yl, 4'-thiohamamelose nucleosides, and the phosphoramidate derivatives

Compound	cLog P
 226	-3.5
 79	-1.6
 80	-2.1
 231	0.9

 <p>232</p>	0.4
 <p>115</p>	-0.5
 <p>116</p>	-0.84
 <p>233</p>	0.54
 <p>234</p>	0.42

 <p style="text-align: center;">235</p>	-1.34
 <p style="text-align: center;">236</p>	0.42

It can be seen that when comparing hamamelose **230** to 4'-thiohamamelose **235**, the clog P value increased from -2.56 to -1.34. Conversion of the 4'-thiohamamelose **235** to phosphoramidate **236** improves the clog P value further. The same is true of the 3,3- and 4,4-bis(hydroxymethyl)-thietan-2-yl nucleosides. The clog P values improve from oxetane **226** to thietane **80**, and the phosphoramidate moiety **231** has improved clog P value versus thietane **80**. The ideal log P values lie between 0 and 5, so any improvement from more negative values to the specified range has the potential to improve availability of these compounds to the cell, and therefore increase the concentration of potentially active NTP in the cell.

5.3 Closing Statement

Small molecule nucleosides offer the greatest potential as potent anti-viral compounds versus other anti-viral agents as they are able to directly halt viral replication. The 3,3- and 4,4-bis(hydroxymethyl)-thietan-2-yl nucleosides could potentially overcome kinase-polymerase bias due to the fact that the pseudo-north and pseudo-south conformations are assumed to be recognised by kinases and viral polymerases. This is based on observations of active oxetane and thietane nucleosides which showed anti-viral activity that could only have occurred if the nucleoside was phosphorylated then incorporated into a viral genome to prevent replication. Phosphoramidate versions of these compounds offer the potential to improve their chemical properties still further, by increasing intracellular NTP concentrations. The 4'-thiohamamelose compounds also offer these potential

benefits, and along with the thietanes discussed, have the potential to overcome PNP hydrolysis that reduces the half-life and efficacy of ribose and oxetane nucleosides. Small molecule nucleosides in general are potent anti-viral compounds due the ability of these compounds to halt viral genome replication. Non-nucleoside compounds are known to act on allosteric sites, but have an increased rate of resistance evolving toward them versus nucleosides. Therefore, by improving the chemical properties and stability of thietane and 4'-thiohamamelose nucleosides, significant increases in anti-viral activities could be achieved whilst reducing the chance of viral resistance from evolving.

5.4: References

- (1) Kharb, R.; Yar, M. S.; Sharma, P. C. *Mini-Rev Med Chem* **2011**, 11, 84.
- (2) Jordheim, L. P.; Durantel, D.; Zoulim, F. *et al. Nat Rev Drug Discov* **2013**, 12, 447.
- (3) De Clercq, E. *Nat Rev Drug Disc* **2007**, 6, 1001.
- (4) Summa, V.; Ludmerer, S. W.; McCauley, J. A. *et al. Antimicrob Agents Chemother* **2012**, 56, 4161.
- (5) Boyer, P. L.; Julias, J. G.; Marquez, V. E. *et al. J Mol Biol* **2005**, 345, 441.
- (6) Dejmek, M.; Hrebabecky, H.; Sala, M. *et al. Bioorg Med Chem* **2014**, 22, 2974.
- (7) Sofia, M. J.; Bao, D.; Chang, W. *et al. J Med Chem* **2010**, 53, 7202.
- (8) Sofia, M. J.; Chang, W.; Furman, P. A. *et al. J Med Chem* **2012**, 55, 2481.
- (9) Gardelli, C.; Attenni, B.; Donghi, M. *et al. J Med Chem* **2009**, 52, 5394.
- (10) Chang, W.; Bao, D.; Chun, B. *et al. ACS Med Chem Lett* **2011**, 2, 130
- (11) Murakami, E.; Niu, C.; Bao, H. *et al. Antimicrob Agents Chemother* **2008**, 52, 458.
- (12) Tomassini, J. E.; Getty, K.; Stahlhut, M. W. *et al. Antimicrob Agents Chemother* **2005**, 49, 2050.
- (13) Naka, T.; Minakawa, N.; Abe, H. *et al. J Am Chem Soc* **2000**, 122, 7233.
- (14) Dyson, M. R.; Coe, P. L.; Walker, R. T. *J Med Chem* **1991**, 34, 2782.
- (15) Desgranges, C.; Rabaud, G. R. M.; Bricaud, H. *et al. Biochem Pharmacol* **1983**, 32, 3583.
- (16) Liang, Y.; Hnatiuk, N. E.; Rowley, J. M. *et al. J Org Chem* **2011**, 76, 9962.
- (17) Norbeck, D. W.; Patent, U. S., Ed.; Abbott Laboratories: United States, 1995; Vol. US005420276A, p 30.
- (18) Rode, J. E.; Dobrowolski, J. Cz. *Chem Phys Lett* **2002**, 360, 123.
- (19) Balsamo, A.; Ceccarelli, G.; Crotti, P. *et al. J Org Chem* **1975**, 40, 473
- (20) Jonckers, T. H.; Vandyck, K.; Vandekerckhove, L. *et al. J Med Chem* **2014**, 57, 1836.
- (21) Ichikawa, E. K., K *Synthesis* **2002**, 1, 1.
- (22) Du, J.; Chun, B. K.; Mosley, R. T. *et al. J Med Chem* **2014**, 57, 1826.
- (23) Masuda, A.; Kitigawa, M.; Tanaka, A. *et al. J antibiotics* **1993**, 46, 1034.
- (24) Nishizono, N.; Akama, Y.; Agata, M. *et al. Tetrahedron* **2011**, 67, 358.
- (25) Nishizono, N.; Sugo, M.; Machida, M. *et al. Tetrahedron* **2007**, 63, 11622.

- (26) Nishizono, N.; Kioke, N.; Yamagata, Y.*et al. Tet Lett* **1996**, 37, 7569.
- (27) Choo, H.; Chen, X.; Yadav, V.*et al. J Med Chem* **2006**, 49, 1635.
- (28) Secrist, J. A.; Riggs, R. M.; Tiwari, K. N.*et al. J Med Chem* **1992**, 35, 533.
- (29) Secrist, J. A.; Tiwari, K. N.; Riordan, J. M.*et al. J Med Chem* **1991**, 34, 2361.
- (30) Garegg, P. J.; Samuelsson, B. *J Chem Soc Perkin Trans 1* **1980**, 2866.
- (31) Toyohara, J.; Kumata, K.; Fukushi, K.*et al. J Nucl Med* **2006**, 47, 1717.
- (32) Marquez, V. E.; Tseng, C. K. H.; Mitsuya, H.*et al. J Med Chem* **1990**, 33, 978.

Chapter 6:

Experimental

Chapter 6: Experimental

^1H and ^{13}C NMR spectroscopic analysis was obtained using a Bruker DPX 400MHz or a Nanobay 400 MHz spectrometer and spectra were recorded in deuterated chloroform or DMSO unless otherwise stated. Infrared analyses were recorded using a Paragon 1000 FT IR (Perkin Elmer, UK) spectrometer and absorptions are quoted in wave numbers. The data was obtained by placing samples onto an ATR diamond. Mass spectrometry data was recorded on a Fisons VG Autospec Mass Spectrometer using electrospray ionisation. Data is reported as the mass/charge ratio. Melting points were determined using Electrothermal digital melting point apparatus and are uncorrected. Purification was performed using a Biotage SP1 automated column chromatography system unless otherwise stated. Purity reported obtained by HPLC using Waters Agilent 2 HPLC with a UV detector and is reported in percent. All reagents were used as supplied by Sigma Aldrich, Alfa Aesar, TCI, Fluorochem, and Fischer Scientific. TLC analysis was performed on aluminium back silica gel with pore size 60Å and stained with either KMnO_4 , CAM, Vanilin or sugar dip. Purification by column chromatography used silica gel with pore size 60Å and compounds were pre-absorbed onto silica prior to running the column. Cell viability assay: SHS-Y5Y cells were cultured in Duplecos eagle medium (thermofischer) with fetal bovine serum (labtech) and penicillin-streptomycin (thermofischer) antibiotics. The cells were plated for experiments using 96 well plates obtained from VWR. The absorbance was measured using a Spectramax spectrophotometer from Molecular Devices.

General Procedures for the Synthesis of Thietane nucleosides

General Procedure A: To an oven dried round bottom flask under argon the pyrimidine nucleobase (2 equivs) was suspended in HMDS (0.14M relative to the nucleobase) and $(\text{NH}_4)_2\text{SO}_4$ (0.05 equivs) was then added to the reaction mixture. The reaction was heated to reflux (145° C) until the solution became clear. The solution was allowed to cool to room temperature and the HMDS was removed *in vacuo* to give a viscous oily residue. The residue was dissolved in DCM (0.2M relative to the fluorothietane) and the fluorothietane (1 equiv) was added followed by SnCl_2 (1 equiv) and AgClO_4 (1 equiv). The solution was reacted under argon at room temperature for 18 – 24 hours or until TLC analysis (1: 1 hexane : ethyl acetate)

showed complete consumption of the starting material. The reaction was diluted with ethyl acetate (equal to reaction volume) and the inorganic material filtered off. The ethyl acetate was partitioned with water (equal to one reaction volume) and organic layer removed. The aqueous phase washed 3 times with 5 times the reaction volume of ethyl acetate and the combined organic phases were washed with 3 times the reaction volume of saturated brine. The combined organic phases were dried with Na_2SO_4 , the solvent filtered then removed *in vacuo*. The residue was purified by column chromatography using 1:1 hexane:ethyl acetate unless otherwise stated.

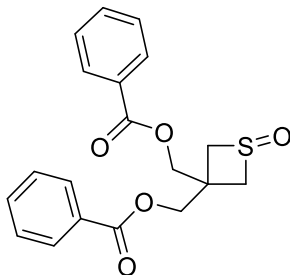
General Procedure B: To an oven dried round bottom flask under argon the pyrimidine nucleobase (2 equiv) was suspended in MeCN (0.48M relative to the fluorothietane) and then *N,O*-BSA (1.1 equiv) was added and then the reaction was heated to 70° C for 1 hour or until the solution became clear. The reaction was cooled to room temperature and the fluorothietane (1 equiv) was added followed by SnCl_2 (1 equiv) and AgClO_4 (1 equiv). The solution was reacted under argon at room temperature for 18 – 24 hours or until TLC analysis (1: 1 hexane : ethyl acetate) showed complete consumption of the starting material. The reaction was diluted with ethyl acetate (equal to reaction volume) and the inorganic material filtered off. The organic phase was partitioned with water (equal to one reaction volume) and organic layer removed. The aqueous phase washed 3 times with 5 times the reaction volume of ethyl acetate and the combined organic phases were washed with 3 times the reaction volume of saturated brine. The combined organic phases were dried with Na_2SO_4 the solvent filtered then removed *in vacuo*. The residue was purified by column chromatography using 1:1 hexane:ethyl acetate unless otherwise stated.

General Procedure C: To an oven dried round bottom flask under argon the benzoyl protected thietanose nucleoside was added (1 equiv) and methylamine (33% in ethanol, 14 ml, 17 equivs) was added. The reaction was stirred at room temperature for 3 hours. The mixture was concentrated *in vacuo* and purified by column chromatography using 9:1 chloroform:methanol as eluent unless otherwise stated.

General Procedure D: To an oven dried round bottom flask under argon the benzoyl protected thietanose nucleoside (1 equiv) was dissolved in methanol (5 ml). Solid NaOMe was added (2.5 equivs) and the reaction stirred at room temperature for 24 hours. The reaction was quenched with excess solid carbon dioxide and then the

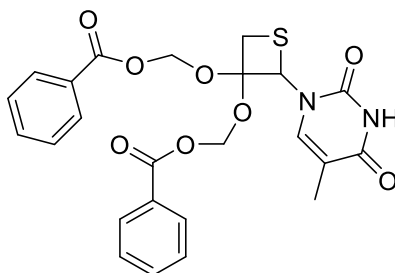
solvent removed *in vacuo*. The residue was purified by column chromatography using 9:1 chloroform:methanol unless otherwise stated.

Synthesis of 3,3-bis(benzoylmethoxy)-thietane-1-oxide **65**



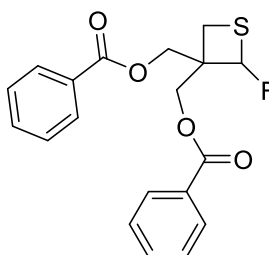
This procedure was modified from Nishizono *et al.*¹ To an oven dried round bottom flask under argon, 3,3-bis(benzoylmethoxy)-thietane **77** (1 g, 2.92 mmol, 1 equiv) was dissolved in methanol (60 ml) and sodium periodate (750 mg, 3.5 mmol, 1.2 equiv) was added. The reaction was stirred vigorously for 24 hours at room temperature. The crude reaction mixture was filtered and the solvent was evaporated *in vacuo*. The residue was purified by column chromatography using biotage on a 100 g column eluting with heptane : ethyl acetate 1 : 2 to yield the title compound as a white solid. Yield: 84%, 830 mg. MP 114 - 115° C Lit: 115 – 116 °C ¹H NMR (400 MHz CDCl₃) δ: 3.44 (2H, d, *J* = 13.0 Hz, SCH_{2a}) 3.80 (2H, d, *J* = 13.0 Hz, SCH_{2b}) 4.44 (2H, s, OCH₂) 4.48 (2H, s, OCH₂) 7.48 – 7.52 (4H, m, ArH) 7.61 – 7.66 (4H, m, ArH) 8.08 – 8.12 (2H, m, ArH) ¹³C NMR (100 MHz CDCl₃) δ: 36.6 (C(CH₂O)₂) 56.1 (2xCH₂S) 66.7 (OCH₂) 67.5 (OCH₂) 128.7 (ArC) 129.7 (ArC) 133.6 (ArC) 166.0 (2xC=O)) IR (u_{max} = cm⁻¹) 3416, 3066, 3031, 2954, 2878, 2322, 1980, 1713, 1383, 1277, 1069 HRMS EI calc: [C₁₉H₁₈SO₄Na⁺] 381.0773 obs: [C₁₉H₁₈SO₄Na⁺] 381.0767

Synthesis of 3,3-bis(benzoylmethoxy)-thietan-2-yl-thymine 66



This procedure was modified from Nishizono *et al.*¹ Synthesis of the title compound followed general procedure A to give the title compound as a white powder after purification by column chromatography. Yield: 57%, 100 mg. ¹H NMR (400 MHz CDCl₃) δ: 1.80 (3H, s, CH₃) 3.02 (1H, d, *J*= 9.5 Hz, CH₂S) 3.26 (1H, d, *J*= 9.5 Hz, CH₂S) 4.42 (1H, d, *J*= 12.0 Hz, OCH₂) 4.58 (1H, d, *J*= 12.0 Hz, OCH₂) 4.65 (1H, d, *J*= 11.5 Hz, OCH₂) 4.83 (1H, d, *J*= 11.5 Hz, OCH₂) 6.27 (1H, s, SCHN) 7.41 – 7.49 (4H, m, ArH) 7.55 – 7.61 (2H, m, ArH) 7.93 – 8.11 (5H, m, ArH and NCH=C(CH₃)) ¹³C NMR (100 MHz CDCl₃) δ: 12.4 (CH₃) 25.0 (CH₂S) 53.5 (C(OCH₂)₂) 56.6 (SCHN) 63.0 (OCH₂) 65.8 (OCH₂) 128.6 (ArC) 128.8 (ArC) 133.5 (ArC) 156.5 (NC=O) 156.8 (CCH₃C=O) 166.1 (OCH₂C=O) 171.1 (NC=O) IR (ν_{max} = cm⁻¹) 3004, 2360, 2342, 1732, 1718, 1696, 1672, 1600, 1450, 1109, 1024 MP: 177 – 178 °C HRSM EI calc: [C₂₄H₂₂N₂O₆SH⁺] 467.1271 obs: [C₂₄H₂₂N₂O₆SH⁺] 467.1265

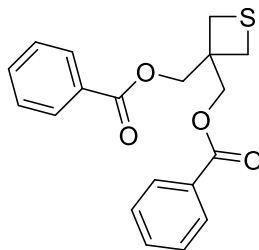
Synthesis of 3,3-bis(benzoyloxymethoxy)-2-fluorothietane 76



This procedure was modified from Nishizono *et al.*¹ To an oven dried round bottom flask under argon, 3,3-bis(benzoylmethoxy)-thietane **77** (250 mg, 0.73 mmol, 1 equiv) was added and it was dissolved in dry DCM (7 ml). SbCl₃ (17 mg, 0.073 mmol, 0.1 equiv) was added and Deoxo-fluor (2.92 ml, 1.5 equiv) was then added dropwise. The reaction was stirred for 72 hours at room temperature and completion was determined by TLC analysis. The reaction was quenched with cold ethyl acetate (14

ml) and washed with saturated sodium bicarbonate solution, then brine (50 ml), then dried over Na_2SO_4 . The solvent was filtered and evaporated *in vacuo*. The crude material was purified by column chromatography using biotage on a 25 g column eluting with heptane ethyl acetate (6:1) to yield the title compound as a white solid, yield: 84%, 220 mg. ^1H NMR (400 MHz CDCl_3) δ : 2.98 (1H, t, $J = 9.0$ Hz, CH_2S) 3.26 (1H, d, $J = 9.0$ Hz, CH_2S) 4.58 (2H, s, OCH_2) 4.79 (1H, d, $J = 2$ Hz, OCH_2) 4.83 (1H, d, $J = 2$ Hz, OCH_2) 6.10 (1H, d, $J = 63.0$ Hz), CHF) 7.41-7.54 (4H, m, ArH) 7.57-7.61 (2H, m, ArH) 8.00-8.07 (4H, m, ArH) ^{13}C NMR (100 MHz CDCl_3) δ : 25.6 (CH_2S) 53.1 ($\text{C}(\text{CH}_2\text{SCHF})(\text{OCH}_2)_2$) 62.9 (OCH_2) 65.0 (OCH_2) 93.6 (CHF , d, $J = 248$ Hz) 128.6 (ArC) 129.6 (ArC) 133.5 (ArC) 166.1 ($\text{CH}_2\text{OC}=\text{O}$) IR ($\nu_{\text{max}} = \text{cm}^{-1}$) 3064, 2955, 1718, 1601, 1584, 1492, 1261, 1095, 705. MP: 71 - 73 °C HRSM EI calc: $[\text{C}_{19}\text{H}_{18}\text{O}_4\text{SFNa}^+]$ 383.0729 obs: $[\text{C}_{19}\text{H}_{18}\text{O}_4\text{SFNa}^+]$ 383.0722

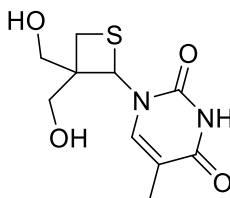
Synthesis of 3,3-bis(benzoylmethoxy)-thietane 77



This procedure was modified from Nishizono *et al.*¹ To an oven dried round bottom flask under argon, 3,3-bis(hydroxymethyl) thietane **95** (720 mg, 5.4 mmol, 1 equiv) was added and dissolved in dry DCM. Benzoyl chloride (3.10 ml, 27.0 mmol, 5 equiv) was added dropwise followed by triethylamine (2.55 ml, 16.1 mmol, 3 equiv) and DMAP (6.6 mg, 54 μmol , 0.01 equiv). The reaction was stirred overnight at room temperature and was monitored by TLC analysis (7:1 hexane : ethyl acetate) until all the starting material was consumed. The reaction was quenched by the addition of sat. NaHCO_3 until a neutral pH was observed. The aqueous phase was washed with ethyl acetate (3 x 30 ml) and the combined organic phases were dried over Na_2SO_4 , filtered and evaporated *in vacuo*. The crude was recrystallized from isopropyl alcohol to give a white solid. Yield: 78%, 1.44 g. ^1H NMR (400 MHz CDCl_3) δ : 3.14 (4H, s, $2\times\text{CH}_2\text{S}$) 4.42 (4H, s, $2\times\text{CH}_2\text{O}$) 7.37 (4H, t, $J = 4.0$ Hz) ArH) 7.46-7.50 (2H, m, ArH) 8.01 (4H, d, $J = 8.0$ Hz, ArH) ^{13}C NMR (100 MHz CDCl_3) δ : 28.8 ($2\times\text{CH}_2\text{S}$) 46.3 ($\text{C}(\text{OCH}_2)_2$) 66.9 ($2\times\text{OCH}_2$) 127.1 (ArC) 129.7 (ArC) 134.5 (ArC) 166.4 ($\text{CH}_2\text{OC}=\text{O}$)

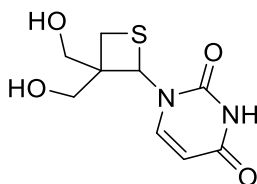
IR (ν_{\max} = cm^{-1}) 3416, 3066, 3031, 2954, 2878, 2322, 1980, 1713, 1383, 1277, 1169
MP: 79 - 82 °C Lit: 79 – 82 °C. HRMS EI calc: $[\text{C}_{19}\text{H}_{18}\text{O}_4\text{SNa}^+]$ 343.0999 obs: $[\text{C}_{19}\text{H}_{18}\text{O}_4\text{SNa}^+]$ 343.1004

Synthesis of 3,3-bis(hydroxymethyl)-thietan-2-yl-thymine 79



This procedure was modified from Nishizono *et al.*¹ Synthesis of the title compound followed general procedure C to give the title compound as a white powder after purification by column chromatography. Yield: 98%, 68 mg. HPLC purity: 98.6%. MP: 154-157 °C. ^1H NMR (400 MHz DMSO) δ : 1.86 (3H, s, CH_3) 2.80 (1H, d, J = 9.0 Hz, SCH_2) 2.88 (1H, d, J = 9.0 Hz, SCH_2) 3.34 (1H, d, J = 11.0 Hz, OCH_2) 3.48 (2H, d, J = 13.0 Hz, OCH_2) 3.60 (1H, d, J = 11.0 Hz, OCH_2) 4.66 (1H, t, J = 4.0 Hz, OH) 5.00 (1H, t, J = 4.0 Hz, OH) 5.86 (1H, s, SCHN) 8.20 (1H, s, $\text{CH}=\text{CCH}_3$) 11.23 (1H, br, NH) ^{13}C NMR (100 MHz DMSO) δ : 12.3 (CH_3) 24.1 (SCH_2) 55.8 (SCHN) 59.9 (CH_2OH) 63.6 (CH_2OH) 79.2 ($\text{C}(\text{CH}_2\text{OH})_2$) 108.0 ($\text{CH}=\text{CCH}_3$) 138.2 ($\text{CH}=\text{CCH}_3$) 151.0 ($(\text{CCH}_3)\text{C}=\text{O}$) 163.8 ($\text{NC}=\text{O}$) IR (ν_{\max} = cm^{-1}) 3411, 3362, 2931, 3602, 2496, 1705, 1653, 1474, 1444, 1397, 1301, 1246, 1231, 1216, 1172, 1064 HRSM EI calc: $[\text{C}_{10}\text{H}_{14}\text{N}_2\text{O}_4\text{SH}^+]$ 259.0747 obs: $[\text{C}_{10}\text{H}_{14}\text{N}_2\text{O}_4\text{SH}^+]$ 259.0749

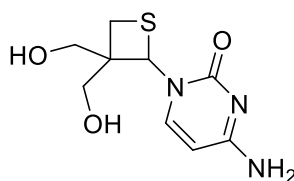
Synthesis of 3,3- bis(hydroxymethyl)-thietan-2-yl-uracil 80



This procedure was modified from Nishizono *et al.*¹ Synthesis of the title compound followed general procedure D to give the title compound as a white powder after purification by column chromatography. Yield: 93%, 138 mg. HPLC purity: 97.9% MP: 161 – 164 °C. ^1H NMR (400 MHz DMSO) δ : 2.75 (1H, d, J = 9.0 Hz, SCH_2) 2.90 (1H, d, J = 9.0 Hz, SCH_2) 3.35 (1H, d, J = 4.5 Hz,

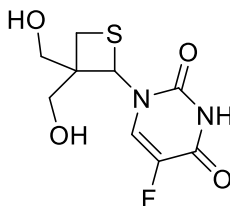
OCH₂) 3.50 (2H, m, OCH₂) 3.60 (1H, d, $J = 11.0$ Hz, OCH₂) 4.70 (1H, t, $J = 4.5$ Hz, OH) 5.00 (1H, t, $J = 4.5$ Hz, OH) 5.63 (1H, d, $J = 8.0$ Hz, CH=CH) 5.86 (1H, s, SCHN) 8.34 (1H, d, $J = 8.1$ Hz, CH-CH) 11.23 (1H, s, NH) ¹³C NMR (100 MHz DMSO) δ : 55.80 (SCHN) 24.0 (SCH₂) 55.8 (C(CH₂OH)₂) 60.1 (CH₂OH) 63.5 (CH₂OH) 99.9 (CH=CH) 142.8 (CH=CH) 151.2 (=CHC=O) 163.6 (NC=O) IR ($\nu_{\max} = \text{cm}^{-1}$) 3428, 3356, 3051, 2952, 2925, 2534, 2494, 2303, 1705, 1667, 1650, 1457, 1418, 1240, HRSM EI calc: [C₉H₁₂N₂O₄SH⁺] 245.0591 obs: [C₉H₁₂N₂O₄SH⁺] 245.0591

Synthesis of 3,3- bis(hydroxymethyl)-thietan-2-yl-cytosine 81



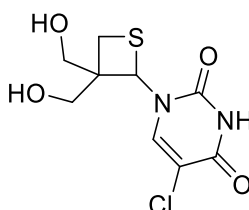
This procedure was modified from Nishizono *et al.*¹ Synthesis of the title compound followed general procedure C to give the title compound as a white powder after purification by column chromatography. Yield: 36%, 47 mg. HPLC purity: 75.1% MP: 244-251° C ¹H NMR (400 MHz DMSO) δ : 2.77 (2H, d, $J = 4.0$ Hz, SCH₂) 3.17 (1H, d, $J = 11.0$ Hz, CH₂OH) 3.39 (1H, d, $J = 11.0$ Hz, CH₂OH) 3.44 (1H, d, $J = 11.0$ Hz, CH₂OH) 4.60 (1H, d, $J = 5.0$ Hz, OH) 4.91 (1H, d, $J = 5.0$ Hz, OH) 5.76 (1H, d, $J = 7.0$ Hz, CH=CH) 5.81 (1H, s, SCHN) 7.20 (2H, d, $J = 43.0$ Hz, NH₂) 8.16 (1H, d, $J = 7.4$ Hz, CH=CH) ¹³C NMR (100 MHz DMSO) δ : 24.3 (SCH₂) 55.8 (C(CH₂OH)₂) 58.1 (SCHN) 61.8 (CH₂OH) 64.7 (CH₂OH) 93.9 (CH=CH) 143.4 (CH=CH) 156.6 (CNH₂) 165.6 (NC=O) IR ($\nu_{\max} = \text{cm}^{-1}$) 3332, 3175, 3916, 2868, 1665, 1639, 1592, 1519, 1476, 1395, 1297, 1178, 1146, 1116 HRSM EI calc: [C₉H₁₃N₃O₃SH⁺] 244.0750 obs: [C₉H₁₃N₃O₃SH⁺] 244.0752

Synthesis of 3,3- bis(hydroxymethyl)-thietan-2-yl-(5-fluoro)uracil 84



This procedure was modified from Nishizono *et al.*¹ Synthesis of the title compound followed general procedure C to give the title compound as a white powder after purification by column chromatography. Yield: 77%, 64 mg. HPLC purity: 94.5%. ¹H NMR (400 MHz DMSO) δ : 2.80 (1H, d, J = 9.0 Hz, SCH₂) 2.88 (1H, d, J = 9.0 Hz, SCH₂) 3.31 (1H, d, J = 11.0 Hz, CH₂OH) 3.42 (1H, d, J = 11.0 Hz, CH₂OH) 3.53 (1H, d, J = 11.0 Hz, CH₂OH) 3.61 (1H, d, J = 8.0 Hz, CH₂OH) 4.9 (1H, s, OH) 5.1 (1H, s, OH) 5.90 (1H, s, SCHN) 8.57 (1H, d, J = 7.0 Hz, CH=CF) ¹³C NMR (100 MHz DMSO) δ : 24.5 (SCH₂) 56.4 (SCHN) 60.0 (CH₂OH) 63.6 (CH₂OH) 127.7 (CH=CF) 137.8 - 140.1 (d, J = 228 Hz, CH=CF) 149.6 (CFC=O) 157.2 (NC=O) IR (ν_{\max} = cm⁻¹) 3378, 2944, 1702, 1660, 1558, 1434, 1136 HRSM EI calc: [C₁₀H₁₄N₂O₄SH⁺] 263.0496 obs: [C₁₀H₁₄N₂O₄SH⁺] 263.0498

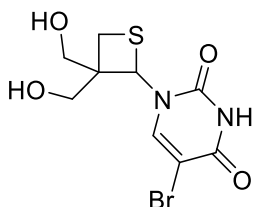
Synthesis of 3,3-bis(hydroxymethyl)-thietan-2-yl-(5-chloro)-uracil 85



This procedure was modified from Nishizono *et al.*¹ Synthesis of the title compound followed general procedure D to give the title compound as a white powder after purification by column chromatography. Yield: 88%, 102 mg. MP: 182-183° C. ¹H NMR (400 MHz DMSO) δ : 2.80 (1H, d, J = 9.0 Hz, SCH₂) 2.88 (1H, d, J = 9.0 Hz, SCH₂) 3.29 (1H, d, J = 10.0 Hz, CH₂OH) 3.40 (1H, d, J = 10.0 Hz, CH₂OH) 3.48 (1H, d, J = 10.0 Hz, CH₂OH) 3.59 (1H, d, J = 10.0 Hz, CH₂OH) 4.8 (1H, s, OH) 5.05 (1H, s, OH) 5.83 (1H, s, SCHN) 8.58 (1H, s, CH=CCl) ¹³C NMR (100 MHz DMSO) δ : 23.8 (SCH₂) 55.5 (C(CH₂OH)₂) 60.1 (CH₂OH) 63.6 (CH₂OH) 105.7 (CH=CCl) 139.9 (CH=CCl) 150.2 (CClC=O) 159.1 (NC=O) IR (ν_{\max} = cm⁻¹) 3432, 3384, 3016, 2935,

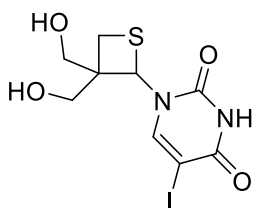
1713, 1673, 1618, 1456, 1424, 1204, 1060 HRSM EI calc: $[\text{C}_9\text{H}_{11}\text{N}_2\text{O}_4\text{S}^{35}\text{ClH}^+]$ 279.0200 obs $[\text{C}_9\text{H}_{11}\text{N}_2\text{O}_4\text{S}^{35}\text{ClH}^+]$ 279.0201 calc $[\text{C}_9\text{H}_{11}\text{N}_2\text{O}_4\text{S}^{37}\text{ClH}^+]$ 281.0170 obs $[\text{C}_9\text{H}_{11}\text{N}_2\text{O}_4\text{S}^{37}\text{ClH}^+]$ 281.0171

Synthesis of 3,3-bis(hydroxymethyl)-thietan-2-yl-(5-bromo)-uracil 86



This procedure was modified from Nishizono *et al.*¹ Synthesis of the title compound followed general procedure D to give the title compound as a white powder after purification by column chromatography. Yield 96%, 285 mg. MP: 191-192° C. ^1H NMR (400 MHz DMSO) δ : 2.79 (1H, d, $J = 9.0$ Hz, SCH_2) 2.87 (1H, d, $J = 9.0$ Hz, SCH_2) 3.30 – 3.60 (4H, m, CH_2OH) 4.80 (1H, m, OH) 5.0 (1H, m, OH) 5.8 (1H, s, SCHN) 8.6 (1H, s, $\text{CH}=\text{CBr}$) ^{13}C NMR (100 MHz CDCl_3) δ : 25.0 (SCH_2) 53.2 ($\text{C}(\text{OCH}_2)_2$) 57.5 (SCHN) 62.8 (OCH_2) 66.2 (OCH_2) 96.7 ($\text{CH}=\text{CBr}$) 149.9 ($\text{CH}=\text{CBr}$) 166.1 ($\text{CH}_2\text{OC}=\text{O}$) IR ($\nu_{\text{max}} = \text{cm}^{-1}$) 3015, 2813, 1708, 1994, 1609, 1495, 1450, 1423, 1357, 1325, 1215, 1154, 1059, 1040, 1027 calc: $[\text{C}_9\text{H}_{11}\text{N}_2\text{O}_4\text{S}^{79}\text{BrH}^+]$ 322.9696 obs $[\text{C}_9\text{H}_{11}\text{N}_2\text{O}_4\text{S}^{79}\text{BrH}^+]$ 322.9698 calc $[\text{C}_9\text{H}_{11}\text{N}_2\text{O}_4\text{S}^{81}\text{BrH}^+]$ 324.9674 obs $[\text{C}_9\text{H}_{11}\text{N}_2\text{O}_4\text{S}^{81}\text{BrH}^+]$ 324.9675

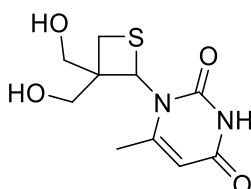
Synthesis of 3,3-bis(hydroxymethyl)-thietan-2-yl-(5-iodo)-uracil 87



This procedure was modified from Nishizono *et al.*¹ Synthesis of the title compound followed general procedure D to give the title compound as a colourless oil after purification by column chromatography. Yield: 90%, 173 mg. ^1H NMR (400 MHz DMSO) δ : 2.79 (1H, d, $J = 9.0$ Hz, SCH_2) 2.89 (1H, d, $J = 9.0$ Hz, SCH_2) 3.3 – 3.6 (4H, m, CH_2OH) 4.79 (1H, t, $J = 5.0$ Hz, OH) 5.03 (1H, t, $J = 5.0$ Hz, OH) 5.81 (1H, s, SCHN) 8.63 ($\text{CH}=\text{CI}$) ^{13}C NMR (100 MHz DMSO) δ : 23.7 (SCH_2) 55.4 ($\text{C}(\text{CH}_2\text{OH})_2$)

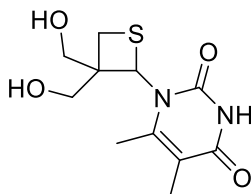
56.6 (SCHN) 60.2 (CH₂OH) 63.6 (CH₂OH) 146.9 (CH=Cl) 150.8 (CH=Cl) 160.5 (=ClC=O) IR (ν_{\max} = cm⁻¹) 3432, 3004, 1707, 1662, 1598, 1417, 1297, 1153, 1059
calc: [C₉H₁₁N₂O₄SiH⁺] 370.9557 obs [C₉H₁₁N₂O₄SiH⁺] 370.9557

Synthesis of 3,3-bis(hydroxymethyl)-thietan-2-yl-(6-methyl)-uracil 885



This procedure was modified from Nishizono *et al.*¹ Synthesis of the title compound followed general procedure D to give the title compound as a white powder after purification by column chromatography. Yield: 98%, 174 mg. MP: 173 - 174° C. ¹H NMR (400 MHz DMSO) δ : 2.01 (3H, s, CH₃) 2.39 (1H, d, J = 9.0 Hz, SCH₂) 3.0 – 3.7 (5H, m, 1H=SCH₂ 4H=CH₂OH) 4.53 (1H, s, OH) 5.1 (1H, s, OH) 5.48 (1H, s, CH₃C=CH) 5.85 (1H, s, SCHN) 11.21 (1H, s, NH) ¹³C NMR (100 MHz DMSO) δ : 17.8 (CH₃) 28.6 (SCH₂) 53.5 (SCHN) 54.3 (C(CH₂OH)₂) 61.3 (CH₂OH) 63.0 (CH₂OH) 101.9 (CH₃C=CH) 154.9 (=CHC=O) 162.9 (NC=O) IR (ν_{\max} = cm⁻¹) 3367, 2944, 1651, 1417, 1363, 1032 HRSM EI calc: [C₁₀H₁₄SO₄N₂Na⁺] 281.0564 obs: [C₁₀H₁₄SO₄N₂Na⁺] 281.0566

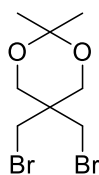
Synthesis of 3,3-bis(hydroxymethyl)-thietan-2-yl-(5,6-dimethyl)-uracil 89



This procedure was modified from Nishizono *et al.*¹ Synthesis of the title compound followed general procedure D to give the title compound as a white powder after purification by column chromatography. Yield: 95%, 129 mg. MP: 176 - 177° C. ¹H NMR (400 MHz DMSO) δ : 1.79 (3H, s, CH₃) 2.20 (3H, s, CH₃) 2.23 (1H, d, J = 9.0 Hz, SCH₂) 3.07 (1H, d, J = 9.0 Hz, SCH₂) 3.40 (1H, d, J = 5.0 Hz, OCH₂) 3.50 (1H, d,

$J = 5.0$ Hz, OCH_2) 3.82 (2H, d, $J = 5.0$ Hz, OCH_2) 4.50 (1H, t, $J = 5.0$ Hz, OH) 5.15 (1H, t, $J = 5.0$ Hz, OH) 5.27 (1H, s, SCHN) 11.26 (1H, s, NH) ^{13}C NMR (100 MHz DMSO) δ : 11.4 (CH_3) 16.8 (CH_3) 29.2 (SCH_2) 55.1 ($\text{C}(\text{CH}_2\text{OH})_2$) 59.7 (SCHN) 61.1 (CH_2OH) 62.7 (CH_2OH) 149.9 ($\text{CCH}_3\text{C}=\text{O}$) 163.3 ($\text{NC}=\text{O}$) IR ($\nu_{\text{max}} = \text{cm}^{-1}$) 3350, 3167, 3038, 2946, 2604, 2498, 1720, 1614, 1472, 1266, 1109, 1050 HRSM EI calc: $[\text{C}_{11}\text{H}_{16}\text{SO}_4\text{N}_2\text{Na}^+]$ 295.0723 obs: $[\text{C}_{11}\text{H}_{16}\text{SO}_4\text{N}_2\text{Na}^+]$ 295.0725

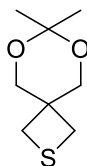
Synthesis of 2,2-bis(bromomethyl)-1,3-O-isopropylidene-1,3-propanediol **93**



This procedure was modified from Nishizono *et al.*¹ To an oven dried round bottom flask under argon 2,2-bis(bromomethyl)-1,3-propanediol **92** (50 g, 0.25 mol) and dissolved in acetone (380 ml). 2,2-Dimethoxypropane (164 ml, 1.76 mol) and *p*-toluene sulfonic acid monohydrate (476 mg, 2.5 mmol) were then added. The reaction was stirred for 2 hours. The reaction was monitored by TLC analysis (6:1 hexane : ethyl acetate) until all of the starting material was consumed. The reaction was quenched with sat. NaHCO_3 (380 ml) and the organic phase separated and concentrated *in vacuo*. The residue was partitioned between ether (380 ml) and water (380 ml) and extracted with ether (3 x 380 ml). The organic phases were combined and dried over MgSO_4 . The solvent was evaporated *in vacuo* and the residue was recrystallized from isopropanol to give the title compound as a white solid. Yield: 91 %, 68.62 g. ^1H NMR (400 MHz CDCl_3) δ : 1.42 (6H, s, $2\times\text{CH}_3$) 3.58 (4H, s, $2\times\text{CH}_2\text{Br}$), 3.80 (4H, s, $2\times\text{OCH}_2$) ^{13}C NMR (100 MHz CDCl_3) δ : 23.5 ($2\times\text{CH}_3$) 35.9 ($2\times\text{CH}_2\text{Br}$) 64.9 ($2\times\text{OCH}_2$) 98.9 (CH_3CCH_3) 38.3 ($\text{OCH}_2\text{OCH}_2\text{CCH}_2\text{BrCH}_2\text{Br}$) IR ($\nu_{\text{max}} = \text{cm}^{-1}$) 2994, 2982, 2868, 1209 MP: 60 – 62 °C Lit: 59 – 60 °C HRMS EI calc: $[\text{C}_8\text{H}_{14}\text{O}_2\text{Br}_2\text{H}^+]$ 300.9438 obs: $[\text{C}_8\text{H}_{14}\text{O}_2\text{Br}_2\text{H}^+]$ 301.1416

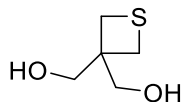
Synthesis of 3',3'-isopropylidene-3,3-bis(hydroxymethyl)-thietane

94



This procedure was modified from Nishizono *et al.*¹ To an oven dried round bottom flask under argon 2,2-bis(bromomethyl)-1,3-O-isopropylidene-1,3-propanediol **93** (5 g, 16.56 mmol) was dissolved in dry DMF (60 ml). Na₂S.9H₂O (5.97 g, 25.48 mmol) was added and the mixture was heated to 110° C for 24 hours whilst stirring. The reaction was cooled to room temperature and then diluted with ether (60 ml) and then partitioned between water (60 ml). The aqueous phase was then extracted with *tert* butyl methyl ether (3 x 60 ml) and the combined organic phases were washed with 1 M LiCl solution (120 ml). The organic phase was dried over MgSO₄, filtered, and then evaporated *in vacuo*. The residue was recrystallized from isopropyl alcohol to give the title compound as a yellow solid. Yield: 94%, 2.71 g. ¹H NMR (400 MHz CDCl₃) δ: 1.40 (6H, s, 2xCH₃) 2.96 (4H, s, 2xCH₂S), 3.87 (4H, s, 2xOCH₂) ¹³C NMR (100 MHz CDCl₃) δ: 23.8 (2xCH₃) 30.6 (2xCH₂S) 68.1 (2xOCH₂) 98.4 (CH₃CCH₃) 41.1 (CCH₂SCH₂S) IR (u_{max} = cm⁻¹) 2997, 2931, 2861, 1182, 1193, 1370, 1378, 1430, 1480 MP: 48 – 52 °C Lit: 51 – 52 °C. HRMS EI calc: [C₈H₁₄O₂SH⁺] 175.0787 obs: [C₈H₁₄O₂SH⁺] 175.0788

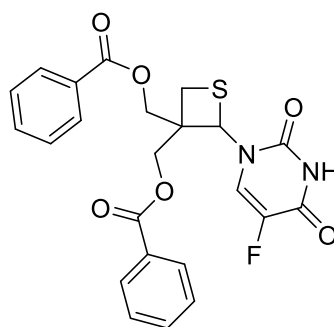
Synthesis of 3,3-bis(hydroxymethyl)-thietane **95**



This procedure was modified from Nishizono *et al.*¹ To an oven dried round bottom flask under argon, 3',3'-isopropylidene-3,3-bis(hydroxymethyl) thietane **94** (5.1 g, 0.03 mol, 1 equiv) was added and dissolved in methanol (263 ml). *p*-Toluene sulfonic acid (1.14 g, 6 mmol, 0.2 equiv) was added and the reaction was monitored by TLC analysis (2:1 toluene : acetone) until all the starting material was consumed. The crude reaction mixture was quenched with solid NaHCO₃ until a neutral pH was observed with pH paper, and then the solvent was evaporated. The residue was

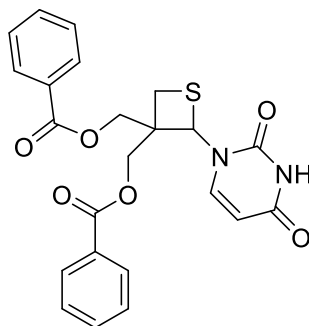
dissolved in DCM (100 ml) and filtered to remove inorganic compounds. The compound was purified by gradient elution on a biotage 100 g column (100% toluene to 2:1 toluene:acetone over 20 CV) to give the title compound as a white solid. Yield: 86%, 3.48 g. MP: 73 – 74 °C ^1H NMR (400 MHz CDCl_3) δ : 2.17 (2H, d, J = 5.0 Hz, OH) 2.96 (4H, s, $2\times\text{CH}_2\text{S}$), 3.89 (4H, d, J = 5.0 Hz, OCH_2) ^{13}C NMR (100 MHz CDCl_3) δ : 28.7 ($2\times\text{CH}_2\text{S}$) 48.0 ($2\times\text{OCH}_2$) 68.2 ($\text{C}(\text{CH}_2\text{OH})_2(\text{CH}_2)_2\text{S}$) IR (ν_{max} = cm^{-1}) 3224, 2963, 2933, 2869, 1489, 1451, 1121, 1023 MP: 72 – 74 °C. HRMS EI calc: $[\text{C}_5\text{H}_{10}\text{O}_2\text{SH}^+]$ 135.0479 obs: $[\text{C}_5\text{H}_{10}\text{O}_2\text{SH}^+]$ 135.0479

Synthesis of 3,3-bis(benzoylmethoxy)-thietan-2-yl-(5-fluoro)-uracil 100



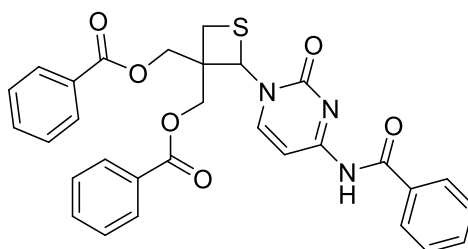
This procedure was modified from Nishizono *et al.*¹ Synthesis of the title compound followed general procedure A to give the title compound as a white powder after purification by column chromatography. Yield: 45%, 60 mg. MP: 219 – 220 °C. ^1H NMR (400 MHz DMSO) δ : 3.17 (1H, d, J = 10.0 Hz, CH_2S) 3.28 (1H, d, J = 10.0 Hz, CH_2S) 4.51 (1H, d, J = 12.0 Hz, OCH_2) 4.64-4.74 (3H, m, OCH_2) 6.20 (1H, s, SCHN) 7.52-7.61 (4H, m, ArH) 7.20-7.74 (2H, m, ArH) 7.92 (2H, d, J = 7.5 Hz, ArH) 8.11 (2H, d, J = 7.6 Hz, ArH) 8.78 (1H, d, J = 7.1 Hz, $\text{CH}=\text{CF}$) 12.00 (1H, s, NH) ^{13}C NMR (100 MHz DMSO) δ : 24.6 (CH_2S) 52.3 ($\text{C}(\text{OCH}_2)_2\text{CH}_2\text{S}$) 56.3 (SCHN) 62.5 (OCH_2) 66.3 (OCH_2) 126.5 ($\text{C}=\text{CF}$) 128.7 (ArC) 129.4 (ArC) 133.6 (ArC) 149.6 ($\text{C}=\text{CF}$) 156.5 ($\text{NC}=\text{O}$) 156.8 ($\text{CFC}=\text{O}$) 165.5 ($\text{CH}_2\text{OC}=\text{O}$) IR (ν_{max} = cm^{-1}) 3069, 2922, 1704, 1651, 1451, 1341, 1269, 1243, 1111, 1025 MP: 219 – 220 °C HRSM EI calc: $[\text{C}_{23}\text{H}_{19}\text{N}_2\text{O}_6\text{SFH}^+]$ 471.1021 obs: $[\text{C}_{23}\text{H}_{19}\text{N}_2\text{O}_6\text{SFH}^+]$ 471.1017

Synthesis of 3,3-bis(benzoylmethoxy)-thietan-2-yl-uracil 101



This procedure was modified from Nishizono *et al.*¹ Synthesis of the title compound followed general procedure B to give the title compound as a white powder after purification by column chromatography. Yield: 64% 404 mg. MP 196 – 198 °C. ¹H NMR (400 MHz DMSO) δ : 3.19 (1H, d, J = 10.0 Hz, CH₂S) 3.25 (1H, d, J = 10.0 Hz, CH₂S) 4.52 (1H, d, J = 12.0 Hz, OCH₂) 4.58 – 4.69 (2H, m, OCH₂) 4.73 (1H, d, J = 12.0 Hz, OCH₂) 5.68 (1H, d, J = 8.0 Hz, CH=CH) 6.26 (1H, s, SCHN) 7.52 – 7.61 (4H, m, ArH) 7.73 (2H, m, ArH) 7.90 (2H, d, J = 7.0 Hz, ArH) 8.10 (2H, d, J = 7.4 Hz, ArH) 8.45 (1H, d, J =8.1 Hz, CH=CH) 11.47 (1H, s, NH) ¹³C NMR(100 MHz DMSO) δ : 24.4 (CH₂S) 52.5 (C19) (C(OCH₂) 55.8 (SCHN) 62.4 (OCH₂) 66.0 (OCH₂) 101.3 (CH=CH) 128.8 (ArC) 129.4 (ArC) 134.2 (ArC) 142.0 (CH=CH) 151.1 (NC=O) 162.7 (HCC=O) 165.5 (CH₂OC=O) IR (ν_{\max} = cm⁻¹) 3050, 2952, 2540, 2303, 1705, 1667, 1650, 1418, 1457, 1240, 1173, 1060 HRSM EI calc: [C₂₃H₂₀N₂O₆SH⁺] 453.1115 obs: [C₂₃H₁₉N₂O₆SH⁺] 453.1118

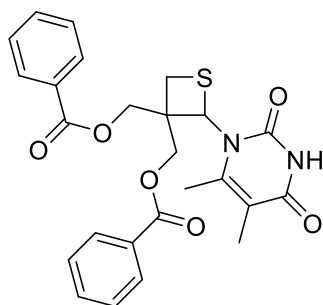
Synthesis of 3,3-bis(benzoylmethoxy)-thietan-2-yl-(*N*⁴-benzoyl)cytosine 102



This procedure was modified from Nishizono *et al.*¹ Synthesis of the title compound followed general procedure A to give the title compound as a white powder after purification by column chromatography 2:1 Ethyl acetate:hexane. Yield 47%, 366 mg.

MP 208 – 211 °C. ^1H NMR (400 MHz CDCl_3) δ : 2.96 (1H, d, $J = 10.0$ Hz, CH_2S) 3.34 (1H, d, $J = 10.0$ Hz, CH_2S) 4.44 (1H, d, $J = 12.0$ Hz, OCH_2) 4.59 (1H, d, $J = 12.0$ Hz, OCH_2) 4.76 (1H, d, $J = 11.5$ Hz, OCH_2) 4.95 (1H, d, $J = 11.5$ Hz, OCH_2) 6.49 (1H, s, SCHN) 7.35-7.63 (12H, m, ArH) 7.75 – 7.85 (3H, m, ArH) 7.94 (1H, d, $J = 7.5$ Hz, CH=CH) 8.12 (1H, d, $J = 7.5$ Hz, CH=CH) 8.12 (1H, d, $J = 7.5$ Hz, NH) ^{13}C NMR (100 MHz CDCl_3) δ : 24.8 ($\text{C}(\text{OCH}_2)_2$) 53.2 (CH_2S) 58.4 (SCHN) 63.1 (OCH_2) 66.7 (OCH_2) 128.6 (ArC) 129.8 (ArC) 133.4 (ArC) 166.1 ($\text{NC}=\text{O}$) 165.9 ($\text{CH}_2\text{OC}=\text{O}$) 166.2 ($\text{NC}=\text{O}$) IR ($\nu_{\text{max}} = \text{cm}^{-1}$) 3326, 1708, 1693, 1617, 1547, 1428, 1293, 1114, HRSM EI calc: $[\text{C}_{30}\text{H}_{25}\text{N}_3\text{O}_6\text{SH}^+]$ 556.1537 obs: $[\text{C}_{30}\text{H}_{25}\text{N}_3\text{O}_6\text{SH}^+]$ 556.1539

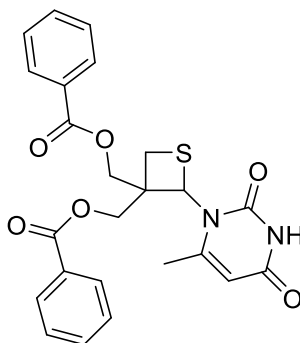
Synthesis of 3,3-bis(benzoylmethoxy)-thietane-2-yl-(5,6-dimethyl)-uracil 103



This procedure was modified from Nishizono *et al.*¹ Synthesis of the title compound followed general procedure A to give the title compound as a white powder after purification by column chromatography. Yield: 53%, 283mg. MP: 208-209° C. ^1H NMR (400 MHz CDCl_3) δ : 1.76 (3H, s, CH_3) 2.04 (3H, s, CH_3) 2.85 (1H, d, $J = 9.0$ Hz, SCH_2) 3.94 (1H, d, $J = 9.0$ Hz, SCH_2) 4.37 (1H, d, $J = 11.5$ Hz, OCH_2) 4.92 (2H, s, OCH_2) 5.01 (1H, d, $J = 11.5$ Hz, OCH_2) 5.44 (1H, s, SCHN) 7.37 – 7.47 (4H, m, ArH) 7.55 – 7.62 (2H, m, ArH) 7.83 (2H, d, $J = 8.0$ Hz, ArH) 8.03 (2H, d, $J = 8.0$ Hz, ArH) 8.22 (1H, s, NH) ^{13}C NMR (100 MHz CDCl_3) δ : 11.4 (CH_3) 17.4 (CH_3) 29.5 (SCH_2) 53.2 ($\text{C}(\text{OCH}_2)_2$) 59.5 (SCHN) 63.8 (OCH_2) 66.7 (OCH_2) 110.0 ($\text{C}=\text{C}$) 128.5 (ArC) 129.4 (ArC) 133.6 (ArC) 162.7 ($\text{CH}_2\text{OC}=\text{O}$) IR ($\nu_{\text{max}} = \text{cm}^{-1}$) 2924, 1711, 1651, 1600, 1474, 1464, 1268, 1266, 1192, 1049 HRSM EI calc: $[\text{C}_{25}\text{H}_{25}\text{SO}_6\text{N}_2]$ 481.1427 obs: $[\text{C}_{25}\text{H}_{25}\text{SO}_6\text{N}_2]$ 481.1428

Synthesis of 3,3-bis(benzoylmethoxy)-thietan-2-yl-(6-methyl)-uracil

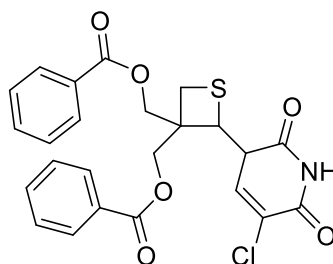
104



This procedure was modified from Nishizono *et al.*¹ Synthesis of the title compound followed general procedure A to give the title compound as a white powder after purification by column chromatography. Yield: 49%, 320mg. MP: 222-223° C. ¹H NMR (400 MHz CDCl₃) δ: 2.07 (1H, d, *J* = 8.0 Hz, SCH₂) 2.10 (3H, s, CH₃) 2.83 (1H, d, *J* = 8.0 Hz, SCH₂) 3.95 (1H, d, *J* = 11.5 Hz, OCH₂) 4.44 (1H, d, *J* = 11.5 Hz, OCH₂) 5.41 (1H, s, SCHN) 5.48 (1H, s, CH₃C=CH) 7.37 – 7.46 (4H, m, ArH) 7.60 (2H, m, ArH) 7.87 (2H, d, *J* = 7.0 Hz, ArH) 8.01 (2H, d, *J* = 7.0 Hz, ArH) 9.0 (1H, s, NH) ¹³C NMR (100 MHz CDCl₃) δ: 21.2 (CH₃) 29.3 (SCH₂) 53.2 (C(OCH₂)₂) 59.1 (SCHN) 63.6 (OCH₂) 66.7 (OCH₂) 104.2 (CH₃C=CH) 128.9 (ArC) 129.7 (ArC) 133.7 (ArC) 150.6 (CH₃C=CHC=O) 153.0 (NC=O) 166.4 (CH₂OC=O) IR (u_{max} = cm⁻¹) 2970, 1711, 1667, 1601, 1450, 1286, 1108, 1070 HRSM EI calc: [C₂₄H₂₂SO₆N₂] 466.1199 obs: [C₂₄H₂₂SO₆N₂] 467.1270

Synthesis of 3,3-bis(benzyolmethoxy)-thietan-2-yl-(5-chloro)-uracil

105

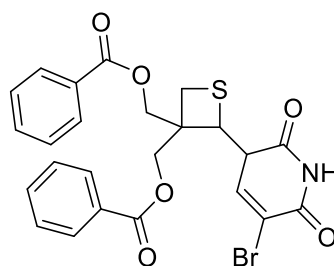


This procedure was modified from Nishizono *et al.*¹ Synthesis of the title compound followed general procedure B to give the title compound as a white powder after

purification by column chromatography. Yield: 48%, 258 mg. MP: 197-199° C. ^1H NMR (400 MHz CDCl_3) δ : 3.05 (1H, d, $J = 10.0$ Hz, SCH_2) 3.26 (1H, d, $J = 10.0$ Hz, SCH_2) 4.41 (1H, d, $J = 11.5$ Hz, OCH_2) 4.57 (1H, d, $J = 11.5$ Hz, OCH_2) 4.61 (1H, d, $J = 11.5$ Hz, OCH_2) 4.81 (1H, d, $J = 11.5$ Hz, OCH_2) 6.21 (1H, s, SCHN) 7.41 – 7.50 (4H, m, ArH) 7.57 - 7.62 (2H, m, ArH) 7.94 – 7.95 (2H, d, $J = 7.0$ Hz, ArH) 8.1 (2H, d, $J = 7.0$ Hz, ArH) 8.46 (1H, s, $\text{CH}=\text{CCl}$) ^{13}C NMR (100 MHz CDCl_3) δ : 25.0 (SCH_2) 53.2 ($\text{C}(\text{OCH}_2)_2$) 57.5 (SCHN) 62.8 (OCH_2) 66.2 (OCH_2) 109.0 ($\text{CH}=\text{CCl}$) 128.6 (ArC) 129.8 (ArC) 133.9 (ArC) 149.6 ($\text{CH}=\text{CCl}$) 165.7 ($\text{CH}_2\text{OC}=\text{O}$) IR ($\nu_{\text{max}} = \text{cm}^{-1}$) 3024, 2844, 1720, 1702, 1615, 1450, 1428, 1286, 1255, 1113, 1059 HRSM EI calc: $[\text{C}_{23}\text{H}_{19}\text{SO}_6\text{N}_2^{35}\text{ClH}^+]$ 487.0652 obs: $[\text{C}_{23}\text{H}_{19}\text{SO}_6\text{N}_2^{35}\text{ClH}^+]$ 487.0725 $[\text{C}_{23}\text{H}_{19}\text{SO}_6\text{N}_2^{37}\text{ClH}^+]$ 489.0693 obs: $[\text{C}_{23}\text{H}_{19}\text{SO}_6\text{N}_2^{37}\text{ClH}^+]$ 489.0696

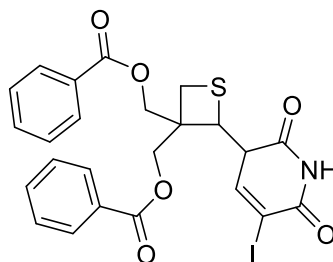
Synthesis of 3,3-bis(benzyoxymethoxy)-thietan-2-yl-(5-bromo)-uracil

106



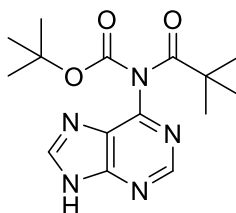
This procedure was modified from Nishizono *et al.*¹ Synthesis of the title compound followed general procedure B to give the title compound as a white powder after purification by column chromatography. Yield: 66%, 491 mg. MP: 216-217° C. ^1H NMR (400 MHz CDCl_3) δ : 3.06 (1H, d, $J = 10.0$ Hz, SCH_2) 3.26 (1H, d, $J = 10.0$ Hz, SCH_2) 4.40 (1H, d, $J = 12.5$ Hz, OCH_2) 4.58 (1H, d, $J = 12.5$ Hz, OCH_2) 4.63 (1H, d, $J = 12.5$ Hz, OCH_2) 4.83 (1H, d, $J = 12.5$ Hz, OCH_2) 6.21 (1H, s, SCHN) 7.42 – 7.49 (4H, m, ArH) 7.56 - 7.62 (2H, m, ArH) 7.96 (2H, d, $J = 7.0$ Hz, ArH) 8.1 (2H, d, $J = 7.0$ Hz, ArH) 8.54 (1H, s, $\text{CH}=\text{CBr}$) ^{13}C NMR (100 MHz CDCl_3) δ : 25.0 (SCH_2) 53.2 ($\text{C}(\text{OCH}_2)_2$) 57.5 (SCHN) 62.8 (OCH_2) 66.2 (OCH_2) 96.7 ($\text{CH}=\text{CBr}$) 128.6 (ArC) 129.8 (ArC) 133.9 (ArC) 149.9 ($\text{CH}=\text{CBr}$) 166.1 ($\text{CH}_2\text{OC}=\text{O}$) IR ($\nu_{\text{max}} = \text{cm}^{-1}$) 3009, 2835, 1704, 1683, 1651, 1450, 1317, 1259, 1087 HRSM EI calc: $[\text{C}_{23}\text{H}_{19}\text{SO}_6\text{N}_2^{79}\text{BrNa}^+]$ 553.0039 obs: $[\text{C}_{23}\text{H}_{19}\text{SO}_6\text{N}_2^{79}\text{BrNa}^+]$ 553.0044 $[\text{C}_{23}\text{H}_{19}\text{SO}_6\text{N}_2^{81}\text{BrNa}^+]$ 555.0019 obs: $[\text{C}_{23}\text{H}_{19}\text{SO}_6\text{N}_2^{81}\text{BrNa}^+]$ 555.0022

Synthesis of 3,3-bis(benzyloxymethoxy)-thietan-2-yl-(5-iodo)-uracil 107



This procedure was modified from Nishizono *et al.*¹ Synthesis of the title compound followed general procedure B to give the title compound as a white powder after purification by column chromatography. Yield: 66%, 491 mg. MP: 199-201° C. ¹H NMR (400 MHz CDCl₃) δ: 3.04 (1H, d, *J* = 10.0 Hz, SCH₂) 3.27 (1H, d, *J* = 10.0 Hz, SCH₂) 4.38 (1H, d, *J* = 12.5 Hz, OCH₂) 4.57 (1H, d, *J* = 12.5 Hz, OCH₂) 4.62 (1H, d, *J* = 12.5 Hz, OCH₂) 4.80 (1H, d, *J* = 12.5 Hz, OCH₂) 6.21 (1H, s, SCHN) 7.44 – 7.50 (4H, m, ArH) 7.60 - 7.61 (2H, m, ArH) 7.96 (2H, d, *J* = 7.0 Hz, ArH) 8.1 (2H, d, *J* = 7.0 Hz, ArH) 8.61 (1H, s, CH=Cl) ¹³C NMR (100 MHz CDCl₃) δ: 25.0 (SCH₂) 53.3 (C(OCH₂)₂) 57.3 (SCHN) 62.8 (OCH₂) 66.2 (OCH₂) 128.6 (ArC) 129.8 (ArC) 133.9 (ArC) 145.7 (CH=Cl) 150.4 (CH=Cl) 159.2 (NC=O) 166.0 (CH₂OC=O) IR (ν_{max} = cm⁻¹) 3001, 2828, 1702, 1644, 1597, 1450, 1317, 1257, 1085 HRSM EI calc: [C₂₃H₁₉SO₆N₂INa⁺] 553.0039 obs: [C₂₃H₁₉SO₆N₂INa⁺] 553.0044

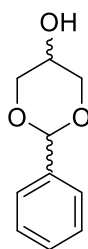
Synthesis of N⁶-Di(*t*-Boc)-Adenine 114



This procedure followed Michel *et al.*² To an oven dried round bottom flask under argon, adenine (2.5 g, 18.5 mmol, 1 equiv) was suspended in dry THF (125 mL). Di-*Tert*-butyl-dicarbonate (8.73 g, 40 mmol, 4 equiv) was then added, followed by DMAP (226 mg, 1.85 mmol, 1 equiv) and the reaction was stirred at room temperature for 24 hours. The solvent was evaporated *in vacuo* and the oily residue was redissolved in EtOAc (250 mL) and the organic phase was washed once with cold 1N HCl (40 mL)

and then brine (3 x 60 mL). The organic phase was then dried using sodium sulfate, and the solvent was filtered and removed *in vacuo*. The crude residue was redissolved in methanol (140 mL) and saturated sodium bicarbonate (60 mL) was added. The reaction was heated to 50 ° C for 1 hour under argon. The crude reaction mixture was cooled to room temperature and the product was extracted with chloroform (3 x 120 mL). The organic phase was dried over sodium sulfate and the solvent was removed *in vacuo*. The crude product was then purified by column chromatography using gradient elution using ethyl acetate:hexane (7:3 – 100% EtOAc) to give the title product as a beige solid. Yield: 85%. ¹H NMR (400 MHz CDCl₃) δ: 1.40 (18H, s, C(CH₃)₃) 8.55 (1H, s, CH) 8.92 (1H, s, CH) ¹³C NMR (100 MHz CDCl₃) δ: 27.8 (C(CH₃)₃) 84.9 (C(CH₃)₃) 145.0 (CH) 151.1 (C=O) 153.3 (CH) IR (u_{max} = cm⁻¹) 3239, 2988, 2360, 1780, 1737, 1584, 1453, 1330, 1254, 1129

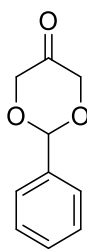
Synthesis of 2-phenyl-1,3-dioxan-5-ol 147



This procedure was modified from Kim *et al.*³ To an oven dried round bottom flask under nitrogen, benzaldehyde dimethyl acetal (9.12 g, 60 mmol, 1 equiv) was dissolved in toluene (30 ml), and *p*-toluene sulfonic acid (1 g, 6 mmol, 0.1 equiv) was added. Glycerol (5.52 g, 60 mmol, 1 equiv) was added slowly and the reaction heated to 40° C *in vacuo* (200 mbar) for 6 hours. The crude reaction mixture was washed with sat. NaHCO₃ (150 ml) and the organic phase separated. The aqueous phase was then washed with chloroform (3 x 50 ml) and the combined organic phases were dried over MgSO₄. The organic phase was then filtered and the solvents evaporated *in vacuo* to give an off white residue. The crude residue was then dissolved in minimal chloroform and recrystallized from petroleum ether 60-40 to give the title compound as white crystals. Yield: 62%, 6.5 g. MP: 69 - 70° C Lit: 70 - 71 ° C. ¹H NMR (400 MHz CDCl₃) δ: 1.75 (1H, d, *J* = 6.0 Hz, OCH₂ cis) 3.05 (1H, d, *J* = 6.0 Hz, OCH₂ cis) 3.5 (1H, d, *J* = 10.0 Hz, CHOH trans) 3.99 (1H, o, *J* = 5.0 Hz, CHOH cis) 4.12 (2H, d, *J* = 11.0 Hz, OCH₂ trans) 4.18 (2H, d, *J* = 11.0 Hz, OCH₂

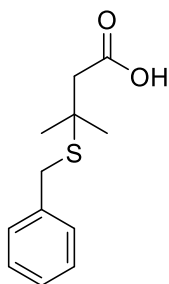
trans) 4.31 (2H, dd, $J = 5.0$ Hz, OCH_2 cis) 5.43 (1H, s, PhCHO_2 trans) 5.59 (1H, s, PhCHO_2 cis) 7.33 – 7.41 (6H, m, ArH) 7.46 – 7.51 (4H, m, ArH) ^{13}C NMR (100 MHz CDCl_3) δ : 61.2 (CHOH cis) 64.0 (CHOH trans) 71.7 (OCH_2 cis) 72.3 (OCH_2 trans) 101.0 (PhCHO_2 trans) 101.6 (PhCHO_2 cis) 126.1 (ArC) 129.2 (ArC) 137.8 (ArC) IR ($\nu_{\text{max}} = \text{cm}^{-1}$) 3348, 2972, 2865, 1452, 1386, 1235, 1220, 1147, 1079, 1029) HRMS EI calc: $[\text{C}_{10}\text{H}_{11}\text{O}_3]$ 180.0786 obs $[\text{C}_{10}\text{H}_{11}\text{O}_3]$ 180.0859

Synthesis of 2-phenyl-1,3-dioxan-5-one 148



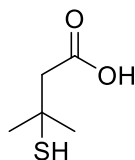
This procedure was modified from Tewes *et al.*⁴ To an oven dried round bottom flask under nitrogen, 2-phenyl-1,3-dioxan-5-ol **147** (2 g, 11 mmol, 1 equiv) was dissolved in DCM (440 ml) and cooled to 0° C. Dess Martin Periodinane (6.93 g, 16 mmol, 1.5 equiv) was then added and the reaction was warmed to room temperature and stirred for three hours. The crude reaction mixture was washed with sat. NaHCO_3 solution (200 ml) and the organic phase was separated. The aqueous phase was then extracted with DCM (3 x 120 ml) and the combined organic phases were then washed with sat. NaCl solution (3 x 120 ml). The combined organic phase were dried over MgSO_4 , filtered and removed *in vacuo*. The crude residue was purified by flash column chromatography using hexane: ethyl acetate (8:2) to afford the title compound as a clear yellow oil. Yield: 80%, 1.57 g. ^1H NMR (400 MHz CDCl_3) δ : 4.47 (2H, d, $J = 17.5$ Hz, OCH_2) 4.48 (2H, d, $J = 17.5$ Hz, OCH_2) 5.87 (1H, s, PhCHO_2) 7.38 – 7.43 (3H, m, ArH) 7.51 – 7.55 (2H, m, ArH) ^{13}C NMR (100 MHz CDCl_3) δ : 51.6 (OCH_3) 66.5 (OCH_2) 70.1 (OCH_2) 100.8 (CH) 114.9 ($\text{C}=\text{CH}$) 126.1 (ArC) 128.4 (ArC) 129.1 (ArC) 137.7 (ArC) 150.0 ($\text{C}=\text{CH}$) 165.8 ($\text{C}=\text{O}$) IR ($\nu_{\text{max}} = \text{cm}^{-1}$) 3067, 3038, 2978, 1740, 1454, 1221 HRMS EI cal: $[\text{C}_{10}\text{H}_{10}\text{O}_3]$ 178.0630 obs: $[\text{C}_{10}\text{H}_{10}\text{O}_3]$ 178.0444

Synthesis of 3-(benzylthio)-3-methyl-butanoic acid **155**



This procedure followed Pattenden *et al.*⁵ To an oven dried round bottom flask under argon, 3-methyl but-2-enoic acid (5 g, 0.05 mol, 1 equiv) was added and dissolved in 10 mL piperidine. Benzyl mercaptan (5.87 mL, 0.05 mol, 1 equiv) was added dropwise. The reaction was heated to reflux overnight and was then cooled to room temperature. Cold concentrated HCl (50 mL) was then added and extracted with diethyl ether (2 x 50 mL). The ether phase was then washed with saturated sodium carbonate (3 x 50 mL) and the extracted aqueous phase was re-acidified with concentrated HCl (3 x 50 mL). The aqueous phase was then re-extracted with fresh diethyl ether (3 x 50 mL). The organic phase was then dried with sodium carbonate and the solvent removed *in vacuo* to give a colourless oil. Yield: 75%. ¹H NMR (400 MHz CDCl₃) δ: 1.51 (6H, s, CH₃) 2.55 (2H, s, CCH₂) 3.83 (2H, s, SCH₂) 7.5 (5H, m, ArH) ¹³C NMR (100 MHz CDCl₃) δ: 28.6 (CH₃) 33.3 ((C(CH₃)₂) 43.6 (SCH₂) 46.9 (CCH₂) 126.9 (ArC) 128.5 (ArC) 129.1 (ArC) 137.5 (ArC) 177.8 (CO₂H). Data matched literature values.

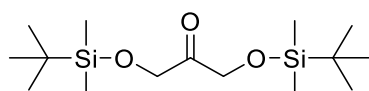
Synthesis of 3-thio-3-methyl-butanoic acid **156**



This procedure followed Pattenden *et al.*⁵ To an oven dried round bottom flask under argon, 3-(benzylthio)-3-methylbutanoic acid **155** (2.5 g, 11 mmol, 1 equiv) was dissolved in dry THF (9 mL). The reaction was cooled to -78 °C and 9mL of freshly distilled liquid ammonia was allowed to condense in the reaction vessel. Sodium metal (282 mg, 12 mmol, 1.1 equiv) was added portionwise until a steady royal blue colour was obtained. The reaction was stirred for 4 hours and was then allowed to

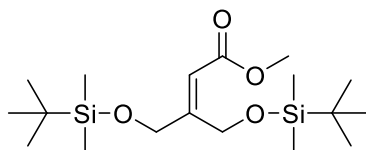
reach room temperature and a stream of nitrogen was used to remove any remaining ammonia. The reaction was quenched with IPA (50 mL) and dilute 1N HCl was added (50 mL) and the crude reaction mixture was extracted with diethyl ether (50 mL). The organic phase was then extracted with saturated sodium carbonate solution (50 mL), and the aqueous phase was re-acidified with concentrated 1N HCl (50 mL). The aqueous phase was extracted with chloroform (3 x 50 mL) to give the title compound as a colourless oil. Yield: quant. ^1H NMR (400 MHz CDCl_3) δ : 1.83 (6H, s, CH_3) 2.86 (1H, s, SH) 3.80 (2H, s, CH_2) ^{13}C NMR (100 MHz CDCl_3) δ : 21.6 (CH_3) 22.3 ($(\text{C}(\text{CH}_3)_2)$) 49.1 (SCH_2) 65.3 (CH_2) 201.6 (CO_2H). Data matched literature values.

Synthesis of 1,3-di-*O*-(*t*-butyldimethylsilyloxy)-propanone **166**



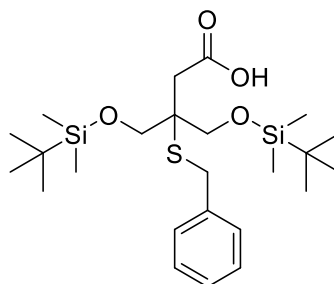
This procedure was modified from Beaulieu *et al.*⁶ To an oven dried round bottom flask under nitrogen, 1,3-dihydroxy acetone dimer **165** (5.66 g, 0.031 mol, 1 equiv) was added to dry DCM (56 ml) followed by imidazole (18.8 g, 0.125 mol, 3 equiv) and *t*-butyl dimethyl silyl chloride (6.39 g, 0.094 mol, 4 equiv) and the reaction was stirred at room temperature overnight. The crude mixture was washed with water (100 ml) and extracted with chloroform (3 x 30 ml). The combined organic layers were dried over MgSO_4 , the solvents filtered and removed *in vacuo*. The crude oil was purified by column chromatography using gradient elution (100% petroleum ether to 8:2 petroleum ether: ethyl acetate) on a pre-packed 100g biotage column to give a golden oil, yield: 9.07 g, 92%. ^1H NMR (400 MHz CDCl_3) δ : 0.1 (12H, s, SiCH_3), 0.8 (18H, s, $\text{C}(\text{CH}_3)_3$), 4.3 (4H, s, OCH_2) ^{13}C NMR (100 MHz CDCl_3) δ : 0.00 (SiCH_3) 26.9 ($\text{C}(\text{CH}_3)_3$) 68.1 (OCH_2) 78.8 ($\text{C}(\text{CH}_3)_3$) 210.1 ($\text{C}=\text{O}$) IR (ν_{max} cm^{-1}) 3011, 2936, 2856, 1738, 1365, 1217 HRSM EI calc: $[\text{C}_{35}\text{H}_{42}\text{Si}_2\text{O}_3\text{Na}^+]$ 341.1944 obs: $[\text{C}_{35}\text{H}_{42}\text{Si}_2\text{O}_3\text{Na}^+]$ 341.2000

Synthesis of methyl-4-(*tert*-butyldimethyl silyloxy)-3-(*tert*-butyldimethylsilyl methoxy)-but-2-enoate **167**



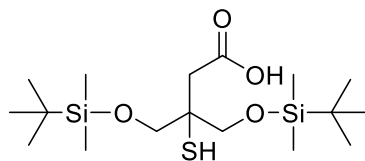
This procedure was modified from Takahashi *et al.*⁷ To an oven dried round bottom flask under argon NaH (377 mg, 9.43 mmol, 1.5 equiv) was added followed by dropwise addition of dry THF (50 ml). Methyl diethylphosphonoacetate (1.14 ml, 6.29 mmol) was added slowly and the mixture was stirred for one hour at room temperature. After effervescence had ceased 1,3-di-O-(*t*-butyldimethylsilyloxy)-propanone **166** (2 g, 6.29 mmol, 1 equiv) was added to the reaction mixture. The reaction was stirred overnight and completion was determined by TLC analysis (petroleum ether: ethyl acetate 9:1). The reaction was cooled to 0° C by dropwise addition of ice cold water (100 ml) and the aqueous phase extracted with DCM (3 x 200 ml). The combined organic phases were dried over MgSO₄, the solvents filtered and evaporated *in vacuo*. The crude oil was purified by gradient elution (100% petroleum ether to 95:5 petroleum ether: ethyl acetate) on a biotage system with a 100 g pre packed column. The title compound was obtained as a clear, golden oil; yield: 1.01 g, 70%. ¹H NMR (400 MHz CDCl₃) δ: 0.00 (6H, s, SiCH₃) 0.02 (6H, s, SiCH₃), 0.83 (9H, s, C(CH₃)₃), 0.86 (9H, s, C(CH₃)₃), 3.6 (3H, s, OCH₃), 4.40 (2H, d, *J* = 1.1 Hz, CH₂), 4.8 (2H, d, *J* = 1.1 Hz, CH₂), 5.9 (1H, t, *J* = 2.0 Hz, C=CH) ¹³C NMR (100 MHz CDCl₃) δ: 0.00 (SiCH₃), 20.4 (C(CH₃)₃) 25.6 (C(CH₃)₃), 51.4 (OCH₃), 77.0 (CH₂), 78.2 (CH₂), 111.0 (C=CH), 161.6 (C=CH), 166.8 (C=O), IR (ν_{max} cm⁻¹) 2954, 2886, 1718, 1655, 1453 HRSM EI calc: [C₁₈H₃₈Si₂O₄H⁺] 375.2384 obs: [C₁₈H₃₈Si₂O₄H⁺] 375.2381

Synthesis of methyl-[3-(benzylthio)-4-(*t*-butyldimethylsilyloxy)-3-(*t*-butyldimethyl silylmethoxy)]-butanoic acid **178**



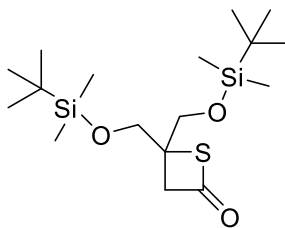
This procedure was modified from Nicolaou *et al.*⁸ To an oven dried round bottom flask under argon, methyl-[3-(benzylthio)-4-(*t*-butyldimethylsilyloxy)-3-(*t*-butyldimethyl silylmethoxy)]-butanoate **182** (1 g, 2 mmol, 1 equiv) was dissolved in dry 1,2-dichloroethane (20 ml) and trimethyltin hydroxide (2.16 g, 12 mmol, 6 equiv) was added and the reaction heated to 80° C for 96 hours. The solvent was removed *in vacuo* and the residue dissolved in ethyl acetate (50 ml). The organic phase was washed with 0.01N KHSO₄ (3 x 20 ml) and then the organic phase was washed with brine. The organic phase was then dried over Na₂SO₄, the solvent filtered and then removed *in vacuo*. The product was further dried under high vacuum to give the title compound as a clear oil. Yield 87%, 854 mg. ¹H NMR (400 MHz CDCl₃) δ: 0.00 (12H, s, SiCH₃) 0.83 (18H, s, C(CH₃)₃) 2.73 (2H, s, CH₂) 3.65 (2H, d, *J* = 10.0 Hz, OCH₂) 3.76 (2H, d, *J* = 10.0 Hz, OCH₂) 3.86 (2H, s, SCH₂) 7.15 - 7.27 (5H, m, ArH) ¹³C NMR (100 MHz CDCl₃) δ: 0.00 (SiCH₃) 18.3 (C(CH₃)₃) 25.8 (C(CH₃)₃) 32.8 (SCH₂) 39.4 (CH₂) 57.7 (CCH₂) 66.2 (OCH₂) 127.1 (ArC) 128.6 (ArC) 129.1 (ArC) 137.8 (ArC) 174.2 (CO₂H) IR (ν_{max} cm⁻¹) 2953, 2929, 2855, 1707, 1495, 1472, 1462, 1388, 1360, 1337, 1282, 1250, 1208, 1137, 1096, 1065, 1028, 1007 HRSM EI calc: [C₂₄H₄₄Si₂SO₄Na⁺] 507.2397 obs: [C₂₅H₄₆Si₂O₄Na⁺]

Synthesis of methyl-[3-(thio)-4-(*t*-butyldimethylsilyloxy)-3-(*t*-butyldimethyl silylmethoxy)]-butanoic acid **179**



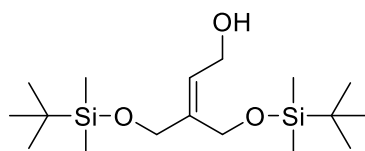
This procedure was modified from Pattenden *et al.*⁵ To an oven dried round bottom flask under nitrogen, methyl-[3-(benzylthio)-4-(*t*-butyldimethylsilyloxy)-3-(*t*-butyldimethyl silylmethoxy)]-butanoic acid **178** (1.1 g, 2.29 mmol, 1 equiv) was dissolved in dry THF (1.8 ml). The mixture was cooled to -78° C and 1.8 ml of freshly distilled liquid ammonia was allowed to condense in the reaction vessel. Sodium metal (58 mg, 2.52 mmol, 1.1 equiv) was added portionwise and the reaction was stirred for 4 hours. The reaction was allowed to warm to room temperature and a stream of nitrogen was used to remove any remaining ammonia. The reaction was then quenched with IPA (5 ml) and acidified to pH 4 with 0.01N HCl. The crude reaction mixture was then extracted with chloroform (3 x 10 ml) and the combined organic phases were dried with MgSO₄. The organic phase was then filtered and removed *in vacuo* to yield the title compound as a colourless oil. Yield: 77%, 700 mg. ¹H NMR (400 MHz CDCl₃) δ: 0.00 (12H, s, SiCH₃) 0.84 (18H, s, C(CH₃)₃) 2.25 (1H, s, SH), 2.61 (2H, s, CH₂CO₂H) 3.58 (2H, d, *J* = 10.0 Hz, OCH₂) 3.66 (2H, d, *J* = 10.0 Hz, OCH₂) ¹³C NMR (100 MHz CDCl₃) δ: 0.00 (SiCH₃) 18.6 (C(CH₃)₃) 25.7 (C(CH₃)₃) 39.3 (CH₂CO₂H) 50.5 (CCH₂) 66.3 (OCH₂) 176.0 (CO₂H) IR (ν_{max} cm⁻¹) 3345, 2930, 2857, 1732, 1687, 1645, 1530, 1516, 1463, 1450, 1387, 1352, 1286, 1211, 1168, 1102, 1059, 1007 HRSM EI calc: [C₁₇H₃₈Si₂SO₄H⁺] 395.2102 obs: [C₁₇H₃₈Si₂SO₄H⁺] 395.3103

Synthesis of 4,4-bis(*t*-butyldimethylsilylmethoxy)-thietan-2-one 180



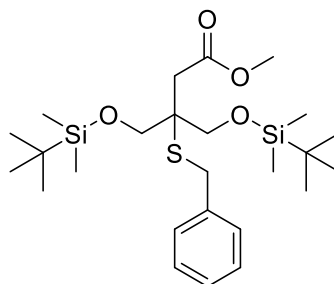
This procedure was modified from Pattenden *et al.*⁵ To an oven dried round bottom flask under nitrogen, methyl-[3-(thio)-4-(*t*-butyldimethylsilyloxy)-3-(*t*-butyldimethylsilylmethoxy)]-butanoic acid **179** (150 mg, 0.38 mmol, 1 equiv) was dissolved in dry DCM (0.61 ml) and triethylamine (0.11 ml, 0.76 mmol, 2 equiv) was added and the reaction was cooled to -10° C. Isobutylchloroformate (57 mg, 0.42 mmol, 1.1 equiv) was added dropwise and the reaction was stirred for 1 hour. The reaction was allowed to warm to room temperature and was quenched with water (5 ml) and the aqueous phase was extracted with DCM (5 x 10 ml). The combined organic phases were dried with MgSO₄, filtered and the solvent removed *in vacuo*. The crude material was purified by gradient flash column chromatography using hexane: ethyl acetate (1:0, 19:1) to give the title compound as a colourless oil. Yield: 37%, 52 mg. ¹H NMR (400 MHz CDCl₃) δ: 0.00 (12H, s, SiCH₃) 0.81 (18H, s, C(CH₃)₃) 3.40 (2H, s, CH₂C=O) 3.82 (2H, d, *J* = 10.0 Hz, OCH₂) 3.85 82 (2H, d, *J* = 10.0 Hz, OCH₂) ¹³C NMR (100 MHz CDCl₃) δ: 0.00 (SiCH₃) 18.3 (C(CH₃)₃) 25.8 (C(CH₃)₃) 47.7 (C(CH₂)₂) 57.8 (CH₂C=O) 66.0 (OCH₂) 190.4 (C=O) IR (ν_{max} cm⁻¹) 2954, 2928, 2857, 1767, 1471, 1463, 1253, 1088, 1005 HRSM EI calc: [C₁₇H₃₆Si₂SO₃Na⁺] 399.1816 obs: [C₁₇H₃₆Si₂SO₃Na⁺] 399.1817

Synthesis of 4-(*tert*-butyldimethyl silyloxy)-3-(*tert*-butyldimethylsilylmethoxy)-but-2-ene-1-ol **181**



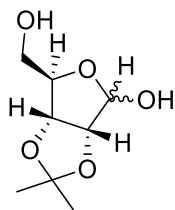
This procedure was modified from Patwardhan *et al.*⁹ To an oven dried round bottom flask under argon, methyl-4-(*t*-butyldimethyl silyloxy)-3-(*t*-butyldimethylsilyl methoxy)-but-2-enoate **167** (1 g, 2.67 mmol, 1 equiv) was dissolved in THF (5 ml) and cooled to -78° C. Diisobutyl aluminium hydride (1.5 M in toluene, 5.3 ml, 8.02 mmol, 3 equiv) was added dropwise and the reaction was stirred for three hours. The reaction was then warmed to room temperature and quenched with water (20 ml), 2M NaOH (10 ml) and water (10 ml). Rochelle's salt was added until no precipitate remained. The aqueous phase was extracted with chloroform (3 x 30 ml) and the combined organic phases were dried over MgSO₄. The solvent was filtered and then removed *in vacuo*. The crude residue was purified by gradient elution column chromatography (100% hexane, 8:2 hexane : ethyl acetate) to give the title compound as a colourless oil. Yield: 740 mg, 80%. ¹H NMR (400 MHz CDCl₃) δ: 0.00 (12H, s, SiCH₃) 0.8 (18H, s, SiC(CH₃)₃) 2.1 (1H, s, OH) 4.1 (2H, m, CH₂OH) 4.13 (4H, m, SiOCH₂) 5.72 (1H, m, C=CH) ¹³C NMR (100 MHz CDCl₃) δ: 0.00 (SiCH₃) 18.2 (Si(C(CH₃)₃) 25.8 (Si(C(CH₃)₃) 59.1 (SiOCH₂) 59.3 (SiOCH₂) 64.4 (CH₂OH) 125.5 (C=CH) 141.0 (C=CH) IR (ν_{max} cm⁻¹) 3354, 2954, 2885, 1252, 1067 HRMS EI calc: [C₁₂H₁₄O₃H⁺] 347.2432 obs: [C₁₂H₁₄O₃H⁺] 347.2433

Synthesis of methyl-[3-(benzylthio)-4-(*t*-butyldimethylsilyloxy)-3-(*t*-butyldimethyl silylmethoxy)]-butanoate **182**



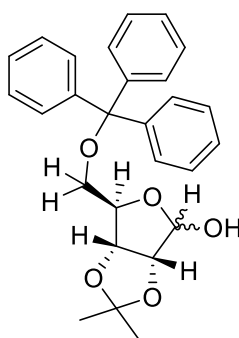
This procedure was modified from Pattenden *et al.*⁵ To an oven dried round bottom flask under argon, methyl-4-(*t*-butyldimethyl silyloxy)-3-(*t*-butyldimethylsilyl methoxy)-but-2-enoate **167** (2 g, 5.34 mmol, 1 equiv) was added followed by piperidine (1.07 ml) and toluene thiol (0.63 ml, 1 equiv). The reaction was heated to reflux for 96 hours. The reaction was allowed to cool to room temperature and was quenched with water (10 ml) and partitioned with chloroform (10 ml). The aqueous phase was extracted with chloroform (3 x 10 ml) and the combined organic phase was dried with MgSO₄, the solvent filtered and removed *in vacuo*. The residue was purified by flash column chromatography hexane: ethyl acetate 8:2 to give the title compound as a golden brown oil. Yield: 88%, 2.34 g. ¹H NMR (400 MHz CDCl₃) δ: 0.01 (3H, s, SiCH₃) 0.85 (3H, s, C(CH₃)₃) 2.60 (2H, s, CH₂) 3.62 (3H, s, OCH₃) 3.70 (2H, d, *J* = 10.0 Hz, OCH₂) 3.78 (2H, d, *J* = 10.0 Hz, OCH₂) 3.89 (2H, s, SCH₂) 7.11 – 7.27 (5H, m, ArH) ¹³C NMR (100 MHz CDCl₃) δ: 0.00 (SiCH₃) 22.7 (C(CH₃)₃) 25.9 (C(CH₃)₃) 32.8 (CH₂) 37.7 (SCH₂) 42.3 (CCH₂) 51.4 (OCH₃) 53.3 (CCH₂) 65.3 (OCH₂) 127.4 (ArC) 128.7 (ArC) 138.3 (ArC) 171.2 (C=O) IR (ν_{max} cm⁻¹) 2952.1, 2928.3, 2855.9, 1738.4, 1470.8, 1251.2, 1198.2, 1096.2 HRSM EI calc: [C₂₅H₄₆Si₂O₄Na⁺] 521.2542 obs: [C₂₅H₄₆Si₂SO₄Na⁺] 521.2548

Synthesis of 2,3-isopropylidene-D-ribose **200**



This procedure was modified from Jin *et al.*¹⁰ To an oven dried round bottom flask under argon D-ribose (150 g, 1 mole, 1 equiv) was suspended in acetone (1.25 L) and concentrated sulfuric acid (4.5 ml, 30 μ L/g) was added dropwise over 2 hours and was stirred under argon for 4 hours. The reaction was quenched with solid sodium bicarbonate (168 g) until neutral. The reaction mixture was filtered and the solvent removed *in vacuo* to give the title compound as a colourless oil. Yield: 100%, 202 g. α_D^{20} (C= 0.1, chloroform): -19.82° $\alpha:\beta$ ratio 1:1 ^1H NMR (400 MHz DMSO) δ : 1.32 (3H, s, CH_3) 1.49 (3H, s, CH_3) 3.45 (1H, s, OH) 3.77 (2H, m, CH_2OH) 4.49 (1H, d, $J = 5.0$ Hz, CH_βOH) 4.59 (1H, d, $J = 6.0$ Hz, CH) 4.85 (1H, d, $J = 6.0$ Hz, CH) 5.44 (1H, d, $J = 5.0$ Hz, $\text{CH}_\alpha\text{OH}$) ^{13}C NMR (100 MHz DMSO) δ : 24.7 (CH_3) 26.4 (CH_3) 63.7 (CH_2OH) 81.4 (CH) 86.9 (CH) 87.8 (CH_βOH) 103.1 ($\text{CH}_\alpha\text{OH}$) 112.0 ($\text{C}(\text{CH}_3)_2$) IR ($\nu_{\text{max}} = \text{cm}^{-1}$) 3400, 2942, 1373, 1209, 1158, 1033 HRSM EI calc: $[\text{C}_8\text{H}_{14}\text{O}_5\text{Na}^+]$ 213.0740 obs: $[\text{C}_8\text{H}_{14}\text{O}_5\text{Na}^+]$ 213.0744

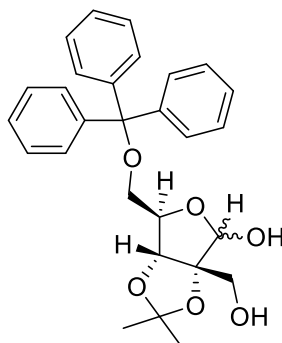
Synthesis of 2,3-isopropylidene-5-O-trityl-D-ribose **201**



This procedure was modified from Beigelman *et al.*¹¹ To an oven dried round bottom under argon flask 2,3-isopropylidene-D-ribose **200** (5g, 0.026 mol, 1 equiv) was dissolved in pyridine (104 ml). DMAP (32 mg, 0.26 mmol) 0.01 equiv) was added followed by trityl chloride (10.9 g, 0.039 mol, 1.5 equiv) and the mixture was stirred overnight at room temperature. The pyridine was removed *in vacuo* and the crude

residue was dissolved in ethyl acetate (150 ml) and partitioned with saturated brine (50 ml) and then extracted ethyl acetate (3 x 150 ml). The organic extracts were combined and dried over MgSO_4 , and the solvent was filtered and removed *in vacuo*. The residue was purified by gradient flash column chromatography hexane : ethyl acetate (9:1 to 8:2) to give the title compound as a white solid. Yield: 82% 6.9 g. α_D^{20} ($C = 0.17$, chloroform): -14.68° MP: $50\text{--}52^\circ\text{C}$ $\alpha:\beta$ 1:5 ^1H NMR (400 MHz DMSO) δ : 1.34 (3H, s, CH_3) 1.48 (3H, s, CH_3) 3.40 (1H, d, $J = 3.5$ Hz, CH_2) 3.42 (1H, d, $J = 3.0$ Hz, CH_2) 3.89 (1H, d, $J = 9.0$ Hz, CH_β) 4.35 (1H, t, $J = 3.0$ Hz, CH) 4.67 (1H, d, $J = 9.0$ Hz, CH_β) 5.32 (1H, d, $J = 9.0$ Hz, CH_βOH) 5.75 (1H, dd, $J = 3.0$ Hz, 9.0 Hz, $\text{CH}_\alpha\text{OH}$) 7.22 - 7.26 (6H, m, ArH) 7.26 - 7.33 (6H, m, ArH) 7.38 - 7.41 (3H, m, ArH) ^{13}C NMR (100 MHz DMSO) δ : 25.1 (CH_3) 26.2 (CH_3) 65.1(CH_2) 79.5 ($\text{C}(\text{Ph})_3$) 81.9 (CH) 87.1 (CH) 98.0 ($\text{CH}_\alpha\text{OH}$) 103.6 (CH_βOH) 113.1 (CH) 125.0 (ArC) 127.2 (ArC) 127.5 (ArC) 128.0 (ArC) 128.1 (ArC) 128.6 (ArC) 128.7 (ArC) IR ($\nu_{\text{max}} = \text{cm}^{-1}$) 3426, 2938, 1596, 1490, 1448, 1373, 1319, 1210, 1158, 1067, 1001 HRSM EI calc:[$\text{C}_{27}\text{H}_{28}\text{O}_5\text{Na}^+$] 455.1826 obs:[$\text{C}_{27}\text{H}_{28}\text{O}_5\text{Na}^+$] 455.1829

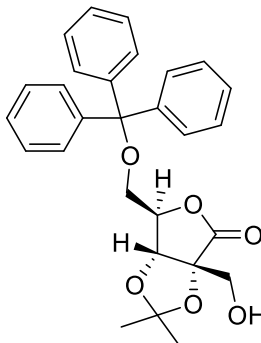
Synthesis of 2,3-isopropylidene-5-O-trityl-D-hamamelose 202



This procedure was modified from Beigelman *et al.*¹¹ To an oven dried round bottom flask under argon, 2,3-isopropylidene-5-O-trityl-D-ribose **201** (4.54 g, 1 equiv, 0.01 mol) was dissolved in methanol (42 ml) and potassium carbonate (1.66 g, 1.1 equiv, 0.012 mol) was added. 39% formaldehyde in water (25 ml) was added dropwise over an hour and the mixture was heated at 65°C for 24 hours. The reaction was cooled to room temperature and quenched with chloroform (150 ml) and partitioned with water (150 ml), then the aqueous phase was extracted with chloroform (3 x 150 ml). The organic phase was dried over Na_2SO_4 , the solvent was filtered and then removed *in vacuo*. The residue was used crude in the next step. Crude yield: 82%,

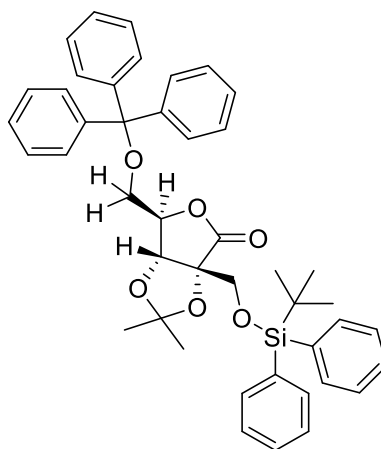
4.5 g. ($\nu_{\max} = \text{cm}^{-1}$) 3308, 2937, 1597, 1490, 1448, 1371, 1216, 1153, 1065 HRSM EI
calc: $[\text{C}_{28}\text{H}_{30}\text{O}_6\text{Na}^+]$ 485.1931 obs: $[\text{C}_{28}\text{H}_{30}\text{O}_6\text{Na}^+]$ 485.1935

Synthesis of 2,3-isopropylidene-5-O-trityl-D-hamamelolactone **203**



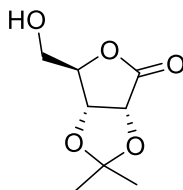
This procedure was modified from Stewart *et al.*¹² To an oven dried round bottom flask under argon, 2,3-isopropylidene-5-O-trityl-D-hamamelose **202** (1 g, 2.16 mmol, 1 equiv) was dissolved in dry DCM (3 ml). K_2CO_3 (447 mg, 1.5 equiv, 3.24 mmol) was added and the reaction was cooled to 0° C and bromine (1.21 ml, 1.1 equiv) was added dropwise over 1 hour. The reaction was allowed to warm to room temperature and was reacted for a further 24 hours. The crude reaction mixture was quenched with saturated sodium thiosulfate solution (10 ml) and the aqueous phase was extracted with DCM (5 x 10 ml). The combined organic phases were dried over Na_2SO_4 , the solvent filtered and removed *in vacuo*. The residue was crude in the next step. Crude yield: 11%, 111 mg. HRSM EI calc: $[\text{C}_{28}\text{H}_{29}\text{O}_6\text{Na}^+]$ 483.1784 obs: $[\text{C}_{28}\text{H}_{29}\text{O}_6\text{Na}^+]$ 483.1791

Synthesis of 2-(*tert*-butyldiphenyl silylmethoxy)-2,3-isopropylidene-5-*O*-trityl-D-hamamelolactone **204**



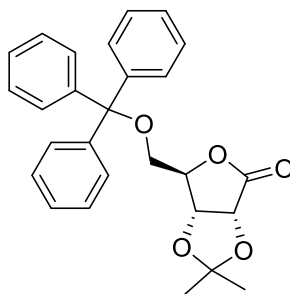
This procedure was modified from Beaulieu *et al.*⁶ To a dry round bottom flask 2,3-isopropylidene-5-*O*-trityl-D-hamamelose **203** (187 mg, 0.14 mmol, 1 equiv) was dissolved in dry DCM (0.82 ml) and imidazole (42 mg, 0.61 mmol, 1.5 equiv) was added followed by *t*-butyldiphenylsilyl chloride (113 mg, 0.41 mmol, 1 equiv). The reaction was stirred overnight at room temperature under argon and then quenched with water (5 ml). The aqueous phase was extracted with 5x5 ml chloroform, the combined organic phases were dried with MgSO₄, the solvent filtered and then removed *in vacuo*. The residue was purified by gradient flash column chromatography hexane: ethyl acetate (19:1, 9:1, 17:2, 8:2) to give the title compound as a colourless oil. Yield: 44%, 127 mg. ¹H NMR (400 MHz DMSO) δ: 0.9 (9H, s, C(CH₃)₃) 1.35 (3H, s, CH₃) 1.41 (3H, s, CH₃) 3.40 (2H, s, *J* = 6.0 Hz, CH₂OSi) 3.88 (1H, d, *J* = 11.0 Hz, CH₂OTr) 3.91 (1H, d, *J* = 11.0 Hz, CH₂OTr) 4.47 (1H, t, *J* = 1 Hz, CH) 4.66 (1H, d, *J* = 1 Hz, CH) 7.2 – 7.7 (25H, m, ArH) ¹³C NMR (100 MHz DMSO) δ: 19.2 (C(CH₃)₃) 26.9 (C(CH₃)₃) 27.0 (CH₃) 63.2 (CH₂OSi) 63.7 (CH₂OTr) 80.0 (CH) 83.1 (CH) 127.8 (ArC) 128.1 (ArC) 135.2 (ArC) IR (ν_{max} = cm⁻¹) HRSM EI calc:[C₄₄H₄₆O₆Na⁺] 721.2961 obs:[C₄₄H₄₆O₆Na⁺] 723.3115

Synthesis of 2,3-isopropylidene-ribo lactone 215



This procedure was modified from Stewart *et al.*¹² To a round bottom flask D-ribose (5 g, 26.2 mmol, 1 equiv) was dissolved in water (21 mL). Potassium carbonate (5.44 g, 1.5 equiv, 39.4 mmol) and the reaction was cooled to 0 ° C. Bromine (4.64 g, 1.1 equiv, 29.0 mmol) was added dropwise and the reaction was stirred for 1 hour. The reaction was allowed to warm to room temperature and left to react further overnight. The reaction was quenched with saturated sodium thiosulfate (21 mL), and then the aqueous phase was extracted with DCM (4 x 40 mL). The organic phase was washed with brine before being dried over the solvent was removed *in vacuo*. The residue was boiled in EtOAc (50 mL) for 10 minutes and then cooled to 0 ° C. The product was crystallised using petroleum ether 40-60 and the resulting white crystals were dried under high vacuum. Yield: quant. ¹H NMR (400 MHz CDCl₃) δ: 1.39 (3H, s, CH₃) 1.48 (3H, s, CH₃) 2.80 (1H, s, OH), 3.80 (1H, d, *J* = 11.0 Hz, CH) 3.99 (1H, d, *J* = 11 Hz, CH) 4.64 (1H, m, CH), 4.79 (1H, d, *J* = 5.0 Hz, CH₂OH) 4.84 (1H, d, *J* = 5.0 Hz, CH₂OH) ¹³C NMR (100 MHz CDCl₃) δ: 25.1 (CH₃) 26.8 (CH₃) 61.8 (2xCH) 76.7 (CH) 82.9 (CH₂OH) 113.1 (C(CH₃)₂) 175.2 (C=O). Data matches literature.

Synthesis of 2,3-isopropylidene-5-O-trityl-ribo lactone 216



This procedure was modified from Stewart *et al.*¹² To an oven dried round bottom flask, 2,3-isopropylidene-5-O-trityl-D-ribose (1 g, 2.4 mmol, 1 equiv) was dissolved in dry DCM (3 mL). Potassium carbonate (470 mg, 3.4 mmol, 1.5 equiv) was added and

the reaction was cooled to 0 °C. Bromine (0.14 mL, 2.6 mmol, 1.1 equiv) was added dropwise. The reaction was stirred overnight under argon. The reaction was warmed to room temperature slowly and quenched with saturated sodium thiosulfate (15 mL) and extracted with DCM (3 x 15 mL). The organic was dried over sodium sulfate and the solvents were removed *in vacuo*. The residue was purified by gradient flash column chromatography hexane: ethyl acetate (9:1, 8:2) to give the title compound as a gel. Yield: 43%, 432 mg. ¹H NMR (400 MHz DMSO) δ: 1.34 (3H, s, CH₃) 1.47 (3H, s, CH₃) ¹³C NMR (100 MHz DMSO) δ: 25.9 (CH₃) 27.0 (CH₃) 63.0 (2xCH) 77.8 (CH₂OTr) 81.6 (CH) 113.1 (C(CH₃)₂) 126.2 (ArC) 127.3 (ArC) 129.2 (ArC) 130.3 (ArC) 143.8 (OC(Ph)₃) 174.5 (C=O) IR (u_{max} = cm⁻¹) HRSM EI calc:[C₄₄H₄₆O₆Na⁺] 430.1780 obs:[C₄₄H₄₆O₆Na⁺] 430.1782

Cell Viability Assay: SHS-Y5Y cells were cultured using standard methods and plated out into 96 well plates (100 μL) for experiments.¹³ Each compound (serially diluted from 100 μM) was added to SHS-Y5Y cells and allowed to incubate for 24 hours at 37° C and 5% CO₂. A solution of XTT (2,3-bis-(2-methoxy-4-nitro-5-sulfophenyl)-2*H*-tetrazolium-5-carboxanilide) was prepared by mixing 1 mg/ml XTT in cell culture media (no serum) with 1.6 mg/ ml phenazine methasulfate and was added to each well. The plate was incubated for an additional 4 hours at 37° C and 5% CO₂. Cell viability was measured by comparing the optical density (Spectramax Spectrophotometer, Molecular Devices) in wells containing cells and test compounds to the vehicle control wells. A positive control of 10 μM of H₂O₂ was used to determine that the assay was measuring a decrease in cell viability.

6.1 References

- (1) Nishizono, N.; Sugo, M.; Machida, M.*et al. Tetrahedron* **2007**, 63, 11622.
- (2) Michel, B. Y.; Strazewski, P. *Tetrahedron* **2007**, 63, 9836.
- (3) Kim, Y.-A.; Park, M.-S.; Kim, Y. H.*et al. Tetrahedron* **2003**, 59, 2921.
- (4) Tewes, B.; Frehland, B.; Schepmann, D.*et al. Bioorg Med Chem* **2010**, 18, 8005.
- (5) Pattenden, G.; Shiker, A. J. *J Chem Soc Perkin Trans 1* **1992**, 1215.
- (6) Beaulieu, P. L.; Organisation, W. I. P., Ed. 2009; Vol. WO/2009/076747 A1.
- (7) Takahashi, S.; Nakata, T. *J Org Chem* **2002**, 67, 5739.
- (8) Nicolaou, K. C.; Estrada, A. A.; Zak, M.*et al. Angew Chem Int Ed Engl* **2005**, 44, 1378.
- (9) Patwardhan, A. P.; Thompson, D. H. *Langmuir* **2000**, 16, 10340
- (10) Jin, Y. H.; Liu, P.; Wang, J.*et al. J Org Chem* **2003**, 68, 9012.
- (11) Beigelman, L.; Ermolinsky, B. S.; Gurskaya, G. V.*et al. Carbohydr Res* **1987**, 166, 219.
- (12) Stewart, A. J.; Evans, R. M.; Weymouth-Wilson, A. C.*et al. Tet Asymm* **2002**, 13, 2667.
- (13) Tominaga, H.; Ishiyama, M.; Ohseto, F.*et al. Anal. Commun* **1999**, 36, 47.

Appendix

Below is the raw data for the cell viability assays performed on thymine **79** uracil **80**, 5FU **84** and 5,6-DMU **89**.

Table A.1.1: Raw data for thymine **79**

1 μ M	1 μ M	10 μ M	10 μ M	100 μ M	100 μ M	DMSO	H ₂ O ₂
1.0656	1.1861	1.0152	0.9992	0.9287	0.9446	0.9771	0.2599
1.0674	1.0858	0.9907	1.0958	0.936	1.004	1.0725	0.2631
1.1749	1.0656	0.8364	1.1281	0.9528	1.0571	0.9227	0.2472
1.1465	1.1352	1.2281	1.1588	1.0241	1.0339	0.932	0.2473
1.2792	1.0173	1.0737	1.368	1.029	0.9925	0.9675	0.2743
0.9334	1.1286	1.3661	1.1742	1.0674	0.8744	0.9994	0.2679
0.7035	1.3037	0.4966	0.8438	0.7331	0.4835	0.9538	0.2515
0.876	1.4938	0.7179	1.3565	0.701	0.7564	1.0041	0.2611
0.9459	1.1679	0.6827	1.2532	0.9376	1.3003	0.9242	0.2704
0.9226	0.9695	1.0201	1.2467	1.1835	1.1789	0.9481	0.3058
1.0621	0.9852	1.1748	1.1349	1.1723	1.0779	1.1347	0.3866
0.986	0.9918	1.1663	1.034	1.0722	1.0322	1.0684	0.2856
1.3058	1.5584	1.376	1.4697	1.6986	1.1363	1.1886	0.2632
1.3191	1.4394	1.1937	1.4033	1.5953	1.3317	1.3275	0.2663
1.3191	1.403	1.3803	1.5497	1.6512	1.5608	1.4072	0.2451
1.3822	1.0543	1.4063	1.7165	1.5878	1.5428	1.3809	0.2618
1.3425	1.4339	1.3299	1.4011	1.5073	1.3782	1.3663	0.2584
1.2853	1.3665	1.4049	1.3804	1.2576	1.169	1.4337	0.2499

Table A.1.2: Raw data for uracil **80**

1 μ M	1 μ M	10 μ M	10 μ M	100 μ M	100 μ M	DMSO	H ₂ O ₂
0.9176	0.9033	0.9171	0.9087	0.9118	0.8662	0.889	0.3412
0.9902	0.9718	0.8777	0.805	0.8361	0.8467	0.9349	0.3395
1.0047	0.9741	0.9337	0.8701	0.9107	0.8531	0.9156	0.3459
0.9565	0.9595	0.9291	0.85	0.8917	0.9108	0.8737	0.3562
0.9649	0.9325	0.8682	0.8798	0.8757	0.8491	0.9016	0.3676
0.8583	0.9642	0.8723	0.8572	0.8712	0.8555	0.8872	0.3676
0.8549	0.8535	0.773	0.7367	0.8374	0.8087	0.9818	0.2459
0.9736	0.9701	0.9053	0.9106	0.7745	0.926	0.9713	0.2382
1.007	0.9647	0.9682	0.9033	0.7754	0.873	0.9654	0.2328

0.9845	0.9711	1.0188	0.8239	0.776	0.8663	0.9524	0.2295
0.9857	0.926	0.9124	0.7842	0.8179	0.8668	0.9524	0.2266
0.7387	0.7581	0.7638	0.8914	0.8139	0.79	0.8005	0.228
0.9419	0.7629	0.8513	0.8608	0.9333	0.6809	0.8037	0.2519
0.8068	0.8756	0.9546	1.157	1.1378	0.9747	1.0789	0.2313
0.8197	0.7964	1.1232	1.157	1.239	1.0262	1.0538	0.2312
0.7937	0.8036	1.0797	1.0985	1.0713	1.0833	0.9851	0.2487
0.9065	0.9302	1.0423	0.877	1.0788	0.9839	1.0083	0.232
0.9143	0.9253	0.7431	0.7547	0.9737	0.7696	0.9377	0.2219

Table A.1.3: Raw data for 5FU **84**

1 μM	1 μM	10 μM	10 μM	100 μM	100 μM	DMSO	H₂O₂
0.9015	0.9291	0.9422	0.9677	0.9184	0.9589	0.9016	0.4145
0.9861	0.9109	0.8552	0.9394	0.8251	0.8035	0.8846	0.3597
1.0705	0.9423	1.0249	0.9985	0.7547	0.7933	0.9442	0.3468
1.0022	0.7672	1.0533	0.9819	0.7566	0.7874	1.0767	0.4073
1.0194	0.9918	1.0607	1.0095	0.7845	0.7957	1.0189	0.4097
0.9514	0.9529	0.9724	1.0085	0.7561	0.8558	0.949	0.3706
0.8537	0.8988	0.8813	0.9034	0.9297	0.925	0.9344	0.2614
0.9578	0.8439	0.8901	0.9986	0.8855	0.8144	1.063	0.2567
1.0099	0.9871	0.9523	0.9483	0.8372	0.8288	1.0334	0.2504
0.9296	0.9013	0.8407	1.0105	0.8404	0.8254	1.03	0.2519
0.9882	1.0073	0.8922	0.9684	0.8126	0.9231	1.0274	0.2487
0.8928	1.0425	0.8876	0.84	0.8257	0.8908	0.7834	0.2466
0.6342	0.9923	0.4832	0.9667	0.5007	1.2152	0.9729	0.245
0.9212	1.1115	0.7101	1.1128	0.5331	0.9622	1.011	0.2432
1.0286	1.1299	0.9053	0.8008	0.5766	1.5858	0.9685	0.2144
0.9507	1.0352	1.2361	1.226	0.9539	2.269	1.079	0.2385
0.9301	0.8811	0.6312	0.5993	0.8768	2.0582	0.9495	0.2267
0.9269	1.0259	0.9057	1.0095	0.9569	2.0045	0.95	0.2855

Table A.1.4: Raw data for 5,6-DMU **89**

1 μM	1 μM	10 μM	10 μM	100 μM	100 μM	DMSO	H₂O₂
0.8856	0.924	0.9315	0.8812	0.838	0.8732	0.8964	0.3722
0.9151	0.973	0.9217	0.8834	0.8526	0.8236	0.9292	0.392
0.8696	0.956	0.9429	0.9179	0.9763	0.8772	0.9305	0.3498
0.9828	0.8974	0.9401	0.9954	0.9702	0.9303	0.9938	0.363

1.0372	0.9283	0.9671	1.0269	1.0192	0.9306	0.9575	0.3516
0.98	0.9973	0.9534	1.0478	0.9942	0.8939	0.9303	0.3497
0.895	0.8322	0.8934	0.8299	1.0139	0.8276	0.8475	0.2583
1.1019	0.9848	1.0635	1.0901	0.9228	0.9658	1.0797	0.2689
1.0133	1.009	1.0975	0.967	0.8659	0.9397	1.0523	0.2727
1.0589	1.0021	1.0366	0.9534	0.8587	0.9851	1.0721	0.2636
1.0677	1.0803	1.0775	1.0396	0.8156	0.9529	1.0207	0.2642
0.9089	0.842	0.8827	0.8106	0.7437	0.6898	0.8067	0.2655
0.5453	0.7694	0.5745	0.7872	0.3387	0.4342	0.8332	0.279
0.582	0.7949	0.6703	1.0176	0.3227	0.6477	0.9354	0.2534
0.5941	0.7606	0.8583	0.995	0.3487	0.7368	1.0425	0.2289
0.6239	0.8133	1.0067	1.0013	0.3573	0.8698	1.0233	0.2183
0.7093	0.7559	1.0238	0.8938	0.504	1.0092	1.0143	0.2443
0.7222	0.8487	0.7701	0.8209	0.5439	0.9831	0.9762	0.2028

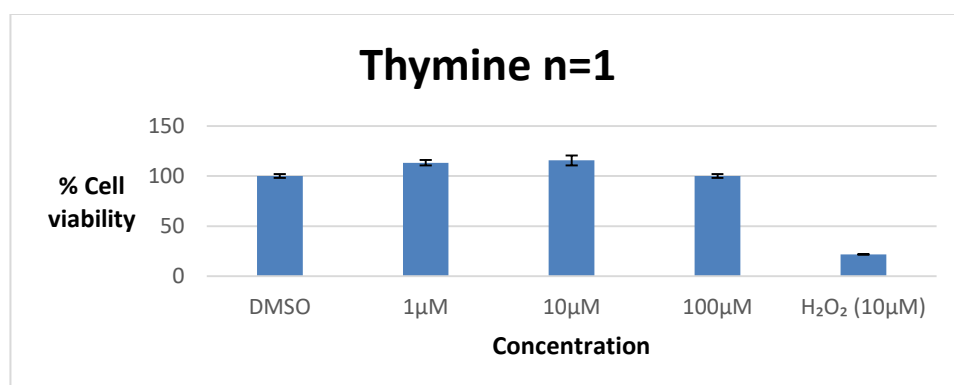


Figure A1.1: Thymine **79** replicate 1

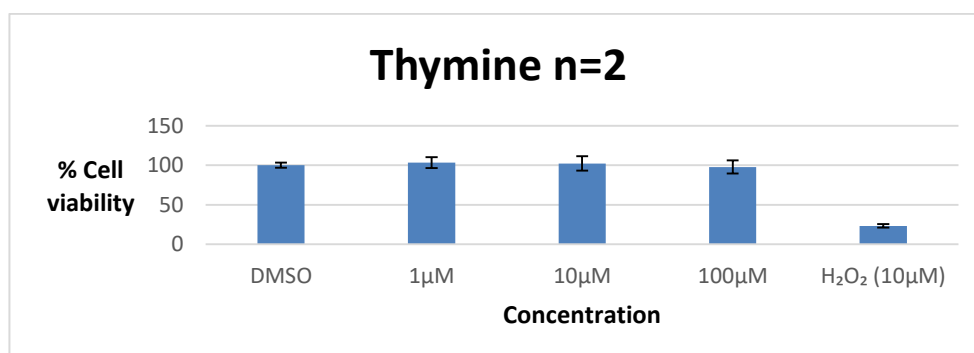


Figure A.1.2: Thymine **79** replicate 2

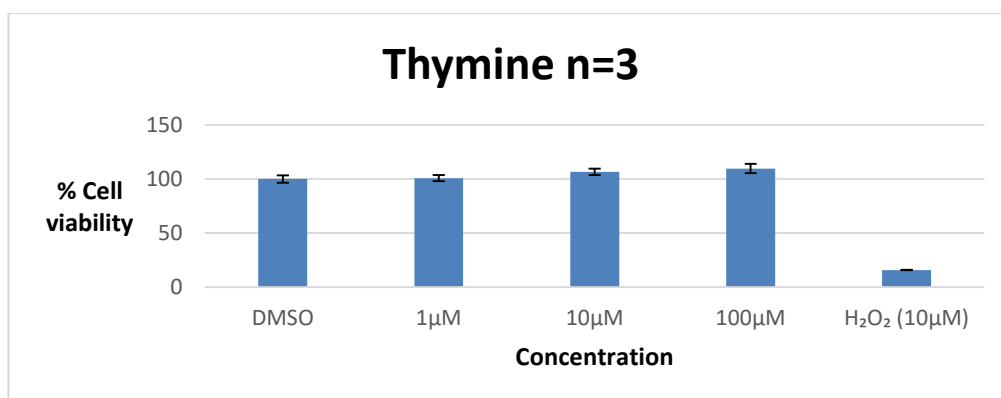


Figure A.1.3: Thymine **79** replicate 3

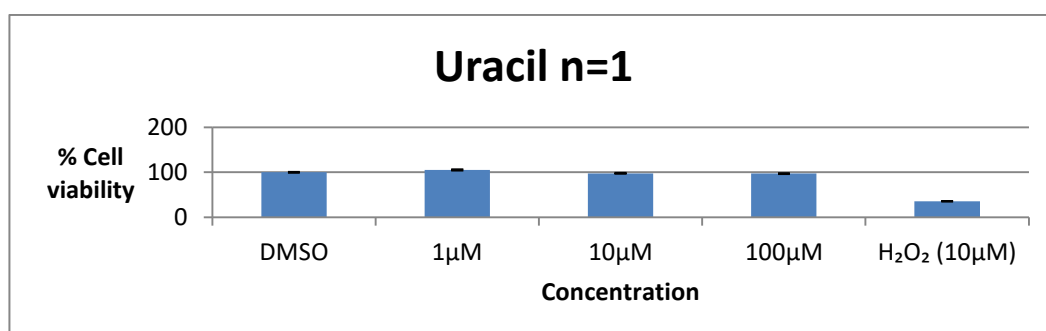


Figure A.1.4: Uracil **80** replicate 1

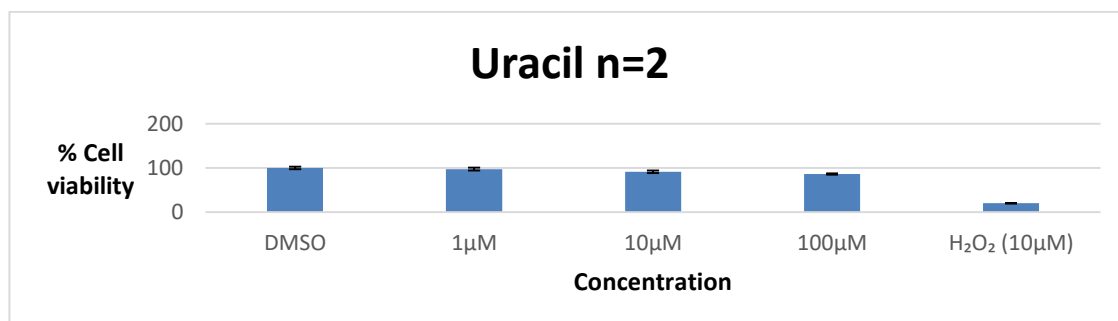


Figure A.1.5: Uracil **80** replicate 2

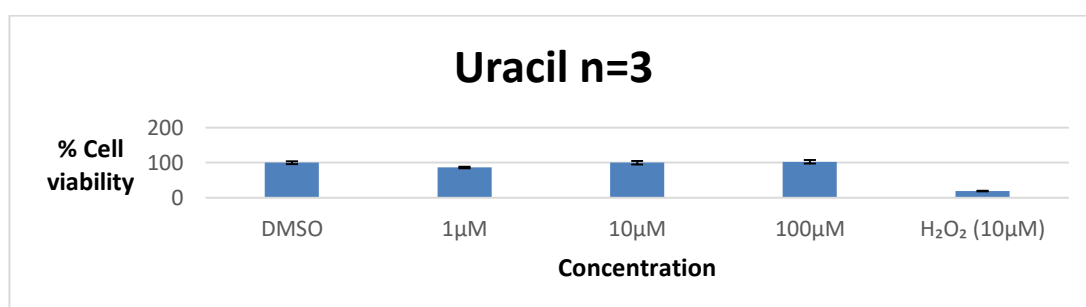


Figure A.1.6: Uracil **80** replicate 3

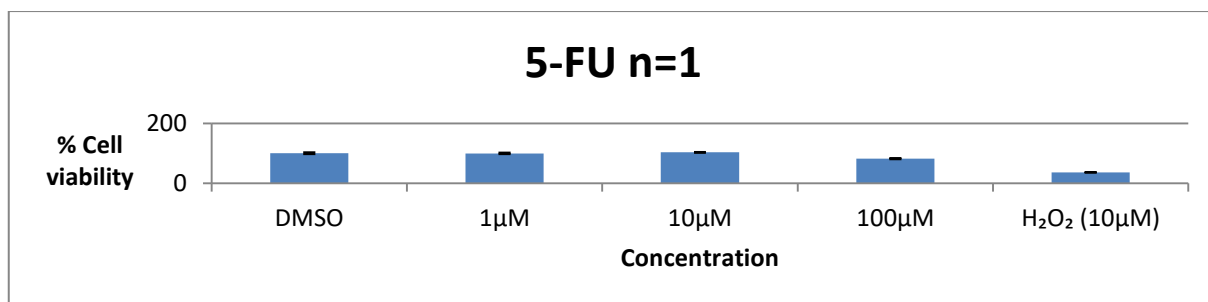


Figure A.1.7: 5FU 84 replicate 1

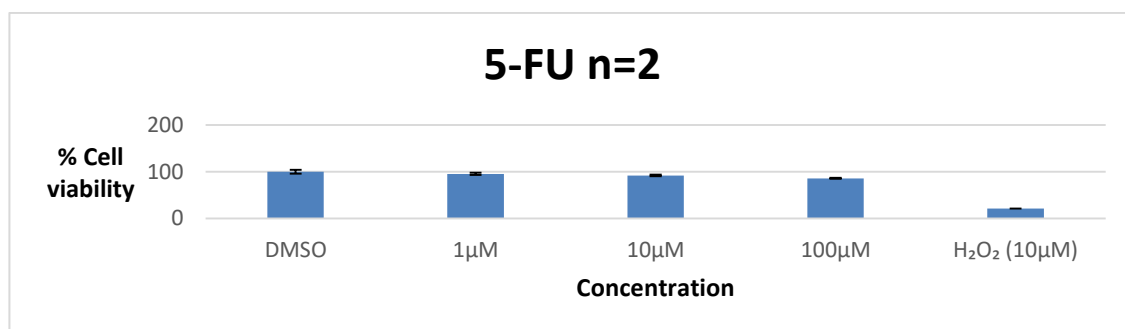


Figure A.1.8: 5FU 84 replicate 2

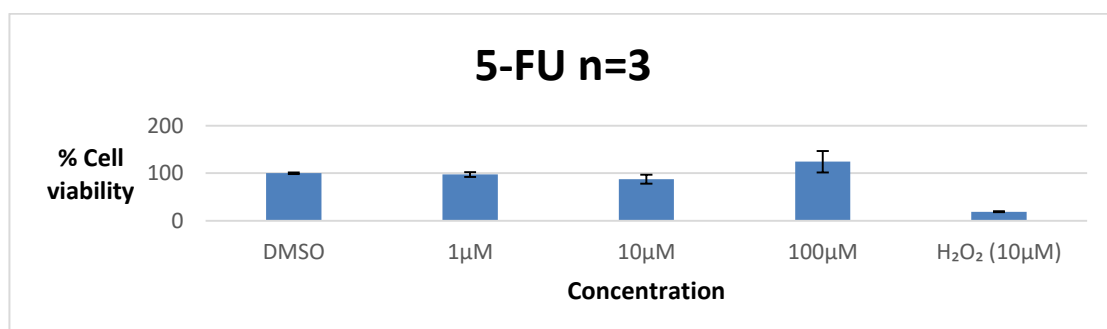


Figure A.1.9: 5FU 84 replicate 3

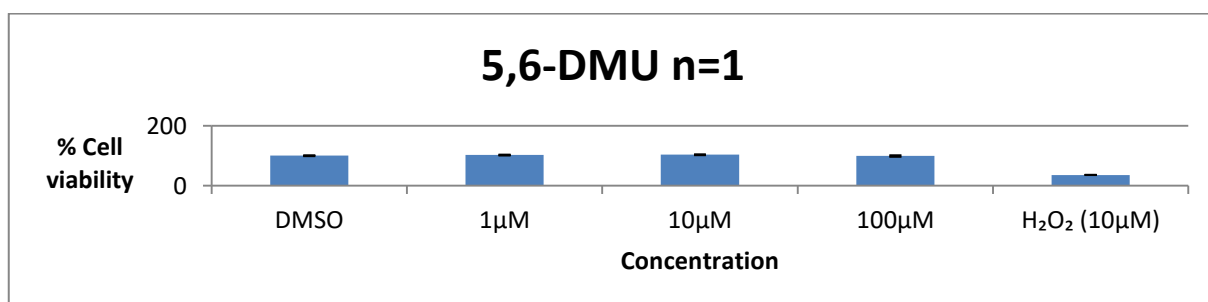


Figure A.1.10: 5,6-DMU 89 replicate 1

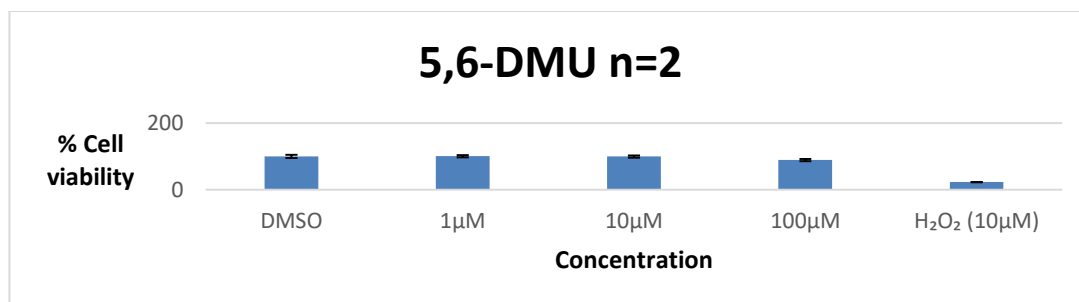


Figure A.1.11: 5,6-DMU 89 replicate 2

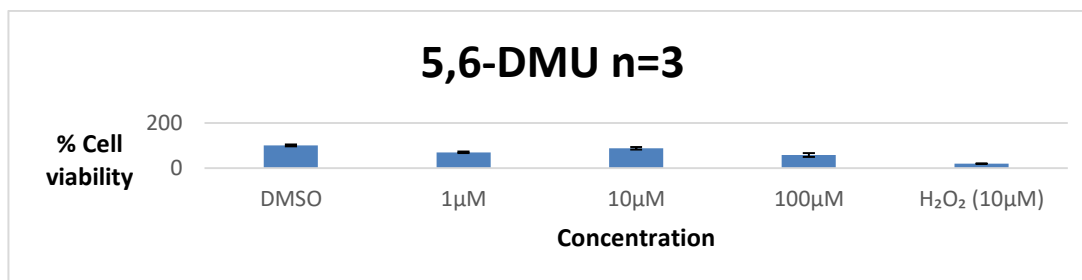


Figure A.1.12: 5,6-DMU 89 replicate 3